EXPLORING THE ROLE OF HYPOXIA IN NEUROINFLAMMATORY DISEASE AND THE USE OF OXYGEN AS A THERAPY

Mario Amatruda

UCL Institute of Neurology

A thesis submitted for the degree of

Doctor of Philosophy (Ph.D)

I, Mario Amatruda confirm that the research presented in this thesis is my own, unless stated otherwise.

Behavioural assessments and histological analyses on EAE (experimental autoimmune encephalomyelitis) were carried out in collaboration with Miss Alina Matis, M.Res, Miss Kate Harris, M.Sc, and Miss Sufaanah Sheikh, M.Res.

Isolation of encephalitogenic T-cells from rMOG immunized rats was carried out by Mr Daniel McElroy, M.Sc

Gene expression analysis on EAE samples was performed in collaboration with Mr Daniel McElroy, M.Sc.

Intravenous injection of pimonidazole and the *in-vivo* measurement of the oxygen tension in the spinal cord of rats with EAE were carried out in collaboration with Dr Roshni Desai, Ph.D, and Dr Andrew Davies, Ph.D.

ABSTRACT

Multiple sclerosis (MS) is an inflammatory-demyelinating disease of the central nervous system (CNS). Pathological studies have revealed that MS lesions can have hypoxia-like properties, raising the possibility that the inflamed CNS may suffer an energy deficit. We recently demonstrated that the spinal cord of rats with active experimental autoimmune encephalomyelitis (EAE, a model of MS) is hypoxic, and that hypoxia can be reversed by inspiring oxygen-enriched air. This thesis examines the contribution of hypoxia to the neurological deficits, and the use of oxygen as a therapy. Demyelinating and non-demyelinating models of EAE in rats were evaluated, namely active and passive EAE respectively. Room air controls were used for comparison. Assessment of neurological deficits in active EAE revealed that oxygen (95%) promptly improved neurological function in paralysed rats, within only 1 hour of exposure. Furthermore, prolonged administration of oxygen (75%) applied either prophylactically (from the day of immunisation for 23 days) or therapeutically from the onset of disease (for 24, 48 or 72 hours) produced a greater and long-lasting amelioration of disease severity. Interestingly, oxygen treatment from disease onset reduced oligodendrocyte cell-stress and death, demyelination, microglial activation and macrophage infiltration in the spinal cord, without exacerbating oxidative damage. The protective effect was proportional to the duration of the treatment and significant in rats treated for 72 hours. Other experiments have revealed that the spinal cord of rats with passive EAE is also hypoxic and oxygen treatment significantly ameliorated disease progression when administered prophylactically. We also tested polynitroxylated pegylated hemoglobin (PNPH) as an alternative oxygen-based treatment in active EAE, revealing an acute improvement of the neurological function 1 hour after the injection of PNPH. We conclude that hypoxia contributes to neurological deficits and demyelination in inflammatory autoimmune demyelinating disease, and that oxygen therapy can reduce both the deficits and the demyelination.

TABLE OF CONTENTS

ABBREVIATIONS

4E-BP1	4E binding protein 1
8-OHdG	8-hydroxy-2'-deoxyguanosine
ANOVA	Analysis of variance
Arg1	Arginase-1
ATP	Adenosine triphosphate
BiP	Immunoglobulin-heavy-chain-binding protein
BBB	Blood-brain barrier
Ca^{2+}	Calcium
CAD	C-terminal transactivation domain
CBF	Cerebral blood flow
CBP	CREB-binding protein
CBV	Cerebral blood volume
CC1	Adenomatous poli coli protein, clone CC1
Ccr5	C-C chemokine receptor 5
CCSVI	Chronic cerebrospinal venous insufficiency
CD3	Cluster of differentiation-3
CFA	Complete Freund's adjuvant
CGT	Ceramide galactosyltransferase
CNS	Central nervous system
CSF	Cerebrospinal fluid
DA	Dark Agouti
DAB	Diaminobenzidine
DISC	Death-induced signal complex
DMF	Dymethil fumarate
DMEM	Dulbecco's modified eagle medium
DNA	Deoxyribonucleic acid
EAE	Experimental autoimmune encephalomyelitis
EDSS	Expanded disability status scale
(p-)eIF2α	(phosphorylated-) Eukaryotic elongation factor 2-alpha
eIF4E	Eukaryotic elongation factor 4E
eIF4G	Eukaryotic elongation factor 4G
eNOS	Endothelial nitric oxide synthase
EP	Evoked potential
ER	Endoplasmic reticulum
FA2H	Fatty acid 2-hydroxylase
FIH	Factor inhibiting HIF
Foxp3	Forkhead box P3
GABA	γ-aminobutyric acid
G-CSF	Granulocyte colony stimulating factor

GFAP	Glial fibrillary acidic protein
GFP	Green fluorescent protein
GLUT-1	Glucose transporter-1
GTP	Guanosine triphosphate
$FADH_2$	Flavin adenine dinucleotide dihydrogen
H_2O_2	Hydrogen peroxide
HBOT	Hyperbaric oxygen therapy
HIF1	Hypoxia inducible factor-1
HLA	Human leukocyte antigen
HNO_2	Nitrous acid
HRE	Hypoxia responsive element
Kir	Inwardly rectifying potassium channels
Iba1	Ionised calcium binding adaptor-1
IFA	Incomplete Freund's adjuvant
IFNγ	Interferon-γ
IL	Interleukin
iNOS	Inducible nitric oxide synthase
IRE1	Inositol-requiring protein 1
LDH	Lactate dehydrogenase
LFB	Luxol fast blue
LPS	Lipopolysaccharide
mAb	Monoclonal antibody
MAG	Myelin associated glycoprotein
MBP	Myelin basic protein
MCT	Monocarboxylate transporter
MHC	Major histocompatibility complex
MLKL	Mixed-lineage kinase like
MOG	Myelin oligodendrocyte glyocoprotein
MRI	Magnetic resonance imaging
MS	Multiple sclerosis
mTOR	Mechanistic target of rapamycin
NaBH4	Sodium borohydride
NaCl	Sodium chloride
NADH	Nicotinamide adenine dinucleotide hydrogen
NADPH	Nicotinamide adenine dinucleotide phosphate
Na^+/K^+	Sodium/potassium
NAWM	Normal appearing white matter
NeuN	Neuronal nuclei
NO	Nitric oxide
NO^-	Nitroxyl ion
NO_2	Nitrogen dioxide
NOS	Nitric oxide synthase
nNOS	Neuronal nitric oxide synthase
O_2	Oxygen

OCT	Optimum cutting temperature
OH^-	Hydroxyl radical
$ONOO^-$	Peroxynitrite
ONOOH	Peroxynitrous acid
OPCs	Oligodendrocyte precursor cells
p70S6K	Ribosomal protein S6 kinase
pAb	Polyclonal antibody
PaO_2	Partial pressure of oxygen
PEG	Polyethylene glycol
PERK	protein RNA-like endoplasmic reticulum kinase
PBS	Phosphate buffered saline
PFA	Paraformaldehyde
PFK-2	Phosphofructokinase-2
PHD	Prolyl hydroxylate
PKR	Protein kinase R
Pimo	Pimonidazole adducts
PML	Promyelocytic leukaemia tumour suppressor
PMN	Polymorphonuclear leukocytes
PLP	Proteolipid protein
PNPH	Polynitroxylated pegylated haemoglobin
PPMS	Primary progressive MS
RECA1	Rat endothelial cell antigen-1
rMOG	Recombinant myelin oligodendrocyte glycoprotein
RNA	Ribonucleic acid
RNS	Reactive nitrogen species
ROS	Reactive oxygen species
RPMI	Roswell Park Memorial Institute medium
RRMS	Relapsing-remitting MS
RT	Room temperature
RT-PCR	Real time – polymerase chain reaction
SOD	Superoxide dismutase
S.E.M	Standard error of mean
SPMS	Secondary progressive MS
S1P	Sphingosine-1-receptor
TGFβ	Transforming growth factor beta
Th1	T-helper 1
Th17	T-helper 17
TNFα	Tumour necrosis factor-alpha
TNFR1	TNFα receptor-1
TRAIL	TNFα-related apoptosis inducing ligands
Treg	T-regulatory cells
VEGF	Vascular endothelial growth factor
VEP	Visual evoked potential
VHL	von Hippel-Lindau

LIST OF FIGURES

1. INTRODUCTION

2. NORMOBARIC OXYGEN-ENRICHED AIR FOR THE TREATMENT OF NEUROLOGICAL DEFICITS IN AN INFLAMMATORY DEMYELINATING MODEL OF MULTIPLE SCLEROSIS

3. HYPOXIA AND NEUROLOGICAL DEFICITS IN AN INFLAMMATORY NON-DEMYELINATING MODEL OF MULTIPLE SCLEROSIS

4. ADMINISTRATION OF AN OXYGEN-CARRYING BLOOD SUBSTITUTE FOR THE TREATMENT OF NEUROLOGICAL DEFICITS IN A MODEL OF MULTIPLE SCLEROSIS

5. GENERAL DISCUSSION

LIST OF TABLES

CHAPTER 1

1. INTRODUCTION

1.1.0.0 Multiple Sclerosis

Multiple sclerosis (MS) is a chronic inflammatory disease of the central nervous system (CNS) which causes debilitating neurological dysfunction in young adults and affects almost 2.5 million individuals worldwide (Noseworthy *et al.*, 2000). MS was first described as a distinct disease in 1868 by the French neurologist Jean-Martin Charcot, and it represents the prototypical demyelinating disease of the CNS. MS usually starts early in adulthood with a relapsing-remitting disease course (relapse-remitting MS; RRMS), in which periodic attacks of neurological deficits are alternated with complete or partial recovery of neurological function (Compston and Coles, 2008). After a variable period of time, the majority of patients with RRMS (~65%) suffer a progressive and persistent accumulation of the deficits without remission, termed secondary progressive MS (SPMS) (Compston and Coles, 2008). In some cases, patients with MS (~20%) experience a progressive disease course directly from the beginning of the first neurological signs and in the absence of any recovery of neurological function (primary progressive MS; PPMS) (Compston and Coles, 2008).

MS is characterised by multifocal demyelinating lesions within the CNS, which consist of well-demarcated areas of myelin loss and parallel formation of an astrocytic scar (Lassmann, 2013). Neurological deficits are widely believed to be due to demyelination (Noseworthy *et al.*, 2000), given that the absence of myelin impairs normal axonal conduction (McDonald and Sears, 1970; Waxman *et al.*, 1977; Smith *et al.*, 1979; Smith, 1994). As the disease progresses, demyelination and inflammation can lead to irreversible axonal destruction and neurodegeneration (Noseworthy *et al.*, 2000). In particular, demyelinated axons may suffer a series of pathological changes resulting in axonal swelling and transection (Trapp *et al.*, 1998; Nikic *et al.*, 2011). These processes may finally result in neuronal death and tissue atrophy, causing irreversible disabilities (Friese *et al.*, 2014).

MS lesions can develop throughout the CNS, although they arise more often in particular locations such as the optic nerves, periventricular white matter, brain stem, cerebellum and spinal cord white matter (Noseworthy *et al.*, 2000). Depending on their anatomical location, MS lesions can cause a variety of neurological signs and symptoms including: visual problems, limb weakness, sensory disturbance, gait instability and ataxia (Hauser and Oksenberg, 2006; Compston and Coles, 2008). Many patients also describe augmented fatigue during normal daily activities, accompanied by physiological increase in body temperature (Noseworthy *et al.*, 2000).

MS is commonly diagnosed based on an evaluation of the neurological signs and symptoms in combination with neuroimaging and laboratory tests. Especially at the early stage of disease, the clinical signs alone are difficult to attribute specifically to MS due to their similarities with other neurological disorders (Compston and Coles, 2008). The most commonly used diagnostic procedure includes the application of the revised McDonald criteria (Polman *et al.*, 2011). The McDonald criteria emphasize the need for combining an evaluation of neurological deficits with magnetic resonance imaging (MRI) used to localize demyelinating lesions disseminated in space (different locations) and time (Polman *et al.*, 2011). Laboratory tests such as the analysis of cerebrospinal fluid (CSF) and evoked potential (EP) can additionally be used to achieve an earlier and more uniform diagnosis of MS (Polman *et al.*, 2011). In particular, the electrophoretic analysis of CSF is used to disclose the presence of oligoclonal bands of IgG, a neuroinflammatory marker found in about 75-80% of patients with MS (Link and Huang, 2006). The EP evaluates the functional response of the brain to a specific stimulus. The electrical potentials are measured by placing electrodes on the scalp in the area of the brain that responds to the stimulation. Decreased speed in electrical transmission implies the presence of a demyelinated lesion.

In the past, three different EP tests were used to detect MS lesions in the brain, namely: visual evoked potentials (VEP), brainstem auditory evoked potentials and sensory evoked potentials. More recently, only the VEP is used for the diagnosis of MS (and optic neuritis). VEP discloses delays in the electrical transmission along the optic nerve, which is an early feature in many patients with MS and it is commonly present even in the absence of evident visual impairment (McDonald, 1980).

The expanded disability status scale (EDSS) is used to assess the magnitude of disability in patients with MS, and to monitor how the severity of the neurological deficit

changes over time. The EDSS is commonly used to assess the efficacy of therapies in clinical trials.

Current treatments for MS include a number of anti-inflammatory and immunomodulatory drugs that have beneficial effects mainly in patients with RRMS but that are only poorly, or not, effective in patients with SPMS or PPMS (Winkelmann *et al.*, 2016). Glucocorticoids are often used at high doses for the treatment of acute exacerbations of the neurological deficits in MS (Winkelmann *et al.*, 2016). The anti-inflammatory effects of glucocorticoids consist of a reduced production of numerous inflammatory mediators and reduced extravasation of inflammatory cells across the BBB (Winkelmann *et al.*, 2016). Disease modifying treatments (described below) are instead used to attenuate disease progression in the long term. Interferon-β (IFN-β) is a cytokine whose mechanism of action is complex and involves downregulation of immune recognition molecules such as MHC class II antigens, co-stimulatory molecules and adhesion molecules, modulation of the balance between pro-inflammatory and anti-inflammatory cytokines, and reduction of lymphocyte migration into the CNS (Winkelmann *et al.*, 2016). Glatiramer acetate is a synthetic polymer that decreases the expression of MHC class II molecules, deactivates macrophages and monocytes, and shifts the lymphocyte activation from a pro-inflammatory (T-helper 1; Th1) to an anti-inflammatory (T-helper 2; Th2) phenotype (Winkelmann *et al.*, 2016). Fingolimod is a first-in-class sphingosine- 1-phosphate (S1P) receptor activator. The activation of the S1P receptor on T-cells blocks their emigration from lymph nodes into the CNS and recent evidence suggest that the activation of S1P receptors by fingolimod on glial cells could also promote reparative processes (Aktas *et al.*, 2010; Winkelmann *et al.*, 2016). Dimethyl fumarate (DMF, also known as BG12) is another treatment option for MS. This drug acts on MS by attenuating the activity of pro-inflammatory Th1 and Th-17 cells, and by scavenging toxic oxygen metabolites (Winkelmann *et al.*, 2016). Teriflunomide is an inhibitor of the enzyme dihydroorotate dehydrogenase, which is essential for *de-novo* pyrimidine synthesis by proliferating T-cells, and it preferentially diminishes the activity of antigen-activated T lymphocytes (Winkelmann *et al.*, 2016). Azathioprine is an immunosuppressive drug whose effect derives from its analogy with purines: it inhibits DNA synthesis, mostly affecting highly proliferative cells such as T-cells (Winkelmann *et al.*, 2016). Natalizumab is a humanized monoclonal antibody that binds

α4 integrins and disrupts their interaction with the adhesion molecule VCAM-1, resulting in reduced migration of leukocytes from the blood to the CNS (Winkelmann *et al.*, 2016). These drugs have proven, to some extent, to be effective in attenuating the severity of neurological deficits, and to delay the progression of the disease, in patients with RRMS, but they also have side effects as they can cause leukopaenia and increased risk of viral, bacterial and fungal infections (Winkelmann *et al.*, 2016).

Although several studies have shown that the risk of developing MS is increased by genetic and environmental factors (Ramagopalan *et al.*, 2010), the initial cause of MS remains unknown. A common proposed idea is that MS is an autoimmune disease. The proposed autoimmune aetiology of MS, which has come to be known as the *"outside-in"* hypothesis, consists of the idea that an aberrant immune response against the CNS is the primary event that triggers the disease (McFarland and Martin, 2007). In brief, auto-reactive lymphocytes against CNS antigen(s) migrate from the blood stream (the "*outside*") into the CNS parenchyma ("*-in"*), eliciting an inflammatory, autoimmune reaction that causes tissue damage and demyelination (McFarland and Martin, 2007). This hypothesis is supported by some features of MS (see following). One feature is that MS, similarly with other well-recognized human autoimmune diseases, often present a relapsing-remitting course (Wildner and Kaufmann, 2013) and it has an increased incidence in female population compared with male individuals (2:1) (Noseworthy *et al.*, 2000; Ngo *et al.*, 2014). However the latter aspect seems not to be applicable in the case of PPMS in which the incidence of the disease is similar between men and women (1:1) (Noseworthy *et al.*, 2000). Another indication in support of the *outside-in* hypothesis was provided by the genetic association between specific types of the human leukocyte antigen class-II (HLA-II) with higher risk of developing MS (McFarland and Martin, 2007; Ramagopalan *et al.*, 2010). It has been suggested that these HLA-II molecules associated with MS, might bind preferentially specific CNS epitopes and subsequently prime an antigenic T-cell response against the CNS, although this mechanism has not been directly proven (McFarland and Martin, 2007). In the last four decades a considerable effort has been expended in identifying the CNS antigen that triggers the autoimmune response in MS (McFarland and Martin, 2007). The demyelinating nature of MS and its similarity with animal models in which a similar pathology is triggered by an autoimmune reaction against myelin, led to focus the

attention on myelin proteins (McFarland and Martin, 2007). A greater number of $CD4^+$ T-cells reactive against encephalitogenic epitopes of myelin was found in MS patients (Bielekova *et al.*, 2004), but the specificity of these T-cells for the antigens was very similar to that of T-cells found also in healthy individuals (Bielekova *et al.*, 2004; McFarland and Martin, 2007). Interestingly, the immunodominant epitopes found in patients with MS showed a predicted low affinity to HLA-II molecules, suggesting a role for thymic selection in the generation of the autoimmune T-cell repertoire (Bielekova *et al.*, 2004). It has been suggested that MS-associated HLA molecules could poorly bind CNS epitopes causing a dysfunctional negative selection of self-reactive T-cells in the thymus during early life, possibly leaving in circulation a larger pool of auto-reactive lymphocytes that could eventually trigger the autoimmune response against the CNS (Bielekova *et al.*, 2004; McFarland and Martin, 2007). However, the HLA-related genetic susceptibility to MS may account only for a subgroup of patients with MS, and it cannot explain the development of the disease in patients in which these MS-associated alleles are not present. Nevertheless, the investigation of the mechanisms underlying the autoimmune aetiology of MS has yielded much information about the immune responses in this disease, leading to the development of useful medications. Indeed, a panel of twelve immunomodulatory therapies exists and these drugs have been shown to ameliorate both the severity of the neurological deficits and delay the onset of new relapses (Winkelmann *et al.*, 2016). However, these therapies are effective only in patients with RRMS and not in the progressive phase of the disease (PPMS and SPMS) (Winkelmann *et al.*, 2016), suggesting that other pathological mechanisms, in addition to inflammation and autoimmunity, can contribute to the disease progression.

An alternative hypothesis suggests that MS is a cytodegenerative disease, where autoimmunity is an important, but only a subsequent reaction that occurs in predisposed hosts (Stys, 2010). This hypothesis is known as an "*inside-out*" hypothesis. The "*inside-out*" hypothesis suggests that MS develops from an intrinsic degeneration of CNS cells (the *"inside"*), possibly oligodendrocytes, which only later result in the recruitment of inflammatory cells into the CNS parenchyma (*"-in"*), which can subsequently elicit an autoimmune response (Stys, 2010). The *"inside-out"* hypothesis is based on recent evidence that has begun to challenge the *"outside-in"*

hypothesis. In particular, pathological studies on newly forming lesions in MS have revealed early loss of oligodendrocytes in the absence of conspicuous T- and B-lymphocyte infiltrates and with only macrophages scavenging myelin debris (Henderson *et al.*, 2009). In addition, ultrastructural analysis of biopsy samples in areas proximal to foci of maximal inflammation, revealed that a large number of the myelinated axons still present exhibted widening of the inner myelin lamellae, but intact outer myelin layers (Rodriguez and Scheithauer, 1994). It has been pointed out that if an autoimmune reaction is the initial cause of the myelin damage, it would be expected that an early event would be the disruption of the external layers of the myelin sheaths, given that these layers are more exposed to the attack of inflammatory cells and mediators, rather than an initial alteration of the innermost, and thereby protected myelin lamellae (Stys, 2010). In addition, the fact that PPMS and SPMS patients have a worsening of the neurological deficits while the inflammatory/autoimmune response decreases (Stys, 2010; Lassmann, 2013), has been used to support the hypothesis that an intrinsic cytodegeneration of the CNS drives the disease (Stys, 2010). However, this view does not exclude the possibility that an autoimmune response causes the initial CNS damage, which might be asymptomatic in some individuals (for example in patients with PPMS), while the progression of the neurological deficits is driven by autoimmune-independent pathological mechanisms such as the nitrative/oxidative stress and mitochondrial dysfunction, which have also been revealed to be prominent in MS lesions (Smith and Lassmann, 2002; Dutta *et al.*, 2006; Haider *et al.*, 2011; Lassmann and Van Horssen, 2011; Fischer *et al.*, 2012; Mahad *et al.*, 2015).

While the causative mechanisms of MS seem to be still far from being understood, it is becoming clearer that several pathological events can contribute to the damage of the CNS including autoimmunity, inflammation, oxidative and nitrative stress, hypoxia, mitochondrial dysfunction and an energy deficit (Bo *et al.*, 1994; Smith and Lassmann, 2002; Aboul-Enein *et al.*, 2003; Dutta *et al.*, 2006; McFarland and Martin, 2007; Trapp and Stys, 2009; Haider *et al.*, 2011; Lassmann and Van Horssen, 2011; Fischer *et al.*, 2012; Mahad *et al.*, 2015). Interestingly, evidence revealed that demyelinating lesions in MS can have different appearances suggestive of one or more of these pathological mechanisms (Lucchinetti *et al.*, 2000; Aboul-Enein and Lassmann, 2005). Indeed, some lesions indicate an autoimmune aetiology while others indicate a primary

oligodendrocyte dystrophy and a hypoxic cause (Lucchinetti *et al.*, 2000). Therefore, it has been suggested that MS may be a series of syndromes with different causes and pathogenic mechanisms (Noseworthy *et al.*, 2000). Therefore, a combinatorial treatment that targets different pathogenic mechanisms at the same time may be especially effective in delaying or even stopping the progression of the disease. Concurrently, neuro-regenerative approaches (e.g. neural stem cells) could be important in repairing the damaged CNS and restoring normal neurological function (Franklin *et al.*, 2012).

1.2.0.0 Animal models of MS: experimental autoimmune encephalomyelitis (EAE)

Important knowledge about the pathogenic mechanisms in MS has been sought by the study of inflammatory-demyelinating models of encephalopathy in rodents. These models also represent a useful tool to develop and test therapeutic approaches before these are applied in MS patients. The most commonly used animal model of MS is experimental autoimmune encephalomyelitis (EAE) (Constantinescu *et al.*, 2011). EAE is an autoimmune-mediated inflammatory disease of the CNS, triggered by $CD4^+$ T-cells reactive against a specific antigen, typically of the myelin sheath. Two major types of EAE are commonly used in preclinical studies, namely active and passive EAE. Active EAE is induced by the injection of a myelin encephalitogenic antigen emulsified in a mineral oil-based adjuvant (Freund's adjuvant) (Freund *et al.*, 1947; Stromnes and Goverman, 2006a). The immunization of susceptible rodents with the antigen primes an autoimmune response in which reactive T-cells enter the CNS, causing myelin damage (Stromnes and Goverman, 2006a). Passive EAE is instead induced via the administration of encephalitogenic T-cells reactivated *in vitro* against the antigen before being injected in the recipient animal (Stromnes and Goverman, 2006b).

Various factors, including genetic susceptibility, species, age and sex of the immunized animal, in addition to type, preparation, dose and administration route of the immunogen, can influence the pathogenesis, sensitivity and clinical course of EAE (Mannie *et al.*, 2009). Accordingly, each animal species and type of EAE, potentially allows the study of one or more aspects of MS. In the majority of susceptible rodent

strains, the disease presents as an ascending flaccid paralysis, beginning with tail weakness and progressing to hind limb paralysis. In severe cases it can even lead to forelimb paralysis and death. However, rodents with EAE less commonly develop lesions in the brain or optic nerves. This pattern is unlike MS (Simmons *et al.*, 1982), a point which was often ignored and that has not been entirely understood.

Although no known animal model reflects the entire pathological spectrum of the human disease, EAE shows neurological signs, and immunological and histopathological similarities with MS (Hohlfeld and Wekerle, 2001). Both active and passive EAE are autoimmune-mediated models of CNS inflammation, but whether they are accurate models of MS remains uncertain.

1.2.1.0 Active EAE

Active EAE refers to the disease resulting from the co-injection, with adjuvant, of spinal cord homogenate or myelin antigens such as myelin basic protein (MBP), myelin proteolipid protein (PLP) or myelin oligodendrocyte glycoprotein (MOG). Active EAE has the advantage that, as in MS, many aspects of the acquired immune system play important roles, and the prominent inflammation commonly occurs in conjunction with the structural damage of the CNS, including demyelination and degeneration. In active EAE, $CD4^+$ T-cells are primed by the interaction between the T-cell receptor and the injected antigen presented by MHC class II complexes in the peripheral immune system, leading to the differentiation of T-naïve in T helpers 1 and and 17 (Stromnes and Goverman, 2006a). In contrast to resting T-cells, T-cells primed for CNS-antigens gain the ability to enter the CNS parenchyma (Ludowyk *et al.*, 1992; Hickey, 2001; Larochelle *et al.*, 2011) via a multi-step process known as leukocyte extravasation (or diapedesis, described below). However, some molecular factors involved in the specific interaction and extravasation of these cells through cerebral capillaries and post-capillary venules in EAE remain unknown (Wilson *et al.*, 2010). Briefly, leukocyte diapedesis involves adhesion of leukocytes to the endothelial surface (Liu *et al.*, 2003; Engelhardt and Wolburg, 2004), and their migration either through the inter-endothelial cell junctions (paracellular migration), or through the endothelial cells themselves (transcellular migration) (Engelhardt and Wolburg, 2004). The first step of this process represents the rolling of leukocytes over the luminal surface of endothelial cells,

mediated by weak interactions between adhesion molecules on leukocytes (such as L-selectin, PSGl-1 and Syalil Lewis X) and their ligands on endothelial cells (such as P-, E-selectin, Glycam-1, CD34 and MadCAM-1) (van Buul and Hordijk, 2004). Subsequently, loosely attached leukocytes can be activated by chemotactic cytokines presented on the apical surface of the endothelium, and firmly adhere to the endothelium through immobilized chemoattractants and adhesion molecules such as integrins on the leukocytes and CAMs on the endothelium (van Buul and Hordijk, 2004). Finally, leukocyte migration through the endothelial cell-cell junctions (paracellular extravasation) involves homophilic-binding molecules such as the JAMs, PECAM-1, CD99 and VE-cadherin (van Buul and Hordijk, 2004). Although there is a lack of evidence regarding the specific molecular components involved in the transcellular migration, it has been speculated that at least some molecules involved in the junctional migration may also play a critical role for transcellular migration (Engelhardt and Wolburg, 2004).

In the CNS, infiltrated myelin-specific T-cells are reactivated via an interaction with resident antigen presenting cells (Wekerle *et al.*, 1986; Stromnes and Goverman, 2006a). Once reactivated, these cells start to produce inflammatory cytokines and chemokines (IL-1, IL-17, TGFβ, etc.) initiating an inflammatory cascade that recruits predominantly macrophages to the sites of T-cell activation (Stromnes 2006). Pro-inflammatory mediators secreted by macrophages, such as TNFα, ROS and matrix metalloproteinase can also directly and indirectly (via neuroglial cells) increase the permeability of the BBB via disruption of the endothelial tight junctions, alteration of the vascular basement membrane, and increased expression of chemokines and CAMs by endothelial cells, resulting in a further extravasation of leukocytes into the CNS (Stromnes and Goverman, 2006a; Larochelle *et al.*, 2011). Furthermore, macrophages, along with other inflammatory cells (such as T- and B-cells) and mediators (e.g. antibodies) contribute to CNS tissue damage and demyelination in EAE (von Budingen *et al.*, 2001; Kuchroo *et al.*, 2002; Stromnes and Goverman, 2006a; Fletcher *et al.*, 2010; O'Brien *et al.*, 2010).

Active EAE is commonly used in mice and rats, producing a chronic-progressive or relapsing-remitting disease with demyelination, depending on the species and strain immunised. A common encephalitogen is MOG (or MOG peptides), a minor myelin component. MOG elicits an encephalitic T-cell response, but also widespread antibody-mediated CNS demyelination (Johns *et al.*, 1995; Gold *et al.*, 2006), resulting in a chronic relapsing or progressive disease in mice (Stromnes and Goverman, 2006a).

MOG is commonly used to induce active EAE in C57BL/6 and SJL mouse strains, which are maybe the most commonly used rodents for the study of MS (Stromnes and Goverman, 2006a). C57BL/6 is a popular strain used in EAE studies because most transgenic and gene knockouts are generated in this background (Al-Izki *et al.*, 2012). C57BL/6 mice with active EAE develop a chronic disease in which animals rapidly accumulate permanent disabilities (Stromnes and Goverman, 2006a; Al-Izki *et al.*, 2012). The fast progression of the disease may represent a clear disadvantage, as it can be an endpoint for experimental design (Al-Izki *et al.*, 2012). SJL is likewise a commonly used mouse strain for the induction of active EAE. Sensitization of SJL mice with MOG leads to a relapsing-remitting disease course in which the frequency of relapses can be quite variable (Brown *et al.*, 1982; Al-Izki *et al.*, 2012). Furthermore, SJL mice with active EAE undergo an aggressive disease course often characterized by hindlimb and forelimb paralysis that can lead to the death of the animal within a relatively short period after the onset of deficits (Brown *et al.*, 1982; Al-Izki *et al.*, 2012). The Biozzi AB/H mouse is another commonly used strain for the induction of active EAE. Although Biozzi AB/H mice respond to a variety of myelin epitopes including MOG, immunization with spinal cord homogenate has most consistently produced a high incidence of relapsing disease and does not require co-injection of pertussis toxin and co-adjuvant (Al-Izki *et al.*, 2012), as instead required for the induction of active EAE in other mice strains such as SJL and C57BL/6 (see also below). Active EAE in Biozzi AB/H mice results in a predictable relapsing-remitting disease that reproduces several characteristics of MS (Baker *et al.*, 1990; Al-Izki *et al.*, 2012). The disease course in Biozzi AB/H mice is less aggressive compared with C57BL/6 and SJL mice with active EAE, and in this model relapses are more easily distinguished (Baker *et al.*, 1990; Al-Izki *et al.*, 2012). Moreover, Biozzi AB/H mice with active EAE, after a first relapsing-remitting phase, slowly develop a secondary progressive disease course in which

neurological disabilities accumulate concomitantly with persistent demyelination, gliosis, glial cell activation and neuronal loss (Baker *et al.*, 1990; Al-Izki *et al.*, 2012). Importantly, it has been shown that Biozzi AB/H mice during the progressive phase of EAE are resistant to immunosuppressive treatments, similarly to patients with progressive MS (Al-Izki *et al.*, 2011). Thus, it represents a useful model in which to study the mechanisms underlying the progression of the neurological deficits in advanced stages of the disease, allowing the development of new therapeutic approaches for the treatment of patients with progressive MS (Al-Izki *et al.*, 2012).

MOG also induces EAE in the female dark agouti (DA) rat, and yields a relatively predictable and reliable disease course that, similarly with Biozzi AB/H mice, more fully represents the pathology and clinical course of MS than other EAE models available (Storch *et al.*, 1998). DA rats are particularly susceptible to the development of EAE, and a single injection of MOG (50-100μg) emulsified in incomplete Freund's adjuvant (IFA) is sufficient to elicit the autoimmune response in the great majority of immunised animals (incidence: ~95%) (Storch *et al.*, 1998), causing an initial relapsing-remitting disease course followed by a chronic progression of the neurological deficits (Mannie *et al.*, 2009). In contrast, C57BL/6 and SJL mice develop only a progressive or a relapsing-remitting disease course respectively, and they are less prone to develop EAE compared with DA rats. Indeed, in order to induce EAE in these mice, the immunogen has to be emulsified in adjuvant supplemented with inactivated *Mycobacteria tuberculosis* (complete Freund's adjuvant; CFA), in order to enhance an adequate inflammatory reaction. Furthermore, higher doses of antigen are required to induce EAE in C57BL/6 and SJL mice, as the emulsion containing MOG has to be injected twice through two immunisations interspersed by 1-week (50-100μg for each administration) (Stromnes and Goverman, 2006a; Sadeghian *et al.*, 2016). Moreover, and in contrast with DA rats (Mannie *et al.*, 2009), in these mice the immunisations are usually followed by the injection of pertussis toxin to increase blood-brain barrier (BBB) permeability and this facilitates the immune cells and mediators to enter the CNS parenchyma (Stromnes and Goverman, 2006a; Sadeghian *et al.*, 2016).

In DA rats, it has been shown that a greater percentage of MOG-immunised animals can develop inflammatory-demyelinating lesions in the optic nerves (~36%) and in the cerebellum (~12%), in conjunction with the typical lesions in the spinal cord (Storch *et*

al., 1998). By contrast, lesions in the optic nerves and cerebellum are rarely observed in classically MOG-immunised mice (Stromnes and Goverman, 2006a), and only occur in certain strain/antigen combinations (Muller *et al.*, 2000; Bettelli *et al.*, 2003; Stromnes and Goverman, 2006a) and on a background of IFNγ deficiency (Wensky *et al.*, 2005; Stromnes and Goverman, 2006a).

Thus, MOG-immunised DA rats can represent one of the better active EAE models in which to study the different factors related to MS.

1.2.2.0 Passive EAE

Passive EAE is induced via an adoptive transfer of encephalitogenic $CD4^+$ T-cells isolated from an actively immunised syngenic animal and injected in the proposed recipient (Stromnes and Goverman, 2006b). Passive immunization of rats with encephalitogenic T-cells reactive against MOG, yields an ascending paresis/paralysis of tail and hind limbs similar to active EAE, but in the absence of major structural damage of the CNS such as demyelination and degeneration, and in a relatively mild inflammatory environment (Linington *et al.*, 1993). Indeed, one advantage of passive EAE relative to active EAE is the comparative immunological and pathological simplicity, which allows studying the effects of inflammation in relative isolation. The injection of encephalitogenic T-cells in naïve syngeneic rats induces an extensive T-cell mediated inflammatory reaction in the spinal cord (Linington *et al.*, 1993), but a milder severity of the neurological deficits compared with actively induced EAE. The failure to induce gross neurological deficits has been attributed to the fact that passive EAE leads to a limited infiltration of activated macrophages in the spinal cord, which in this model are largely confined in the perivascular areas (Linington *et al.*, 1993) and not widely diffused in the CNS parenchyma as observed in active EAE (Davies *et al.*, 2013). Another aspect, can be that the passive transfer of encephalitogenic T-cells does not result in spinal cord demyelination (Linington *et al.*, 1993), but demyelination only occurs when the T-cells are co-transferred with MOG-specific monoclonal antibodies (mAb) (Linington *et al.*, 1993). Indeed, the co-transfer of MOG-specific mAb synergizes with the encephalitogenic T-cells, causing increased macrophage recruitment in the spinal cord, and white matter demyelination (Linington *et al.*, 1993). Therefore, it has been suggested that the T-cells reactive against MOG are sufficient in yielding an

encephalitogenic (inflammatory) response in the CNS, but an autoantibody response against myelin is necessary to initiate demyelination (Linington *et al.*, 1993). Intriguingly, the mechanisms underlying the neurological deficits, caused by the encephalitogenic T-cells alone, in the absence of demyelination and pronounced macrophage infiltration, remain unclear.

Another important advantage of passive EAE is the possibility to label the T-cells before the transfer, so that their location and activity can be monitored in the recipient (Stromnes and Goverman, 2006b).

1.3.0.0 Pathology of MS lesions

The pathology of MS is characterized by multifocal, perivascular inflammation and demyelination. Demyelination was traditionally considered a white matter phenomenon, but now it is known that it also affects the grey matter (Lassmann, 2013). Different molecular mechanisms can take place in different regions of the same MS lesion (Lassmann, 2013), making it difficult to understand the sequence of events that initiate the tissue damage. Characteristics of white matter MS lesions include demyelination, oligodendrocytes loss, inflammation, the formation of an astrocytic scar (Lassmann, 2013) and the preferential degeneration of small caliber axons (Evangelou *et al.*, 2001). Inflammation is present at all stages of the disease, although the abundance of the inflammatory infiltrate and its composition can vary with the stage of disease (Lassmann, 2013) and it can differ between different types of MS lesions (Lucchinetti *et al.*, 2000). It has been observed that the inflammatory component is more pronounced in patients with RRMS compared with patients in the progressive stage (Frischer *et al.*, 2009; Lassmann, 2013). In early stages of MS new lesions in the white matter are characterized by gadolinium-enhancement at MRI examination, indicating damage of the BBB and inflammation as driving forces (Grossman *et al.*, 1988; Miller *et al.*, 1988). In contrast, new lesions, and particularly gadolinium-enhancing lesions, become rare when patients have entered the progressive phase (Grossman *et al.*, 1988; Miller *et al.*, 1988; Lassmann, 2013). The autoimmune and inflammatory response in MS appears intricate, with many cell types of the innate and adaptive immune system taking part in the formation and progression of the lesions. T-helper lymphocytes (Th1 and Th17)

have been shown to be implicated in the pathogenesis of MS and EAE, while cytotoxic T-cells ($CD8^+$), B-cells/plasma cells and macrophages have been recognized to play a major role in the development of demyelinating lesions and the progression of neurological deficits (Magliozzi *et al.*, 2007; McFarland and Martin, 2007; Ajami *et al.*, 2011; Hemmer *et al.*, 2015). Relatively little is known about the role of granulocytes in MS, such as neutrophils, which comprise the greatest percentage of leukocytes circulating in the blood stream. Recent studies in MS (Naegele *et al.*, 2012; Rumble *et al.*, 2015) and EAE (Rumble *et al.*, 2015) raised the possibility that neutrophils may play an important role in causing damage of the CNS. Naegele and colleagues (2012) reported that neutrophils in patients with MS are more numerous and they often exist in an activate state consisting of enhanced degranulation and activation of the oxidative burst. Rumble and colleagues (2015) also reported an increased number of neutrophils in the blood of patients with MS, and such neutrophils were characterized by elevated expression of CXC chemokines (such as CXCL1 and CXCL5) that correlated with the extension of MS lesions and the severity of clinical disabilities (Rumble *et al.*, 2015). Mice with EAE deficient for the granulocyte colony stimulating factor (G-CSF) receptor and treated with a CXCL1 antagonist showed a reduced number of activated neutrophils in the blood and less severe neurological deficits compared with controls, suggesting that also neutrophils can play an important role in the pathogenesis of EAE (Rumble *et al.*, 2015).

Patients with RRMS are characterized by a large number of active demyelinating lesions in the CNS, which present elevated lymphocyte and macrophage infiltration and profound microglial activation (Brück *et al.*, 1995; Frischer *et al.*, 2009). Furthermore, active lesions localize in perivenular regions characterized by gadolinium enhancement upon MRI examination (Grossman *et al.*, 1988; Miller *et al.*, 1988; Noseworthy *et al.*, 2000). Active lesions can in turn be divided in early and late active lesions (Lassmann, 2013). The distinction between early and late active lesions is based on the amount of phagocytic macrophages present in the lesion (greater in early active lesions), and the type of myelin-degradation products contained in their lysosomes (Brück *et al.*, 1995; Lassmann, 2013). Phagocytic degradation of minor, small myelin proteins (e.g. MOG, and MAG) occurs rapidly, within 1 to 3 days, and the presence in macrophages of degradation products derived from these proteins indicates early active demyelination

(Brück *et al.*, 1995; Popescu *et al.*, 2013). By contrast, larger and more abundant myelin proteins such as MBP and PLP are digested more slowly and may persist in macrophages for up to 10 days (Brück *et al.*, 1995; Popescu *et al.*, 2013). Thus, the presence within macrophages of degradation products derived from the phagocytosis of major myelin proteins (PLP and MBP) in the absence of minor degradation products (MOG and MAG), demarcates late active lesions (Brück *et al.*, 1995; Popescu *et al.*, 2013). In the area surrounding active lesions there is an initial or pre-phagocytic zone (Barnett and Prineas, 2004; Marik *et al.*, 2007). Here, myelin is largely intact but there are apoptotic oligodendrocytes, microglial activation (Barnett and Prineas, 2004; Henderson *et al.*, 2009) and cells positive for oxidized DNA and lipids (Haider *et al.*, 2011).

Although sometimes the white matter of patients with MS can appear normal at a superficial morphological analysis or at the MRI examination, it can instead be affected by biochemical and histological alterations. Indeed, while no evidence of demyelination or leukocyte infiltration is observed in the normal appearing white matter (NAWM) of patients with MS (De Groot *et al.*, 2001), other peculiar alterations can occur. The NAWM often shows activated clusters of microglial cells expressing MHC class-II molecules (De Groot *et al.*, 2001). Furthermore, the microglial clusters are usually associated with stressed olidodendrocytes (van Noort *et al.*, 2010) and elevated levels of inflammatory cytokines (van Horssen *et al.*, 2012). These lesions are named pre-active lesions and can occur throughout the CNS of patients with MS, but often develop in the proximity of active lesions (van Horssen *et al.*, 2012). As not all the pre-active lesions progress in demyelinating active lesions, it is possible that the pre-active lesion may be the earliest, and potentially reversible, stage of the development of an MS plaque.

Patients in the chronic or progressive stage of MS are characterized by a higher number of inactive lesions in the CNS (Lassmann, 2013). In these lesions the inactive core show extensive demyelination and axonal degeneration, and it is surrounded by a narrow rim of activated microglia and macrophages, few of which contain products of myelin degradation, suggesting a slow expansion of the lesion (Prineas *et al.*, 2001; Lassmann, 2013). Furthermore, inactive lesions show both moderate perivascular cuffs and signs of acute inflammation (Prineas *et al.*, 2001). Interestingly, inactive lesions are

particularly frequent in the cortex of patients with progressive MS (Kutzelnigg *et al.,* 2005). Here, lymphocytic inflammation is present in the meningeal areas proximal to the demyelinated plaques, while perivascular, parenchymal infiltration of lymphocytes is rare or absent (Magliozzi *et al.*, 2010; Lassmann, 2013). A minor demyelinating activity is associated with the activated microglia at the border between the cortical plaques and the NAWM (Magliozzi *et al.*, 2010; Lassmann, 2013). This observation raises the possibility that the cortical demyelination at late stages of the disease is induced by soluble factors produced by the meningeal infiltrates that activate microglial cells, which in turn can directly or indirectly cause demyelination (Magliozzi *et al.*, 2007; Choi *et al.*, 2012; Lassmann, 2013).

Interestingly, in the progressive phase of MS, inflammatory cells are frequently seen around vessels with intact BBB (Hochmeister *et al.*, 2006; Lassmann, 2013), suggesting that at this stage of disease the inflammatory response could be "trapped" within the CNS (Lassmann, 2013). Therefore, it is possible that the “trapped” inflammation and other cytodegenerative processes, rather than further inflammatory cells entering from the periphery, can drive the expansion of lesions in the progressive stage of MS.

Remyelination can occur throughout the disease (Lassmann, 2013). However, neuropathological studies have revealed that remyelination is more often observed at late stages of MS, although it is usually incomplete (Lassmann, 2013). Remyelinated lesions usually show weak staining for myelin upon histological examination, and they are often referred to as “shadow plaques” (Lassmann, 2013).

1.3.1.0 Heterogeneity of MS lesions

In addition to the previously described classification in early and late active lesions, early active MS lesions show additional features which can permit them to be further sub-classified. Lucchinetti and colleagues (2000) recognised four different subtypes (pattern I-IV) of active demyelinating lesions based on their histological characteristics, which are also suggestive of different pathogenic mechanisms (Lucchinetti *et al.*, 2000). Indeed, while pattern I and II suggest an inflammatory-autoimmune aetiology, pattern III and IV are indicative of oligodendrocyte dystrophic causes.

Pattern I and II share some similarities with inflammatory-demyelinating lesions observed in animals with active EAE (Lucchinetti *et al.*, 2000). In particular, in these subtypes of lesion, demyelination is centered on blood vessels and it is associated with prominent perivascular lymphocyte infiltration and partial remyelination (Lucchinetti *et al.*, 2000). In addition, Pattern-II lesions present specific deposition of immunoglobulin and complement (Lucchinetti *et al.*, 2000). Pattern-III lesions are also characterized by perivascular inflammation, but in this pattern demyelination is not centered on blood vessels, and a rim of myelinated axons is often preserved in the area surrounding the vessels (Lucchinetti *et al.*, 2000). Furthermore, pattern-III lesions are associated with apoptosis of oligodendrocytes, selective loss of myelin-associated glycoprotein (MAG, a protein located in the innermost lamellae of the myelin sheaths) and increased expression of hypoxia inducible factor 1α (HIF1α) (Lucchinetti *et al.*, 2000; Aboul-Enein *et al.*, 2003). Pattern-III lesions share these characteristics with demyelinating lesions due to ischaemic stroke; raising the possibility that hypoxia-like events could contribute to its pathogenesis (Aboul-Enein *et al.*, 2003). Pattern-IV lesions also show abundant inflammation, dominated by T-cells and macrophages, but this lesion subtype is characterized by apoptosis of oligodendrocytes specifically in a small rim of the periplaque, adjacent to the active lesion (Lucchinetti *et al.*, 2000). Intriguingly, in pattern-IV lesions oligodendrocyte death was revealed by the presence of nuclear DNA fragmentation, but these cells did not show the classical morphological features of apoptotic oligodendrocytes (Lucchinetti *et al.*, 2000).

One school of thought considers that MS lesions belong to the same subtype in a given patient (Lucchinetti *et al.*, 2000; Noseworthy *et al.*, 2000). However, other investigators report that different subtypes of lesion can co-exist in the same patient. In particular, the presence of two different types of lesion has been reported in patients with MS within the same individual, with some lesions indicating oligodendrocyte dystrophy and others suggesting an inflammatory/autoimmune aetiology (Barnett and Prineas, 2004). This finding suggests that a stage-dependent evolution of the lesion may occur. Possibly a first stage is represented by a primary apoptosis of oligodendrocyte that can subsequently elicit a T-cell mediated inflammatory response (second stage) (Barnett and Prineas, 2004).

Interestingly, recent findings revealed that there are some mechanisms of tissue damage which are common in all MS lesions at all stages of the disease, such as the oxidative/nitrative damage and mitochondrial dysfunction (Stadelmann *et al.*, 2005; Dutta *et al.*, 2006; Marik *et al.*, 2007; Trapp and Stys, 2009; Haider *et al.*, 2011; Lassmann and Van Horssen, 2011; Fischer *et al.*, 2012). Evidence in active EAE has shown that both oxidative and nitrative stress can directly harm axonal mitochondrial function (Nikic *et al.*, 2011), raising the possibility that the mitochondrial impairment occurring in MS lesions (Mahad *et al.*, 2008; Witte *et al.*, 2014) can be due to similar mechanisms. Impaired mitochondrial function can lead to an energy crisis which can explain many pathological features of MS, such as demyelination, oligodendrocyte apoptosis, axonal degeneration and functional alterations of astrocytes and oligodendrocytes progenitor cells (Lassmann and Van Horssen, 2011).

1.3.2.0 Energy insufficiency and mitochondrial dysfunction

Increasing evidence suggests that an energy insufficiency may represent a key event in MS (Aboul-Enein and Lassmann, 2005; Mahad *et al.*, 2008). Indeed, an insufficient energy supply of the CNS is hypothesized to be one of the main mechanisms involved in axonal degeneration (Trapp and Stys, 2009). Large amounts of ATP are produced via oxidative mitochondrial respiration; it represents the energy currency of the cells and it is required for a number of physiological processes, including signal transduction, ionic balance and protein synthesis and transport. It is not surprising that ATP depletion can have devastating consequences on cellular function and survival. Essentially, any mechanism that impairs ATP production during inflammatory demyelination is likely to result in energy insufficiency. In the CNS, ATP is of pivotal importance for the maintenance of the ionic membrane gradient through the activity of the Na^+/K^+ ATPase, which uses more than 50% of total CNS energy (Ames 3rd, 2000). ATP deficiency can severely affect the function of the Na^+/K^+ ATPase, potentially leading to remarkable alterations of vulnerable, polarised cell types such as oligodendrocytes (Kettenmann *et al.*, 1983), astrocytes (Bolton *et al.*, 2006) and neurons (Trapp and Stys, 2009). Impaired activity of the Na^+/K^+ ATPase can limit the extrusion of sodium cations from the cell. It has been shown that sodium cations can quickly accumulate in demyelinated axons due to the redistribution of sodium channels, which are normally confined in the

nodes of Ranvier (Ritchie and Rogart, 1977; Waxman *et al.*, 1977), along the axolemma (Bostock and Sears, 1978; Foster *et al.*, 1980; Waxman, 2006). Furthermore, demyelinated axons can be intrinsically more excitable than myelinated axons due to increased spontaneous depolarization of the membrane (Smith and McDonald, 1980; Felts *et al.*, 1995; Hamada and Kole, 2015), which leads to a greater influx of sodium cations. In demyelinated axons, the conduction of the electric impulse has been suggested to be also energetically more expensive due to the need of restoring the trans-axolemmal Na^+/K^+ gradient on a larger non-myelinated surface (Trapp and Stys, 2009). Therefore, in demyelinated axons, both the increased axonal excitability and elevated energy cost to sustain the electrical conduction may cause mitochondrial stress.

Elevated concentration of sodium cations into demyelinated axons, caused by the increased excitability and the reduced extrusion of these ions through the Na^+/K^+ ATPase, can reverse the operation of the sodium-calcium exchanger, increasing the influx of calcium cations (Ca^{2+}) (Stys *et al.*, 1992; Stys, 1998; Bechtold and Smith, 2005; Waxman, 2006; Smith, 2007). Increased cellular concentration of Ca^{2+} can trigger cell death via either necrotic or apoptotic pathways (Orrenius *et al.*, 2003), and it has been suggested as a mechanism of axonal degeneration in MS (Smith, 2007; Trapp and Stys, 2009). Indeed, evidence shows signs of Ca^{2+}-mediated protease activity in demyelinated axons of patients with MS, such as fragmented neurofilaments, depolymerised microtubules and organelle disruption (Dutta *et al.*, 2006). Interestingly, studies demonstrated that sodium and calcium channel blockers can protect from axonal degeneration (Kapoor *et al.*, 2003).

Mitochondrial dysfunction is increasingly recognised as a source of energy insufficiency and axonal damage in both acute and chronic MS lesions (Mahad *et al.*, 2008; Witte *et al.*, 2014). Indeed, defects in the mitochondrial respiratory chain have been described in MS (see following). In particular, impaired activity of complex-IV has been found in pattern-III active MS lesions, and dysfunctional complex-I has been observed in chronic MS lesions (Mahad *et al.*, 2008). In the motor cortex of patients with MS an impaired activity of both mitochondrial complexes-I and III has been detected, in combination with reduced expression of nuclear mitochondrial genes (Dutta *et al.*, 2006). Here, the reduced activity of these complexes has been associated with decreased inhibitory

input from γ-aminobutyric acid (GABA) (Dutta *et al.*, 2006). It is possible that GABA signal is implicated in the transcriptional regulation of mitochondrial genes in neuronal nuclei (Dutta *et al.*, 2006). Furthermore, decreased inhibitory innervation of cortical neurons may exacerbate the energy deficit by increasing the firing of downstream demyelinated axons, which have higher than normal energy demands and an impaired ability to produce ATP (Dutta *et al.*, 2006).

Increasing evidence in MS and animal models has partially revealed the sequence of events that can impair the activity of axonal mitochondria during neuroinflammation. A recent study in active EAE, showed that depolarised mitochondria, a sign of mitochondrial dysfunction, can appear in non-demyelinated axons even before the onset of neurological deficits (Sadeghian *et al.*, 2016). In demyelinated axons, mitochondria increase in number, size and speed of movement and tend to accumulate in demyelinated regions (Nikic *et al.*, 2011; Ohno *et al.*, 2014). This has been suggested as an axonal mitochondrial response to demyelination (Ohno *et al.*, 2014; Mahad *et al.*, 2015). It is believed that the increased number of mitochondria in demyelinated areas of the axon, provides energetic support to the energetically costly conduction in this region (Ohno *et al.*, 2014; Mahad *et al.*, 2015). However, as the disease progresses, inflammatory mediators, such as free radicals, damage the mitochondria causing mitochondrial DNA deletion, depolarisation of the mitochondrial membrane, and dysfunction of the mitochondrial respiratory chain (Dahlgren and Karlsson, 1999; Nikic *et al.*, 2011; Guo *et al.*, 2013; Mahad *et al.*, 2015). Over time the mitochondrial dysfunction may be amplified via both the clonal expansion of mitochondria with DNA deletions and decreased levels of nuclear-derived mitochondrial transcripts (Dutta *et al.*, 2006; Mahad *et al.*, 2015); exacerbating the energy deficit in a vicious cycle that can lead to axonal transection and degeneration (Trapp and Stys, 2009; Witte *et al.*, 2014).

A number of factors can compromise the normal activity of mitochondria (Mahad *et al.*, 2008; Trapp and Stys, 2009) and some of these are present during the early phases of an inflammatory response, including nitric oxide (NO) and reactive oxygen and nitrogen species (ROS/RNS) (Brown and Cooper, 1994; Cleeter *et al.*, 1994; Bolaños *et al.*, 1997; Clementi *et al.*, 1998; Haider *et al.*, 2011; Nikic *et al.*, 2011; Fischer *et al.*, 2012).

Recently, specific types of ceramides have also been found enriched in the CSF of patients with MS, and these are able to impair the mitochondrial respiration of cultured neurons via unknown mechanisms (Vidaurre *et al.*, 2014).

Interestingly, Nikic and colleagues (2011) have shown that, especially at early stage of injury, axonal degeneration can be rescued by neutralizing the free radical-mediated mitochondrial damage (Nikic *et al.*, 2011). This suggests the possibility that the mitochondrial dysfunction and energy deficit may be reversible, and therapies targeting these mechanisms could potentially protect the CNS from axonal degeneration and loss of neurological function.

1.3.3.0 Free radical mediators of tissue damage

1.3.3.1 Nitric oxide and nitrative damage

The inflammatory response is characterized by release of a number of inflammatory mediators that can cause tissue damage. Some of these mediators include free radicals, which have been found to play a direct effect in damaging the CNS during MS (Stadelmann *et al.*, 2005; Marik *et al.*, 2007; Haider *et al.*, 2011; Lassmann and Van Horssen, 2011; Nikic *et al.*, 2011; Fischer *et al.*, 2012). An important role is played by nitric oxide (NO) and other NO-derived free radicals (reactive nitrogen species; RNS) (Smith and Lassmann, 2002; Moncada and Bolanos, 2006). NO is synthesized by an enzymatic reaction mediated by nitric oxide synthases (NOS) (Bredt, 1999). NOS catalyzes the reaction of arginine with molecular oxygen to produce citrullin and NO (Bredt, 1999). Three forms of NOS have been identified, named: endothelial-NOS (eNOS), neuronal-NOS (nNOS) and inducible-NOS (iNOS) (Alderton *et al.*, 2001). eNOS and nNOS are constitutionally expressed in the CNS, as the names suggest, by endothelial and neuronal cells respectively, and contribute to the basal, low concentration of NO in the tissue (Alderton *et al.*, 2001). In contrast, the expression of iNOS is transcriptionally regulated and it is responsible for the synthesis of high levels of NO within sites of inflammation (Koprowski *et al.*, 1993). Interestingly, elevated concentrations of iNOS have been found within active MS lesions, expressed mainly by infiltrated macrophages and activated microglia (Stadelmann *et al.*, 2005; Marik *et al.*, 2007). Furthermore, increased levels of nitrate (derived from NO) have been detected

in the CSF of patients with MS (Giovannoni, 1998), and they seem to correlate with the severity of disease (Rejdak *et al.*, 2004). However, in chronic lesions, as the inflammation becomes less prominent, the expression of iNOS also diminishes (Oleszak *et al.*, 1998; Smith and Lassmann, 2002).

NO is a reactive molecule that gives rise to several other RNS, including: nitroxyl ion (NO^-), nitrous acid (HNO_2), nitrogen dioxide (NO_2), peroxynitrite ($ONOO^-$) and peroxynitrous acid (ONOOH) (Smith and Lassmann, 2002). The forms that NO takes at the site of inflammation are not known (Smith and Lassmann, 2002), so in this thesis we will refer to them by simply using the term “NO”. NO is a potent signalling molecule which plays several physiological roles, but at higher concentrations it can mediate tissue damage (see following). One important physiological function of NO is its potent, endogenous vasodilator effect (Kobari *et al.*, 1993). During MS the vasodilator effect of NO may exacerbate the inflammatory response in the CNS. Indeed, vessel vasodilation decreases the velocity of blood flow, and this may give more time for inflammatory cells to adhere at the endothelial surface and migrate into the CNS parenchyma (Smith and Lassmann, 2002). Furthermore, it has been shown that NO can increase the BBB permeability (Mayhan, 2000; Martinelli *et al.*, 2009) contributing to the extravasation of inflammatory cells such as lymphocytes (Martinelli *et al.*, 2009) and mediators into the CNS. However, anti-inflammatory effects of NO such as the inhibition of antigen presentation and T-cell proliferation have also been reported (Albina and Henry, 1991; Sicher *et al.*, 1994).

NO can have direct toxic effects via a variety of molecular mechanisms that potentially affect all cell types. NO can damage cells by reacting with proteins, nucleic acids and lipids. Nitration is a common NO-mediated protein modification, and nitrotyrosine levels have been found increased in inflammatory lesions of patients with MS, as well as in animals with EAE (Liu *et al.*, 2001; Smith and Lassmann, 2002; Schuh *et al.*, 2014). An interesting protein modification mediated by NO is the S-nitrosation of cysteins, which can give rise to new self-antigens and antibodies against these NO-modified epitopes have been found increased in patients with MS (Boullerne *et al.*, 1995). In addition, NO can damage nuclear and mitochondrial DNA both directly, via altering the chemical structure of DNA through a peroxynitrite-mediated reaction, and indirectly by inhibiting various DNA-repair processes (Zhang *et al.*, 1994; Graziewicz *et al.*, 1996). Studies *in-vitro* revealed that oligodendrocytes are more susceptible than astrocytes and microglia

to peroxynitrite-toxicity, although they experience a similar degree of DNA damage (Mitrovic *et al.*, 1994, 1995). A possible explanation can be that peroxynitrite induces not only strand breakdown of DNA (Zhang *et al.*, 1994; Witte *et al.*, 2014), but also triggers lipid peroxidation, which can alter the fluidity and permeability of cell membranes (van der Veen and Roberts, 1999). This detrimental effect may be more severe in oligodendrocytes given the larger surface of their plasma membrane.

Interestingly, a study revealed that NO at elevated concentration can reversibly block axonal conduction of both normal and demyelinated axons (Redford *et al.*, 1997). The mechanisms through which NO impairs axonal conduction are not clear, but it has been suggested that the conduction block may be caused by a NO-mediated structural modification of sodium channels (Renganathan *et al.*, 2002; Smith and Lassmann, 2002). In addition, an NO-mediated damage of mitochondrial function may also play a relevant role. NO affects mitochondria in three principal ways: reversible inhibition of respiration; irreversible inactivation of mitochondrial enzymes; and induction of the mitochondrial permeability transition (Murphy, 1999) (see also paragraph 1.3.3.2). NO can compete with oxygen for binding to complex-IV blocking oxidative phosphorylation (Cooper *et al.*, 2003). The NO-mediated impairment of mitochondrial complex-IV in MS lesions has been previously defined as “virtual hypoxia” (Trapp and Stys, 2009), because the resulting reduction in cellular ATP synthesis can be similar to what would be observed in conditions of decreased oxygen supply (*true hypoxia*). Furthermore, NO may initiate a destructive cascade of peroxynitrite-mediated mitochondrial damages (Murphy, 1999). Peroxynitrite is generated by the reaction of NO with superoxide (O_2^-, a reactive oxygen species) (Pacher *et al.*, 2007), and its detrimental effects on mitochondria are described in the next paragraph.

1.3.3.2 Oxidative damage

Inflammation can also generate reactive oxygen species (ROS) (Dahlgren and Karlsson, 1999). Superoxide (O_2^-) is a free radical produced by transfer of one electron to molecular oxygen, and it is the precursor of many other forms of ROS (Beckman and Koppenol, 1996). Dismutation of superoxide generates hydrogen peroxide (H_2O_2), which can be fully reduced in water, or partially reduced in the hydroxyl radical (OH^-). The reaction between superoxide and NO can give rise to peroxynitrite ($ONOO^-$), which is highly reactive and toxic for cells (Beckman and Koppenol, 1996; Murphy, 1999;

Pacher *et al.*, 2007). Inflammatory cells of the innate response can generate superoxide through an enzymatic reaction which occurs on the outer plasma-membrane and that involves NADPH oxidase and molecular oxygen, in a process known as the respiratory (or oxidative) burst (Dahlgren and Karlsson, 1999).

In MS, a large amount of ROS is produced by reactive microglia and macrophages. Indeed, increased expression of the active form of NADPH oxidase has been detected in these cells within active MS lesions (Fischer *et al.*, 2012). ROS can be generated also in mitochondria, particularly when these are dysfunctional (Murphy, 2009), a condition that has been well characterized in MS (Mahad *et al.*, 2008). Some components of the mitochondrial electron transport chain can leak electrons and such electrons can be directly transferred to molecular oxygen forming superoxide (Murphy, 2009). The rate of superoxide production is dependent from the amount of molecular oxygen available (Murphy, 2009). Interestingly, it has been shown that hypoxia, as well as hyperoxia, can exacerbate oxidative stress through mechanisms that are not entirely clear (Xu *et al.*, 2004; Strapazzon *et al.*, 2016) (see also Chapter 5; paragraph 5.3.0.0).

ROS can mediate a variety of mechanisms toxic for the cells, including DNA (Cooke *et al.*, 2003) and lipid (Ayala *et al.*, 2014) oxidation. Notably, these markers of oxidative damage have been found to be increased within active MS lesions (Haider *et al.*, 2011; Fischer *et al.*, 2012). As mentioned before, ROS can also severely damage mitochondria (Nikic *et al.*, 2011; Witte *et al.*, 2014). Here, ROS can either damage mitochondrial constituents directly, oxidizing mitochondrial DNA and lipids, or form peroxynitrite by reacting with NO (Smith, 2011). Peroxynitrite can permanently nitrate tyrosine residues of mitochondrial proteins, affecting their functionality (Smith, 2011). In addition, peroxynitrite can irreversibly damage mitochondria by reacting with iron-sulphur domains contained in respiratory chain complexes I, II and III, and in Kreb's cycle enzymes (Hausladen and Fridovich, 1994; Radi *et al.*, 1994; Rubbo *et al.*, 1994; Lizasoain *et al.*, 1996; Murphy, 1999). Peroxynitrite can also induce mitochondrial calcium efflux by oxidizing the thiols of mitochondrial membrane proteins that can finally lead to the mitochondrial permeability transition (Packer and Murphy, 1994, 1995; Scarlett *et al.*, 1996; Murphy, 1999). The mitochondrial permeability transition is induced by oxidative stress in conjunction with elevated calcium, and consists in the

formation of a 2–3nm diameter protein pore in the mitochondrial inner membrane with subsequent depolarization, swelling of the mitochondrion, and release of solutes from the matrix (Murphy, 1999; Biasutto *et al.*, 2016). Depolarization of mitochondria and induction of the permeability transition cause the release in the cytosol of elevated amount of Ca^{2+} (Gunter *et al.*, 1994; Richter *et al.*, 1994). Indeed, mitochondria are particularly enriched in Ca^{2+} because they directly modulate cellular Ca^{2+} concentrations acting as a sink for excessive cytosolic-Ca^{2+} (Gunter *et al.*, 1994; Murphy, 1999). Increased cytosolic Ca^{2+} concentrations, caused by mitochondrial damage, can cause cell death via both apoptotic and necrotic pathways (Orrenius *et al.*, 2003). Moreover, damaged mitochondria can in turn produce more ROS, which can further damage the mitochondria and the surrounding tissue, setting up a vicious cycle (Smith, 2011).

In addition, as the generation of ROS and RNS involves the use of molecular oxygen as substrate, their production in sites of inflammation can deprive the surrounding tissue of oxygen, causing hypoxia. Therefore, in MS, the increased expression of enzymes involved in the synthesis of both ROS and NO/RNS, in combination with evidence of dysfunctional mitochondria, suggest a high risk of an energy deficit within MS lesions (Trapp and Stys, 2009).

1.3.4.0 Inflammatory mediators of tissue damage: TNFα-mediated necroptosis

The level of pro-inflammatory cytokines such as TNFα has been shown to be increased in active MS lesions as well as in the serum and CSF of patients with MS (Sharief and Hentges, 1991). TNFα and TNFα-related apoptosis-inducing ligands (TRAILs) activate caspase-8 and -10, pro-apoptotic enzymes that lead to the assembly of a multi-protein death-induced signal complex (DISC), culminating in the endoproteolysis of several cellular proteins and the formation of apoptotic bodies which are then cleared from the tissue by scavenger cells (Dhib-Jalbut and Kalvakolanu, 2015). However, under conditions of failed caspase activation, possibly due to the inhibition caused by FLICE-inhibitor protein (cFLIP) and/or oxidized caspase active sites (Dhib-Jalbut and Kalvakolanu, 2015) it has been shown that TNFα can lead to cell death also via a finely

regulated necrotic pathway, which has been defined as necroptosis (Pasparakis and Vandenabeele, 2015; Newton and Manning, 2016). Although it has been shown that necroptosis can be activated by a number of pro-inflammatory stimuli including IFNs, Toll-like receptors, TRAILs and Fas-ligands the molecular pathway triggered by TNFα is the better characterized one and it will be discussed here (Pasparakis and Vandenabeele, 2015; Newton and Manning, 2016; Su *et al.*, 2016). In MS, it has been shown that necroptosis occurs in oligodendrocytes (Selmaj and Raine, 1988; Jurewicz *et al.*, 2005; Dhib-Jalbut, 2007) and neurons (Dhib-Jalbut and Kalvakolanu, 2015) within active lesions and it is largely triggered by the activation of the TNFα receptor-1 (TNFR1) (Sharief and Hentges, 1991; Dhib-Jalbut and Kalvakolanu, 2015; Ofengeim *et al.*, 2015). Upon activation of TNFR1 and under apoptosis deficient conditions (inactive caspase-8), the kinase RIPK1 interacts with RIPK3 to induce its phosphorylation and to form a RIPK1/RIPK3-containing complex, known as complex IIb or necrosome, a critical regulator of necroptosis (Dhib-Jalbut and Kalvakolanu, 2015; Ofengeim *et al.*, 2015). The necrosome phosphorylates mixed-lineage kinase like (MLKL), which can then form trimers that are able to penetrate cell membranes creating pores in the membrane of the cells and organelles (Dhib-Jalbut and Kalvakolanu, 2015). These pores permeabilize cellular contents causing the release of solutes (such as Ca^{2+}) from organelles and the consequent osmotic swelling and necrosis of the cell (Dhib-Jalbut and Kalvakolanu, 2015). In addition, RIPK3 can activate, by phosphorylation, a number of enzymes such as glycogen phosphorylase, glutamate-ammonia ligase, and glutamate dehydrogenase, resulting in high levels of ROS production that in turn can further cause mitochondrial damage and a necrotic demise of cells (Dhib-Jalbut and Kalvakolanu, 2015). Recently, Ofengeim and colleagues (2015) showed that the inhibition of RIPK1 protects from oligodendrocyte death both *in-vivo* (in mice with active EAE) and *in-vitro*, suggesting that targeting RIPK1 and the necroptosis pathway may represent a new therapeutic strategy for MS (Ofengeim *et al.*, 2015).

1.4.0.0 The integrated stress response

Inflammation, ROS/RNS, endoplasmic reticulum (ER) stress, energy deficiency and hypoxia are all factors that can cause severe cellular stress (Donnelly *et al.*, 2013). In

the CNS of patients with MS, all these factors can potentially occur and stress susceptible cells. Cells try to counteract the stress insult by activating a number of molecular mechanisms that form the so-called integrated stress response (Way *et al.*, 2016). The hallmark of integrated stress response is the phosphorylation of the eukaryotic initiation factor 2α (eIF2α) (Lin and Popko, 2009), a key player in protein synthesis. The phosphorylation of eIF2α (p-eIF2α) leads to a reduction in the rate of general protein synthesis, but selectively promotes the transcriptional expression and translation of cytoprotective and cell-repairing genes (Lin and Popko, 2009; Donnelly *et al.*, 2013). Therefore, the integrated stress response protects cells by reducing normal physiological activities (such as protein synthesis), focusing the cellular efforts on mechanisms that increase cellular endurance. However, if the stress persists, a prolonged inhibition of the protein synthesis is not sustainable, pro-apoptotic genes are expressed and the cell dies (Tabas and Ron, 2011).

The activation of the integrated stress response has been reported in several neurodegenerative disorders, including Alzheimer disease, Parkinson disease, cerebral ischemia and MS (Roussel *et al.*, 2013). Histological analyses of CNS samples of patients with MS, revealed increased levels of p-eIF2α predominantly in activated microglia, macrophages and astrocytes within the lesions (Allen *et al.*, 2001; Kutzelnigg *et al.,* 2005; Cunnea *et al.*, 2011; McMahon *et al.*, 2012; Ní Fhlathartaigh *et al.*, 2013), and such increased p-eIF2α expression has been also associated with the expression of hypoxia-related markers (McMahon *et al.*, 2012). Elevated levels of p-eIF2α have been detected also in mice with active EAE, and especially in neurons and oligodendrocytes (Chakrabarty *et al.*, 2004). Notably, oligodendrocytes appeared to be particularly susceptible to the activation of the integrated stress response during active EAE (Chakrabarty *et al.*, 2004; Lin and Popko, 2009). Indeed, while oligodendrocytes are mainly negative for p-eIF2α upon histological examinations in healthy mice, p-eIF2α expression increases significantly during active EAE (Chakrabarty *et al.*, 2004; Lin and Popko, 2009). It is possible that the MS studies did not detect oligodendrocytes positive for p-eIF2α (Allen *et al.*, 2001; Kutzelnigg *et al.,* 2005; Cunnea *et al.*, 2011; McMahon *et al.*, 2012; Ní Fhlathartaigh *et al.*, 2013) due to the advanced stage of disease at which the samples were examined. Probably in these studies, olidogendrocytes within the

inspected MS lesions had already undergone cell death, but eIF2α phosphorylation in oligodendrocytes could have occurred at earlier stages.

Studies in active EAE have revealed that the integrated stress response in oligodendrocytes can be triggered by the inflammatory cytokine interferon-γ (IFNγ), via activation of the protein RNA-like endoplasmic reticulum kinase (PERK) (Lin and Popko, 2009). In mice with active EAE, Lin and colleagues demonstrated that augmented release of IFNγ in the CNS increases PERK activation and eIF2α phosphorylation particularly in oligodendrocytes, and this phenotype is rescued in mouse knockouts for the expression of PERK (Lin *et al.*, 2006, Lin *et al.,* 2012; Lin and Popko, 2009). Interestingly, the investigators observed that the IFNγ-mediated enhancement of the integrated stress response can both ameliorate and exacerbate the progression of EAE, dependent upon whether the stress response is induced before or after the onset of the disease (Lin *et al.*, 2006, 2007). In particular, IFNγ preconditioning, before the onset of neurological deficits in actively immunized EAE mice, delays the onset and attenuates the severity of disease by both reducing demyelination and promoting oligodendrocyte survival (Lin *et al.*, 2007). By contrast, treatment with IFNγ during the symptomatic-phase in mice with active EAE exacerbates disease progression, worsens demyelination and impairs remyelination and oligodendrocyte survival (Lin *et al.*, 2006; Roussel *et al.*, 2013). Possibly, the stress preconditioning of the CNS prepares oligodendrocytes to face the upcoming injury, whereas, once the disease is established, a persistent inhibition of protein synthesis may impair the self-repair capacity of oligodendrocytes, suppress remyelination, and lead to apoptosis.

1.5.0.0 Cerebral blood flow and oxygenation

The brain has a high demand for energy, such that although it comprises only 2% of body weight it takes 20% and 25% of the total oxygen and glucose consumption respectively, and 15% of cardiac output (Clarke and Sokoloff, 1999). The adequate supply of nutrients and oxygen to the CNS is guaranteed by a finely regulated cerebral blood flow (CBF). CBF promptly increases in activated areas of the CNS in order to provide a sufficient supply of nutrients to ratify increased demand; for example, CBF

increases in the visual cortex after a visual input (Ances *et al.*, 1999; Lu *et al.*, 2004) or in the motor cortex during finger movement (Allison *et al.*, 2000). Evidence has shown that under physiological conditions, cerebral activity is followed by a 50% local increase in both CBF and glucose uptake, but only a 5% increase in oxygen consumption (Fox and Raichle, 1986; Fox *et al.*, 1988). More recently, elevated lactate concentration has been detected in activated areas of the brain (Figley and Stroman, 2011), suggesting that at least part of the energy demand is fulfilled by glycolysis (Figley and Stroman, 2011). Lactate is emerging as an important energy source for the CNS (Schurr *et al.*, 1999; Smith *et al.*, 2003; Gallagher *et al.*, 2009; Bélanger *et al.*, 2011). Complexes designated for the entrance and oxidation of lactate, such as the monocarboxylate transporter isoforms 1 and 2 (MCT-1 and 2) and lactate dehydrogenase (LDH), have been found expressed in the inner membrane of neuronal mitochondria, and associated with components of oxidative respiration (Hashimoto *et al.*, 2008). Recent observations suggest that neurons can even "prefer" lactate over glucose when both are available (Itoh *et al.*, 2003; Bouzier-Sore *et al.*, 2006; Bélanger *et al.*, 2011) and utilize lactate as a metabolic substrate for oxidative phosphorylation (Walz and Mukerji, 1988; Magistretti and Pellerin, 1999; Schurr, 2006). Recently, oligodendrocytes have been suggested to supply lactate to axons (Fünfschilling *et al.*, 2012; Jones, 2012; Lee *et al.*, 2012). Axons have very high-energy demands but are isolated from extracellular metabolites by their myelin sheaths (Jones, 2012). Therefore, it is possible that axons depend on energy substrates provided by oligodendrocytes (Jones, 2012). Oligodendrocytes produce lactate via anaerobic glycolysis (Fünfschilling *et al.*, 2012; Lee *et al.*, 2012), and the lactate may then be transferred to axons via the MCT-1 expressed in the myelin sheaths (Lee *et al.*, 2012). Then, axons could use lactate (as well as glucose) in mitochondrial oxidative phosphorylation in order to accomplish their energy need.

More than 90% of the oxygen imported into the brain is used by mitochondria for oxidative phosphorylation to produce energy in the form of ATP (Sciamanna and Lee, 1993). The process of oxidative phosphorylation yields up to 34 moles of ATP from just one mole of glucose compared to a meager two moles of ATP for every mole of glucose produced via anaerobic glycolysis. It has been estimated that almost 80% of the ATP is utilized to support electrical (e.g. synaptic) activity (Sibson *et al.*, 1998; Rothman *et al.*, 2003), most of which is consumed by the Na^+/K^+ ATPase, while the other 20% is used

to maintain basic cellular and neuronal functions such as protein synthesis (Attwell and Laughlin, 2001). Therefore, an adequate and continuous supply of nutrients and oxygen is essential to maintain neuronal survival and normal brain function. Accordingly, cessation of oxygen and glucose supply leads to unconsciousness within less than 10 seconds (Clarke and Sokoloff, 1999). It is understandable why oxygen is essential to ensure an efficient rate of energy production.

1.6.0.0 Hypoxia and the CNS

Hypoxia refers to a decrease in the availability of inspired oxygen, or decreased oxygen tension (oxygen partial pressure, PaO_2) within the tissue (LaManna, 2007). At physiological pressure of inspired oxygen (around 16 kPa), arterial haemoglobin is almost saturated with oxygen (97-99%), and even a slight decrease in the ambient oxygen does not influence the haemoglobin saturation, so that tissue oxygenation remains the same (LaManna, 2007). In mild hypoxic conditions (below 12 kPa but above 6 kPa), successful long-term adaptation occurs, and it is these adaptations that allow mammals to live at high altitudes (e.g. up to 3500 meters of altitude) (LaManna *et al.*, 2004). However, at oxygen pressures between 4 and 6 kPa (e.g. up to 5000 m of altitude) permanent brain damage may occur. Indeed, longer exposure at severe hypoxic conditions (below 4 kPa; e.g. at more than 5000 m of altitude) cause loss of consciousness and neurodegeneration (Fayed *et al.*, 2006; LaManna, 2007; Di Paola *et al.*, 2008). Systemic compensatory changes begin in response to mild hypoxia including increased ventilation, increased erythropoiesis, decreased core temperature and weight loss (LaManna *et al.*, 2004); furthermore organ-specific compensations also occur. To maintain normal tissue oxygenation, the CNS regulates regional and total blood flow at a constant rate over a wide range of blood pressures, through a process known as “cerebral auto-regulation” (Johnston and Czosnyka, 2003). These adaptations include increased CBF (Kety and Schmidt, 1948) and cerebral blood volume (CBV) (Shockley and LaManna, 1988; Julien-Dolbec *et al.*, 2002). Furthermore, neovascularisation occurs approximately after 1 week of prolonged hypoxia (LaManna *et al.*, 2004). The increased vascular bed is not the only factor that enhances the intake of metabolites into the tissue. Indeed, angiogenesis is accompanied by an increased expression of

glucose transporter-1 (GLUT-1) on endothelial cells (Xu and Lamanna, 2006) that results in a greater migration of glucose from the bloodstream into the CNS.

1.7.0.0 Hypoxia and MS

Increasing evidence suggests that hypoxia and an energy deficit may occur in patients with MS and contribute to the pathogenesis and progression of CNS lesions. As mentioned before (paragraph 1.3.1.0), Lucchinetti *et al.* (2000) have demonstrated that demyelinated Pattern-III MS lesions present "hypoxia-like" characteristics showing pathological similarities with white matter lesions forming due to ischaemic stroke (Aboul-Enein *et al.*, 2003). In pattern-III lesions, increased expression of HIF1α, predominantly in oligodendrocytes, astrocytes and some endothelial cells (Aboul-Enein *et al.*, 2003), can be indicative of an actual low concentration of oxygen (see introduction 1.10.1.0). Interestingly, a microarray study disclosed the over-expression of other hypoxia-related genes in the NAWM of patients with MS (Graumann *et al.*, 2003), raising the possibility that tissue hypoxia may be an early feature of newly forming lesions. However, these findings have been typically attributed to an energy deficit resulting from NO-mediated mitochondrial dysfunction (*virtual hypoxia*), rather than an actual insufficiency of oxygen (*true hypoxia*) within the lesion.

Interestingly, the brain of patients with MS can suffer from reduced blood perfusion (reviewed in D'haeseleer *et al.*, 2015). It is easy to image that diminished blood supply to the CNS can cause hypoxia. Initially, it was suggested that the decreased CBF in patients with MS was a consequence of the decreased metabolic demand due to axonal degeneration and CNS atrophy. However, recent evidence has shown that in MS, the NAWM can also suffer from a number of alterations in cerebral haemodynamics including prolonged arterial bolus arrival time (Paling *et al.*, 2014) and decreased CBF (Varga *et al.*, 2009; D'haeseleer *et al.*, 2015). Varga and colleagues (2009) observed reduced CBF in the NAWM of patients with MS already in the first five years of disease, and before the formation of sub-cortical grey matter lesions. These findings suggest that the widespread reduction in cerebral blood perfusion is not secondary to axonal degeneration and brain atrophy. However, the mechanisms

underlining the cerebral hypoperfusion in MS remain enigmatic, and they will be discussed later in this thesis (Chapter 5; paragraph 5.1.0.0).

Although further studies are needed to disclose the sequence of events leading to cerebral hypoperfusion in MS, it is becoming clearer that perfusion abnormalities are present even at the very early stages of disease, when loss of neuronal activity is still not prominent and CNS atrophy is absent (reviewed in D'haeseleer *et al.*, 2015). If so, the decreased CBF may not be a consequence of tissue loss and reduced cell activity that would require less blood supply, but rather, it may be a factor involved in causing tissue damage and disease progression.

1.8.0.0 Hyperbaric oxygen treatment in MS

The suggestion that hyperbaric oxygen therapy (HBOT) could slow or reverse the progression of MS, has led to a number of clinical trials in which HBOT was tested in patients with MS. The early use of HBOT in MS was clearly not based on the recent observations that MS lesions can have hypoxia-like characteristics (Lucchinetti *et al.*, 2000; Aboul-Enein *et al.*, 2003; Aboul-Enein and Lassmann, 2005) or suffer of reduced blood perfusion (D'haeseleer *et al.*, 2015) and energy deficit (Trapp and Stys, 2009). Instead, HBOT in MS was taken in consideration in part because some MS lesions share similarities, including perivenular location of the lesions and vessel reactivity, with lesions caused by gas embolism and decompression illness in which HBOT has therapeutic beneficial effects (Bennett and Heard, 2010), and in part because HBOT has been shown to have an immunosuppressive effect in rats with active EAE (Warren *et al.*, 1978).

HBOT efficacy in MS was evaluated in several clinical trials during the 1980's (Fischer *et al.*, 1983; Murthy *et al.*, 1985; Massey *et al.*, 1985; Neiman *et al.*, 1985; Wood *et al.*, 1985; Confavreux *et al.*, 1986; Harpur *et al.*, 1986; Wiles C. M., Clarke C. R. A., Irwin H. P., 1986; Barnes *et al.*, 1987; Oriani *et al.*, 1990). All these trials examined the role of HBOT in patients with chronic MS, the treatment consisted in exposure to hyperbaric oxygen-enriched (~70%) air at pressures between 1.75 and 2.5 ATA for only 60-90 minutes per day, for a maximum of 20 exposures in total. Interestingly, some trials

reported beneficial effects after treatment (Fischer *et al.*, 1983; Murthy *et al.*, 1985; Barnes *et al.*, 1987; Oriani *et al.*, 1990). These beneficial effects were usually transient and mainly included improvements in bladder functionality, fatigue, and in few cases also in motor functions. Only in one trial (Fischer *et al.*, 1983) was a long-lasting beneficial effect achieved, and the disease severity was attenuated up to six months after treatment cessation. However, a number of other independent trials reported no changes in disease severity after the administration of HBOT (Massey *et al.*, 1985; Neiman *et al.*, 1985; Wood *et al.*, 1985; Confavreux *et al.*, 1986; Harpur *et al.*, 1986). Recently, Bennett and Heard (2010) performed a critical meta-analysis of all the data arising from these trials in order to establish whether HBOT is a valid treatment for MS, or not. They did not identify plausible benefits of HBOT on the clinical course of MS, concluding that the routine treatment of MS with HBOT is not recommended (Bennett and Heard, 2010), despite that some neurologists and MS patients claimed a beneficial effect of HBOT in ameliorating the neurological deficits.

Some weak aspects in the design of HBOT clinical trials can be identified, and they can possibly explain the overall failure of those trials. First, the number of MS patients examined in each trial was small. Indeed, the majority of the trials included only 30-60 patients with MS (Fischer *et al.*, 1983; Murthy *et al.*, 1985; Wood *et al.*, 1985; Confavreux *et al.*, 1986; Oriani *et al.*, 1990), in some cases even less than 30 patients were examined (Massey *et al.*, 1985; Neiman *et al.*, 1985), while only Wiles (1986) and Harpur (1986) included a slightly bigger number of patients in their trials, respectively 88 and 82 patients with MS. Interestingly, Barnes and colleagues (1987) examined the efficacy of HBOT in a relatively larger number of patients with MS (n = 120), and their study was one of the trials that disclosed the greatest, though transient, beneficial effect (Barnes *et al.*, 1987). This raises the possibility that only a subgroup of patients with MS can benefit from HBOT and therefore a clinical trial that employs a larger cohort of patient is more likely to be informative. Second, as mentioned before, HBOT was tested only in patients with chronic MS. The advanced stage of disease may have reduced the efficacy of the therapy given that in patients with chronic MS, it is unlikely to achieve an amelioration of the neurological deficits. In support to these hypotheses, a recent trial with HBOT, that included a large cohort of patients with MS, was performed in the 2000s and the results were recently published (2009) exclusively online (no authors

formally recognized; reviewed in Bennett and Heard, 2010). In this trial, 703 patients with MS were examined, of which: 417 with chronic-progressive, 43 with chronic-static and 167 with relapsing-remitting MS (Bennett and Heard, 2010). Thus, also different stages of MS were considered. Interestingly, transient improvements at the disability score were detected in many patients exposed to HBOT and in particular in the ones with RRMS (Bennett and Heard, 2010). Therefore, it is possible that HBOT may be effective in a subgroup of MS patients and mainly when administered during the acute phase of disease. This aspect may not have been clearly identified at the time of the clinical trials conducted in the 1980's, due to the advanced stage of disease and the small number of patients examined.

In addition, the hyperbaric pressures of oxygen could have affected the efficacy of the therapy in MS. It is now known that high concentrations of inspired oxygen result in increased arterial PaO_2 proportional to the pressure at which oxygen is administered (Nemoto and Betterman, 2007). Indeed, higher pressures of inspired oxygen correspond to greater concentrations of oxygen freely dissolved in the plasma (Nemoto and Betterman, 2007). Although HBOT can result in a greater oxygenation of the tissue compared with normobaric oxygen, recent evidence has shown that HBOT can exacerbate the oxidative/nitrative damage in disease characterized by prominent inflammation such as ischemic stroke (Singhal, 2007; Ding *et al.*, 2014). Therefore it is possible that HBOT could also worsen oxidative damage occurring in active MS lesions. Interestingly, studies in animal models (S. Liu *et al.*, 2006; Shin *et al.*, 2007) and patients (Singhal *et al.*, 2005) with ischaemic stroke revealed that, in contrast with HBOT, oxygen therapy at normobaric pressure ameliorates the neurological deficits without exacerbating the oxidative damage (reviewed in Weaver and Liu, 2015), and it is especially effective when applied in the acute phase of disease (Singhal, 2007). These findings raise the possibility that normobaric oxygen may be beneficial for the treatment of MS, and possibly have fewer side effects than HBOT.

1.9.0.0 Hypoxia in EAE

In a recent study, Davies *et al.* (2013) have demonstrated that the spinal cord of rats with active EAE is hypoxic. The findings have shown that tissue hypoxia is

quantitatively, temporally, and spatially associated with the expression of neurological deficits (Davies *et al.*, 2013). The methods have detected tissue hypoxia both *ex-vivo*, labeling spinal cord sections for markers of hypoxia (pimonidazole and HIF-1α), and *in-vivo*, recording the oxygen tension via a microelectrode oxygen-sensitive probe inserted in the spinal cord (Davies *et al.*, 2013). Furthermore, an enlargement of the spinal blood vessels during the first days of EAE was noticed, followed by an increase in vessel number during relapse, consistent with the observations regarding hypoxia (Davies *et al.*, 2013). Indeed, in hypoxic conditions a prompt vasodilation occurs to increase the local blood supply and then new vessels form to provide a richer vascular bed in the hypoxic region (Xu and Lamanna, 2006). Similar changes in the vasculature were observed also in MS (Holley *et al.*, 2010).

Interestingly, the hypoxia appeared to contribute to neurological dysfunction, because upon administration of normobaric oxygen-enriched air, hypoxia has been promptly reversed and notably the severity of the deficits was also reduced (Davies *et al.*, 2013). These findings suggest that improving the oxygenation of inflammatory lesions may be beneficial as a therapy in MS. The further evaluation of the effects resulting from the administration of normobaric oxygen-enriched air in neuroinflammatory disease, and the optimization of the treatment, are fundamental topics of this thesis.

1.10.0.0 Markers of tissue hypoxia

Although hypoxia plays a key role in the pathophysiology of a number of diseases, it is not routinely measured, in part due to limitations associated with conventional invasive methods such as oxygen microelectrodes. However, the expression of a number of genes is altered in response to hypoxia (Leonard *et al.*, 2003; Manalo *et al.*, 2005; Xia *et al.*, 2009) and they can be used as indirect markers to disclose hypoxic tissue. In particular, the transcription factor HIF1α plays a key role in the adaptive response to low oxygen concentration, and, therefore, its presence within the tissue is often used as an indicator of hypoxia. Pimonidazole, a chemically stable drug that can cross the BBB, is sometimes used in tumour studies and represents another means to detect tissue hypoxia. This drug is thought to facilitate the measurement of oxygen gradients at the

cell level. The mechanisms of action of HIF1α and pimonidazole will be discussed in further detail below.

1.10.1.0 Hypoxia inducible factor 1-alpha (HIF1α)

HIF1 is a heterodimeric transcription factor formed by two constitutively expressed subunits, namely HIF1α and HIF1β (Wang *et al.*, 1995; Semenza, 2002). HIF1α and HIF1β are continuously expressed within the cell, but only HIF1α is subjected to an oxygen-dependent regulation (see following). In normoxic conditions, two conserved prolines (P402 and P564) in HIF1α are hydroxylated by prolyl hydroxylate enzymes (PHDs) in a reaction that consumes oxygen as substrate (Schofield and Zhang, 1999). Hydroxylated HIF1α is ubiquitinated by an E3 ligase (von Hippel-Lindau protein, VHL) and consequently degraded into the proteasome (Figure 1.1) (Maxwell *et al.*, 1999; Ivan *et al.*, 2001; Jaakkola *et al.*, 2001; Klimova and Chandel, 2008). This mechanism contributes to maintaining a very low level of HIF1α in cells. Another oxygen-dependent control of HIF1α is mediated by the hydroxylation of a conserved asparagine (N803) on the c-terminal transactivation domain (CAD) (Figure 1.1) (Coleman and Ratcliffe, 2007). CAD is essential for recruiting the co-transcription factors p300 and CREB-binding protein (CBP) with which HIF1 binds the DNA and activates the transcription of hypoxia-responsive genes, but, when CAD is hydroxylated this function is inhibited (Figure 1.1) (Coleman and Ratcliffe, 2007; Klimova and Chandel, 2008). The factor inhibiting HIF (FIH) is responsible for the hydroxylation of CAD, and similarly to PHD, FIH requires oxygen to catalyze the reaction (Figure 1.1) (Schofield and Ratcliffe, 2004) During hypoxia, PHD and FIH have not enough oxygen to exert their activity. Therefore stabilized HIF1α accumulates within the cell and translocates into the nucleus where it binds the HIF1β subunit, forming the transcriptionally active factor HIF1 (Masson and Ratcliffe, 2003). HIF1 recruits the co-transcriptional factors p300 and CBP (Figure 1.1), and activates the expression of specific genes via the interaction with hypoxia responsive elements (HRE) in their promoter regions (Masson and Ratcliffe, 2003; Klimova and Chandel, 2008). HIF1 mediates the expression of a variety of genes involved in the adaptation of cells to hypoxia, including genes implicated in energy metabolism, cell growth, survival and migration (Coleman and Ratcliffe, 2007). Studies *in-vitro* have estimated that HIF1 directly and indirectly regulates the expression of

more than 50% of the genes responding to hypoxia (Coleman and Ratcliffe, 2007). For example, HIF1 enhances the synthesis of vascular endothelial growth factor (VEGF), a pro-angiogenesis factor, and the endothelial expression of glucose transporter-1 (GLUT-1) (Elvidge *et al.*, 2006). The several adaptation mechanisms to hypoxia that derive from the stabilization of HIF1α make this factor the master regulator of the tissue response to hypoxia.

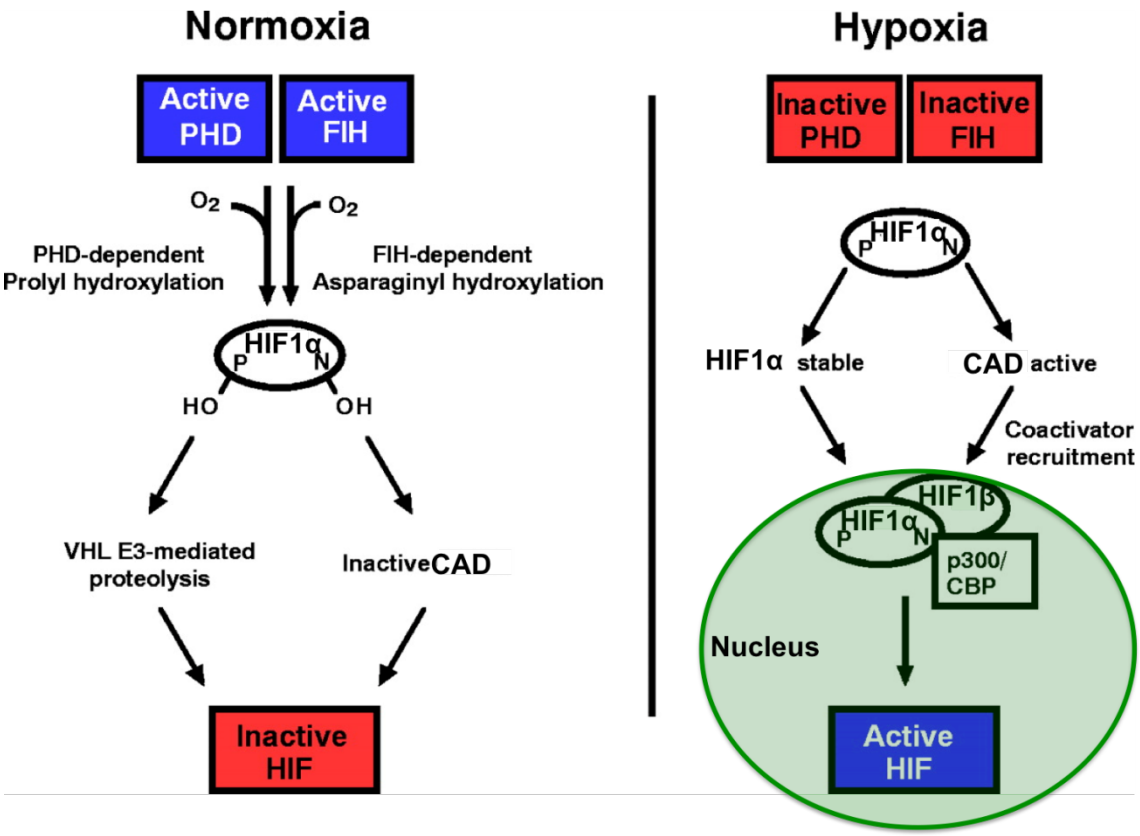

Figure 1.1 - Regulation of HIF1α activity in response to cellular oxygen levels.
In normoxic conditions, oxygen availability allows PHD-dependent hydroxylation of two conserved prolines (P) of HIF1α. This post-translational modification makes HIF1α ubiquitinated by VHL and consequently degraded into the proteasome. Oxygen allows also FIH to inactivate via hydroxylation of a conserved asparagine (N) the CAD domain of HIF1α. Inactivated CAD impairs the transcriptional function of HIF1α. In hypoxia, deficiency of oxygen impairs the activity of both PHD and FIH. Therefore, HIF1α is not degraded and its CAD domain remains active. Stable HIF1α translocates into the nucleus where it dimerizes with HIF1β and binds, at the CAD level, co-transcriptional factors such as p300 and CBP, activating the expression of genes involved in the response to hypoxia. The image was adapted from Masson and Ratcliffe, 2003.

Although HIF1α stabilization within cells is oxygen dependent, recent findings have shown that during hypoxia its expression can also be increased by pro-inflammatory

stimuli and that HIF1α can be involved in the control of the inflammatory response (see following). In naïve T-cells, HIF1α has been discovered to be a key factor regulating the diffentiation of T-naïve cells in Th17, and to inhibit directly T-naïve to T-regulatory (Treg) cell polarisation via degradation of the Forkhead Box-P3 transcription factor (Dang *et al.*, 2011; Shi *et al.*, 2011; Clambey *et al.*, 2012). It has been demonstrated that in naïve T-cells, the inhibition of HIF1α leads to Treg polarization, which consequently enhances an anti-inflammatory response (Dang *et al.*, 2011). Interestingly, Dang *et al.* (2011) showed that HIF1α knockout mice have a reduced incidence of developing EAE upon rMOG immunization, and when sick, these mice experience milder deficits compared with wild-type controls. At the peak of neurological deficits, in these mice the draining lymph nodes, spleen and CNS were found significantly enriched in Treg and impoverished in Th17, in contrast with EAE wild-type mice (Dang *et al.*, 2011).

HIF1α has been reported also to be involved in monocyte-to-macrophage differentiation (Riboldi *et al.*, 2013). Recent studies have demonstrated that pro-inflammatory cytokines (e.g. TGFβ and IL-6), microbial products (e.g. lipopolysaccharide, LPS), and hypoxia can induce monocytes to undertake a M1 pro-inflammatory differentiation via a HIF1α/NFkb dependent pathway (Sica and Mantovani, 2012; Poitz *et al.*, 2013; Riboldi *et al.*, 2013; Tugal *et al.*, 2013). By contrast, the inhibition of HIF1α and the presence of anti-inflammatory signals (e.g. IL-4 and IL-10) can lead monocytes to M2 alternative activation (Lawrence and Natoli, 2011; Sica and Mantovani, 2012; Poitz *et al.*, 2013; Riboldi *et al.*, 2013; Tugal *et al.*, 2013). M2 macrophages express general markers of macrophage activation (e.g. ED-1) and are involved in tissue repair by producing extracellular matrix molecules, anti-inflammatory cytokines and more recently it has been discovered that they are also implicated in the stimulation of oligodendrocyte progenitor cells to differentiate and repair demyelinating lesions (Verreck *et al.*, 2006; Parsa *et al.*, 2012; Miron *et al.*, 2013). Briefly, the overexpression and stabilization of HIF1α in inflammatory precursor cells has been associated with the acquisition of a pro-inflammatory phenotype. Accordingly with these recent discoveries, HIF1α can be considered a double-edged sword in inflammatory diseases. From a therapeutic perspective, the time-point of HIF1α modulation appears crucial. In MS, it has been suggested that before the inflammatory reaction occurs, a preventive activation of

HIF1α via hypoxic preconditioning may protect from the formation of new lesions (Stadelmann *et al.*, 2005; Dore-Duffy *et al.*, 2011) and HIF1α has been demonstrated to protect the brain from ischaemic damage in animal models of stroke (Wacker *et al.*, 2012; Monson *et al.*, 2014), possibly by making tissue more resistant to the upcoming energy deficit. *Vice versa*, when the triggering factor of the inflammatory response is already present (for e.g. after EAE immunisation), a later inhibition of HIF1α may be beneficial, as has been shown in models of autoimmune-inflammatory diseases such as rheumatoid arthritis (Yang *et al.*, 2014) and EAE (Dang *et al.*, 2011), possibly limiting the ability of naïve inflammatory cells (monocytes and T-cells) to acquire a pro-inflammatory phenotype.

1.10.2.0 Pimonidazole

Pimonidazole is a probe that allows the immunohistochemical detection of tissue hypoxia. Pimonidazole consists in a chemical compound that, when administered intravenously can readily reach all tissues in the body, including the CNS (Arteel *et al.*, 1998). In the presence of adequate oxygen concentration, pimonidazole is oxidised to an amine oxide, or conjugated to sulphate groups or glucuronic acid by sulfotransferases and glucuronyl transferases respectively (Figure 1.2) (Arteel *et al.*, 1998). Oxidised or conjugated pimonidazole is then excreted from the body (Arteel *et al.*, 1998). Alternatively, pimonidazole can be also reduced by nitroreductases such as NADPH and NADH to form the nitro-intermediate pimonidazole compound (Figure 1.2) (Arteel *et al.*, 1998). At this stage, oxygen is the limiting factor. At adequate oxygen concentrations, the nitro-intermediate is oxidised back to pimonidazole by oxygen, preventing further reduction of the pimonidazole nitro-intermediate (Arteel *et al.*, 1998). By contrast, if the concentration of oxygen into the cell is low, the pimonidazole nitro-intermediate is further reduced by nitroreductases, gaining the ability to bind thiol-containing molecules, such as glutathione and proteins, forming stable adducts (Figure 1.2) (Arteel *et al.*, 1998). These pimonidazole adducts can be detected in immunohistochemistry by using specific antibodies (Arteel *et al.*, 1998). The localization of these pimonidazole adducts can disclose both the cell types and tissue area suffering of hypoxia, while the intensity of the labelling may be suggestive of the degree of hypoxia.

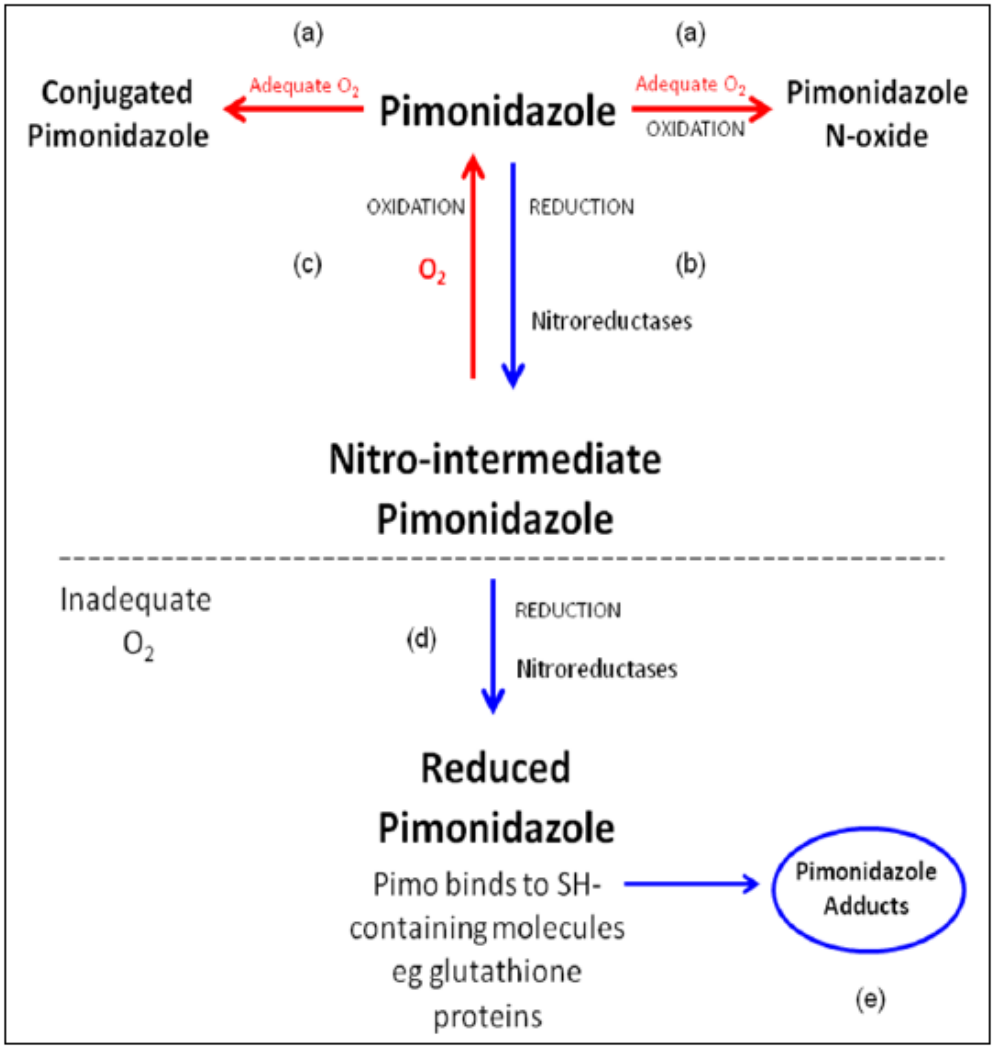

Figure 1.2 - Pimonidazole metabolism *in-vivo*.
In vivo, under normoxic conditions, pimonidazole is rapidly metabolised and eliminated from the body, by oxidation or conjugation. b) In the absence of oxygen, pimonidazole is reduced by nitroreductases to a nitro-intermediate. However, oxygen concentration is the limiting factor at this point, and can oxidise the nitro-intermediate back to pimonidazole (c). In hypoxic cells, the nitro intermediate is subject to a series of reductions (d), until reduced pimonidazole can bind to thiol (SH-) containing molecules resulting in the formation of pimonidazole adducts (e). Adapted from Arteel *et al.*, 1998.

Pimonidazole is used to disclose tissue hypoxia in tumour studies (Raleigh *et al.*, 1998; Wykoff *et al.*, 2000; Janssen *et al.*, 2002; Airley *et al.*, 2003; van Laarhoven *et al.*, 2006). A number of studies have demonstrated a correlation between the localization of pimonidazole adducts and the expression of endogenous markers of tissue hypoxia (Raleigh *et al.*, 1998; Wykoff *et al.*, 2000; Janssen *et al.*, 2002; Airley *et al.*, 2003; van

Laarhoven *et al.*, 2006). For example, in cervical carcinoma, pimonidazole labelling significantly correlated with the expression of HIF1α and GLUT-1 (Airley *et al.*, 2003) whereas it did not correlate with the expression of VEGF (Raleigh *et al.*, 1998). It seems that the correlation between pimonidazole labelling and the expression of other endogenous markers for tissue hypoxia is variable, and it may depend on the model and organ examined. Furthermore, while the expression of endogenous markers related to hypoxia can be affected by other stimuli, the formation of pimonidazole adducts is strictly dependent to the oxygen availability within the cell, making this marker one of the best ways to detect tissue hypoxia.

1.11.0.0 Hypothesis and aims

Our hypothesis is that cerebral hypoxia in MS and EAE can contribute to neurological deficits and CNS damage. We have investigated whether reversing cerebral hypoxia, by increasing the concentration of oxygen in the inspired air or by the systemic administration of a haemoglobin-based oxygen carrier, it is possible to ameliorate the neurological disabilities and reduce CNS damage. To examine this hypothesis we used two animal models of MS, namely active and passive EAE.

The aims of this study are 1) to evaluate whether oxygen treatment can ameliorate neurological deficits due to EAE, and to identify the optimal timing and duration for the treatment, and 2) to examine the effects of oxygen on the pathology of the disease with particular regard to inflammation, demyelination, oxidative stress, hypoxia and metabolic changes.

CHAPTER 2

2. NORMOBARIC OXYGEN-ENRICHED AIR FOR THE TREATMENT OF NEUROLOGICAL DEFICITS IN AN INFLAMMATORY DEMYELINATING MODEL OF MULTIPLE SCLEROSIS

2.0.0.0 Background

Studies have revealed that demyelinating lesions in MS can have different appearances (Lucchinetti *et al.*, 2000; Lassmann, 2013). Four distinct patterns of demyelination have been identified, with some indicating an autoimmune aetiology (Pattern I and II), while others are characterized by diffuse oligodendrocyte dystrophy (Pattern III and IV) in some cases suggestive of a hypoxic cause (Pattern III). Notably, Pattern III lesions show similarities with ischaemic stroke injury including 1) the preferential loss of the myelin protein MAG, 2) lesion non-centered around venules with 3) a rim of preserved myelin in the surrounding (and therefore better oxygenated) regions of blood vessels and 4) the over-expression of hypoxia related antigens (Lucchinetti *et al.*, 2000; Aboul-Enein *et al.*, 2003). Interestingly, a gene expression comparison between patients with MS and healthy controls has revealed a consistent upregulation of genes associated with hypoxic adaptation of the NAWM in MS, thus indicating the presence of tissue hypoxia also in non-demyelinating areas of the CNS parenchyma (Graumann *et al.*, 2003). More recently, MRI studies have revealed that the brain of patients with MS can be characterized by altered cerebral hemodynamics (D'haeseleer *et al.*, 2015) consistent with reduced blood perfusion. These and other evidence suggest that the CNS can suffer an energy failure during MS (Paling *et al.*, 2011; Witte *et al.*, 2014), raising the possibility that at least some neurological deficits may be due to tissue hypoxia and an energy crisis.

A recent study from our group has shown that the spinal cord of rats with active EAE is strongly immunolabelled for markers of tissue hypoxia (HIF1α and pimonidazole) and interestingly, it suffers from an actual reduction of oxygen concentration (Davies *et al.*, 2013). Importantly, Davies and colleagues have shown that by simply giving rats

normobaric oxygen-enriched air to breathe, it is possible to restore normal oxygenation of the spinal cord and reverse tissue hypoxia.

Here, we hypothesized that the administration of normobaric oxygen-enriched air (in this thesis referred simply as “oxygen”) may represent a therapeutic approach for the treatment of the neurological deficits due to inflammatory demyelinating disease. To investigate this possibility we used an inflammatory-demyelinating model of MS, namely active EAE.

2.0.1.0 Aims

- To determine the efficacy of oxygen treatment in improving neurological function in rats with active EAE.
- To explore the optimal timing and duration of oxygen exposure for the treatment of neurological dysfunction in active EAE.
- To evaluate the effects of oxygen administration on the pathology (demyelination, inflammation and metabolic changes) of active EAE.
- To determine the consequences of oxygen administration with regard to oxidative and nitrative damage due to active EAE.

2.1.0.0 Material and methods

2.1.1.0 Animal model: induction of active EAE

Female Dark Agouti (DA; n = 173; 8-9 weeks-old, ~150g, Harlan, UK) rats were kept in standard cages with food and water *ad libitum* on a twelve hour light - dark cycle. One week was left between the arrival of the rats and the induction of active EAE, to acclimatize the rats to their new environment. Active EAE was induced by a subcutaneous injection at the base of the tail of 100µg of rMOG (MOG_{1-124}; synthetised in the laboratory of Prof Christopher Linington, University of Glasgow) in incomplete Freund‘s adjuvant (IFA) (Davies *et al.*, 2013). Control animals received an injection of IFA and saline emulsion alone. Rats that developed cerebellum-like neurological dysfunction, which is difficult to score using our behavioural tests (see below), were

excluded. All experiments were performed in accordance with the UK Animals (Scientific Procedures) Act of 1986, and the ARRIVE guidelines.

2.1.2.0 Behavioural assessment of the neurological deficits

All behaviour assessments and analysis were performed blinded. Disease progression was monitored on a daily basis, including assessment of general health (weight) and neurological function. Neurological function was assessed using a 10-point behavioural test. One point was given for each of the following neurological signs: tail tip weakness, tail weakness, tail paralysis, absence of toe spreading reflex, abnormal gait, left and right hind limb paresis, left and right hind limb paralysis and moribund (Davies *et al.*, 2013). To assess neurological function before and after treatment in more detail, a 30-point scale was also used, and a score from 0 to 2 points per hind limb was given for each of the following functions: stretch withdrawal, toe spreading reflex, spasticity and plantar placement, whereas 0 to 3 points were given for pinch withdrawal and nociception. Tail paresis and paralysis (0 - 3 points), nociceptive response to tail pinch (0 - 3 points), flexion of the hip (0 - 2 points), paralysis per forelimb (0 – 2 points) were also tested. Zero indicates normal function, while ascending scores indicate increasing disabilities.

2.1.3.0 Therapeutic oxygen administration

Oxygen treatment was administered by placing the animals in a chamber (Biospherix, USA) with defined raised oxygen concentration. Control rats were kept in a similar chamber containing room air (21% oxygen). Therapeutic treatment with oxygen was administered after the onset of neurological deficit. To assess the optimal timing and duration of the therapy, independent trials were performed as described below.

2.1.3.1 1-hour oxygen treatment

To study the acute effect of oxygen therapy, 95% oxygen was administered for 1 hour to rats with active EAE (n = 10) at the peak of disease, alternating with 1 hour of room air before and after oxygen exposure. For a more detailed analysis of the efficacy of oxygen the enhanced 30-point neurological scale was employed to assess the neurological deficits before and after the treatment.

2.1.3.2 24 hours oxygen treatment

To study the effects of timing on the efficacy of oxygen treatment, rats with active EAE (n = 72) were randomly assigned to receive either room air or 75% oxygen for 24 hours, starting at different stages of disease progression (first, second or third day from onset of deficits, n = 12 per group). All animals were perfused at the end of the treatment period and the spinal cords were collected for histological analysis. IFA control animals receiving either oxygen for 24 hours (n = 4) or room air (n = 4) were added for comparison.

2.1.3.3 24, 48 and 72 hours of oxygen treatment from the onset of deficits

To study the effects of duration on the efficacy of oxygen treatment, two independent trials of active EAE were performed (n = 74). In the first trial (n = 28) rats with active EAE were randomly assigned to receive 75% oxygen for 24 (n = 6), 48 (n = 8) or 72 (n = 7) hours from the first day of deficits, and active EAE rats that did not receive oxygen (room air, n = 7) were used as controls. All animals were returned to room air after cessation of oxygen treatment and monitored up to the ninth day of disease (second peak of disease) to assess the long-term effects of oxygen treatment. In the second trial (n = 36), rats with active EAE were also treated with oxygen (75%) for 24 (n = 10), 48 (n = 9) or 72 (n = 9) hours from the onset of disease or exposed to room air (n = 8), but in this case animals were perfused three days after the onset of deficits (first peak of disease) for histological analysis aimed to investigate the acute effect of the therapy on the disease. IFA controls (n = 8) were added for comparison.

2.1.4.0 Prophylactic oxygen administration

To evaluate the role of oxygen treatment on the pathogenesis of the disease, rats with active EAE (n = 16) were randomly assigned to receive either oxygen (75%, n = 8) or room air (n = 8) from the day of the immunization (before the onset of deficits) up to 23 days post-immunisation (second peak of disease).

2.1.5.0 Tissue processing and histology

At the end of the experiment (at times indicated previously), animals were deeply anaesthetized with isoflurane (5%) and intracardially perfused with 0.1 M phosphate buffer saline (PBS) containing heparin, followed by fixation with 4% paraformaldehyde (PFA) in PBS. Following perfusion, the spinal cords were excised and post-fixed in 4% PFA overnight. Tissue was subsequently transferred into 30% sucrose in PBS solution for five days for cryoprotection. The spinal cords were embedded in blocks with TissueTek O.C.T and frozen in 2-methylbutan (Sigma, UK) in liquid nitrogen at -150° C. Tissue blocks were stored at -80°C prior to cryosectioning (12 µm transverse sections) and immunohistochemical examination.

2.1.5.1 Neuropathology and immunohistochemistry

Basic neuropathological evaluation was performed on luxol fast blue (LFB) staining. The frozen sections were air dried for more than one hour and dehydrated through a graded alcohol scale (50%, 70%, 90% and 100% ethanol). They were then incubated in neat LFB solution (BDH 34044, BDH International, UK) in acidified 95% ethanol at 50° C overnight. On day 2, tissues were washed in running tap water and differentiated in saturated lithium carbonate for 10 seconds to remove the staining from non-myelinated tissue. Where needed, sections were counterstained with Harris's haematoxylin (VWR International, UK). Each step was followed by washing in running tap water.

Immunohistochemistry was performed on frozen sections air dried for more than one hour, and rehydrated in PBS for at least 5 minutes. Next, the sections were incubated in 0.3% hydrogen peroxide (H_2O_2; Sigma-Aldrich, USA) in neat methanol (BDH International, UK) for 15 minutes, with gentle agitation, to block endogenous peroxidase. Only the sections labelled for 8-OHdG (see below) were not incubated in H_2O_2 as recommended in the manufacturer's instructions (Trevigen; cod. 4354MC050). Where necessary, the sections were treated twice with 1mg/ml sodium borohydride ($NaBH_4$; VWR International, UK) for 5 minutes to reduce aldehyde binding to antigens due to PFA fixation. Each step was followed by washing with PBS. All sections were incubated in the appropriate blocking buffer for at least 15 minutes, to decrease non-specific antibody binding, before incubation with primary monoclonal or polyclonal antibodies, diluted in the same blocking buffer, overnight at 4°C. Negative controls were incubated with blocking buffer alone. The following day, all sections were washed in

PBS prior to incubation with a biotinylated anti-mouse, anti-rabbit or anti-goat secondary antibody, diluted to 1/200 in the appropriate blocking buffer, for at least an hour at room temperature (RT). Next, the sections were incubated with avidin-peroxidase complex (Vectastain Elite: Vector Laboratories Ltd, USA), for at least one hour at RT. PBS washes were carried out between each step. Finally, the sections were exposed to the 3,3'-diaminobenzidine (DAB) reaction mixture (Vector DAB kit; Vector Laboratories Ltd, USA). When the developing brown colour appeared optimal, the sections were quickly immersed in tap water to stop the reaction, and then washed for an additional 10 minutes in PBS. Dehydration through graded alcohol to xylene was performed, before mounting in DPX medium (VWR International, UK). Positive controls were used where available to ensure the staining method was operating as expected. Immunolabelling of myelin was performed by using an antibody against myelin oligodendrocyte glycoprotein (MOG). Microglial activation and macrophage infiltration was detected using a primary antibody against ED-1. Free radical injury mediated by activated microglia and macrophages was detected using antibodies for: inducible nitric oxide synthase (iNOS), 8-hydroxy-2'-deoxyguanosine (8-OHdG) and oxidized phospholipids (E06). Changes in the vasculature were evaluated using the rat endothelial cell antigen-1 (Reca1); hypoxia was detected using antibodies against hypoxia inducible factor-1α (HIF1α), while the activation of the glycolytic pathway was studied using anti-phosphofructokinase-2 (PFK-2). Application and dilution of the above primary antibodies are reported in Table 2.1.

2.1.5.2 Immunofluorescence

Air-dried sections of the spinal cords were rehydrated with PBS for a minimum duration of 5 minutes. The sections were then washed twice with $NaBH_4$ (in PBS, 1mg/ml) for 5 minutes each. PBS washes were carried out between each step. Next, sections were incubated with the appropriate blocking buffer, for a minimum of 30 minutes at room temperature, before incubation with primary antibodies diluted in the appropriate blocking buffer, overnight at 4°C. Negative controls were incubated in blocking buffer alone overnight. The next day, following three washes of PBS, the sections were incubated in secondary Alexa fluor 568 donkey anti-mouse IgG (1/200; Invitrogen) and Alexa fluor 488 donkey anti-goat IgG (1/200; Invitrogen). Single labelling with a mouse anti-cluster of differentiation 3 (CD3) was used to mark T-lymphocytes (T-cells). Double

labelling included the following primary antibody combinations: mouse anti-neuronal nuclei (NeuN) with goat anti-phosphorylated eukaryotic initiation factor 2α (p-eIF2α); and mouse anti-adenomatous poli coli protein (clone CC1) with goat anti p-eIF2α. Application and dilution of the primary antibodies are reported in Table 2.2.

Antibody	Origin	Target	Marker	Dilution	Source
8-OHdG	Mouse (mAb)	8-hydroxy-2'-deoxyguanosine	Oxidized DNA/RNA, oxidative damage	1/200	Trevigen; 4354MC050
CC1	Mouse (mAb)	Adenomatous poli coli protein,clone CC1	Oligodendrocyte cell body	1/200	Abcam; ab16794
CD3	Mouse (mAb)	Cluster of differentiation 3	T-lymphocytes	1/200	AbD Serotec; MCA772
E06	Mouse (mAb)	Oxidized phospholipids	Oxidative damage	1/200	Avanti; 330001
ED-1	Mouse (mAb)	Rat CD68	Activated microglia and macrophages	1/200	AbD Serotec; MCA341G
HIF1α	Rabbit (pAB)	Hypoxia inducible factor-1α	Tissue hypoxia	1/200	Abcam; ab85886
iNOS	Rabbit (pAB)	Inducible nitric oxide synthase	inflammation, nitrative damage	1/200	BD Laboratories; NB300-605
MOG	Mouse (mAb)	Myelin oligodendrocyte glycoprotein	Myelin	1/500	Millipore; MAB5680
NeuN	Mouse (mAb)	Neuronal nuclei	Neuronal cell body	1/200	Millipore; MAB377
peIF2α	Goat (pAb)	Phosphorylated eukaryotic initiation factor-2α	Integrated stress response	1/200	Santa Cruz; sc12412
PFK-2	Goat (pAb)	Phosphofructokinase-2	Glycolisis	1/200	Santa Cruz; sc10091
Reca1	Mouse (mAb)	Rat endothelial cell antigen-1	Blood vessels	1/200	Abcam; ab22492

Table 2.1 - Primary antibodies.
Antibodies were used on rat tissue for immunohistochemistry and/or immunofluorescence as described in the material and methods above. mAb = monoclonal antibody, pAb = polyclonal antibody.

2.1.6.0 Microscopy and histological analysis

Tissue stained with DAB and LFB was viewed using an Axiophot light microscope (Zeiss, Germany) and pictures taken with a Nikon D300 camera (Nikon, USA). Quantification was carried out on 5 different levels of the spinal cord for a total of 10 sections per rat (sacral, lower lumbar, upper lumbar, lower thoracic and upper thoracic; 2 sections per level, 120μm apart). ImageJ software (NIH, USA) was used for image analysis. All quantification was carried out in a blinded manner. Analysis of the immuno-reactivity for ED-1, iNOS, HIF1α, PFK-2, 8-OHdG and E06 was done by making the images binary, tracing the area around the whole spinal cord sections with the freehand selection tool, before counting the number of pixels above a set threshold and expressing the result in percentage coverage of the total cross-sectional spinal cord area. Quantification of RECA1 was performed on binary converted images, with the automated analyse particles tool, to quantify the number and size of vessels. LFB and MOG analysis for demyelination was done by tracing the area around the white matter of the spinal cords and measuring the surface covered by LFB or MOG labelling above

a set threshold. This area was then subtracted from the total area and expressed as the percentage of demyelination of the total white matter. Where no clear demyelinated lesions were detected, a value of zero was given. Fluorescently labelled tissue was viewed, and images acquired, using an AxioImager-Z.2 confocal microscope (Zeiss, Germany). Immunofluorescent labelling was quantified on 4 spinal cord sections per rat at the lumbar level (2 sections for the lower and upper lumbar level respectively; sections in the same spinal cord region were distant 120μm). CC1/peIF2α co-labelling was analysed by counting positive cells within the dorsal column and the anteromedian white matter of the spinal cord. The percentage of double-positive cells was calculated by normalizing the number of cells double positive for CC1/p-eIF2α against the total number of CC1 positive cells. CD3 labelling was quantified by counting the number of positive cells within the dorsal column and the anteromedian white matter of the spinal cord. Isolated groups of CD3 positive cells were considered “clusters” and quantified on the entire surface of the spinal cord cross-sections. Both the number and the size of such clusters were considered. The size of CD3 clusters was quantified by measuring the area covered by CD3 signal above a set threshold. All immunofluorescent analyses were carried out using DAPI to distinguish cells from unspecific labelling artefacts. The quantifications among the different sections of spinal cord were averaged within each rat and used for statistical analysis.

2.1.7.0 RT-PCR

Rats with active EAE (n = 10) were either treated with oxygen (75%, n = 5) for 72 hours from the onset of disease or kept in room air (n = 5, controls). IFA rats (n = 6) were added for comparison. At the peak of disease (three days after onset), all rats were perfused in PBS-heparin and the spinal cords were snap frozen on dry-ice. RNA was extracted from 2 cm frozen sections at the level of the lumbar spinal cord enlargement, using TRIzol Plus purification kit (12183555). RNA quality and integrity was measured using the Agilent Bioanalyzer 6000 Nano LabChip platform. cDNA was synthesized using the Qiagen QuantiTect® Reverse Transcription Kit following the manufacturer’s instructions. Cycling parameters were as follows: first cycle (DNA wipeout step) 42°C for 2 min, after adding reverse transcriptase, reaction buffer and primer mix second cycle: 42°C for 20min, then 3 min for 95°C. Primers were designed from sequences

from the NCBI nucleotide data base, using NCBI Primer Designing Tool software. Primer sequences were tested with BLAST (http://blast.ncbi.nlm.nih.gov/Blast.cgi) and were purchased from Integrated DNA Technologies (UK). Real-time PCR was performed using 1X SYBR Green master mix (Applied Biosystems, USA), 10ng cDNA template, 50 pmol/μl of forward and reverse primers, and distilled water. The reaction was amplified in an Applied Biosystems Fast Real-Time PCR System (ABI 7500, USA) using the following cycle settings: 50°C for 5 min, 95°C for 10 min, followed by 40 cycles of 95°C for 15 seconds, 60°C for 1 minute, and a final dissociation step at 95°C for 15 seconds. Melt curve analysis was then performed between 75–99°C in 1°C increments. The comparative CT method (or the 2-ΔCT method) was used to determine differences in gene expression between control and treated EAE rats. IFA controls were used for comparison. RT-PCR primers and conditions are summarized in Table 2.2.

Gene	Full name	Primer sequences	Size (bp)	Annealing (°C)	Gene bank
Arg1	Arginase-1	FW: 5'-CATATCTGCCAAGGACATCG-3' RV: 5'-GGTCTCTTCCATCACTTTGC-3'	142	56	NM_017134.3
Ccr5	C-C chemokine receptor 5	FW: 5'-GAAGGTGAGACATCCGTTCCC-3' RV: 5'-CAGACGTCCCCTCAGGATTTC-3'	126	60	NC_005107.4
Foxp3	Forkhead box P3	FW: 5'-TTCTCAAGCACTGCCAAGCA-3' RV: 5'-GTCTCCGCACAGCAAACAAG-3'	291	60	NM_001108250.1
IFNγ	Interferon-γ	FW: 5'-GCCCTCTCTGGCTGTTACTG-3' RV: 5'-CCAAGAGGAGGCTCTTTCCT-3'	112	60	NM_138880.2
IL-2	Interleukine-2	FW: 5'-CCAAGCAGGCCACAGAATTG-3' RV: 5'- ACCACAGTTGCTGGCTCATC-3'	208	60	NM_053836.1
IL-12b	Interleukine-12b	FW: 5'-ACCTCTGCCGAAGTCCAATG-3' RV: 5'-AAGCCTCCTCTTAGCCTCCA-3'	172	60	NC_005109.4
IL-17a	Interleukine-17a	FW: 5'-CATCCATGTGCCTGATGCTG-3' RV: 5'-GCCTCCCAGATCACAGAAGG-3'	265	59	NM_001106897.1
IL-23	Interleukine-23	FW: 5'-ATGACCAGCTTCCTTCCACC-3' RV: 5'-TCACCTCACCTCGTTGTTCC-3'	198	60	NC_005106.4
iNOS	Inducible nitric oxide synthase	FW: 5'-GAGACGCACAGGCAGAGG-3' RV: 5'-CAGGCACACGCAATGATGG-3'	121	60	NM_012611.3
Mhc1	Major histocompatibility complex-1	FW: 5'-TGACCAACCTTTCCACAGCAT-3' RV: 5'-CAAGACCAGAGCATCACACCA-3'	198	60	NC_005112.4
TNFα	Tumor necrosis factor-α	FW: 5'-CCCCTTTATCGTCTACTCCTCA-3' RV: 5'-TTCAGCGTCTCGTGTGTTTC-3'	134	58	NM_012675.3

Table 2.2 - RT-PCR primers and conditions.
Abbreviations are: FW = forward primer; RV = reverse primer.

2.1.8.0 Statistical analysis

Graphpad Prism v6.0 (USA) was used for statistical analysis and graph generation. All graphs represent mean ± S.E.M. (standard error of the mean). All statistical analyses were two-tailed and considered significant when $p < 0.05$. The non-parametric Mann Whitney U-test was used to compare the severity of neurological deficits between

groups of treatment. Parametric tests were used for histological and RT-PCR analysis as following. Independent t-test was used when only two groups were compared. One-way ANOVA with multiple comparison tests was used to compare multiple groups when only one variable was present (e.g. group of treatment). Two-way ANOVA with multiple comparison tests was used when multiple groups were compared and more than one variable (e.g. group of treatment and stage of disease) were taken in consideration. Dunnett's correction was used to compare groups of treatment with the control and Sidak's correction was used to analyse differences between groups.

2.2.0.0 Results

2.2.1.0 1-hour of oxygen treatment promptly improves neurological function

To evaluate the acute effect of oxygen on neurological deficits, rats with active EAE (n = 10) were treated with 1 hour of 95% oxygen-enriched air at different levels of disease severity (n = 3 with impairment of tail motility, n = 3 with tail paralysis and hind limb paresis, and n = 4 with tail and hind limb paralysis). For a more detailed analysis of the efficacy of oxygen we employed the enhanced 30-point neurological scale as described in the material and methods (paragraph 2.1.2.0). The oxygen treatment was preceded and followed by 1 hour of room air. One rat experienced an exacerbation of the neurological deficits during the first hour in room air (Figure 2.1), but during the following hour in oxygen, 5 out of 10 rats (1 mild, 1 moderate, 3 severe) improved in tail, hind limb motility and/or nociceptive perception, suggesting that oxygen can promptly ameliorate the neurological function even in paralysed rats (Figure 2.1; $p = 0.02$). However, the neurological deficits returned when the rats were restored to room air for the next hour (Figure 2.1), highlighting a specific but transient beneficial effect of 1-hour oxygen exposure. The remaining rats showed no changes in oxygen (or room air). It remains unclear why some animals responded to oxygen and others did not.

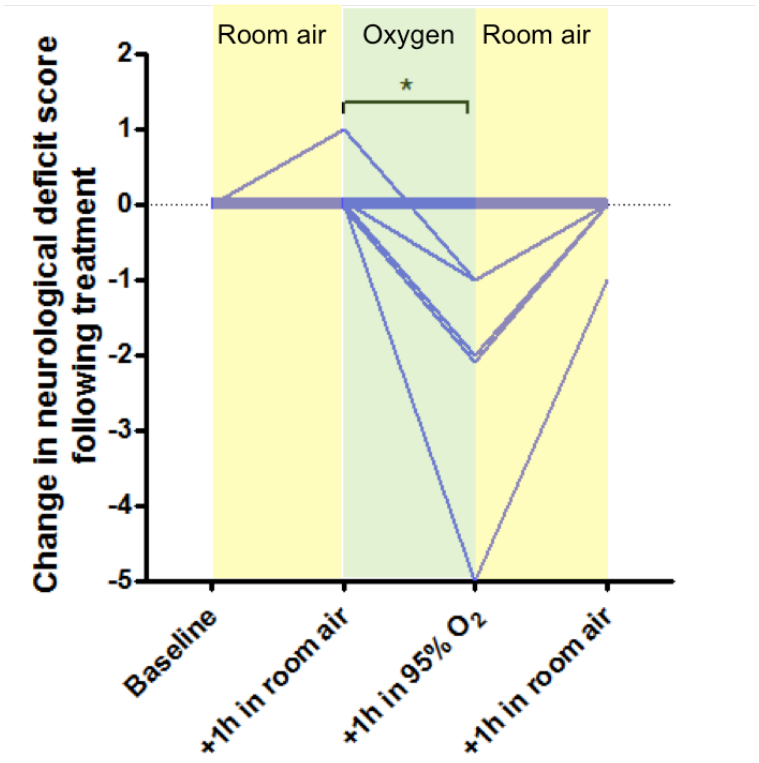

Figure 2.1 - 1 hour of oxygen treatment (95%) at the peak of disease decreases neurological deficits in rats with active EAE.
Rats with active EAE were exposed to 1 hour of 95% oxygen treatment at the peak of disease. The treatment was preceded and followed by 1 hour of room air. Neurological function was assessed using a 30-point behavioural test after each hour, and expressed as a difference in the absolute score after 1 hour compared with the score before entering in treatment. Blue lines represent changes in neurological score for single animals. Zero represents no changes in neurological function, whereas positive and negative scores represent an exacerbation or an improvement of neurological deficits respectively. Oxygen treatment promptly decreased neurological deficits from 1 up to 5 points at the behavioural test in 50% of treated rats after 1 hour of exposure ($p = 0.02$). The beneficial effect disappeared when rats were returned in room air for another hour. Mann-Whitney U-test; $n = 10$.

2.2.2.0 Timing of oxygen treatment: 24 hours of oxygen exposure at different stages of disease

To explore what would be the optimal time to start the treatment, two independent trials of active EAE (Trial1: $n = 18$; Trial 2: $n = 54$) were performed. Rats with active EAE were randomly sorted to receive 75% oxygen or room air for 24 hours, from either the first, second or third day of disease (Trial1: $n = 3$ per group; Trial2: $n = 9$ per group). Both trials showed similar effects of oxygen treatment on the disease progression and the data were grouped and considered together as discussed below (Figure 2.2; $n = 72$,

12 per group). Interestingly, oxygen ameliorated disease progression regardless of whether the treatment was started on the first, second or third day of disease, compared with cohort controls maintained in room air (Figure 2.2). Indeed, we observed that rats breathing room air were affected by a more severe disease course after 24 hours than animals treated with oxygen (Figure 2.2a-d). Interestingly, a significant amelioration of the disease progression was achieved when rats were treated at the first day of deficits. The improvement consisted of a 30% decrease, in the behavioural test, in the severity of neurological deficits compared with controls (Figure 2.2a, d; $p = 0.034$). In this group, all room air controls accumulated new disabilities after 24 hours, experiencing an increase in score of up to 8 points upon neurological testing (mean difference in score after 24 hours = +4.25 ± 0.71; Figure 2.2d). In contrast, 3 out of 12 rats treated with oxygen on the first day of disease did not develop further deficits, and the other 9 animals experienced a milder exacerbation of the disease compared with controls, showing an increase of neurological deficits of maximum 4 points upon neurological testing (mean difference in score after 24 hours = +2.08 ± 0.54; Figure 2.2a, d). A pronounced, although non-significant amelioration of the neurological deficits (reduction of 19% upon neurological testing) was also observed in rats treated with oxygen from the second day of disease compared with time-matched controls (Figure 2.2b). At this stage, 4 animals in both room air and oxygen-treated groups did not develop new deficits; 8 room air controls worsened in their deficit after 24 hours, but only 5 rats treated with oxygen progressed in disease severity. None of the rats exposed to room air improved after 24 hours, but 3 animals treated with oxygen at the second day of disease improved, with a decrease in score of up to 2 points (mean difference in score after 24 hours: room air = +1.91 ± 0.51, oxygen = +0.50 ± 0.49; Figure 2.2b, d). When the treatment started at the third day of disease, a decrease in the mean neurological score was observed in both oxygen-treated rats and room air controls (mean difference in score after 24 hours: room air = -0.5 ± 0.47, oxygen = -0.75 ± 0.41; Figure 2.2c, d), indicating an overall spontaneous remission of the disease. Oxygen administration at this stage of disease resulted in a mild, non-significant improvement (8% in the neurological deficit score) of the neurological function compared with room air controls. Thus, although amelioration in neurological deficit was observed after therapy independently from the time-point of treatment initiation, the greatest improvement was achieved when oxygen was applied at the first day of

deficits, suggesting that the treatment at the very onset of disease expression may produce the best therapeutic effect.

To evaluate further the effects of oxygen on the pathology of the disease, the spinal cord of rats included in Trial1 and 2 were collected and analysed histologically for markers of demyelination, inflammation, hypoxia, and for vascular and metabolic changes.

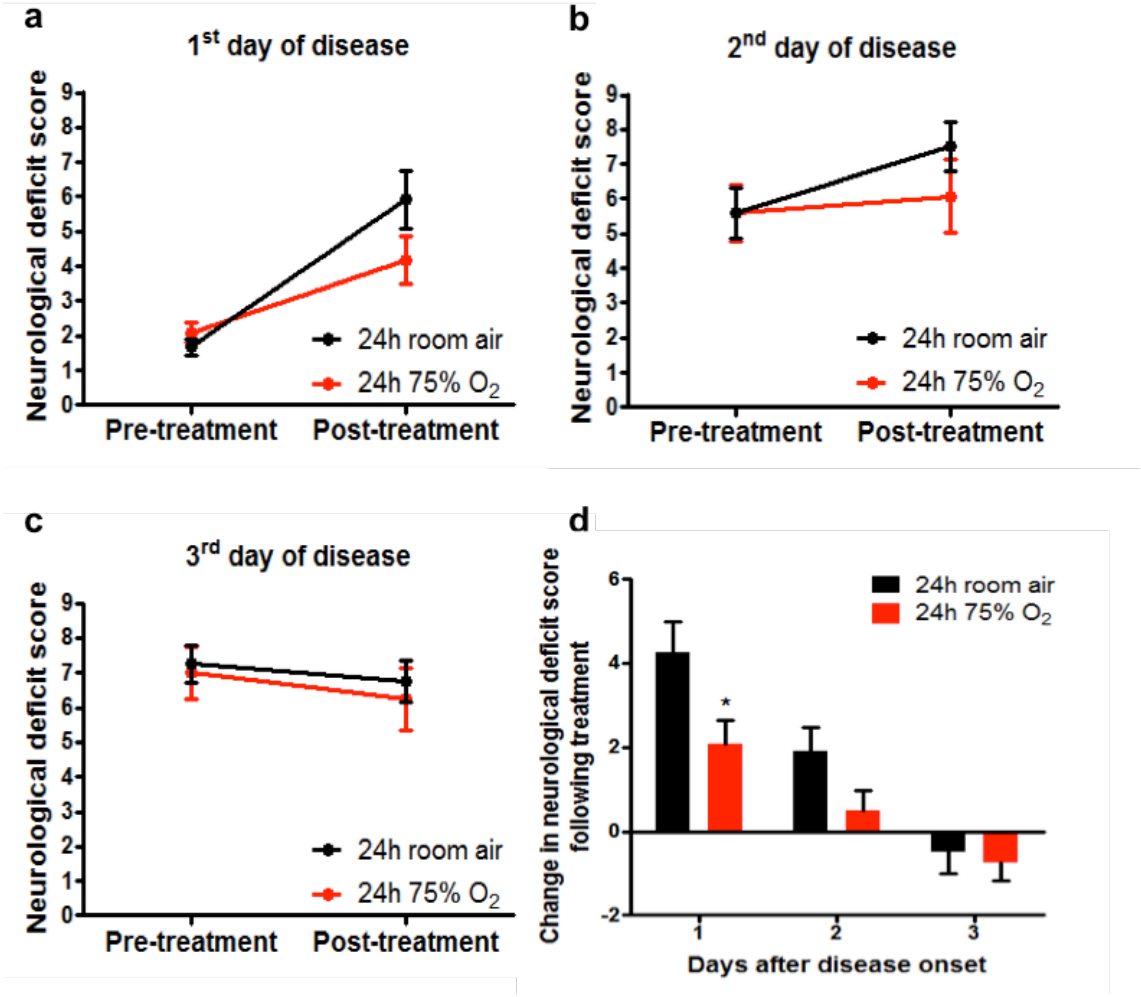

Figure 2.2 - 24 hours of oxygen (75%) treatment ameliorates the expression of neurological deficits when administered at the first, second or third day of disease.
a- c) Neurological deficit score of rats with active EAE exposed to oxygen or room air for 24 hours on either the first, second or third day of disease. Oxygen alleviated the disease progression compared with time-matched room air controls, irrespective of the stage of disease it was administered. **d)** Change in neurological deficit score shows that oxygen-treated rats experienced a milder exacerbation of neurological dysfunction after 24 hours compared with room air controls, and significantly milder when treatment started on the first day of disease ($p = 0.034$), compared with controls. Change in score was calculated as the difference between the absolute score before and after the treatment. Mann-Whitney U-test. N = 12 per group.

2.2.2.1 Spinal cord demyelination after 24 hours of oxygen administration at different stages of disease

We examined demyelination using the luxol fast blue (LFB) staining for myelin in spinal cord cross-sections of rats included in the study described above. LFB is a copper phthalocyanine dye which binds lipoprotein expressed in the myelin sheath. Low or

absent LFB staining indicates partial or complete demyelination respectively. LFB staining of the spinal cords showed that while IFA controls kept in room air or exposed to oxygen for 24 hours did not have any sign of demyelination, EAE rats were characterized by myelin loss in the white matter. Perivascular and sub-meningeal demyelination was observed in rats with active EAE as early as one and two days after the onset of neurological deficits (Figure 2.3a), although not all rats at these early stages showed demyelination (data not shown). At three days after onset, all rats showed demyelination and this appeared more obvious and affected a larger part of the spinal cord white matter (Figure 2.3a and b). Interestingly, at all three stages of disease examined, when present the demyelination most frequently occurred in the dorsal columns (Figure 2.3a) and at the anteromedian area of the spinal cord. Another group (Lin *et al.*, 2007) has also observed demyelination frequently in these spinal cord regions of mice with active EAE, but the mechanisms underlying this peculiar localization of the lesions remain unclear.

We then evaluated whether continuous administration of oxygen for 24 hours from the first, second or third day of disease can protect from spinal cord demyelination. LFB quantification did not show any differences in white matter demyelination between oxygen-treated groups and time-matched room air controls (Figure 2.3a and b).

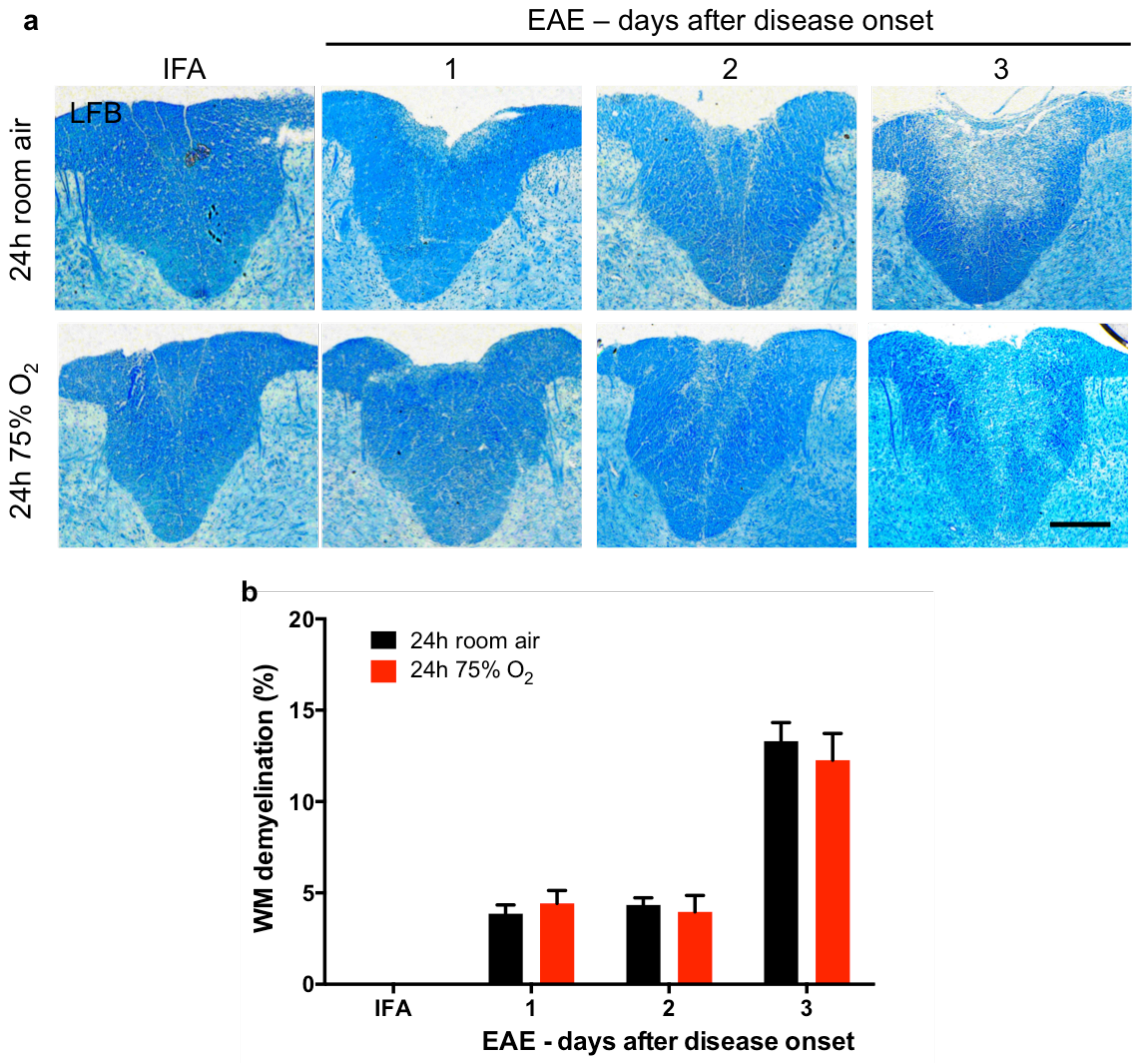

Figure 2.3 - 24 hours of oxygen treatment from either the first, second or third day of disease, does not change white matter demyelination in the spinal cord of rats with active EAE straight after treatment cessation.
a) Lumbar spinal cord dorsal columns of IFA controls and rats with active EAE were stained for LFB (blue). EAE rats received either oxygen (75%) or room air for 24 hours on either the first, second or third day of disease. Absence of blue staining indicates demyelination. IFA controls did not show demyelination. Rats with active EAE were characterized by sub-meningeal and perivascular demyelination in the spinal cord white matter (WM) one and two days after the onset of deficits, whereas demyelination was greater on the third day of disease. Scale bar = 200µm. **b)** Quantification of LFB staining showed no changes after 24 hours of oxygen treatment administered on either the first, second or third day of disease compared with room air controls. Two-way ANOVA with Sidak's correction ($p > 0.05$). IFA: n = 4 per group; EAE: n = 12 per group.

2.2.2.2 Microglial activation, macrophage infiltration and iNOS expression do not change after 24 hours in oxygen

Reactive microglia and infiltrated macrophages are key players of tissue damage during MS and EAE. To determine whether oxygen treatment (24 hours from the first, second or third day of disease) affects the abundance of activated microglia and macrophages in the spinal cord of rats with active EAE, we immunohistochemically labelled these cells using anti- ED-1. ED-1 immunoreactivity was observed in the spinal cord of rats with active EAE in areas characterized by hypercellularity (assessed using haematoxylin) probably due to inflammatory infiltrates, and often in areas that were also demyelinated (loss of LFB staining) (Figure 2.4a). Non-inflamed, non-demyelinated IFA controls did not show ED-1 labelling (Figure 2.4a, b). In animals with active EAE, the number of ED-1 positive cells gradually increased with the progression of the disease (Figure 2.4b, c). One and two days after the onset of the disease, activated microglia and macrophages were mainly observed in the sub-meningeal and perivascular regions of the spinal cord. At the third day of neurological deficits (peak of disease), activated microglia and macrophages were diffused, occupying a larger part of the spinal cord parenchyma (Figure 2.4b, c). ED-1 quantification did not reveal changes in the number of activated microglia and macrophages in rats exposed to oxygen compared with room air controls, 24 hours after treatment initiation on either the first, second or third day of disease (Figure 2.4c; $p > 0.05$).

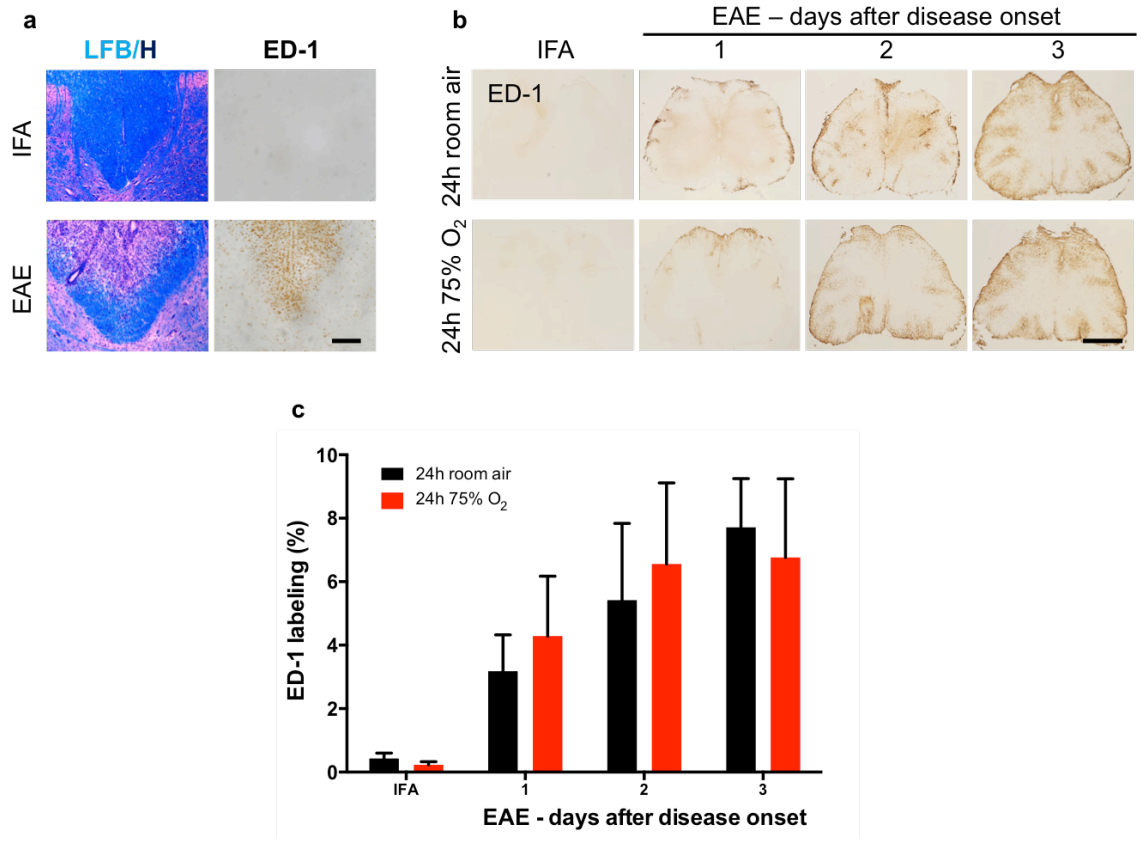

Figure 2.4 - 24 hours of oxygen treatment from either the first, second or third day of disease, does not change microglial activation and macrophage infiltration in the spinal cord of rats with active EAE.

a) Representative images of spinal cord dorsal columns stained for myelin (LFB; light blue) and cell nuclei (haematoxylin, H; dark blue), and labeled for activated microglia and macrophages (ED-1; brown) on adjacent sections. EAE rats showed demyelination (absence of LFB) in areas with hypercellularity (H, probably due to inflammatory infiltrates) and ED-1 positive cells. IFA controls had no demyelination, inflammation and macrophage/microglial activation. Scale bar = 200µm. **b)** Lumbar spinal cord cross-sections labeled for ED-1, of IFA controls and EAE rats exposed to room air or oxygen (75%) for 24 hours from the first, second or third day of disease. Scale bar = 1mm. **c)** Quantification of ED-1 labelling after treatment showed no changes between oxygen and time-matched room air controls. Two-way ANOVA with Sidak's correction ($p > 0.05$). IFA: n = 4 per group; EAE: n = 12 per group.

Activated microglia, infiltrated macrophages and reactive astrocytes have been reported to be the main sources of NO within the inflamed CNS. In these cells, NO is produced via the appearance of the inducible form of NO-synthase, iNOS. Augmented expression of iNOS indicates increased synthesis of NO. NO is an important inflammatory mediator involved in both oligodendrocytic and neuronal damage in MS (Smith and Lassmann, 2002). We followed the expression of iNOS in the spinal cord of rats with active EAE during the first three days of neurological deficits. As expected, iNOS labelling was not detected in non-inflamed IFA controls (Figure 2.5a). Immunohistochemistry for iNOS in EAE rats showed a similar distribution to ED-1 labelling (sub-meningeal and perivascular, Figure 2.5b) during the first two days of disease, confirming the inflammatory association of this enzyme (Figure 2.5a). Surprisingly, the expression of iNOS was higher at the first day of neurological deficits and decreased to control levels by the third day after onset (Figure 2.5a, b). However, while iNOS expression returned to control levels, the severity of neurological deficits increased and was greater three days after the onset of the disease (Figure 2.5 and Figure 2.2); suggesting that iNOS may only partially and transiently account for the neurological dysfunction occurring in active EAE. We then evaluated whether 24 hours of oxygen treatment on the first, second, or third day of disease can affect the spinal expression of iNOS in active EAE. Histological comparison of iNOS expression showed no differences between oxygen-treated rats and time-matched room air controls (Figure 2.5a, b).

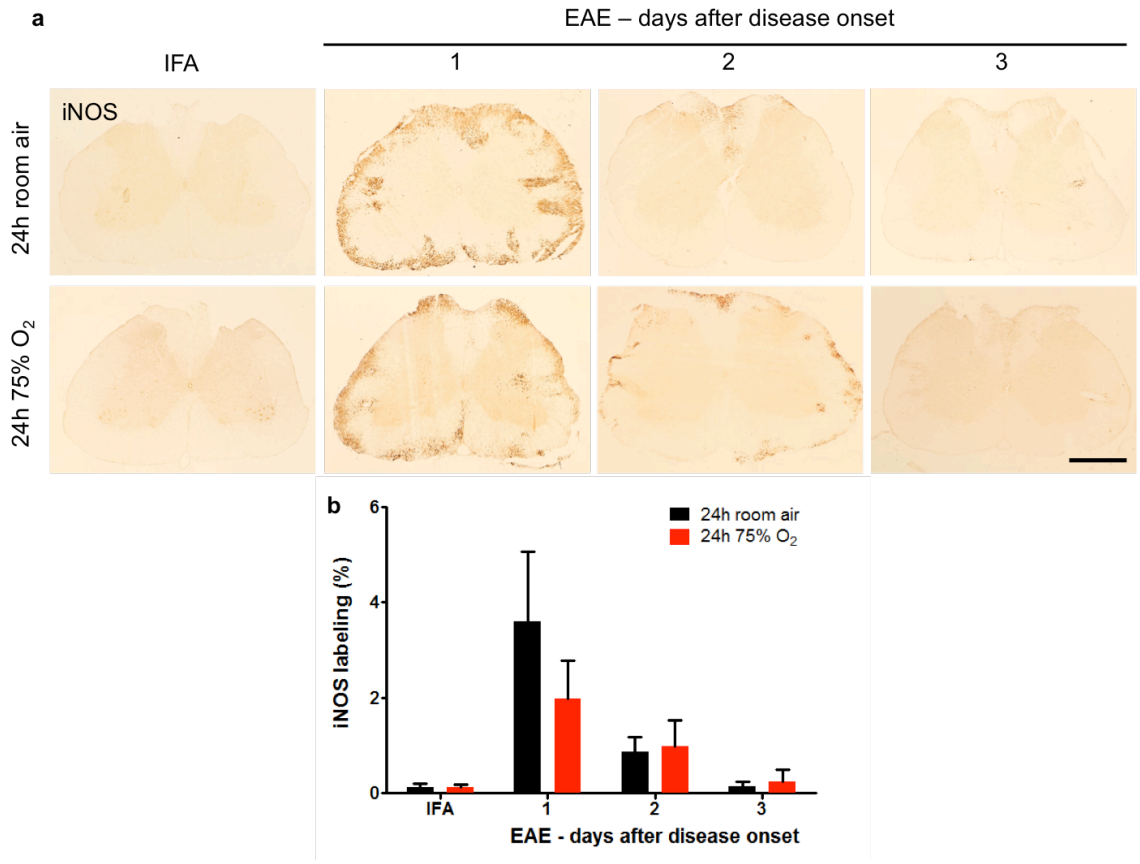

Figure 2.5 - iNOS expression is not affected by 24 hours of oxygen administration on either the first, second or third day of disease.
a) Lumbar spinal cord sections labeled for iNOS from IFA controls and rats with active EAE exposed either to oxygen (75%) for 24 hours, or room air, on either the first, second or third day of disease. EAE rats had higher iNOS expression one day after disease onset, but iNOS labelling gradually decreased on day two and three after onset. Scale bar = 1mm. **b)** iNOS quantification showed that oxygen administration to rats with active EAE on either the first, second or third day of disease, did not change iNOS expression compared with room air controls. Two-way ANOVA with Sidak's correction ($p > 0.05$). IFA: n = 4 per group; EAE: n = 12 per group.

2.2.2.3 HIF1α expression in the spinal cord of rats with active EAE is decreased by 24 hours of oxygen treatment

To evaluate whether 24 hours of oxygen treatment administered at different stages of disease (first, second or third day of deficits) can reverse tissue hypoxia, spinal cord cross sections of rats with active EAE and IFA controls were labeled for HIF1α. Although HIF1α can be increased by inflammation in addition to hypoxia, the expression of HIF1α is tightly correlated with the concentration of oxygen. Indeed, in normoxic conditions HIF1α is hydroxylated through an oxygen-dependent mechanism and it is promptly destroyed via proteasome degradation. In hypoxic conditions, HIF1α is not hydroxylated and therefore degraded; thus it binds the subunit HIF1β and translocates into the nucleus where activates the transcription of genes involved in the response to hypoxia (for more information see Introduction 1.10.1.0). Immunohistochemistry for HIF1α strongly labeled the spinal cord of rats with active EAE. In particular, HIF1α immunoreactivity increased with the progression of the disease and it was more intense three days after the onset (Figure 2.6a). In contrast, IFA controls had very low or absent HIF1α labelling (Figure 2.6a). Interestingly, in rats with active EAE the level of HIF1α was decreased after 24 hours of oxygen exposure from the first, second or third day of disease (Figure 2.6a), and significantly when oxygen was administered on the first ($p = 0.015$) and third ($p = 0.003$) day of disease (Figure 2.6b).

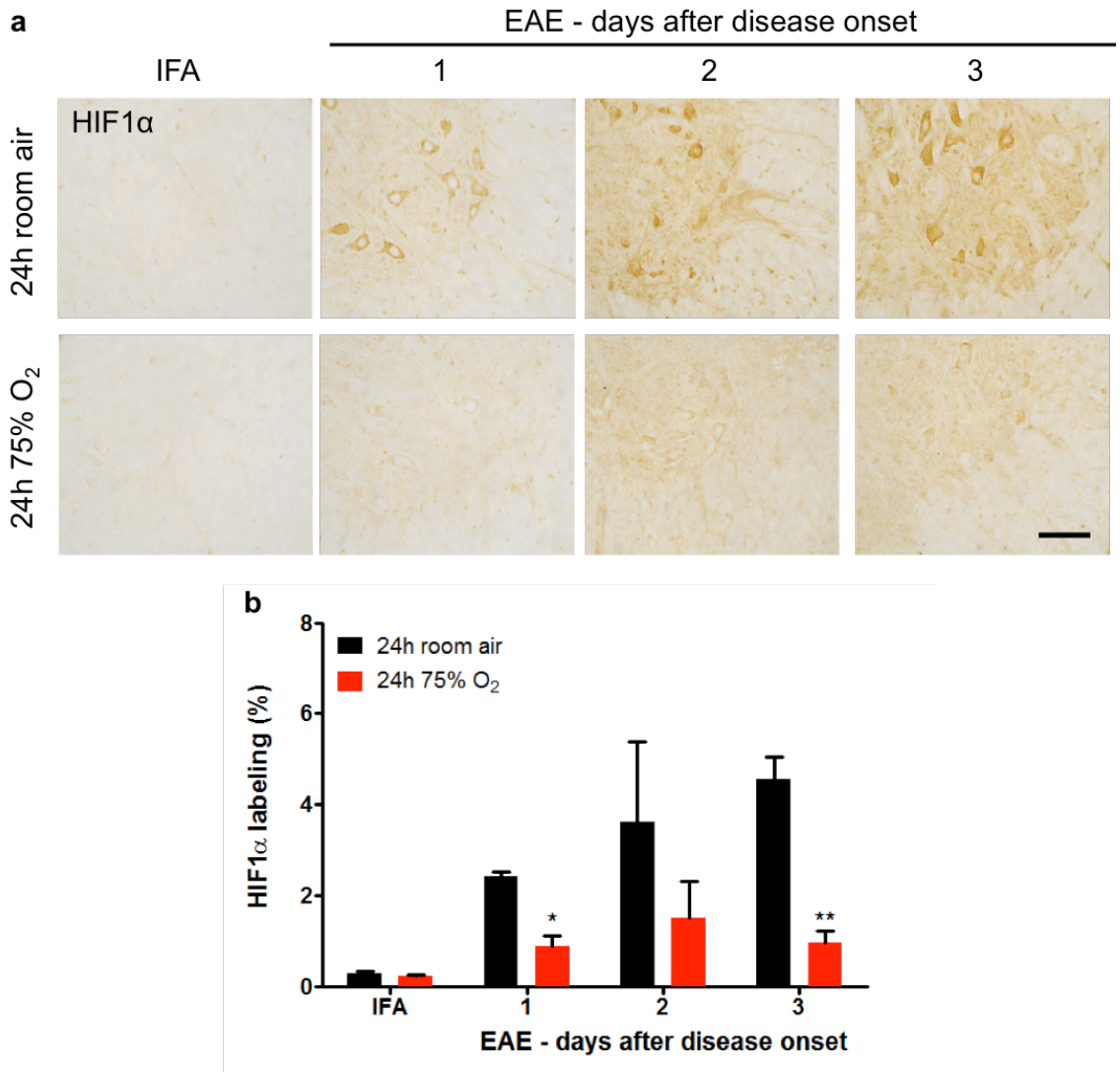

Figure 2.6 - Oxygen treatment for 24 hours from the first, second or third day of disease decreases tissue hypoxia in the spinal cord of rats with active EAE.
a) Immunohistochemical labelling for HIF1α (marker of tissue hypoxia) of spinal cord sections of IFA controls and rats with active EAE exposed to room air or oxygen for 24 hours on either the first, second or third day of disease. Representative images show the ventral grey matter area of the spinal cord. Rats with active EAE were characterized by a greater labelling for HIF1α than IFA controls, with labelling of motor neurons particularly prominent. The level of HIF1α increased with the progression of the disease and it was higher in rats at the third day after the onset of deficits (peak of disease). Rats with active EAE treated with oxygen for 24 hours showed reduced levels of HIF1α compared with room air controls. Scale bar = 200µm. **b)** Quantification of HIF1α immunolabelling shows that oxygen treatment decreased HIF1α expression in rats with active EAE independently of whether the treatment started on the first, second or third day of disease. HIF1α is significantly reduced in rats treated with oxygen on the first ($p = 0.015$) and third day of deficits ($p = 0.003$) compared with time-matched controls. Two-way ANOVA with Sidak's correction. IFA: n = 4 per group; EAE: n = 12 per group.

2.2.2.4 Glycolysis in the spinal cord of rats with active EAE is not affected by oxygen administration

There is evidence that markers of glycolysis are increased in the CNS of animals with active EAE (Sadeghian *et al.*, 2016). Cells may activate glycolysis in an attempt to overcome an energy deficit due to insufficient oxygen to sustain mitochondrial respiration. However, each molecule of glucose leads to the production of 34 ATP molecules via oxidative phosphorylation through the electron transport chain, but only 2 ATP molecules are made by glycolysis, suggesting that glycolysis may be not sufficient to compensate the energy deficit during active EAE. We hypothesized that by restoring tissue oxygenation via the administration of oxygen-enriched air, it may be possible to restore a more physiological cellular respiration able to overcome the activation of glycolysis. To investigate whether 24 hours of oxygen administration can reduce the cellular need for glycolysis, spinal cords of rats with active EAE were histologically labeled for an enzyme involved in glycolysis, namely PFK-2. Consistent with previous observations (Sadeghian *et al.*, 2016), we observed that while PFK-2 labelling was very low in healthy IFA controls, its expression was markedly higher in rats with active EAE (Figure 2.7a). Interestingly, PFK-2 signal was greater one and two days after disease onset, but it returned to control level by the third day of disease (Figure 2.7a, b). Analysis of the PFK-2 immunoreactivity in active EAE rats showed no differences after 24 hours of oxygen administration, independently of whether oxygen was applied on the first, second or third day of disease compared with time-matched cohort of rats kept in room air (Figure 2.7a and b).

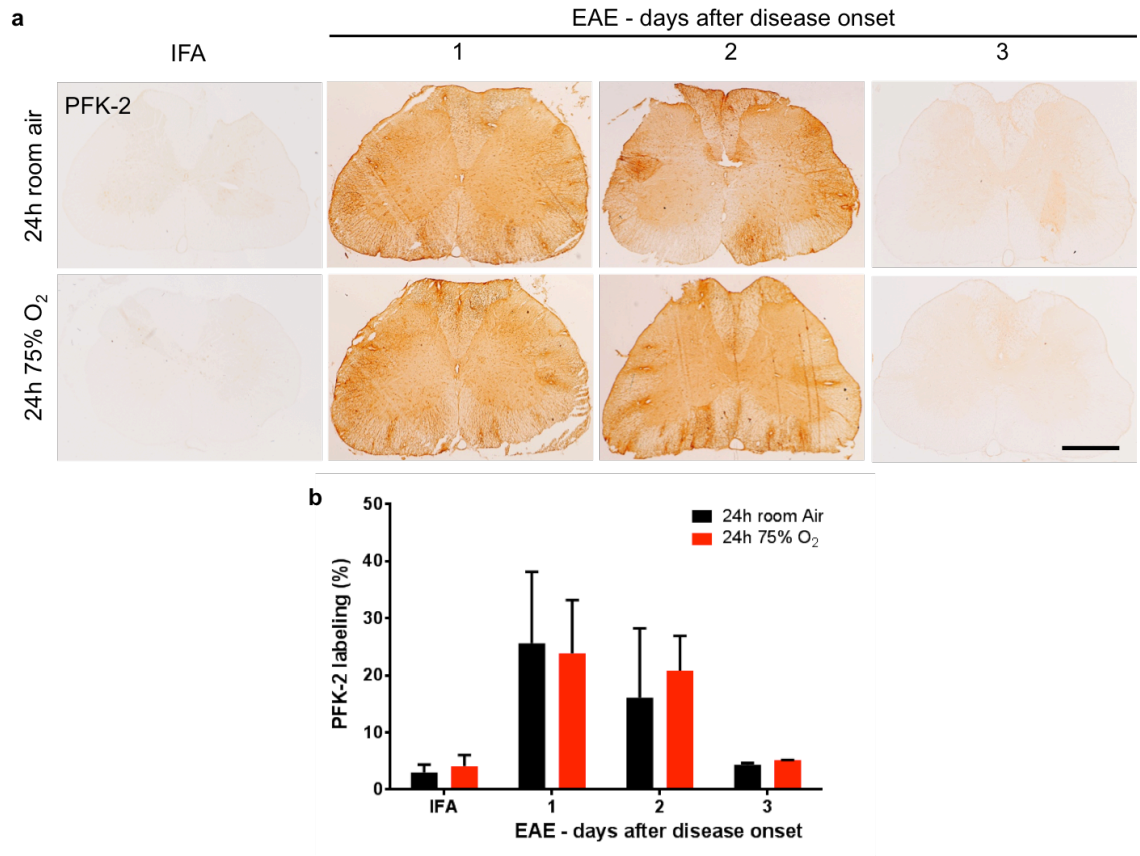

Figure 2.7 - 24 hours of oxygen administration does not change the expression of the glycolysis marker PFK-2 in the spinal cord of rats with active EAE.
a) Lumbar spinal cord cross sections of room air and oxygen-treated IFA controls and rats with active EAE were labeled for PFK-2, a marker of glycolysis. Oxygen was administered for 24 hours starting on either the first, second or third day of disease. Immunolabelling for PFK-2 was low in IFA rats. PFK-2 immunoreactivity was increased one and two days after EAE onset and returned to control levels by the third day after onset. Scale bar = 1mm. **b)** PFK-2 quantifications shows increased level of PFK-2 in rats with active EAE compared with healthy (IFA) controls. PFK-2 levels decreased during the progression of the disease and were not changed by oxygen administration. Two-way ANOVA with Sidak's correction ($p > 0.05$). IFA: n = 4 per group; EAE: n = 12 per group.

2.2.2.5 Oxygen therapy: effects on size and density of spinal cord blood vessels

Changes in blood oxygen concentration can lead to several adaptations aimed at restoring the optimal oxygen supply to the tissue requirements. One of the first organ responses to increased oxygen in the blood stream is the vasoconstriction of capillaries, which results in reduced blood flow to restore a normal oxygenation of the tissue. Therefore, it is reasonable to think that the administration of oxygen-enriched air may cause vasoconstriction that could impede the desired oxygen supply at the inflamed CNS. To evaluate whether oxygen therapy causes vasoconstriction in the CNS of rats with active EAE, the spinal cords were histologically labeled for Reca1, a marker of endothelial cells. Rats with active EAE treated with oxygen for 24 hours from the first, second or third day of disease were compared after treatment cessation with time-matched room air controls and IFA animals (exposed and non-exposed to oxygen for 24 hours). No changes in blood vessel size were observed in IFA controls exposed to oxygen compared with ones kept in room air (Figure 2.8a, b). Consistent with observation by Davies and colleagues (Davies *et al.*, 2013), rats with active EAE were characterized by increased vessel size compared with healthy controls, and this difference was significantly greater two days after disease onset ($p = 0.002$; Figure 2.8a, b). The enlargement of vessels may be a consequence of both inflammation and hypoxia occurring in active EAE. Interestingly, oxygen did not change the size of vessels compared with room air controls at any of the disease stages analysed (Figure 2.8a, b).

Then, we examined whether oxygen treatment affects the vascular network of the spinal cord by counting the number of Reca1 positive vessels. We did not detect any changes in IFA rats exposed to oxygen for 24 hours compared with IFA breathing room air (Figure 2.8a, c). A significant increase in Reca1 labeled vessels was instead measured in rats with active EAE at the second and third day of disease ($p = 0.016$ and $p = 0.032$ respectively) compared with healthy controls (Figure 2.8a, c). Oxygen-treated rats at the first, second or third day of disease for 24 hours did not show any difference compared with their respective controls maintained in room air (Figure 2.8a, c).

Although more sophisticated and precise techniques exist for the evaluation of endothelial function, vasodilation, angiogenesis and tissue vascularisation (Flammer *et*

al., 2012; Simons *et al.*, 2015), our histological data provide a preliminary indication that the administration of oxygen for 24 hours may not affect the size and number of spinal vessels during EAE.

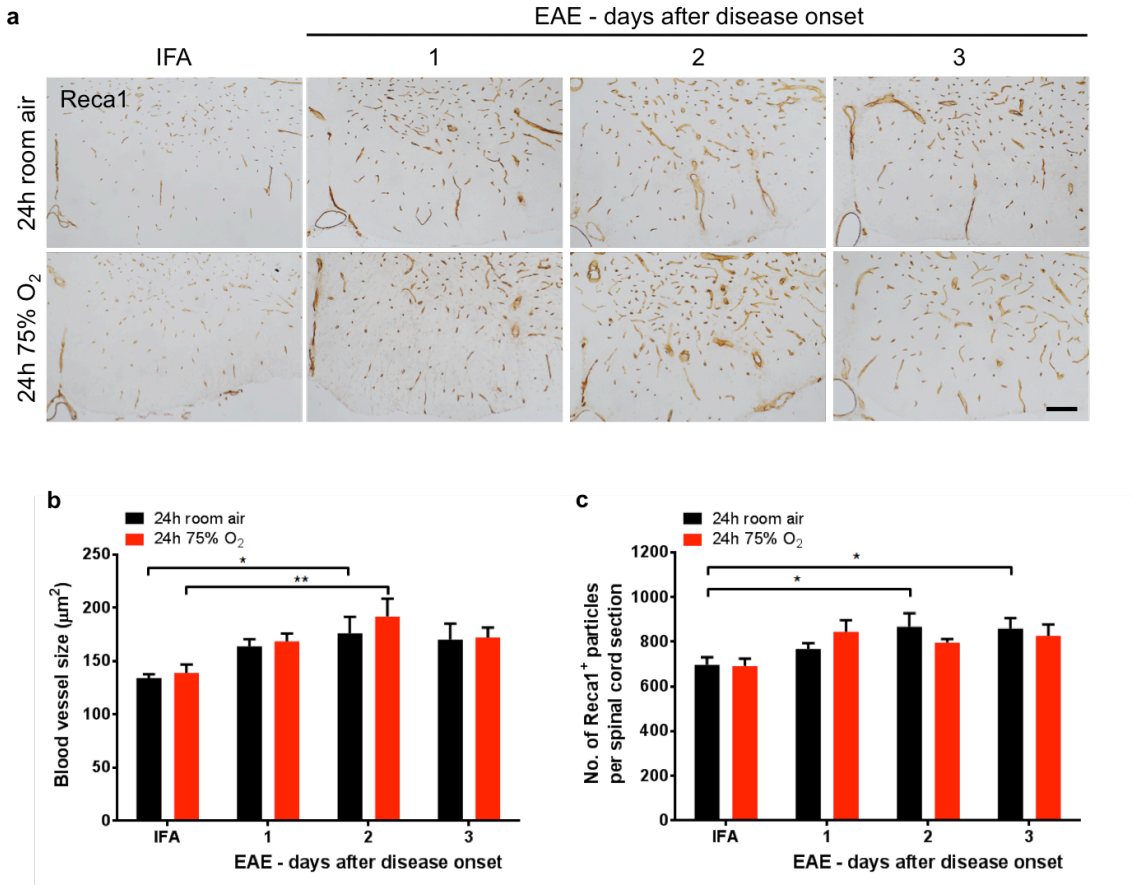

Figure 2.8 - Effects of 24 hours of oxygen administration on either the first, second or third day of disease on the spinal cord blood vessels in animals with active EAE.
a) Representative images show spinal cord anteromedian areas of rats with active EAE and IFA controls labeled for Reca1, a marker of endothelial cells. Rats with active EAE were treated with oxygen (or maintained in room air) for 24 hours from either the first, second or third day of disease and analysed after treatment cessation. IFA controls kept in room air or exposed to oxygen for 24 hours were used for comparison. Scale bar = 100µm. **b)** The size of Reca1-positive vessels appeared increased in rats with active EAE compared with IFA controls, and it was significantly increased in rats treated or untreated with oxygen at the second day of disease ($p = 0.018$ and $p = 0.002$ respectively) compared with their treatment-matched IFA controls. No changes were observed at each stage of disease between rats with active EAE treated with oxygen or kept in room air. **c)** The number of Reca1-positive particles was significantly increased in rats with active EAE at the second and third day of disease ($p = 0.016$ and $p = 0.032$ respectively) compared with IFA controls. No changes were observed between oxygen-treated and room air controls at each stage of disease. Two-Way ANOVA with Dunnett's correction. IFA: n = 4 per group; EAE: n = 12 per group.

2.2.3.0 Duration of oxygen treatment: 24, 48 and 72 hours of oxygen treatment from the onset of deficits

In the previous paragraphs, evidence was provided that oxygen is able promptly to improve neurological function in rats with active EAE even when administered for only 1 hour at the peak of disease, but the specific beneficial effect was transient. Next, we investigated the optimal timing to start the treatment by administering oxygen for longer (24 hours) on either the first, second or third day of disease. Interestingly, we discovered that oxygen treatment can ameliorate the disease progression independently of the stage of disease at which it is administered, although the greatest beneficial effect was observed when oxygen exposure started at the onset of neurological deficits. Thus, the administration of oxygen at the very early stage of disease appeared to be most effective in producing the largest improvement of the disease. Here we examine different durations (24, 48 and 72 hours) of oxygen exposure from the onset of neurological deficits. The aims are 1) to evaluate what is the optimal duration for oxygen therapy, 2) how long the beneficial effect persists after treatment cessation, and 3) whether prolonged exposure to oxygen can change the pathology of active EAE.

2.2.3.1 Oxygen treatment from the onset of neurological deficits ameliorates disease progression

Rats with active EAE (n = 28) were randomly allocated to receive oxygen (75%) for 24, 48 or 72 hours from the onset of disease (respectively: n = 6, n = 8 and n = 7). Control rats were not exposed to oxygen but kept in room air for the entire duration of the trial (n = 8). After treatment with oxygen, the animals were returned in room air, and the magnitude of the neurological deficits was followed up to 9 days after the onset of neurological signs (second peak of disease). Interestingly, we observed that oxygen ameliorated the severity of the disease even when administered only for the first 24 hours (Figure 2.9). During the first peak of disease (first three days after onset) more than 30% of the rats in all treated groups (33% in the 24 hours, 50% in the 48 hours and 43% in the 72 hours oxygen-treated groups) did not develop hind limb paralysis, whereas 75% of animals receiving room air lost voluntary motor control of their hind limbs (score > 8; Figure 2.9). Remarkably, the beneficial effect of oxygen persisted for several days after treatment cessation, and all oxygen-treated groups displayed an average score for neurological dysfunction always lower than the room air control

(Figure 2.9). Notably, rats treated with oxygen for 24, 48 or 72 hours experienced a better recovery of the neurological function after the first attack of disease (remitting phase) compared with controls, and particularly when treated for the first 72 hours (Figure 2.9). However, although oxygen administered at the onset of disease attenuated the overall severity of deficits providing a better and longer recovery during the remitting phase, it did not avoid the development of the second peak of neurological deficits (Figure 2.9).

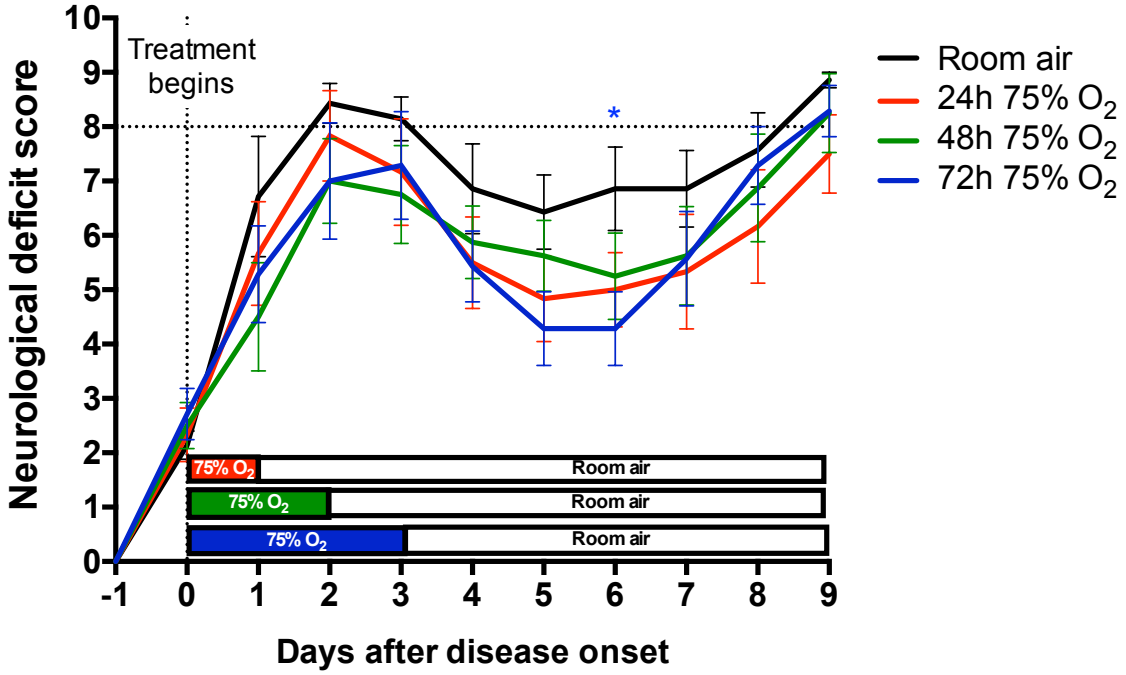

Figure 2.9 - Treatment with oxygen (75%) for 24, 48 or 72 hours from the onset of neurological deficits attenuates disease progression for several days after treatment cessation.
Disease progression in rats with active EAE randomly allocated to receive either oxygen for 24, 48 or 72 hours from the onset of neurological signs (day 0; vertical dashed line), or room air. After treatment, rats were returned to room air and the neurological deficits were monitored for up to 9 days after the onset of deficits (second peak of disease). All durations of oxygen exposure (24, 48 or 72 hours) ameliorated disease progression and the beneficial effect persisted for several days after treatment cessation. In contrast with the room air group, the mean average score of rats treated with oxygen always lay on or below score 8 (indicating hind limb paralysis; horizontal dashed line). Rats treated with oxygen experienced a more pronounced remission of the neurological deficits after the first peak of disease compared with room air controls, which was significant at day six in rats treated for 72 hours with oxygen ($p = 0.039$). Mann Whitney U-test. Room air, $n = 7$; 24h 75% O_2, $n = 6$; 48h 75% O_2, $n = 8$; 72h 75% O_2, $n = 7$.

We then performed another independent active EAE trial (n = 36) in which rats were similarly treated with oxygen from the onset of disease for 24, 48 or 72 hours (respectively: n = 10, n = 9 and n = 9). Rats treated with oxygen for 24 and 48 hours were returned to room air after oxygen administration. Rats with active EAE that received only room air (n = 8) were used as controls. All animals were sacrificed at the third day of disease (peak of disease) for histological analysis. Consistent with the previous trial, we observed that oxygen ameliorated disease severity in all treated groups and the beneficial effect persisted even after rats were returned to room air (Figure 2.10a). At the peak of disease, rats treated with oxygen for 24, 48 or 72 hours showed on average a reduction in the severity of the disease respectively of 18%, 25% and 15% at the neurological examination compared with controls (Figure 2.10a and b). In particular, more than 50% of rats in all oxygen groups did not develop hind limb paralysis (score < 8; Figure 2.10b), whereas 7 out of 8 rats in the room air control group reached score 8 or 9 upon behavioural testing (Figure 2.10b). In particular, rats exposed to oxygen for 48 hours showed the greatest improvement in neurological score compared with controls ($p = 0.038$; Figure 2.10b). Furthermore, we weighed rats with active EAE on a daily base from the day of immunization, and the weight was considered as a parameter of general health. Indeed, healthy rats gradually increase their body weight over time, but they start progressively to lose weight when neurological deficits appear (Figure 2.10c). The magnitude of body weight loss is considered a bad prognosis for disease. Interestingly, we noticed that rats with active EAE treated with oxygen were characterized by reduced body weight loss compared with control rats breathing room air (Figure 2.10c). Notably, the percentage of body weight lost at the peak of disease was significantly decreased in rats treated with oxygen for 72 hours compared with controls ($p = 0.030$; Figure 2.10d).

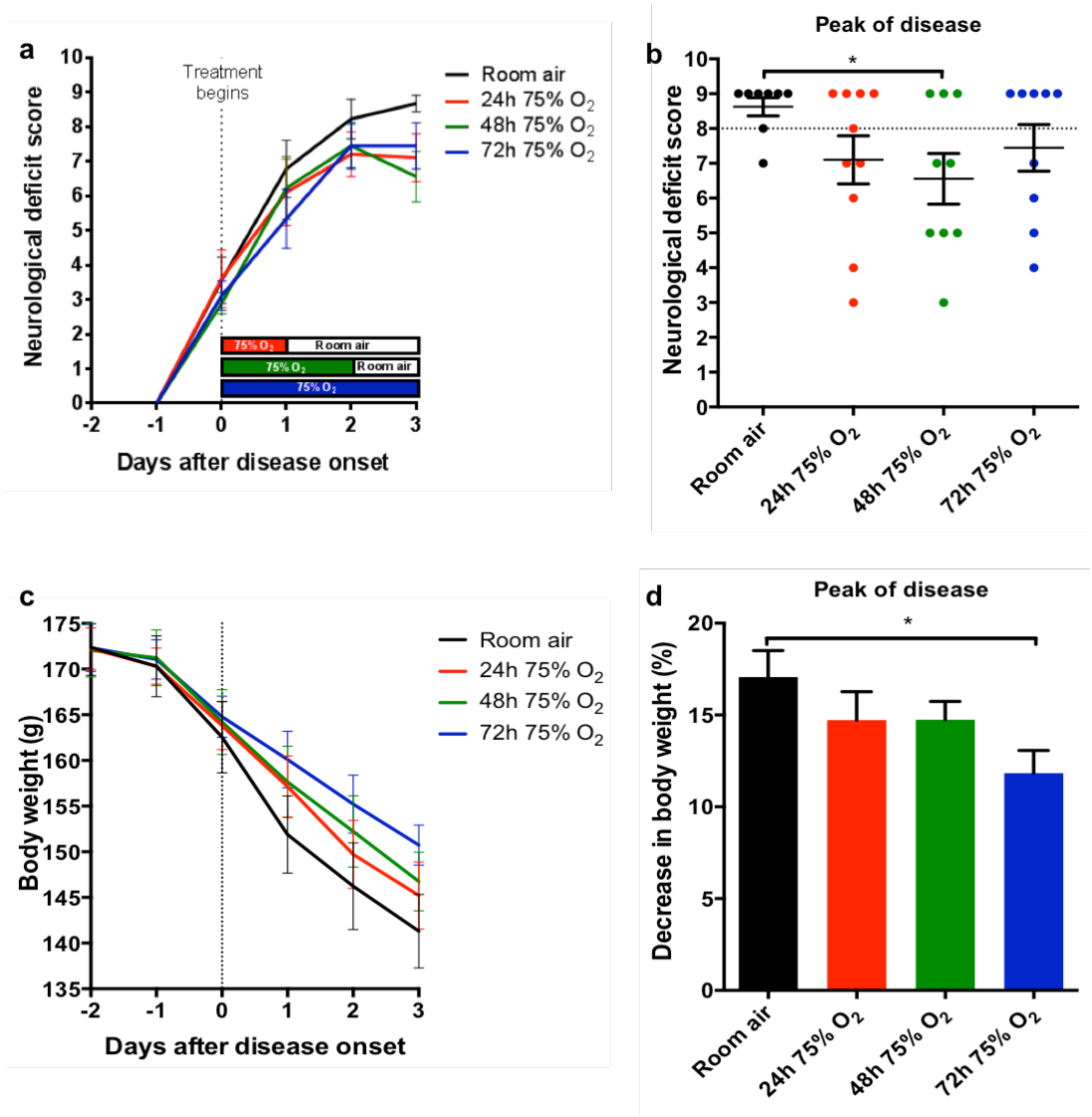

Figure 2.10 - Oxygen treatment (75%) for 24, 48 and 72 hours from the onset of disease ameliorates the severity of neurological deficits at the first peak of disease.
a) Progression of neurological deficits during the first peak of active EAE in rats treated with oxygen from the onset of disease (day 0; vertical dashed line) for 24, 48 or 72 hours or maintained in room air. Rats treated with oxygen for 24 and 48 hours were returned to room air up to the third day of disease. All oxygen-treated groups displayed less severe progression of the disease overall compared with room air controls. **b)** Neurological deficit score at the peak of disease (3 days after onset) shows that more than 50% of rats treated with oxygen did not develop hind limb paralysis (score < 8), whereas only one rat in the room air control group showed a score lower than 8. The severity of neurological dysfunction at the peak of disease was significantly reduced in rats treated with oxygen for 48 hours ($p = 0.038$) compared with room air controls. Mann-Whitney U-test. **c)** Rats with active EAE experienced a gradual decrease in body weight from the onset of neurological deficits (day 0; vertical dashed line) that was less severe in the ones treated with oxygen. **d)** Analysis of body weight loss at the peak of disease shows that rats treated with oxygen lost less weight than room air controls, and significantly less when treated for 72 hours ($p = 0.030$). One-way ANOVA with Dunnett's correction. Room air, n = 8; 24h 75% O_2, n = 10; 48h 75% O_2, n = 9; 72h 75% O_2, n = 9.

As mentioned before, the rats included in this trial were sacrificed at the peak of disease (3 days after onset) and the spinal cords collected for histological and analysis. IFA control rats (n = 8) were included and used for comparison. Demyelination, hypoxia, integrated stress response, inflammation and oxidative damage were evaluated as described in the following paragraphs.

2.2.3.2 Oxygen protects from spinal cord demyelination

Demyelination was evaluated by staining the spinal cord of rats included in the previous trial with LFB, or immunolabelling for MOG. Healthy rats (IFA) were also analysed and used as negative (non-demyelinated) controls. Rats with active EAE were treated with oxygen from the onset of neurological deficits for 24, 48 or 72 hours, whereas control rats were exposed to room air only. All animals were sacrificed and analysed at the third day of disease (peak of neurological deficits). Histology for LFB and MOG showed a similar pattern of demyelination in the white matter (Figure 2.11a). However, immunohistochemistry for MOG disclosed a sharper difference between demyelinated lesions and intact white matter compared with LFB staining (Figure 2.11a); thus MOG labelling was preferred to LFB for the quantification of the extension of demyelinated lesions. Interestingly, we observed that white matter demyelination was reduced in rats treated with oxygen in proportion to the duration of the treatment (Figure 2.11a, b). Indeed, rats treated for 72 hours were the most protected ones compared with room air controls ($p = 0.002$; Figure 2.11b). To investigate which areas of the spinal cord were more affected by demyelination, the sacral, lumbar and thoracic levels of the spinal cord were considered separately (Figure 2.11c). The sacral spinal cord sections were severely demyelinated and such demyelination affected a larger portion of the white matter surface compared with the lumbar and thoracic levels (Figure 2.11c). Interestingly, all oxygen-treated groups showed a general reduction of demyelination at all levels of the spinal cord compared with room air controls, although the protective effect was greater in the sacral segment, and particularly so in rats treated with oxygen for 48 ($p = 0.002$) and 72 ($p < 0.0001$) hours compared with room air controls (Figure 2.11c). These data suggest that oxygen administered at the onset of deficits can reduce the overall spinal cord demyelination at the first peak of disease in a proportional manner to the duration of the treatment and significantly when applied for 72 hours. In

particular, the protective effect occurred only at the sacral level of the spinal cord and in rats treated with oxygen for 48 and 72 hours.

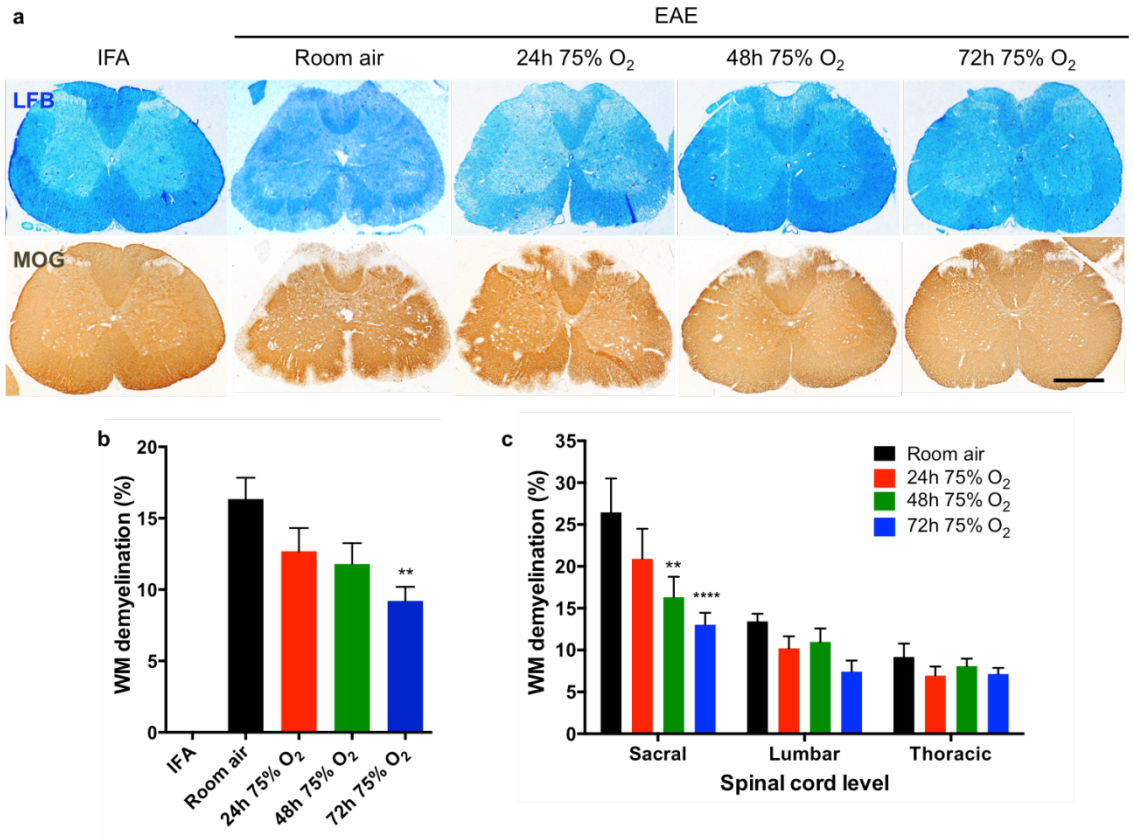

Figure 2.11 - Oxygen administration (75%) for 24, 48 and 72 hours from the onset of neurological deficits protects from spinal cord demyelination at the peak of disease in proportion with the duration of the treatment.
a) Representative images show adjacent lumbar spinal cord sections of IFA controls and EAE rats at the peak of disease stained for LFB (blue) or immunolabeled for MOG (brown). Rats with active EAE were exposed to room air or treated with oxygen from the onset of disease for 24, 48 or 72 hours. Absence of LFB staining or MOG labelling highlights demyelinated areas. IFA controls were not demyelinated. LFB staining and MOG immunolabelling disclosed a similar pattern of white matter (WM) demyelination in rats with active EAE. Scale bar = 1mm. **b)** Quantification of MOG labelling in animals with active EAE showed reduced demyelination in the WM of rats treated with oxygen in proportion to the duration of the treatment. 72 hours treated rats were significantly less demyelinated than room air controls ($p = 0.002$). One-way ANOVA with Dunnett's correction. **c)** Demyelination was more severe in the WM of the sacral level compared with the lumbar and thoracic levels of the spinal cord. Oxygen resulted in reduced demyelination at all levels of the spinal cord, and significantly in the sacral area in rats treated for 48 ($p = 0.002$) and 72 ($p < 0.0001$) hours compared with controls. Two-way ANOVA with Dunnett's correction. IFA, n = 8; Room air, n = 8; 24h 75% O_2, n = 10; 48h 75% O_2, n = 9; 72h 75% O_2, n = 9.

2.2.3.3 HIF1α expression at the peak of disease after 24, 48 and 72 hours of oxygen exposure

We have previously demonstrated that oxygen can decrease the level of HIF1α (a marker of tissue hypoxia) in the spinal cord of rats with active EAE straight after 24 hours of administration, and independently of the stage of disease at which the treatment was applied (paragraph 2.2.2.3). Here, we examine if oxygen therapy administered at the onset of deficits can reduce spinal cord hypoxia at the peak of disease (3 days after onset) even in rats which are returned in room air after oxygen exposure. Rats with active EAE were treated with oxygen from the first day of neurological signs for either 24, 48 or 72 hours. Rats exposed to oxygen for 24 and 48 hours were then returned to room air for two or one extra days respectively. All rats were examined at the peak of disease (third day of disease) and compared with room air controls. HIF1α was labeled histologically to demarcate tissue hypoxia. While IFA controls showed very low HIF1α labelling in the spinal cord, HIF1α expression was higher in rats with active EAE at the peak of disease and diminished in animals treated with oxygen (Figure 2.12a). Indeed, quantification of HIF1α immunoreactivity showed a non-significant trend of reduced HIF1α expression in rats treated with oxygen for 24, 48 or 72 hours from the onset of disease. Notably, this trend of reduced expression of HIF1α was proportional to the duration of the treatment (Figure 2.12b).

Administration of oxygen-enriched air in rats with active EAE from the onset of disease for 24, 48 or 72 hours, did not significantly change the level of tissue hypoxia at the peak of neurological deficits, but it was observed a trend of decreased HIF1α expression compared with room air controls (Figure 2.12). The level of HIF1α was higher in rats that were treated for only 24 or 48 hours and then returned in room air compared with the ones that were exposed to oxygen up to the peak of disease (72 hours; Figure 2.12b). This finding suggests that tissue hypoxia can reappear when rats are returned in room air after oxygen, but such hypoxia is attenuated at least up to two days after treatment cessation compared with room air controls (Figure 2.12b).

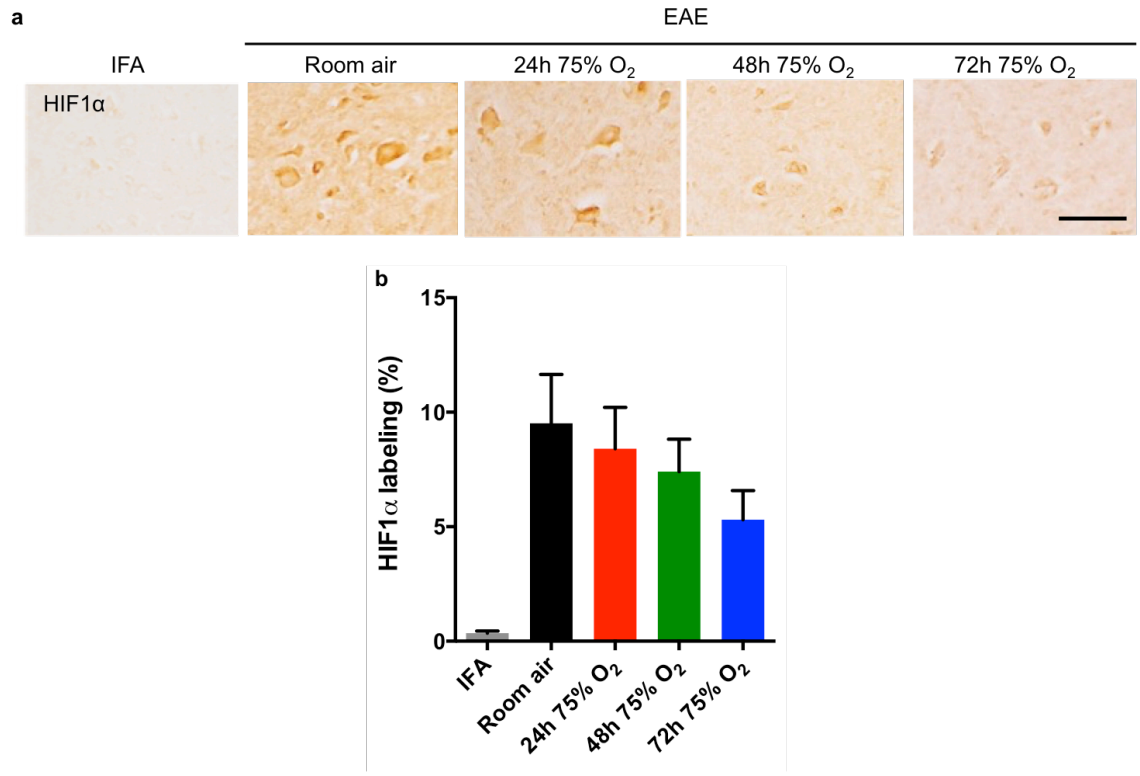

Figure 2.12 - HIF1α expression at the peak of disease is reduced by oxygen administration from the onset of deficit for 24, 48 or 72 hours and proportionally to the duration of the treatment.

a) Immunohistochemistry for HIF1α in spinal cord of rats with active EAE at the peak of disease and in IFA controls. Representative images show the grey matter (ventral horn) of the spinal cords. Rats with active EAE were exposed to room air or treated with oxygen for 24, 48 and 72 hours from the onset of deficits. Increased HIF1α labelling was observed in rats with active EAE compared with IFA controls. The magnitude of HIF1α immunoreactivity inversely correlated with the duration of oxygen treatment. Scale bar = 200μm. **b)** Quantification of spinal cord cross-sections labeled for HIF1α showed diminished HIF1α levels in rats with active EAE that were exposed to oxygen for 24, 48 or 72 hours from the onset of disease compared with room air controls. The reduction in HIF1α labelling was proportional to the duration of the treatment. One-way ANOVA with Dunnett's correction ($p > 0.05$). IFA, n = 8; Room air, n = 8; 24h 75% O_2, n = 10; 48h 75% O_2, n = 9; 72h 75% O_2, n = 9.

2.2.3.4 Oxygen decreases the integrated stress response and promotes oligodendrocyte survival

A number of studies have reported the activation of stress related mechanisms, known as the integrated stress response, in different cells within the CNS during active EAE (Kumagami *et al.*, 1999; Chakrabarty *et al.*, 2004; Lin and Popko, 2009) as well as in MS (Allen *et al.*, 2001; Kutzelnigg *et al.,* 2005; Cunnea *et al.*, 2011; McMahon *et al.*, 2012; Ní Fhlathartaigh *et al.*, 2013). Stress conditions, such as hypoxia, viral infection, glucose deprivation, ER stress and inflammation, have been reported to enhance the integrated stress response (Donnelly *et al.*, 2013). The hallmark of the integrated stress response is the phosphorylation of eIF2α, a key factor involved in protein translation. Phosphorylation of eIF2α (p-eIF2α) leads to a general attenuation of protein synthesis and to downstream expression of cytoprotective genes (Donnelly *et al.*, 2013). Hypoxia is believed to induce phosphorylation of eIF2α in the cellular attempt to save energy by decreasing the rate of protein synthesis (Koumenis *et al.*, 2002). However in active EAE, the phosphorylation of eIF2α has been mainly attributed to inflammation and in particular to a mechanism mediated by IFNγ (Lin and Popko, 2009). Here, we compared cellular stress in rats with active EAE and healthy controls (IFA) by histology, using p-eIF2α as a marker. Furthermore, we evaluated whether the administration of oxygen in EAE rats affected the level of p-eIF2α expression in the inflamed CNS.

P-eIF2α was first evaluated in neurons by labelling the neuronal cell bodies with NeuN (Figure 2.13). Both animals with active EAE and IFA controls were characterized by the presence of p-eIF2α positive foci in the neuronal cytoplasm (Figure 2.13). We did not observe any differences between IFA controls and rats with active EAE, suggesting that part of the eIF2α pool in neurons is normally phosphorylated in the healthy condition, and this does not increase at the first peak of active EAE (Figure 2.13).

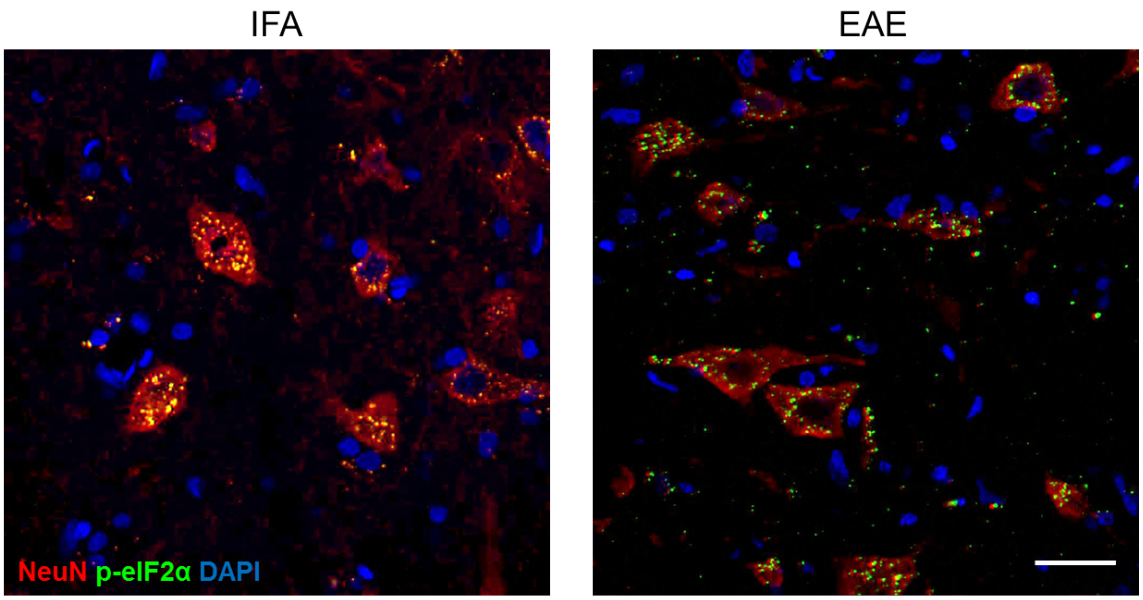

Figure 2.13 - Immunofluorescence of neurons co-labeled for NeuN and p-eIF2α in a rat with active EAE and in an IFA control.
Neurons were co-labeled in immunofluorescence using NeuN (red, a marker of neuronal cell bodies) and p-eIF2α (green, a marker of integrated stress response). DAPI was used to mark cell nuclei. P-eIF2α positive foci were observed in the cytoplasm of neurons of rats with active EAE as well as in IFA controls. Scale bar = 100µm.

Next, we examined the expression of p-eIF2α in CC1 labeled mature oligodendrocytes at the peak of disease (Figure 2.14). Consistent with previous studies (Chakrabarty *et al.*, 2004; Lin and Popko, 2009), while IFA controls did not show any CC1 positive oligodendrocytes co-labeled for p-eIF2α, CC1/p-eIF2α double positive cells were present in the spinal cord of rats with active EAE (Figure 2.14). P-eIF2α positive oligodendrocytes were detected in both oxygen-treated (for 24, 48 or 72 hours from the onset of deficit) and room air control-rats (Figure 2.14).

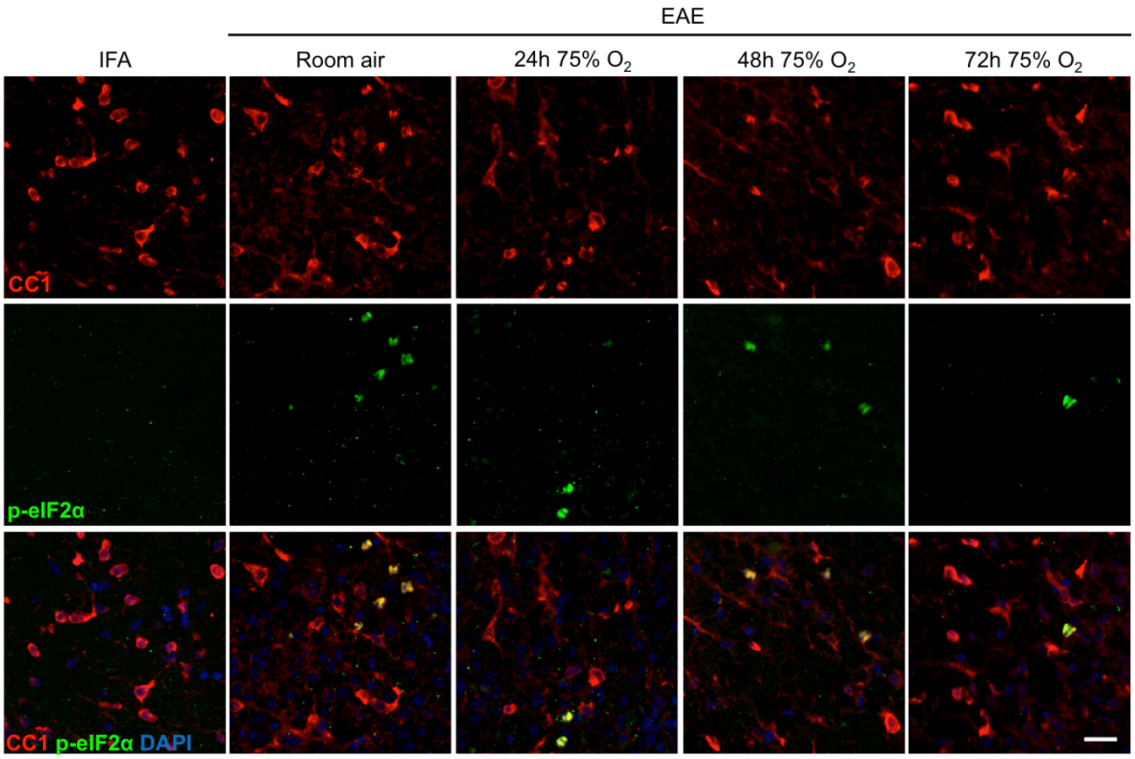

Figure 2.14 - Some oligodendrocytes show p-eIF2α labelling at the peak of active EAE. Immunofluorescence for CC1 (red, marker of mature oligodendrocytes) and p-eIF2α (green) in the spinal cord of IFA controls and rats with active EAE exposed to room air or oxygen for 24, 48 or 72 hours from the onset of disease. DAPI was used to mark cell nuclei. IFA controls did not show CC1 positive oligodendrocytes co-labeled for p-eIF2α. In contrast, CC1/p-eIF2α double positive oligodendrocytes were observed in rats with active EAE at the peak of disease in all oxygen-treated, and in room air controls. Scale bar = 20μm.

We then evaluated whether oxygen treatment administered at the onset of neurological deficits for 24, 48 or 72 hours, changed the number of p-eIF2α positive oligodendrocytes at the peak of disease. CC1/p-eIF2α double positive cells were counted within the dorsal column and the anteromedian area of the spinal cords, as these areas were the most commonly affected by inflammation and demyelination in room air control rats with active EAE. The number of CC1/p-eIF2α double positive cells was then expressed as a percentage of the total number of CC1 positive cells counted in the same areas (see Matherial and Methods 2.1.6.0). We did not find any CC1 positive oligodendrocyte labeled for p-eIF2α in IFA controls (Figure 2.15), but a significantly increased number of p-eIF2α positive oligodendrocytes was detected in rats with active EAE breathing room air ($p = 0.004$; Figure 2.15b). Interestingly, the

amount of CC1/p-eIF2α double-positive cells was decreased in all oxygen-treated groups compared with room air controls, and significantly decreased in rats treated for 72 hours (p = 0.011; Figure 2.15).

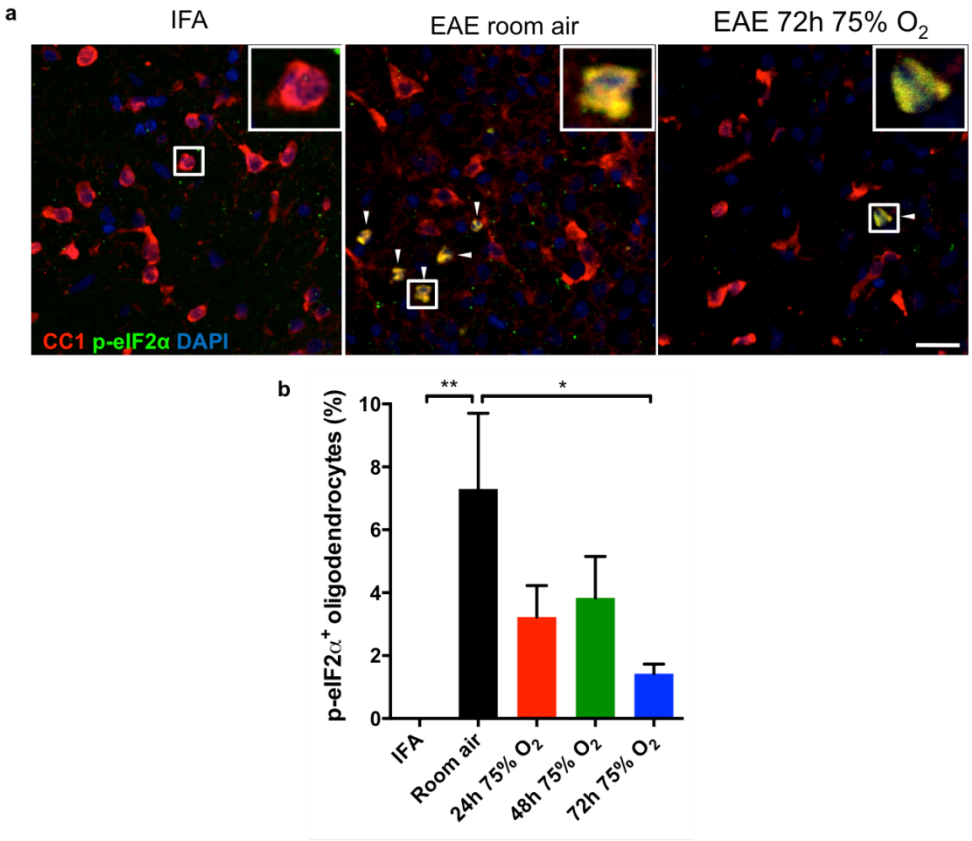

Figure 2.15 - Oxygen treatment for 24, 48 or 72 hours from the onset of neurological deficits reduces the number of p-eIF2α positive oligodendrocytes at the peak of disease. **a)** Immunofluorescence for CC1 (red, oligodendrocytes), p-eIF2α (green) and DAPI (blue, cell nuclei) in the spinal cord of IFA controls and rats with active EAE at the peak of disease after exposure to room air or oxygen for 72 hours. White arrowheads indicate CC1/ p-eIF2α double positive cells. High magnification insets show: absence of p-eIF2α labelling in CC1 positive oligodendrocyte in IFA controls, but CC1/p-eIF2α double labelling in rats with active EAE. Scale bar = 20µm. **b)** Cell counting revealed a significant increase of oligodendrocytes immunoreactive for p-eIF2α in rats with active EAE (p = 0.004) compared with IFA controls. The number of CC1/p-eIF2α double positive oligodendrocytes was decreased after treatment with oxygen, and significantly decreased in animals exposed to oxygen for 72 hours (p = 0.011) compared with room air controls. Scale bar = 20µm. One-way ANOVA with Dunnett's correction. IFA, n = 8; Room air, n = 8; 24h 75% O_2, n = 10; 48h 75% O_2, n = 9; 72h 75% O_2, n = 9.

Although the integrated stress response is a protective mechanism that cells use to tolerate stress conditions, it can lead to apoptosis if the initial insult persists for too long and a physiological rate of protein synthesis is not restored (Tabas and Ron, 2011). Therefore, we investigated whether the reduced phosphorylation of eIF2α in oxygen-treated rats with active EAE was affecting oligodendrocyte survival. We counted the number of CC1 positive oligodendrocytes in rats with active EAE treated and untreated with oxygen and in IFA controls (Figure 2.16). At the peak of disease, rats with active EAE receiving room air experienced a remarkable loss of oligodendrocytes, expressed by a significantly lower number of CC1 positive cells compared to IFA controls ($p = 0.008$; Figure 2.16b). Interestingly, oxygen treatment resulted in an increased oligodendrocyte survival in proportion to the duration of the exposure (Figure 2.16b). Notably, rats treated with oxygen for 72 hours showed a significantly higher number of oligodendrocytes compared with room air controls ($p = 0.005$), and the average number of oligodendrocytes in this group was similar to IFA control (Figure 2.16b).

The findings above suggest that hypoxia can contribute to cellular stress in oligodendrocytes during active EAE. Notably, oxygen administration from the onset of deficit can reduce eIF2α phosphorylation (a marker of cell stress) in these cells at the peak of disease, probably restoring a more physiological rate of protein synthesis. Interestingly, this phenotype was proportional to the duration of oxygen exposure.

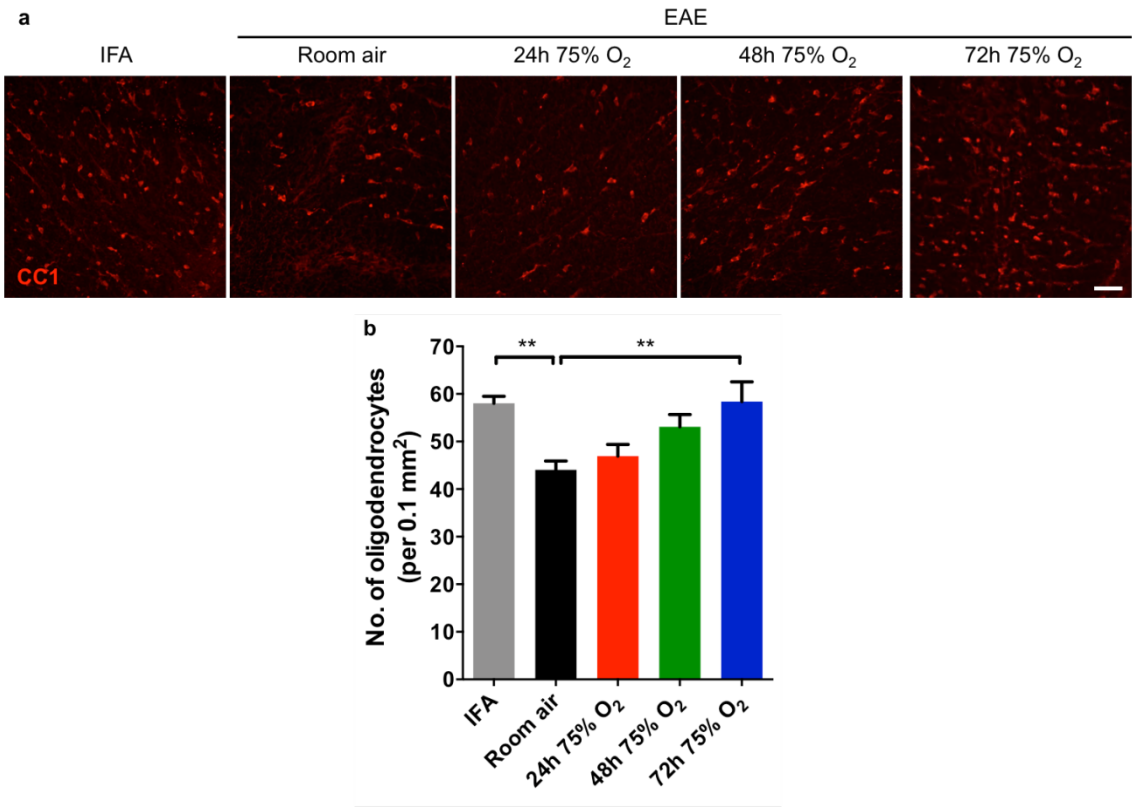

Figure 2.16 - Oxygen treatment (75%) from the onset of neurological deficit for 24, 48 or 72 hours protect from oligodendrocyte loss at the peak of disease.
a) Representative images show immunofluorescence for CC1 (red, oligodendrocytes) in the spinal cord dorsal column of IFA controls and rats with active EAE at the peak of disease. Rats with active EAE were maintained in room air or exposed to oxygen from the onset of deficits for either 24, 48 or 72 hours. Scale bar = 100µm. **b)** CC1 positive cell counts at the peak of disease highlight a significantly decreased number of oligodendrocytes in rats with active EAE breathing room air ($p = 0.008$) compared with IFA controls. Oxygen protected from oligodendrocyte death in proportion to the duration of the treatment and significantly in rats exposed to oxygen for 72 hours ($p = 0.005$) compared with room air controls. One-way ANOVA with Dunnett's correction. IFA, n = 8; Room air, n = 8; 24h 75% O_2, n = 10; 48h 75% O_2, n = 9; 72h 75% O_2, n = 9.

2.2.3.5 Oxygen does not affect T-cell infiltration in the spinal cord

To investigate whether oxygen treatment affects the inflammatory response in rats with active EAE, we evaluated: 1) T-cell infiltration, 2) microglial activation, macrophage infiltration, and iNOS expression, and 3) gene expression of pro- and anti-inflammatory markers.

Here we examined T-cell infiltration in the spinal cord of rats with active EAE maintained in room air or treated with oxygen (75%) from the onset of neurological signs for 24, 48 or 72 hours. All animals were histologically analysed three days after the onset of disease (peak of disease). T-cells were labeled using antibodies against CD3, and isolated T-cells or clusters of T-cells were considered separately (Figure 2.17a). IFA controls did not show any T-cell infiltration into the spinal cord (Figure 2.17a). The number of isolated CD3-positive cells dispersed within the spinal cord parenchyma of rats with active EAE did not change between oxygen-treated groups and rats in room air (Figure 2.17b). Similarly, oxygen treatment did not alter either the number or size of CD3-positive cell clusters compared with room air controls (Figure 2.17c and d).

These data suggest that oxygen treatment administered at the onset of deficits does not change the number of T-cells present in the CNS of rats with active EAE at the peak of disease.

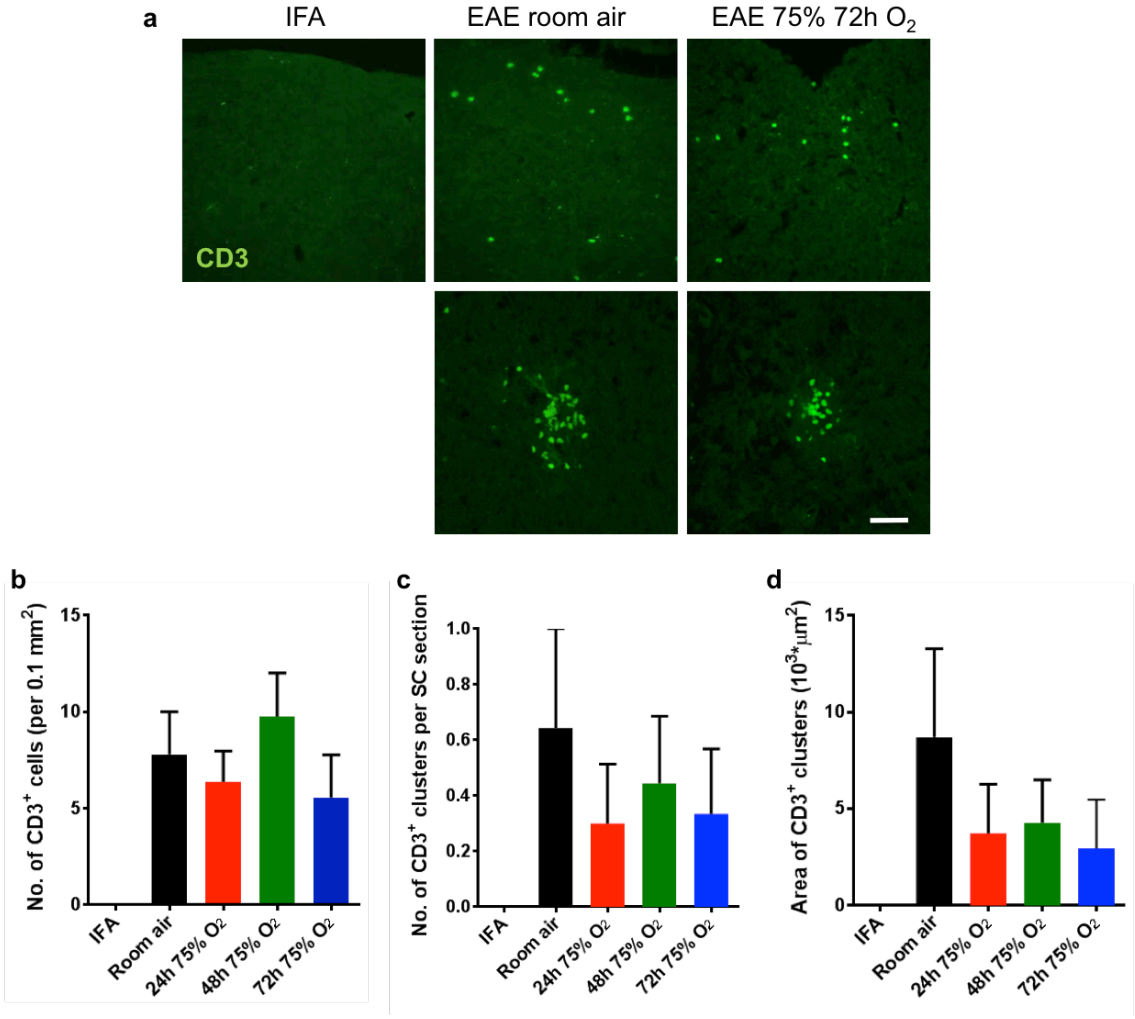

Figure 2.17 - T-cell infiltration at the peak of disease does not change after 24, 48 or 72 hours of oxygen treatment from the onset of deficits in active EAE.
a) T-cells were labeled by immunofluorescence for CD3 (green). Images show isolated T-cells and clusters of T-cells into the spinal cord of rats with active EAE at the peak of disease after room air or oxygen exposure for 72 hours from the onset of deficits. No CD3-positive cells were detected in the spinal cord of IFA controls. Scale bar = 50µm. **b)** Quantification of the number of CD3-positive cells in the spinal cord of rats at the peak of disease did not show changes between room air and oxygen-treated groups. **c-d)** The number and size of CD3-positive clusters within the spinal cord of rats at the peak of disease did not change in animals treated with oxygen for 24, 48 and 72 hours from the onset of deficits, compared with room air controls. One-way ANOVA with Dunnett's correction ($p > 0.05$). IFA, n = 8; Room air, n = 8; 24h 75% O_2, n = 10; 48h 75% O_2, n = 9; 72h 75% O_2, n = 9.

2.2.3.6 Microglial activation and macrophage infiltration is reduced in rats treated with oxygen from the onset of disease

Activated microglia and infiltrated macrophages in the spinal cord of rats with active EAE were immunohistochemically labeled for ED-1. ED-1 has been shown to be expressed by blood-derived monocytes/macrophages and activated microglia during active EAE and ischaemic stroke in rats (Bauer *et al.*, 1994; Nicot *et al.*, 2003; Jacobowitz *et al.*, 2012). However, in the early phase of active EAE, as examined in this study, it has been suggested that only few ED-1$^+$ cells are activated microglia while the majority of ED-1$^+$ cells are infiltrated macrophages (Bauer *et al.*, 1994). Consistent with this observation, in our model the sub-meningeal and perivascular labelling for ED-1 suggests that, at least at the early stage of disease, the largest number of ED-1$^+$ cells may be represented by infiltrated macrophages rather than activated microglia. Nonetheless, as both macrophages and activated microglia can express ED-1 during EAE (Bauer *et al.*, 1994) and we did not separately examine these two cell populations, in the course of this thesis we will refer to ED-1$^+$ cells as activated microglia and infiltrated macrophages. At the peak of neurological deficits, rats with active EAE showed a considerably increased labelling for ED-1 compared with healthy controls (Figure 2.18a). Interestingly, at this stage of disease, ED-1 immunoreactivity was decreased in rats treated with oxygen compared with rats breathing room air (Figure 2.18a). Quantification of ED-1 at the sacral, lumbar and thoracic level of the spinal cord, underlined greater microglial/macrophage activation in the sacral compartment compared with the lumbar and thoracic levels (Figure 2.18b). Furthermore, at the sacral level, ED-1 labelling was significantly reduced in all oxygen-treated groups compared with room air control ($p = 0.001$, $p = 0.043$ and $p = 0.005$ respectively; Figure 2.18b). Average of ED-1 labelling within all segments of the spinal cords disclosed a general reduction of microglial activation and macrophage infiltration in rats exposed to oxygen from the onset of neurological signs, and significantly in animals treated for 72 hours ($P = 0.036$; Figure 2.18c).

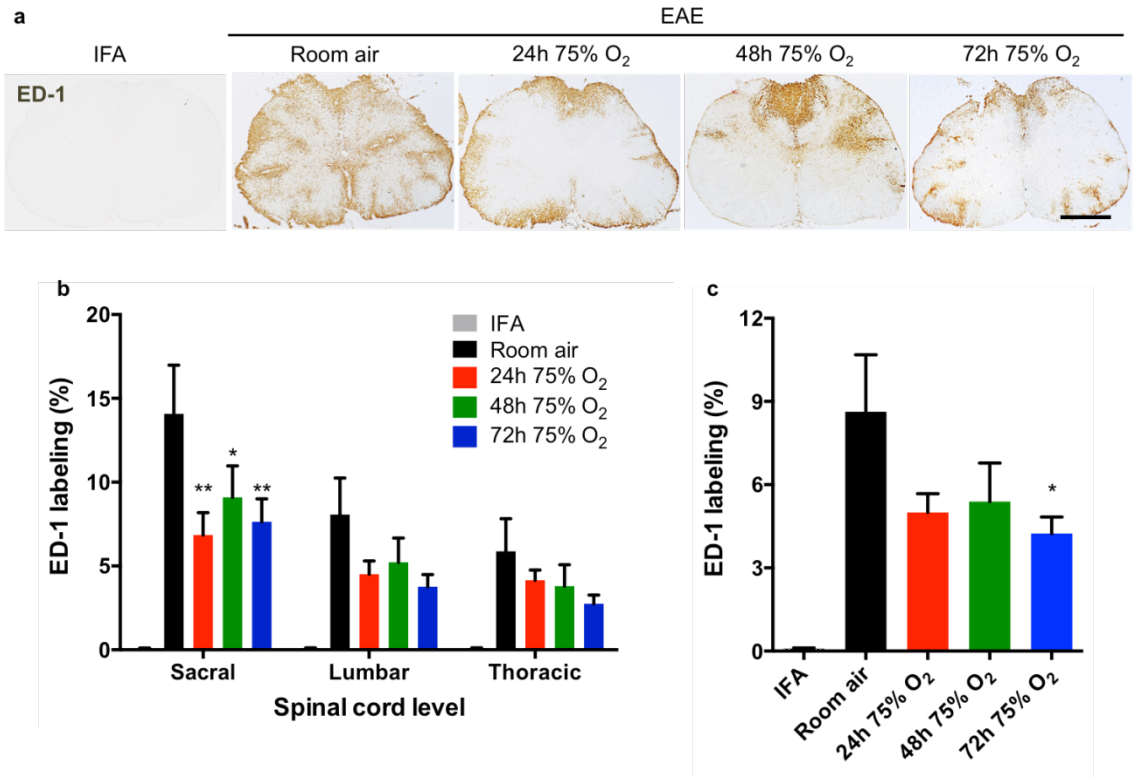

Figure 2.18 - Reduced microglial activation and macrophage infiltration in the spinal cord of rats with active EAE at the peak of disease after 72 hours of oxygen treatment from the onset of deficits.

a) Lumbar spinal cord cross-sections labeled for ED-1 (brown), a marker of macrophages and activated microglia. Rats with active EAE at the peak of disease showed a remarkably stronger labelling for ED-1 compared with IFA controls. ED-1 labelling was reduced in groups treated with oxygen for 24, 48 or 72 hours from the onset of disease compared with room air controls. Scale bar = 1mm. **b)** Histological quantification highlighted greater ED-1 immunoreactivity at the sacral part of the spinal cord compared with the lumbar and thoracic levels. A trend of reduced microglial/macrophage activation was observed in oxygen-treated groups at all levels of the spinal cords, and significantly at the sacral level in rats treated with oxygen for 24, 48 and 72 hours (respectively: $p = 0.001$; $p = 0.043$ and $p = 0.005$) compared with room air controls. Two-way ANOVA with Dunnett's correction. **c)** Overall, ED-1 immunoreactivity was decreased in the spinal cords of rats treated with oxygen and significantly in the ones treated for 72 hours ($p = 0.036$). One-way ANOVA wth Dunnett's correction. IFA, n = 8; Room air, n = 8; 24h 75% O_2, n = 10; 48h 75% O_2, n = 9; 72h 75% O_2, n = 9.

Next, we evaluated the expression of iNOS, a pro-inflammatory mediator mainly up-regulated in active microglia and macrophages, in the spinal cord of rats with active EAE at the peak of disease. At this stage of disease, immunohistochemical labelling showed a higher, although still small number of iNOS positive cells in the spinal cord of rats with active EAE compared with IFA controls (Figure 2.19a), which is consistent with what our data at the peak of neurological deficits and discussed previously in this thesis (paragraph 2.2.2.2). iNOS quantification at the peak of disease did not disclose any differences between rats treated with oxygen (for 24, 48 or 72 hours from the onset of deficits) and room air controls (Figure 2.19b).

Briefly, oxygen treatment administered from the onset of neurological deficits for 24, 48 or 72 hours decreased the number of ED-1-positive cells (activated microglia and macrophages) in the spinal cord of rats with active EAE at the peak of disease. The greatest reduction in ED-1-positive inflammatory cells was observed in rats treated with oxygen for 72 hours compared with room air controls. iNOS expression was not affected by oxygen administration.

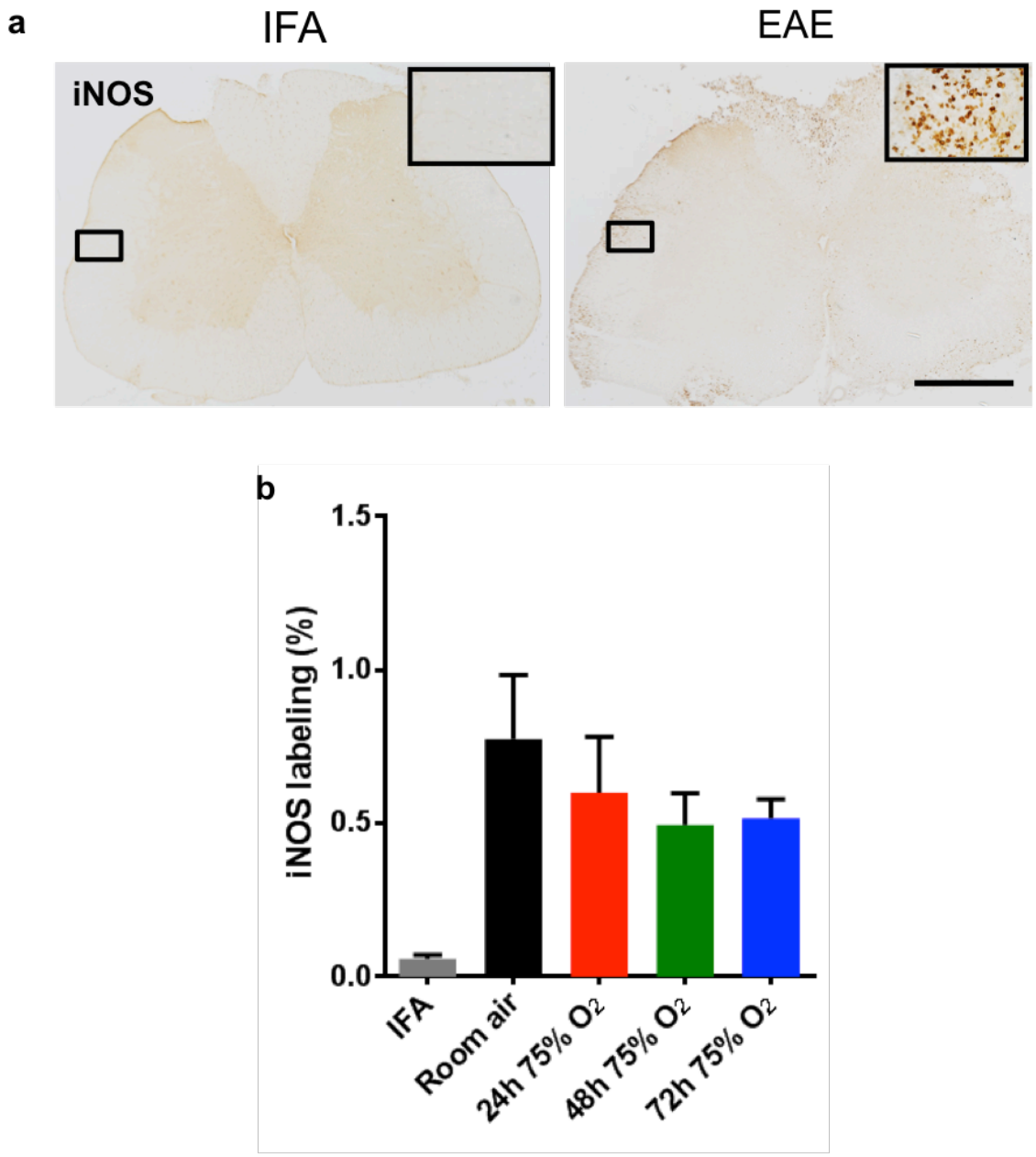

Figure 2.19 - iNOS expression in the spinal cord of rats with active EAE is not changed by oxygen treatment for 24, 48 and 72 hours from the onset of deficits.
a) Lumbar spinal cord cross-section labeled for iNOS in a healthy rat (IFA), and a rat with active EAE at the peak of disease. iNOS labelling is absent in the spinal cord of the IFA control. At the peak of EAE, iNOS is expressed within the white matter of the spinal cord. High magnification inset shows iNOS positive cells in the sub-meningeal area of the spinal cord of a rat with active EAE. Scale bar = 1mm. **b)** Quantification of iNOS labelling showed increased expression of iNOS in the spinal cord of rats with active EAE at the peak of disease compared with IFA controls, but such expression is not changed by oxygen treatment for 24, 48 or 72 hours from the onset of neurological deficits. One-way ANOVA with Dunnett's correction ($p > 0.05$). IFA, n = 8; Room air, n = 8; 24h 75% O_2, n = 10; 48h 75% O_2, n = 9; 72h 75% O_2, n = 9.

2.2.3.7 Gene expression analysis of pro-inflammatory and anti-inflammatory markers after oxygen exposure

To investigate further whether oxygen treatment administered from the onset of deficits changes the inflammatory response in active EAE, the expression of pro- and anti-inflammatory markers was analysed. The RT-PCR analysis was carried out on mRNA extracted from spinal cord of rats included in an independent trial of active EAE (n = 10). In common with the previous trials (paragraph 2.2.3.1), rats with active EAE were randomly sorted to receive room air or be treated with oxygen (for 72 hours) from the onset of deficits (n = 5 per group). The spinal cord were collected and processed for gene expression analysis at the peak of disease (3 days after onset). IFA controls (n = 6) were included for comparison. In this experiment, it was examined only the 72 hours oxygen treatment because, as showed before, this duration of exposure produced the greatest beneficial effect and pathological changes in the spinal cord of rats with active EAE. Consistently with the other EAE trials discussed previously (paragraph 2.2.3.1) also here oxygen again ameliorated the severity of neurological deficits at the first peak of disease compared with room air controls (Figure 2.20).

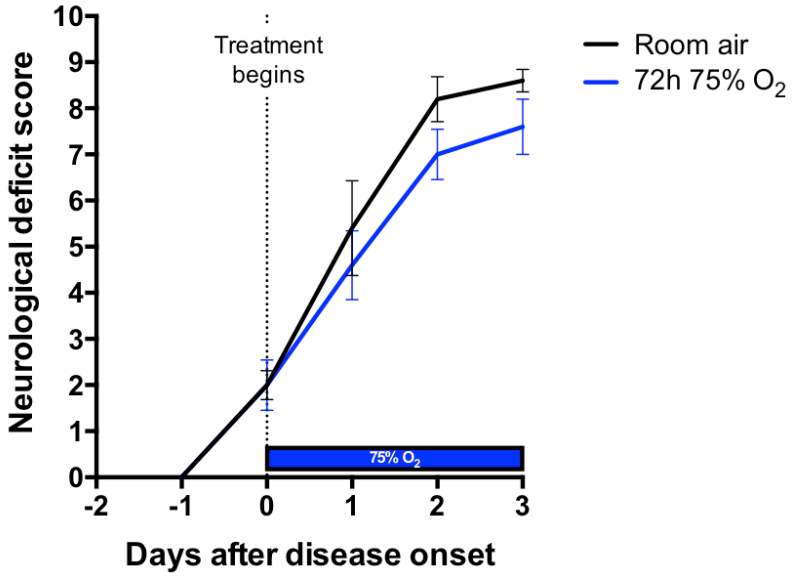

Figure 2.20 - Progression of neurological deficits at the first peak of disease in rats with active EAE exposed to room air or oxygen for 72 hours from the onset of dysfunctions. Rats with active EAE were treated with oxygen for 72 hours from the onset of deficits or maintained in room air. Oxygen treatment ameliorated disease progression compared with room air controls. Mann-Whitney U-test ($p > 0.05$). N = 5 per group.

RT-PCR analysis underlined an increased level of pro-inflammatory markers within the spinal cord of rats with active EAE compared with IFA controls. In particular, high levels of mRNA encoding for surface markers and pro-inflammatory cytokines produced by T-cell effectors and/or activated macrophages and microglia, were detected at the peak of disease, including: Ccr5, IFNγ, IL2, IL17a, IL23a, MHC1 and TNFα (Figure 2.21). Interestingly, an over-expression of pro-inflammatory genes such as iNOS and IL12b, a cytokine produced by macrophages, was not observed in rats with active EAE compared with healthy controls (Figure 2.21). The level of mRNA encoding for iNOS at the peak of neurological deficits was similar to healthy controls and correlated with the reduced quantity of iNOS protein (to control level), observed histologically at the same stage of disease (paragraphs 2.2.2.2 and 2.2.3.6).

Rats with active EAE were also characterized by a greater spinal cord expression of Foxp3 encoding mRNA (Figure 2.21). Foxp3 is the prototypical marker of T-regulatory lymphocytes (Treg), a population of T-cells involved in the control and suppression of inflammatory and autoimmune reactions; these data suggest the presence of anti-inflammatory mechanisms in the spinal cord of rats with active EAE at the peak of disease. However, no changes in Arg1 expression, another anti-inflammatory marker (M2 type microglia/macrophages), were observed between rats with active EAE and IFA controls (Figure 2.21).

Importantly, oxygen administration for 72 hours from the onset of neurological signs did not significantly change the expression of any of these markers compared with time-matched animals breathing room air (Figure 2.21). This finding suggests that oxygen does not affect the overall pro- and anti-inflammatory response in the spinal cord of rats with active EAE.

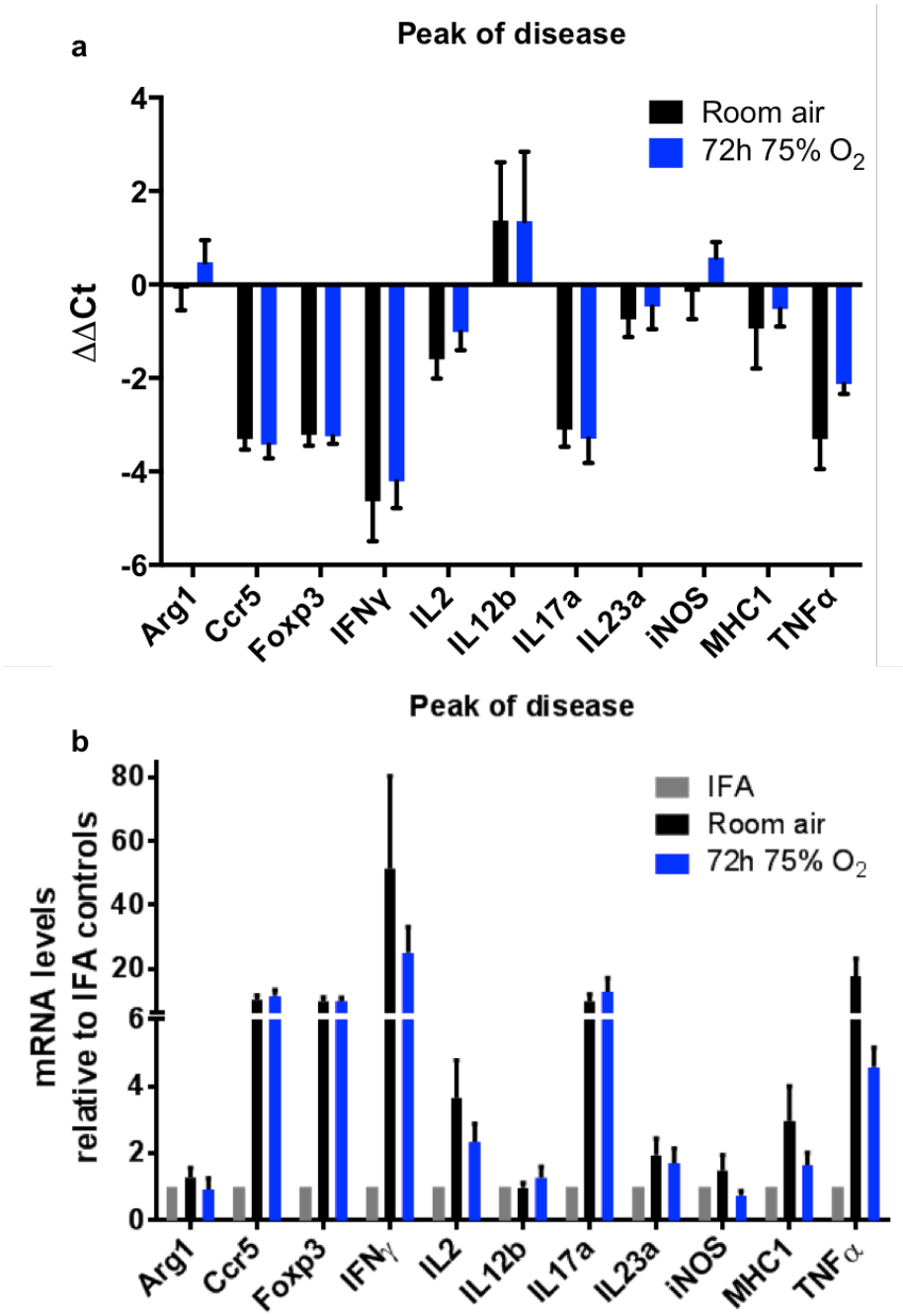

Figure 2.21 - Gene expression analysis for pro- and anti- inflammatory markers in the spinal cord of rats with active EAE at the peak of disease after exposure to room air or oxygen (75%) for 72 hours.

Rats with active EAE were maintained in room air or treated with oxygen for 72 hours from the onset of neurological deficits. At the peak of disease (3 days after onset), RT-PCR analysis showed no changes in the expression of pro- and anti- inflammatory markers between oxygen treated and room air control rats. **a)** ΔΔCt analysis over IFA controls shows the abundance of pro- and anti-inflammatory gene transcripts in the spinal cord of rats with EAE treated and untreated with oxygen. Independent t-test ($p > 0.05$). **b)** Fold change representation of the gene expression analysis relative to IFA controls. IFA, n = 6; EAE, n = 5 per group.

2.2.3.8 Oxygen treatment and oxidative damage

A potential safety concern is that oxygen administration might increase superoxide production causing cell toxicity. The safety of normobaric oxygen therapy in MS is still largely unknown and the usage of oxygen in the clinic has to be considered with caution. In this study, we aimed also to investigate the safety of the treatment in active EAE with particular regard to oxidative stress. We have evaluated the presence of 8-OHdG (a marker for oxidized DNA and RNA; Figure 2.22a) and E06 (marker of oxidized phospholipids; Figure 2.22b) at the peak of disease after 24, 48 or 72 hours of oxygen exposure and in room air and IFA controls. The spinal cord of rats with active EAE showed a significantly higher number of positive cells for 8-OHdG and E06 ($p < 0.0001$ and $p = 0.003$ respectively) compared with IFA control animals (Figure 2.22c and d). Quantification of the labelling showed no increased 8-OHdG and E06 levels in any of the oxygen-treated groups (24, 48 or 72 hours of administration) compared with room air controls (Figure 2.22c and d).

Surprisingly, the level of E06 was significantly decreased in the spinal cord of rats with active EAE treated with oxygen for 72 hours compared with rats breathing room air ($p = 0.014$; Figure 2.22d).

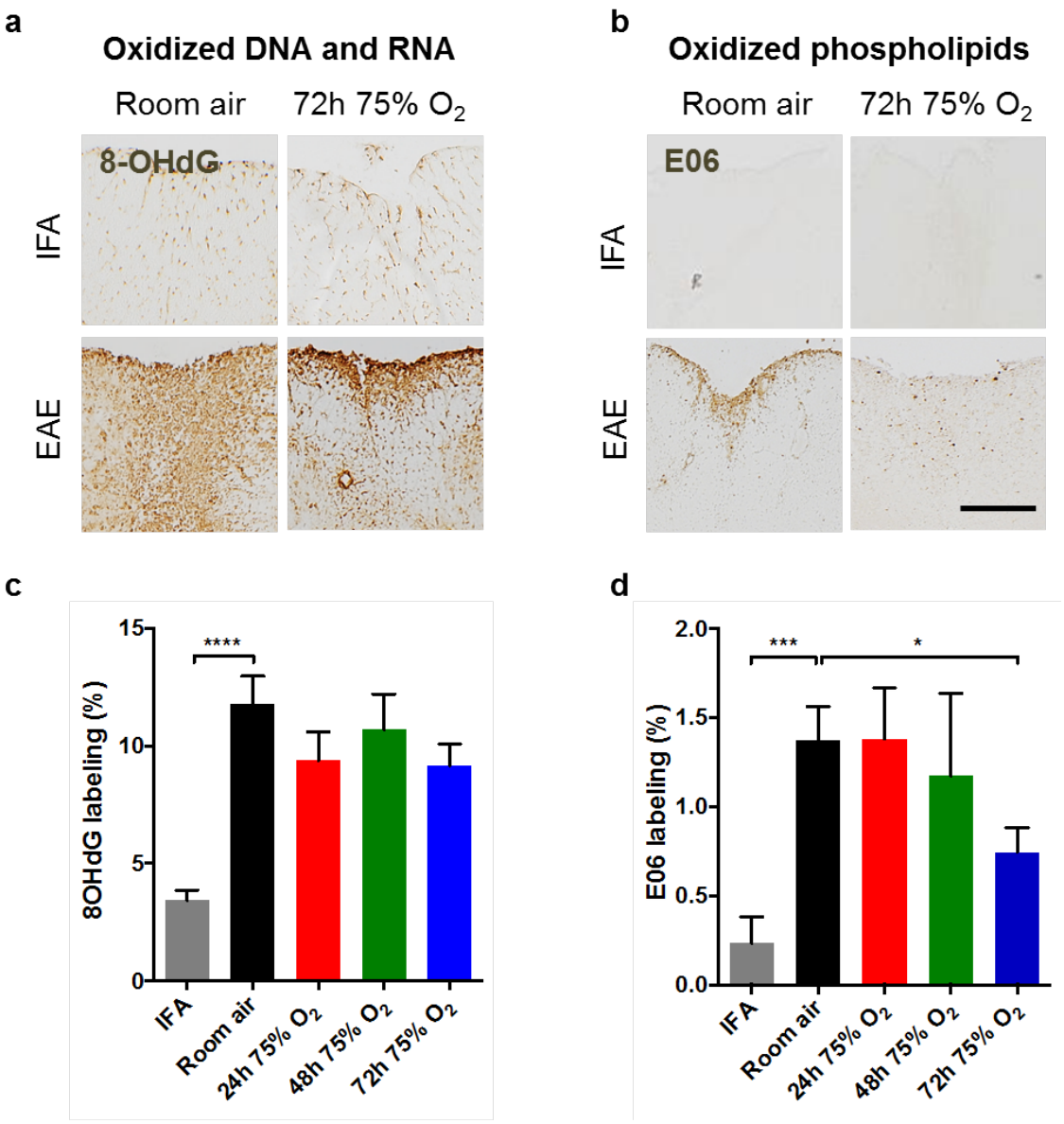

Figure 2.22 - Oxygen administration (75%) from the onset of deficits for either 24, 48, or 72 hours does not exacerbate the oxidative damage at the peak of disease.
a-b) Representative images show spinal cord dorsal columns labeled for 8-OHdG (a marker of oxidized DNA and RNA) or E06 (a marker of oxidized phospholipids) in IFA controls and rats with active EAE exposed to room air or oxygen treatment for 72 hours from the first day of disease. Scale bar = 250µm. **c)** Quantification of 8-OHdG shows increased labelling in rats with active EAE ($p < 0.0001$) compared with healthy controls, but no changes between room air and oxygen-treated groups. **d)** E06 quantification displayed a higher number of E06 positive cells in the spinal cord of rats with active EAE ($p = 0.003$) compared with IFA controls. Phospholipid oxidation was not exacerbated at the peak of disease by oxygen treatment for 24, 48 or 72 hours starting from the onset of deficits. E06 labelling was significantly decreased in rats treated with oxygen for 72 hours ($p = 0.014$) compared with room air controls. One-way ANOVA with Dunnett's correction. IFA, n = 8; Room air, n = 8; 24h 75% O_2, n = 10; 48h 75% O_2, n = 9; 72h 75% O_2, n = 9.

2.2.4.0 Prophylactic oxygen treatment

Oligodendrocyte apoptosis, the expression of hypoxia-related antigens and cerebral hypoperfusion have been identified as early changes in newly forming demyelinating lesions in MS by a number of studies (Lassmann, 2003; Barnett and Prineas, 2004; Juurlink, 2013; D'haeseleer *et al.*, 2015), raising the possibility that treatment with oxygen may be beneficial when applied even before the establishment of a new lesion. Here we examined whether oxygen can modify disease progression when administered prophylactically (before the onset of neurological deficits).

Rats with active EAE (n = 16) were randomly allocated to receive either oxygen (75%, n = 8) from the day of immunisation for 23 days or room air (n = 8). Interestingly, in rats treated with oxygen neurological deficits appeared on average 1 day later (12 d.p.i.) compared with rats kept in room air (11 d.p.i.) (Figure 2.23a, Table 2.3). Furthermore, the prophylactic treatment with oxygen significantly ameliorated the disease progression, decreasing the severity of the neurological disabilities of approximately 38% at the neurological test compared with controls ($p = 0.04$; Figure 2.23a). Notably, only 3 out of 8 rats exposed to oxygen developed a full spectrum of EAE neurological disabilities (tail and bilateral hind limb paralysis, score = 9), whereas the other 5 animals showed only tail paralysis and hind limbs weakness, maintaining the ability to walk with an unsteady gait (score ≤ 6; Table 2.3). In contrast, 7 out of 8 rats breathing room air developed both tail and bilateral hind limb paralysis (score = 9; Table 2.3), losing the ability to walk using their hind limbs. Indeed, the average maximum neurological deficit score reached by rats treated with oxygen was significantly lower ($p = 0.001$) compared with room air controls (Figure 2.23b). Furthermore, the cumulative score 23 days after the immunization that represents another measure of the burden of the disease (Fleming *et al.*, 2005), was significantly reduced in animals treated with oxygen compared with room air controls ($p = 0.026$; Figure 2.23c).

Thus, oxygen administration in the pre-symptomatic phase of the disease, significantly ameliorates and even delays the onset of neurological deficits. However, the effects of prolonged exposure (longer than 72 hours) to high concentration of oxygen have to be better investigated with regard to organ toxicity (e.g. lung) and oxidative damage within the inflamed tissue (e.g. demyelinating lesions).

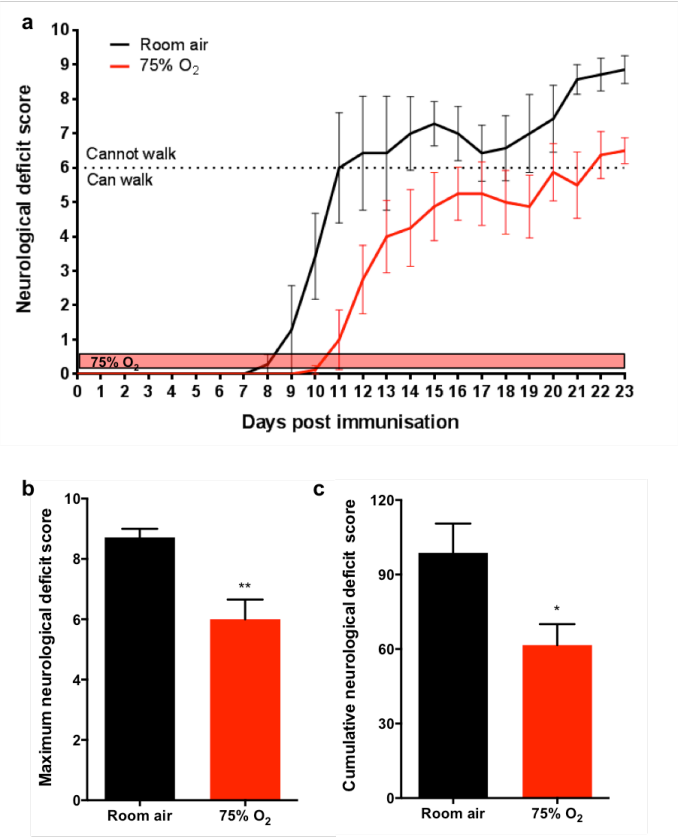

Figure 2.23 - Oxygen treatment (75%) administered from the day of immunization for 23 days delays the onset of neurological deficits and ameliorates the severity of the disease.

a) Oxygen treatment (75%) administered prophylactically from the day of immunization for 23 days, delayed the onset of disease and significantly attenuated disease progression compared with room air controls ($p = 0.044$). In particular the mean score in the oxygen-treated group was always lower than the room air control, and below a score of 6, indicating that rats treated with oxygen preserved the ability to walk using their hind limbs. **b)** The average maximum score for neurological deficit reached by rats treated with oxygen prophylactically was significantly lower compared with room air controls ($p = 0.001$). **c)** Cumulative neurological deficit score at the end of treatment (23 days after immunization) was significantly reduced in rats treated with oxygen prophylactically compared with room air controls ($p = 0.026$). Mann-Whitney U-test. Room air. N = 8 in each group.

	Room air	75% O_2
Number of rats with active EAE	8	8
Treatment	No treatment, room air controls	75% oxygen enriched air applied from the day of immunisation up to 23 days
Asymptomatic	0	0
Day of onset	11 ± 0.68	12 ± 0.55
Rats that developed bilateral hind limb paralysis (score = 9)	7 (85.7%)	3 (37.5%)

Table 2.3 - Table outlining the protocol and outcomes of prophylactically treating rats with active EAE with oxygen.

2.3.0.0 Discussion

2.3.1.0 Demyelination, inflammation, hypoxia and metabolic changes in non-treated animals with active EAE.

The pathology of active EAE is characterised by inflammation and demyelination of the spinal cord (Stromnes and Goverman, 2006a). In active EAE as well as in MS, the loss of neurological function has typically been attributed to demyelination, however studies in passive EAE (Linington *et al*., 1993) and MS (Moreau *et al*., 1996; Bitsch *et al*., 1999) suggest that neuroinflammation *per se* can also cause neurological deficits.

2.3.1.1 Demyelination in active EAE

Interestingly, in this thesis we have seen that demyelination only partially correlates with the severity of the neurological deficits in rats with active EAE. Indeed, at the very early phase of disease (first and second day after disease onset), although neurological deficits were evident, some animals did not show spinal cord demyelination upon histological examination (data not shown), suggesting that other pathological mechanisms contribute to the loss of neurological function. Demyelination was limited (sometimes absent) during the early, symptomatic phase of disease and it became more prominent at the peak of neurological deficits, but it did not increase proportionally with the worsening of neurological function. In particular, we observed that in active EAE, although the neurological deficits were often worse at the second day of deficits compared with the first day of disease, the demyelination at these two time-points appeared similar. Nonetheless, the magnitude of demyelination along the spinal cord spatially correlated with the caudal to rostral severity of the neurological dysfunction,

and indeed, it was more prominent in the sacral region compared with more rostral (lumbar and thoracic) levels of the spinal cord.

2.3.1.2 Inflammation in active EAE: activated microglia and macrophages

As mentioned before, evidence in passive EAE suggests that neuroinflammation alone is sufficient to cause neurological deficits in the absence of demyelination (Linington *et al.*, 1993)(see also Chapter 3). Furthermore, more recent studies in this model revealed that the infiltration of T-cells into the CNS starts before the onset of the deficits (Flügel *et al.*, 2001; Bartholomäus *et al.*, 2009; Murphy *et al.*, 2010) and it is accompanied by the activation of resident microglia (Murphy *et al.*, 2010). Interestingly, in active EAE, it has been shown that the activation of the endogenous microglia correlates with the initiation of disease expression, and it is the subsequent recruitment of macrophages that drives the progression of the disease to severe paralysis (Ajami *et al.*, 2011). Therefore, it is possible that the activation of microglia and the recruitment of macrophages into the spinal cord correlate better with the progression of the disease than does demyelination. Here, we followed microglial activation and macrophage infiltration in the spinal cord of rats with active EAE during the first peak of disease by histologically labelling these cells for ED-1. We noticed an increased number of ED-1 positive cells in rats with active EAE already from the early phase of disease (already present one day after onset of deficits), and their number increased as the disease progressed over the following days. Consistent with this finding, previous studies revealed a higher number of ED-1 positive cells (Davies *et al.*, 2013), and, by MRI, an increased infiltration of magnetic-labeled monocytes (Engberink *et al.*, 2010), into the spinal cord of animals with active EAE at the peak of deficits compared with early stage of the disease. Interestingly, we observed that microglial activation and macrophage infiltration were already evident one day after onset, whereas, as mentioned before, at this stage of disease demyelination was limited, affecting only sub-meningeal and perivascular areas of the spinal cord white matter, and even absent in some sick animals. Beside the temporal correlation between the abundance of activated microglia and macrophages and the severity of deficits, this inflammatory component correlated also with the spatial distribution of neurological dysfunction, and it was greater at caudal levels compared with more rostral regions of the spinal cord. However, the mechanisms

through which activated microglia and macrophages can harm neurological function, in the absence of demyelination, remain largely enigmatic. One possible mechanism includes the release at the site of inflammation of inflammatory mediators such ROS, NO and RNS, which can damage mitochondria causing an energy deficit (Mahad *et al.*, 2008; Nikic *et al.*, 2011; Guo *et al.*, 2013; Witte *et al.*, 2014). In particular, NO has been indicated as a potent mediator of mitochondrial impairment (Brown and Cooper, 1994; Cleeter *et al.*, 1994; Bolaños *et al.*, 1997; Clementi *et al.*, 1998) and during inflammation, it is synthesized by active microglia and macrophages via the enzymatic reaction catalyzed by iNOS (Stadelmann *et al.*, 2005; Marik *et al.*, 2007) (see also Chapter 1; paragraph 1.3.3.1). Dysfunctional mitochondria and the consequent inadequate synthesis of ATP can severely affect the function of neurons, which have high-energy demand to sustain their synaptic activity (Bélanger *et al.*, 2011). Studies revealed that in active EAE (Cross *et al.*, 1996; Schuh *et al.*, 2014) as well as in MS lesions (Stadelmann *et al.*, 2005; Haider *et al.*, 2011; Fischer *et al.*, 2012) the expression of iNOS is prominent. Briefly, NO has a high affinity and competes with oxygen for binding to the oxygen binding-site of mitochondrial complex-IV (Brown and Cooper, 1994; Cleeter *et al.*, 1994). The binding of NO to complex-IV blocks oxidative phosphorylation with consequent reduction of ATP synthesis (Brown and Cooper, 1994). Furthermore, NO reacts avidly with superoxide to form the strong oxidizing agent peroxynitrite (a RNS), which can in turn irreversibly damage the structure, and thereby the activity, of mitochondrial complexes I and IV (Clementi *et al.*, 1998; Smith and Lassmann, 2002; Zhang *et al.*, 2005; Mahad *et al.*, 2008). Interestingly, evidence reveals that NO can block conduction in both normal, and, especially demyelinated, axons (Redford *et al.*, 1997). In this study, we followed histologically the expression of iNOS in the spinal cord of rats with active EAE to understand whether increased synthesis of NO could explain the loss of function. Interestingly, we observed that the spinal expression of iNOS in rats with active EAE was higher during the first days of disease, but returned to control levels by the third day after onset. This histological observation was also confirmed by a gene expression analysis, which highlighted at the third day of disease a similar level of mRNA encoding for iNOS with healthy controls. These results are consistent with previous observations in active EAE (Schuh *et al.*, 2014) and in contrast to what has been described in active MS lesions (Marik *et al.*, 2007; Fischer *et al.*, 2012). The transient expression of iNOS suggests that NO may

contribute to the loss of neurological function at the beginning of disease, but not in more advanced stages. Indeed, while the expression of iNOS decreases, the neurological deficits continue to get worse, underlining the probability that other mechanisms contribute to the deficits.

2.3.1.3 Hypoxia, metabolic changes and cell stress in active EAE

Hypoxia is another possible pathological event that could explain, at least in part, the neurological deficits in active EAE. Interestingly, tissue hypoxia has been reported to correlate closely with the spatial and temporal progression of neurological deficits (Davies *et al.*, 2013). Davies and colleagues (2013) have shown that spinal hypoxia is initially more intense in the sacral level of the spinal cord, and it reaches the lumbar and thoracic levels concomitantly with the extension of the neurological deficits to involve the hind limbs (Davies *et al.*, 2013). Furthermore, the severity of hypoxia has been found to increase proportionally with the severity of the neurological signs (Davies *et al.*, 2013). In this thesis, we confirmed that the spinal cord of rats with active EAE was characterized by tissue hypoxia as exemplified by the expression of HIF1α, and that such hypoxia temporally correlated with the progression of the disease. Indeed, HIF1α expression was already significantly increased at the first day of deficits compared with healthy controls, and its expression increased in the following days in proportion with the severity of the disease. Furthermore, HIF1α expression was augmented also in sick animals that were not characterized by histological signs of spinal demyelination. However, the reason(s) why the inflamed spinal cord becomes hypoxic are still unknown and will be part of the discussion in the next chapter of this thesis (Chapter 3; paragraph 3.3.1.0).

These findings raise the possibility that tissue hypoxia could play a critical role in the onset and progression of neurological deficits due to neuroinflammation. Indeed, insufficient oxygen supply can severely affect CNS function (LaManna, 2007; le Feber *et al.*, 2016) due to reduction in oxidative phosphorylation and the subsequent decrease in ATP synthesis (Solaini *et al.*, 2010), and this detrimental effect could be exacerbated by the inflammatory-mediated damage to mitochondria (Mahad *et al.*, 2008; Nikic *et al.*, 2011; Guo *et al.*, 2013; Witte *et al.*, 2014). In order to survive with an inadequate oxygen availability and in an attempt to restore an adequate oxygen supply, the CNS undertakes a number of adaptations to hypoxia (LaManna *et al.*, 2004). One of the

mechanisms by which a cell can overcome an energy deficit caused by a shortage of oxygen and/or mitochondrial dysfunction is activation of the glycolytic pathway. Glycolysis may compensate for the loss of energy by producing ATP via the anaerobic catabolism of glucose, which may provide enough energy to sustain neuronal activity, or at least neuronal survival (Trapp and Stys, 2009). However, PFK-2 labelling indicates that the activation of glycolysis in rats with active EAE is transient, and gradually returns to control levels three days after the onset of disease. Activation of glycolysis followed a similar pattern to iNOS expression, suggesting that glycolysis may be related to the concentration of NO in the tissue. In support of this hypothesis, a connection between iNOS and glycolysis has previously been described in the brain (Keeney *et al.*, 2013) and in the pancreas (Eckersten and Henningsson, 2012).

Vasodilation of capillaries is another mechanism aimed to increase the blood supply and oxygenation of the tissue during hypoxia. Vasodilation occurs in active EAE from the very early phase of disease, as shown by previous studies (Boroujerdi *et al.*, 2013; Davies *et al.*, 2013), and in this thesis by the increased size of Reca1-positive vessels. Interestingly, Boroujerdi and colleagues (2013) reported a significant increase in vessel size during the pre-symptomatic phase of active EAE. This vasodilation can be caused by inflammation but it could also be indicative of hypoxia- and metabolic-related changes within the CNS of animals with active EAE, which can occur even before the onset of deficits.

Surprisingly, we detected an apparently higher number of Reca1-positive vessels in the spinal cord of rats with active EAE, and the number appeared to increase gradually with the progression of disease. Increased vessel number may reflect angiogenesis in the inflamed spinal cord, but previous reports suggest that the formation of new vessels occurs at later stages of the disease compared to the ones investigated in this thesis (Seabrook *et al.*, 2010; Davies *et al.*, 2013). A possible explanation for the elevated number of vessels detected could be that the increased vessel size resulted in an *apparent* overexpression due to the fact that larger vessels will be more likely to appear in different sections. A stereological analysis of a larger volume of the spinal cord (e.g. by using the Neurolucida Stereoinvestigator, MBF Bioscience, USA) may help in clarifying this doubt.

Hypoxia as well as other conditions such as glucose deprivation, ER stress, viral infection and inflammation, can cause cell stress resulting in the activation of the integrated stress response (Donnelly *et al.*, 2013). We found that the spinal cord of rats with active EAE was characterized by increased expression of p-eIF2α, a marker of the integrated stress response, in oligodendrocytes, consistent with previous observation by other groups (Chakrabarty *et al.*, 2004; Lin and Popko, 2009). In active EAE, this response has been linked to inflammation and in particular to the IFNγ-driven activation of PERK (Lin and Popko, 2009; Lin *et al.*, 2012). However, the fact that by administering oxygen to rats with active EAE we have been able to reduce such cellular stress in oligodendrocytes suggests that at least part of the integrated stress response in active EAE is caused by hypoxia (see also discussion in paragraph 2.3.2.0). The aim behind the integrated stress response mediated by hypoxia, lies in the fact that cells try to save energy by limiting their protein synthesis, while cytoprotective mechanisms try to repair the damage caused by hypoxia. Hypoxia can lead to a state of cellular stress and decreased protein synthesis via a number of different mechanisms (Koumenis *et al.*, 2002; L. Liu *et al.*, 2006; Liu *et al.*, 2008; Wouters and Koritzinsky, 2008). One mechanism includes a condition known as ER stress, which comprises the activation of three ER stress sensors: PERK, inositol-requiring protein 1 (IRE1) and ATF6 (Wouters and Koritzinsky, 2008). These are transmembrane proteins of the ER that signal luminal stress to the cytosol and the nucleus, and are involved in the inhibition of the protein synthesis via the downstream phosphorylation of eIF2α (Wouters and Koritzinsky, 2008). During hypoxia, two mechanisms can trigger the ER-stress response as described below.

In the ER, many chaperones assist nascent proteins to reach their native fold by consuming ATP (Saibil, 2013). In hypoxic conditions, the rate of ATP synthesis decreases due to impaired mitochondrial respiration, therefore an accumulation of misfolded and/or unfolded proteins in the ER may occur due to an insufficient energy supply to the chaperones (L. Liu *et al.*, 2006). Following the accumulation of misfolded/unfolded proteins in the ER a specific chaperone, the immunoglobulin-heavy-chain-binding protein (BiP), which in physiological condition is bound to PERK, IRE1 and ATF6, is taken away from these stress sensors and recruited by the misfolded proteins in the last attempt to drive correct folding (Wouters and Koritzinsky, 2008). In physiological conditions, the binding of BiP to PERK, IRE1 and ATF6 inhibits their

activation, whereas, when BiP is shunted away and recruited by misfolded/unfolded protein, PERK, IRE1 and ATF6 are activated and cause the downstream inhibition of protein synthesis via the phosphorylation of eIF2α and the transcription of several cytoprotective genes (Wouters and Koritzinsky, 2008). Activation of PERK and IRE1 has been reported to occur within minutes when cells are exposed to hypoxia, and the magnitude of the downstream inhibition of protein synthesis has been found to correlate with the intensity and duration of such hypoxia (Wouters and Koritzinsky, 2008). Activation of the third ER stress sensor ATF6 by hypoxia has not been directly demonstrated but is probable, based on the observation that many of its transcriptional targets are induced under hypoxic conditions (Wouters and Koritzinsky, 2008). In addition, hypoxia can cause ER stress by increasing the cellular production of ROS (to see how hypoxia enhances the synthesis of ROS see paragraph 5.3.0.0). ROS can cause ER stress exacerbating the energy deficit by damaging mitochondria, but also, ROS can react directly with proteins changing their structure or interfering with their folding, finally causing an accumulation of misfolded proteins and the activation of the ER stress response as described above (Liu *et al.*, 2008).

Furthermore, hypoxia can lead to a severe decrease in protein synthesis via a mechanism that is independent of the ER stress response. This mechanism involves the inhibition of the mechanistic target of rapamycin (mTOR), a kinase implicated in a multitude of signaling pathways associated with the regulation of cell survival and growth via changes in mRNA translation, ribosomal biogenesis, autophagy and metabolism (Wouters and Koritzinsky, 2008). During hypoxia, the promyelocytic leukaemia tumour suppressor (PML) has been reported to bind mTOR and inactivate it through sequestration in nuclear bodies (Wouters and Koritzinsky, 2008). In the absence of mTOR, the protein kinase R (PKR), a cytosolic kinase, is not phosphorylated and it is active and free to inhibit protein synthesis via the phosphorylation of eIF2α (Wouters and Koritzinsky, 2008). Inhibition of mTOR arrests also the phosphorylation of ribosomal protein S6 kinase (p70S6K) inactivating this kinase. Inactive p70S6K is unable to phosphorylate and activate the ribosomal subunit-6, a molecule needed for the protein synthesis (Wouters and Koritzinsky, 2008). In addition, when mTOR is inhibited, the eukaryotic initiation factor 4E binding protein 1 (4E-BP1), a cap-mediated inhibitor of the eukaryotic elongation factor 4E (eIF4E), is not phosphorylated. Non-phosphorylated 4E-BP1 binds eIF4E masking its binding-site to

the eukaryotic elongation factor 4G (eIF4G); thereby eIF4E cannot dimerize with eIF4G to form the functional complex needed for the protein synthesis (Wouters and Koritzinsky, 2008). Briefly, hypoxia can markedly decrease the rate of protein synthesis in cells via several mechanisms that include the activation of the ER-stress response and/or the inhibition of mTOR (Wouters and Koritzinsky, 2008). In hypoxic conditions, the downstream attenuation of protein synthesis can occur via both the phosphorylation of eIF2α and the inhibition of other factors involved in protein synthesis such as the ribosomal subunit-6 and eIF4E (Wouters and Koritzinsky, 2008). Although a number of studies reports the overexpression of p-eIF2α in the CNS of animals with active EAE (Chakrabarty *et al.*, 2004; Lin and Popko, 2009) and in MS lesions (Allen *et al.*, 2001; Kutzelnigg *et al.,* 2005; Cunnea *et al.*, 2011; McMahon *et al.*, 2012; Ní Fhlathartaigh *et al.*, 2013), the finding that the inflamed CNS can be hypoxic (Davies *et al.*, 2013) raises the possibility that reduced protein synthesis can occur also via molecular pathways which are independent to the phosphorylation of eIF2α.

In summary, we have seen that the spinal cord of rats with active EAE is characterized by remarkable pathological alterations including inflammation, demyelination and a series of metabolic changes suggestive of tissue hypoxia and an energy deficit (HIF1α expression, activation of glycolysis, vasodilation and cell stress). The poor correlation between demyelination and the severity of the neurological deficits suggests that demyelination may not be the only factor causing the functional impairment. In addition, the transient expression of iNOS and PFK-2 is in contrast with the more persistent inflammation, HIF1α expression and neurological deficits, indicating that NO cannot be responsible for the neurological deficits at late stage of disease and glycolysis is not enough to counteract the ongoing energy failure and loss of function. Hypoxia and microglial/macrophage activation instead, appear to correlate better with the severity and distribution of neurological deficits.

2.3.2.0 Oxygen treatment ameliorates neurological deficits in active EAE: insights on optimal timing and duration for an effective therapy

Our findings and previous evidence in MS (Aboul-Enein *et al.*, 2003; Aboul-Enein and Lassmann, 2005; Trapp and Stys, 2009; Steen *et al.*, 2013) and in active EAE (Davies *et al.*, 2013) show the presence of tissue hypoxia during neuroinflammation, raising the

possibility that oxygen therapy may represent a suitable treatment for the neurological deficits due to MS. Here, we have shown that oxygen treatment can effectively ameliorate neurological deficits in an animal model of MS, namely active EAE, and we provide insights on the optimal time and duration for oxygen administration.

We have seen that oxygen is able to improve the neurological function promptly, after just 1 hour of administration, even in paralysed animals. However, the beneficial effect achieved after 1 hour of oxygen exposure was transient, and disappeared after another hour in room air. Furthermore, only 50% of the rats improved after 1 hour of treatment, and why the other animals did not benefit from the therapy is not known. One possible explanation may lie in the different level of spinal expression of iNOS among animals. It is possible that some rats were characterized by a higher expression of NO than others, and this may have counteracted the beneficial effect of oxygen in these rats. Indeed, as mentioned previously, NO can block oxidative phosphorylation via binding to mitochondrial complex-IV (Brown and Cooper, 1994). Therefore, in the presence of elevated concentration of NO, increased oxygen availability may be not sufficient to restore an adequate energy supply, at least for short-term exposure to oxygen such as only 1-hour, because the oxygen-binding site of complex-IV is “occupied” by NO.

We then investigated what the best time point would be to administer oxygen by treating rats with active EAE for 24 hours from either the first, second or third day of disease. Interestingly, oxygen ameliorated disease severity after 24 hours of treatment compared with time-matched controls breathing room air, independently of whether the treatment started on the first, second or third day of deficit. The greatest beneficial effect was achieved when oxygen was applied from the onset of disease. Interestingly, as discussed in the previous paragraph, demyelination is rare during the first days of disease, and when present, it is limited in the spinal cord of rats with active EAE. It is possible that the hypoxia and energy deficit drive, at least in part, neurological deficits during the early stage of disease, and this would explain the greatest beneficial effect achieved with oxygen administration at the beginning of the disease. This hypothesis is in line with a recent study *in-vivo* that showed the presence of an energy deficit in mice during the symptomatic phase of active EAE before the onset of demyelination (Sadeghian *et al.*, 2016), and consistent with findings *in-vitro* that revealed that even

short-term exposure to hypoxia can severely impair the synaptic activity of neurons, and the damage is reversible upon prompt re-oxygenation (le Feber *et al.*, 2016).

To determine the best duration for oxygen administration, we treated rats with active EAE from the onset of disease for 24, 48 or 72 hours. All treatment durations resulted in an attenuation of the disease, and interestingly the severity of neurological dysfunction remained milder compared with room air controls for several days after treatment cessation. Rats treated with oxygen for 72 hours from the first day of neurological signs, experienced a better recovery of the neurological function during the remitting phase of disease, compared with room air controls and oxygen-treated groups for 24 and 48 hours. Furthermore, treatment for 72 hours provided significant protection from some of the main pathological features of active EAE when compared with room air controls, including: loss of body weight, demyelination and death of oligodendrocyte. In summary, oxygen therapy administered from the onset of disease and maintained for the entire duration of the first peak of neurological deficits (72 hours treatment), led to a more pronounced and long-lasting amelioration of the disease and a greater protection from spinal cord damage. The reason responsible for the more pronounced recovery of the neurological function achieved after oxygen treatment for 72 hours from the onset of disease, could be due to the reduced demyelination at the first peak of disease. However, in these rats, oxygen treatment did not protect from the development of the second peak of deficits, possibly because inflammation and hypoxia reappear later in the disease (Davies *et al.*, 2013), suggesting that repeated administrations of oxygen, probably from the onset of the new relapse, may be needed in order to attenuate progression of disease in the long-term.

To evaluate whether oxygen therapy can change the pathogenesis of active EAE, oxygen was administered prophylactically (before the onset of deficit) from the day of immunization for 23 days (second peak of disease). Interestingly, oxygen delayed the onset of disease and significantly ameliorated the severity of neurological deficits compared with rats breathing room air. Prophylactic oxygen treatment resulted in a remarkable protection from loss of neurological function. Indeed, the majority of rats treated with oxygen (almost 75%) did not develop hind limb paralysis, whereas almost all rats (86%) exposed to room air lost motor control of their hind limbs. The outstanding beneficial effect achieved with prophylactic oxygen administration, raises the possibility

that a sub-clinical energy failure may occur even before the onset of clear neurological deficits, possibly caused by the early infiltration of lymphocytes into the CNS (Flügel *et al.*, 2001; Bartholomäus *et al.*, 2009; Murphy *et al.*, 2010). However, other mechanisms may be implicated including a modulation of the autoimmune response by oxygen. A recent study showed that hypoxia can affect the differentiation of naïve T-cells into T-cell effectors (T helper-17, Th17) rather than anti-inflammatory regulatory T-cells (Treg), through a HIF1α-dependent pathway (Dang *et al.*, 2011). Th17 alongside with Th1 cells are the principal lymphocytes involved in the pathogenesis of active EAE (Hemmer *et al.*, 2015). Interestingly, Dang and colleagues (2011) showed that conditional HIF1α knockout mice in T-cells were significantly protected from active EAE induction (Dang *et al.*, 2011). In this regard, it is possible that the prophylactic administration of oxygen has decreased HIF1α level in the body, including HIF1α expression within naïve T-cells, reducing their differentiation in Th17. To address this possibility, we have administered prophylactic oxygen treatment in rats with passive EAE. Passive EAE is induced by the injection in recipient rats of encephalitogenic T-cells reactive against MOG. Differentiated encephalitogenic T-cells are isolated from rats sensitized to rMOG and reactivated *in-vitro* before the injection, thus an effect of oxygen on their differentiation/activation is unlikely. This experiment is part of the next chapter (Chapter 3) and it will be discussed later in this thesis.

However the beneficial effects of oxygen were only partial. Indeed, the disease was only attenuated and not all treated-animals responded to the therapy, implying that some pathological mechanisms were not affected by oxygen. EAE is an autoimmune-mediated encephalopathy, in which an early event is neuroinflammation. Our findings provide the first indications that oxygen may not have a major effect on the inflammation. Thus, it is possible that while oxygen administration plays its beneficial effect by sustaining the energetic demand of neurons and glial cells (e.g. oligodendrocytes), the inflammatory components within the CNS have still exerted a number of detrimental roles. Indeed, the abundance of infiltrating T-cells and mediators (e.g. TNFα) within the CNS of rats with active EAE did not change after oxygen administration. Therefore, it is possible that the inflammation has continued to harm the tissue (e.g. causing necroptosis of oligodendrocytes and neurons), explaining why, though attenuated, the disease did not stop in rats treated with oxygen.

In that case, oxygen may be particularly effective if applied in combination with anti-inflammatory/immunomodulatory treatments, possibly providing a beneficial effect in which the reduced inflammation (provided by the anti-inflammatory/immunomodulatory treatments) could be combined with an increased metabolic support to the CNS (given by oxygen).

2.3.3.0 Effects of oxygen treatment on the pathology of active EAE

2.3.3.1 Hypoxia and metabolic changes in rats with active EAE after exposure to oxygen treatment

Histopathological analysis of spinal cord of rats with active EAE revealed that oxygen is able to reduce the level of HIF1α promptly after 24 hours of exposure compared with room air controls, and significantly when administered at the first or third day of disease. Interestingly, when applied from the onset of disease for 24, 48 or 72 hours, oxygen decreased the expression of HIF1α at the peak of disease in proportion to the duration of the treatment, indicating a reduction of tissue hypoxia. In addition to hypoxia also microglial and macrophage derived inflammatory mediators, in particular TNFα, have been implicated in the upregulation of cellular HIF1α expression (Frede *et al.*, 2007; Imtiyaz and Simon, 2010). Nevertheless, we did not observe changes in microglial activation and macrophage infiltration after 24 hours of oxygen treatment from the first, second or third day of disease, and also, we did not detect significant differences in the gene expression of TNFα and other inflammatory markers after 72 hours of oxygen exposure from the onset of deficits. Furthermore, previous findings from our group have shown that oxygen administration decreases pimonidazole labelling (a direct marker of tissue hypoxia) and restores a physiological oxygen partial pressure in the spinal cord of rats with active EAE (Davies *et al.*, 2013). Thereafter, despite elevated HIF1α expression may result from both hypoxia and inflammation, we believe that the decreased level of HIF1α achieved after oxygen treatment in rats with active EAE is a consequence of reduced tissue hypoxia rather than an effect on inflammation.

Intriguingly, the level of HIF1α at the peak of disease was lower in oxygen-treated rats compared with room air controls even after cessation of oxygen administration. It is reasonable to suppose that the expression of HIF1α remains low as long as a proper

oxygenation of the tissue is provided or until the cause of hypoxia is not removed, raising the question of why the expression of HIF1α is decreased even when the rats are returned to room air. A possible explanation may lie in the fact that the reduced HIF1α signal correlated with reduced demyelination and macrophage/microglial activation. Indeed, both demyelinated axons and active microglia and macrophages can consume vast amount of oxygen to sustain their activities (as described following). Evidence demonstrated that demyelinated axons are intrinsically more excitable (Smith and McDonald, 1980; Felts *et al.*, 1995; Hamada and Kole, 2015) and the conduction of the electric impulse in the absence of myelin is more energy consuming (Trapp and Stys, 2009). As axons rely mainly on mitochondrial respiration to sustain their energy demand (Bélanger *et al.*, 2011), it is easy to image that, when demyelinated, they consume a higher amount of oxygen. In addition, the reduced phagocytic activation of microglia and macrophages, detected in oxygen-treated rats at the peak of disease using ED-1, implies a decreased consumption of oxygen via the oxidative burst (Bellavite, 1988; Banati *et al.*, 1991; Dahlgren and Karlsson, 1999) (see also Chapter 3; paragraph 3.3.1.0).

We hypothesized that by increasing tissue oxygenation it would be possible to overcome the activation of glycolysis in the inflamed spinal cord. As discussed previously, despite tissue hypoxia persisting for several days in rats with active EAE breathing room air, the activation of glycolysis (assessed following PFK-2 expression) was transient and returned to control level by the third day of deficits, showing a similar pattern to iNOS expression. In contrast with our hypothesis, oxygen treatment did not decrease the level of PFK-2 after 24 hours of exposure. One possible explanation is that elevated NO concentration aside from hypoxia, can cause activation of glycolysis. Indeed, evidence indicates that NO-mediated inhibition of mitochondrial respiration leads to the activation of glycolysis in astrocytes (Moncada and Bolanos, 2006). In our EAE rats, iNOS expression did not change after oxygen treatment implying a similar concentration of NO in the spinal cord of oxygen-treated and untreated animals. Interestingly, we have seen that iNOS and PFK-2 immunoreactivity on adjacent spinal cord cross-sections localized in the same areas (Figure 2.24) and PFK-2 labelling showed morphological similarities with reactive astrocytes arguing in favour that, at least part of the PFK-2 positive cells may have been astrocytes. Possibly, elevated NO

concentration within the tissue may have contributed to enhance the activation of the glycolytic pathway despite the re-oxygenation achieved after oxygen treatment.

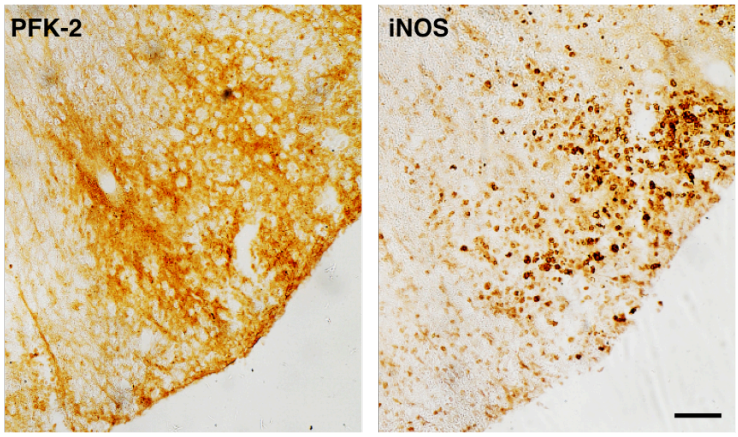

Figure 2.24 - PFK-2 and iNOS labelling of adjacent spinal cord cross sections from a rat with active EAE.
PFK-2 labelling localizes inside, and surrounds foci of, positive iNOS labelling, suggesting that at least part of the activation of glycolysis is due to NO-mediated impairment of mitochondrial respiration. Scale bar = 50µm.

Elevated oxygen supply can lead to the vasoconstriction of capillaries in an attempt to restore normal oxygenation of the tissue by decreasing blood flow. Constriction of blood vessels could therefore occur during administration of oxygen-enriched air and counteract the re-oxygenation of the inflamed spinal cord. However, we did not observe differences in blood vessel size (and number) in rats treated with oxygen for 24 hours at different stages of the disease, compared with time-matched controls. A possible explanation for this finding could be that a rise in oxygen concentration in the blood does not induce vasoconstriction in inflamed hypoxic tissue as instead described under physiological conditions.

2.3.3.2 Demyelination and oligodendrocyte survival in rats with active EAE treated with oxygen

The most prominent and surprising histological finding was that oxygen decreased white matter spinal cord demyelination at the peak of neurological deficits (three days after onset) when administered from the first day of disease for 24, 48 or 72 hours. Instead, when administered for only 24 hours at different stages of disease (from the first, second or third day of deficits) no changes in spinal cord demyelination were observed straight after oxygen treatment, compared with time-matched room air

controls. A possible explanation could be that in rats treated with oxygen for 24 hours on either the first or second day of disease, at this stage, the demyelination was too limited to detect differences compared with controls, whereas, later in the disease, demyelination was already prominent and probably the tissue was too compromised to benefit from late administration of oxygen. These findings suggest that oxygen treatment can protect from demyelination when administered from the very early stage of disease, but the protective effect is delayed and it can be detected in advanced stages of disease, when, in non-treated animals, the demyelination becomes prominent.

Interestingly, as mentioned before, in rats exposed to oxygen from the onset of deficits for 24, 48 or 72 hours, at the peak of disease, the protection from demyelination was proportional to the duration of the treatment, with the 72 hours treated-group showing a significant reduction of demyelination compared with room air control. The reduced demyelination might have been achieved via either enhanced remyelination through the differentiation of oligodendrocyte progenitor cells (OPCs), or via the protection of pre-existing mature oligodendrocytes. Studies investigated the time needed for remyelination to occur in lysolecithin- (Miron *et al.*, 2013) and LPS- (Felts *et al.*, 2005) induced demyelinating lesions. Miron and colleagues (2013) induced demyelination via the stereotaxic injection of lysolecithin in the corpus callosum of mice, and this injection resulted in an almost instant, localized demyelination of the nerve fibers. Interestingly, this study revealed that OPCs migrate and reach the lesion site at the earliest 3-4 days post-lesion, but OPC differentiation and remyelination start only 10-14 days after lysolecithin injection, and demyelination is complete within 21-24 days (Miron *et al.*, 2013). Felts and colleagues (2005) induced focal demyelination in the spinal cord of rats via the injection of LPS into the dorsal column. In this model, demyelination was evident 5-7 days after LPS injection, remyelination started approximately 14 days after LPS injection, and it was mostly complete by 28 days (Felts *et al.*, 2005). Taken together, these findings suggest that remyelination requires several days to occur. Therefore, we believe that the acute reduction of demyelination observed at the peak of disease (only 3 days after onset) in rats treated with oxygen from the onset of deficits, is due to a protective effect on mature oligodendrocytes rather than enhanced remyelination induced by the therapy. In support to this hypothesis, we discovered that,

at the peak of disease, oxygen-treated rats were characterized by an increased survival of mature oligodendrocytes in proportion to the duration of the exposure (24, 48 or 72 hours from onset of disease), which was significant in rats treated with oxygen for 72 hours compared with room air controls.

It has been shown that cell stress conditions can cause apoptosis of oligodendrocytes (Lin and Popko, 2009; Roussel *et al.*, 2013). Interestingly, the decrease in both demyelination and oligodendrocyte loss achieved with oxygen treatment was associated with reduced integrated stress response in oligodendrocytes at the peak of disease, as shown by a lower number of oligodendrocytes positive for p-eIF2α. In particular, a significant reduction of p-eIF2α positive oligodendrocytes was found in rats treated with oxygen for 72 hours from the onset of deficits. Several *in-vitro* and *in-vivo* studies recognized the integrated stress response to be protective in the short-term, but detrimental in the long-term because it can trigger the activation of apoptotic pathways (reviewed in Tabas and Ron, 2011). In addition, in active EAE, the phosphorylation of eIF2α can be both protective and detrimental depending on the stage of disease at which it occurs and on how long eIF2α remains phosphorylated (Lin *et al.*, 2006, Lin *et al.,* 2007, Lin *et al.,* 2013; Lin and Popko, 2009; Way *et al.*, 2016). A recent study demonstrated that by enhancing eIF2α phosphorylation before the onset of active EAE, it is possible to protect animals from neurological deficits and demyelination (Lin *et al.*, 2007). This effect might be a result of a pre-conditioning the tissue to stress, which may have prepared the oligodendrocytes to survive the ensuing damage. By contrast, the same group of researchers (Lin *et al.*, 2006) showed that an increased and persistent activation of the integrated stress response after the onset of dysfunction (symptomatic phase) causes increased oligodendrocyte apoptosis and demyelination, exacerbation of neurological deficits and delayed recovery during the remitting phase (Lin *et al.*, 2006). Thus, it is possible that the reduced p-eIF2α achieved with oxygen therapy during the symptomatic phase of the disease, might have protected oligodendrocytes from apoptosis and demyelination, subsequently ameliorating the disease course in oxygen-treated rats. As discussed previously in this thesis, although several conditions including hypoxia can enhance the integrated stress response (Donnelly *et al.*, 2013), increased expression of p-eIF2α in active EAE has been attributed only to inflammation and in particular to increased levels of IFNγ (Lin and Popko, 2009). Our finding that p-

eIF2α is decreased in oligodendrocytes after oxygen administration, raises the possibility that hypoxia can also contribute to cell stress during active EAE, and the fact that oxygen did not change the spinal levels of inflammatory cytokines (including IFNγ) compared with controls, argues in favour of this hypothesis. Furthermore, we have previously discussed (paragraph 2.3.1.0) that hypoxia can also cause a reduction of protein synthesis via pathways that do not involve p-eIF2α (Wouters and Koritzinsky, 2008). Therefore, it is possible that the quantification of p-eIF2α has even provided an underestimation of the restored protein synthesis resulting from oxygen therapy.

2.3.3.3 Inflammation in rats with active EAE treated with oxygen

To determine whether oxygen exerts its beneficial effect via immunomodulatory mechanisms, we have examined the spinal cord of rats with active EAE for the abundance of T-cells, active microglia and macrophages, and expression of pro- and anti-inflammatory markers. Although we did not detect differences in the number of infiltrating T-cells, we found a decreased number of ED-1 positive microglia and macrophages at the peak of disease in the spinal cord of rats treated with oxygen from the onset of deficits for 24, 48 or 72 hours, and significantly in rats exposed to oxygen for 72 hours compared with controls, raising the possibility that oxygen can play an anti-inflammatory effect. A possible immunomodulatory role of oxygen has been suggested in the 1970's in a study investigating the role of HBOT in active EAE (Warren *et al.*, 1978), however no further evidence has been provided in support of this observation. Nonetheless, recent studies revealed that hypoxia, via changes in pathways regulated by hypoxia-related transcription factors (such as HIF1α and HIF2α) and along with other cytokine-mediated signaling, can modulate the activation of macrophages to a M1 (pro-inflammatory) rather than a M2 (anti-inflammatory) phenotype (Riboldi *et al.*, 2013; Wang *et al.*, 2014; Orihuela *et al.*, 2016). However, at the peak of disease, we did not detect differences in the spinal expression of pro- and anti-inflammatory genes, including markers of M1 (iNOS) and M2 (Arg1) activation, in rats treated with oxygen for 72 hours from the onset of the disease compared with room air controls. This finding argues against an anti-inflammatory effect of oxygen.

A possible explanation for the reduced number of activated microglia and macrophages observed at the peak of disease in oxygen-treated rats from the onset of deficits may be that such reduction was a consequence of the decreased demyelination.

Demyelination releases cell debris in the tissue that has subsequently to be removed by phagocytic cells (Fu *et al.*, 2014). Therefore, a decrease in demyelination would require a reduced number of activated scavenger cells (microglia and macrophages), suggesting that the effect of oxygen on the abundance of phagocytic cells (as detected via ED-1 histological examination) was indirect, rather than direct. In this regard, it is interesting to note that the distribution and abundance of active microglia and macrophages often correlated with the presence and extent of demyelination. Indeed, demyelination and activated microglia and macrophages, often co-localized and were more diffuse at the sacral level of the spinal cord, which in addition, has been shown to be also the more hypoxic region of cord (Davies *et al.*, 2013) and in this thesis, appeared to benefit the most from oxygen therapy.

However, recent studies in cancer have demonstrated that gradients of tissue hypoxia can affect monocyte/macrophage extravasation and migration within organs (Murdoch and Lewis, 2005; Chanmee *et al.*, 2014). Indeed, it has been shown that these cells tend to be attracted to, and to migrate into, hypoxic regions (Murdoch and Lewis, 2005; Chanmee *et al.*, 2014). Therefore, it cannot be excluded that the decreased number of ED-1^{+} cells in the spinal cord of rats treated with oxygen may be also a consequence of reduced macrophage infiltration due to decreased tissue hypoxia.

Evidence in MS (Pikor *et al.*, 2012) as well as in EAE (Linington *et al.*, 1993; Mann *et al.*, 2012) supports an important role for B-cells in the pathogenesis of the disease via antibody-mediated mechanisms. In EAE, it has been shown that the mechanisms through which antibodies trigger demyelination include complement activation on the plasma membrane of oligodendrocytes and Fc receptor engagement (Mann *et al.*, 2012). Complement activation can lead to a greater recruitment of inflammatory cells in the site of inflammation and it can also directly cause oligodendrocyte damage via the formation of a trans-membrane channel, which can lead to osmotic lysis (Peña *et al.*, 2013). Furthermore, antibodies against oligodendrocyte antigens have been shown to stimulate nearby macrophages by interacting with their Fc receptors (Griot-Wenk *et al.*, 1991). *In-vitro*, this coincides with the damage of oligodendrocytes due to increased release of toxic compounds such as ROS and TNFα from the stimulated macrophages (Griot-Wenk *et al.*, 1991). However, in this study we did not investigate whether oxygen affects the recruitment and activation of B-cells into the CNS, or the synthesis/secretion

of antibodies during EAE. We believe that the protective effect of oxygen is mainly mediated by metabolic-related mechanisms, which have increased the resilience of CNS cells against the inflammatory attack, rather than a direct, anti-inflammatory role of the treatment. As discussed before, this hypothesis is partially supported by our findings that oxygen does not change the number of T-cells infiltrating the CNS, and the expression of pro- and anti-inflammatory markers. The reduced p-eIF2α expression in oligodendrocytes upon oxygen administration suggests the restoration of a more physiological rate of protein synthesis in these cells, arguing in favour of this hypothesis (see paragraph 2.2.3.4). Nonetheless, a role of oxygen on B-cell activation cannot be excluded; therefore future experiments should aim to investigate what the effects of oxygen are on the B-cell component during EAE.

Our findings provide preliminary indications that the efficacy of the therapy in attenuating neurological deficits and demyelination may not be mediated by anti-inflammatory mechanisms. Rather, the persistent behavioural effect may be due to resolute, metabolic changes that could make, *inter alia*, oligodendrocytes more resistant to the inflammatory insult.

2.2.3.4 Effects of hypoxia on oligodendrocyte metabolism

As discussed previously, administration of oxygen to rats with active EAE resulted in a prominent protection of oligodendrocytes, suggesting that oxygen may be beneficial by attenuating the energy deficit in these cells. However, although mitochondrial respiration plays an important role in immature oligodendrocytes providing energy for oligodendrocyte differentiation and myelination (Rinholm *et al.*, 2011, 2016; Amaral *et al.*, 2016), a recent study shows that the anaerobic glycolysis is the main source of energy in mature oligodendrocytes (Fünfschilling *et al.*, 2012). In addition, it has been shown that mature oligodendrocytes have fewer mitochondria compared with other glial cells and neurons, and these mitochondria are characterized by fewer cristae in the inner membrane, suggesting a decreased ATP production via oxidative phosphorylation (Rinholm *et al.*, 2016). These findings suggest that mature oligodendrocytes do not require much oxygen to fuel their energy supply. However, other observations may seem conflicting with this hypothesis (see following). An *in-vitro* study has shown that *virtual* hypoxia, induced by the inhibition of the mitochondrial complex-IV, causes injury and death of mature oligodendrocytes and impairs OPCs differentiation (Ziabreva *et al.*,

2010). In addition, mature oligodendrocytes have been reported to be particularly susceptible to ischaemic stroke *in-vivo* (Petito *et al.*, 1998; Dewar *et al.*, 2003) and to be strongly labeled for markers of hypoxia during active EAE (Davies *et al.*, 2013). A possible explanation for the high susceptibility of oligodendrocytes to (*virtual* and *true*) hypoxia might be that in these cells, mitochondria, although less in number and maybe less efficient compared with the mitochondria in other glial cells and neurons, could still account for a small but important portion of the energy supply needed by oligodendrocytes. In addition, this role may be even more relevant in pathological conditions (e.g. demyelination), where the mitochondrial activity could probably increase in order to provide enough energy to repair the damage.

Another possibility is represented by the fact that oxygen is not only important for ATP synthesis but also for lipid homeostasis. Lipid, cholesterol and oxidative metabolism are particularly relevant to produce and support myelin membrane (Blissman *et al.*, 1996). A number of enzymes (oxygenases), which use (heme and non-heme) iron and oxygen as co-factors, have been identified as involved in the homeostasis of myelin (Morell and Toews, 1984; Thompson, 1992; Alderson *et al.*, 2006) (see also General Discussion; paragraph 5.3.0.0). Interestingly, a recent study identified the fatty acid 2-hydroxylase (FA2H), an iron-containing and oxygen-consuming monooxygenase, to be a key enzyme for the synthesis of 2-hydroxy ceramides (Alderson *et al.*, 2006). 2-hydroxy ceramides are relatively minor species of membrane lipids but, in mammals, these lipids are uniquely abundant in myelin galactosylceramides and sulfatides (Alderson *et al.*, 2006). Galactosilceramides and sulfatides (3-sulfate ester of galactoceramides) represent approximately one-third of all lipids in the myelin membrane (Alderson *et al.*, 2006), and they are synthetized by the ceramide galactosyltransferase (CGT) via the transfer of a galactosyl group to a 2-hydroxy ceramide (Alderson *et al.*, 2006). Interestingly, CGT knock-out mice, which lack of galctosylceramides and sulfatides, are characterized by uncompacted myelin and progressive demyelination and hind limb paralysis (Bosio *et al.*, 1996; Coetzee *et al.*, 1996; Fewou *et al.*, 2005). It is possible that also an impaired function of one or more of the upstream enzymes that lead to the final formation of galactosylceramides and sulfatides may have similar effects. For example, insufficient oxygen and/or iron availability could impair the activity of upstream hydroxylases (such as FA2H) reducing the formation of 2-hydroxyl ceramides (the substrate of CGT); and this, similarly to what is observed in CGT knock-out mice, may

alter the formation and homeostasis of myelin. In support of this hypothesis, it has been shown that iron deficiency (Todorich *et al.*, 2009) and hypoxia (Bilali *et al.*, 2008) are associated with hypomyelination of the developing brain during the post-natal life. Although it is easy to imagine that myelin synthesis is prominent during development (Baumann and Pham-Dinh, 2001), relatively little is known about myelin lipid turnover in the adult brain, although studies in mice indicate a necessity to renew myelin lipids in adulthood (Ando *et al.*, 2003; Chrast *et al.*, 2011). Presumably, the turnover of myelin lipids may be augmented during pathological conditions such as demyelination, and this could lead to higher demand for oxygen to sustain the enzymatic activities, raising the possibility that oxygen therapy in active EAE exerts its protective role on oligodendrocytes, at least in part supporting lipid homeostasis. However, it is still unknown what the impact of lipid biogenesis is on oligodendrocytic oxygen consumption, and how long and severe the exposure to hypoxia has to be in order to impair these mechanisms in the adult CNS.

2.2.3.5 Oxygen therapy and oxidative damage in active EAE

A big concern about the use of oxygen for the treatment of MS is that it can increase oxidative damage (Haider *et al.*, 2011; Fischer *et al.*, 2012). Interestingly, we have seen that increased concentration of oxygen not only did not increase the expression of markers of oxidative damage in the inflamed spinal cord, but resulted in a significant reduction of oxidized phospholipids (E06) in rats exposed to oxygen for 72 hours from the onset of deficits, compared with room air controls. The reduced phospholipid oxidation observed at the peak of disease after 72 hours of oxygen therapy could result from the decreased tissue hypoxia in these rats, given that hypoxia (as well as hyperoxia) can contribute to the production of reactive oxygen species (Xu *et al.*, 2004; Strapazzon *et al.*, 2016) (see also Chapter 5; paragraph 5.3.0.0). Interestingly, reduced phospholipid oxidation may have contributed to oligodendrocyte survival, as oligodendrocytes are especially sensitive to phospholipid oxidation due to the high content of polyunsaturated fatty acid in their myelin sheaths (Dewar *et al.*, 2003). Oxidative damage has been reported to be one of the mechanism causing cell stress (including eIF2α phosphorylation) and apoptosis (Liu *et al.*, 2008; Donnelly *et al.*, 2013). However, E06 positive cells were mainly observed in the sub-meningeal areas whereas p-eIF2α positive oligodendrocytes were diffusely located throughout the entire white

matter, suggesting a poor correlation between these two markers. Nonetheless, it cannot be excluded that the decreased phospholipid oxidation achieved after oxygen treatment also occurred in oligodendrocytes, contributing to the reduced integrated stress response observed in these cells. Future experiments, including the co-labelling of oligodendrocytes with markers for phospholipid oxidation (E06) and p-eIF2α, will help to clarify this aspect. In addition, other markers have to be considered in order to establish the safety of oxygen therapy in neuroinflammatory diseases, including markers of nitrative damage such as nitrotyrosine. However, the transient expression of iNOS suggests that the nitrative damage caused by NO could be also transient, and limited to only the early stage of disease. Our preliminary results provide encouraging indications that oxygen therapy could be a safe treatment to avoid neurological deficits and demyelination due to neuroinflammation (see also Chapter 5; paragraphs 5.3.0.0 and 5.4.0.0).

2.3.4.0 Conclusion

The data support the hypothesis that oxygen therapy can decrease the neurological deficit due to active EAE. Oxygen was able promptly to attenuate the severity of the deficits when administered for only 1 hour, and it produced a long-lasting amelioration of the disease when applied for longer (24, 48 or 72 hours) from the onset of the disease. Prolonged administration (from 24 up to 72 hours) of treatment, starting at the first day of deficits, ameliorated disease progression, and the beneficial effect persisted for several days after treatment cessation, indicating a disease-modifying role of oxygen. Oxygen treatment from the onset of disease resulted in reduced oligodendrocytes loss, demyelination, microglial activation and macrophage infiltration at the peak of disease, but it did not change T-cell infiltration and the level of pro- and anti- inflammatory markers in the inflamed spinal cord. We have seen that oxygen treatment starting at the onset of disease decreased the integrated stress response in oligodendrocytes by preventing the inhibition of the protein synthesis machinery, possibly contributing to the greater oligodendrocytes survival achieved after oxygen exposure. However, it cannot be entirely excluded that the increased survival of oligodendrocytes achieved by oxygen administration may be due to an anti-inflammatory effect of the treatment. Although we have seen that oxygen does not

change T-cell infiltration and the expression of some pro- and anti-inflammatory markers in the CNS, we did not examine the effects of oxygen on B-cells (Mann *et al.*, 2012), or whether the trafficking and migration of macrophages is decreased by the reduced tissue hypoxia in the spinal cord (Murdoch and Lewis, 2005; Chanmee *et al.*, 2014) (see also paragraph 2.3.3.3). While the role of oxygen on the B-cell driven damage to oligodendrocytes (such as antibody-mediated) (Griot-Wenk *et al.*, 1991; Mann *et al.*, 2012; Pikor *et al.*, 2012) remains to be examined, the gene expression analysis provides preliminary indications that the macrophage-mediated death of oligodendrocytes may not be affected by oxygen. Recent studies have demonstrated that macrophages can cause cell death via the secretion of inflammatory mediators that can trigger apoptosis and necroptosis in oligodendrocytes and neurons during EAE (Jurewicz *et al.*, 2005, 2006; Ofengeim *et al.*, 2015). Here, we have shown that oxygen treatment increases oligodendrocyte survival but does not change the overall expression of two major cytokines involved in the inflammation-mediated cell death (via apoptosis and necroptosis), such as TNFα and IFNγ (Newton and Manning, 2016), raising the possibility that hypoxia may also contribute to the death of oligodendrocytes during active EAE. However, before excluding any direct effect of oxygen on the macrophage-mediated necroptosis of oligodendrocytes, further experiments are necessary in order to evaluate whether oxygen changes macrophage trafficking into the CNS and/or the expression of other macrophage-derived mediators of tissue damage (such as TRAILs).

Importantly, oxygen applied at the onset of disease for up to 72 hours did not increase oxidative damage in the inflamed spinal cord, suggesting that oxygen (75%, normobaric) may be an effective treatment for neurological deficits with relative low side effects.

Interestingly, we discovered that oxygen is particularly beneficial when administered prophylactically (before the onset of neurological signs). Prophylactic treatment with oxygen delayed the onset and attenuated the deficits, suggesting a potential role of oxygen in changing the pathogenesis of the disease.

CHAPTER 3

3. HYPOXIA AND NEUROLOGICAL DEFICITS IN AN INFLAMMATORY NON-DEMYELINATING MODEL OF MULTIPLE SCLEROSIS

3.0.0.0 Background

Evidence has shown that inflammation in the CNS of patients with MS can induce neurological deficits even in absence of further demyelination (Moreau *et al.*, 1996), leading to the paradigm that neuroinflammation alone can cause loss of neurological function (Bitsch *et al.*, 1999, 2000). However, the mechanisms by which inflammation alters regular neuronal activity are not entirely clear. We hypothesized that hypoxia and the consequent energy deficit, possibly caused by inflammation, can contribute to the genesis of neurological dysfunction in absence of demyelination. To address this possibility we used an animal model of MS, namely passive EAE, in which neurological deficits occur in the absence of major structural damage in the CNS, including demyelination. Passive EAE is induced in rodents via the administration of exogenous encephalitogenic T-cells auto-reactive against MOG (Linington *et al.*, 1993; Stromnes and Goverman, 2006b). In passive EAE, the absence of myelin degradation does not promote prominent macrophage recruitment and microglial activation in the CNS, resulting in a short-term inflammatory reaction (Linington *et al.*, 1993). Indeed, in this model the duration of neurological deficits entirely depends on the persistency in the circulation of the injected encephalitogenic T-cells, and the disease spontaneously recovers when these T-cells die (Linington *et al.*, 1993). In passive EAE, first we studied if the spinal cord of sick animals is hypoxic and then, if the hypoxia contributes to the neurological deficits in this model.

Furthermore, we speculated that in passive EAE, oxygen treatment should not be able to induce an anti-inflammatory response because the disease is mainly driven by the exogenous T-cells, reactivated *in-vitro*, and therefore the encephalitogenic response is unlikely to be changed once these cells are injected in the recipient rat. Thus, if

observed, a beneficial effect of oxygen therapy would argue in favour of a metabolic-mediated mechanism rather than an anti-inflammatory role of oxygen, consolidating the hypothesis of a prominent role of hypoxia in contributing to the neurological dysfunction.

3.0.1.0 Aims

- To determine whether the inflamed spinal cord of rats with passive EAE is hypoxic.
- To investigate the contribution of hypoxia to the neurological deficits in passive EAE and whether oxygen therapy can play a beneficial effect.
- To examine the role of oxygen treatment on the pathogenesis of the disease.

3.1.0.0 Material and methods

3.1.1.0 Animal model: induction of passive EAE

Female DA rats (n = 65; 8-9 weeks-old, ~150g, Harlan, UK) were kept in standard cages with food and water *ad libitum* on a twelve-hour light - dark cycle. One week, between the arrival of the rats and induction of passive EAE, was left to acclimatize the rats at the new environment. Passive EAE was induced by the injection of encephalitogenic T-cells reactive against MOG. Encephalitogenic T-cells were isolated from donor DA rats sensitized to rMOG (active EAE) obtained from Prof. Christopher Linington (University of Glasgow, UK). T-cells were then reactivated in-vitro as described below, before being injected in the recipient rats. First, T-cells were thawed and cultured for 1 day in T-cell grow factor medium (complete DMEM + 15% horse serum + 15% MLA supernatant). The next day, T-cells were centrifuged, washed with fresh DMEM without serum and co-cultured with irradiated (30 Gy) thymocytes (10^8 thymocytes with 2-4 x 10^6 T-cells) for 3 days in T-cell restimulation medium (complete DMEM + 1% rat serum + 10µg/mL rMOG). After 3 days T-cells were forming clusters indicating proliferation and reactivation against the antigen (rMOG). At this stage, live T-cells were counted using trypan blue (irradiate thymocytes were dead by the third day in culture), and suspended in RPMI medium in order to have 5 million T-cells per millilitre. 5 million reactive T-cells (in 1mL of RPMI medium) were injected intraperitoneally in recipient rats to induce passive EAE (n = 52). Control rats received

an injection of 1mL RPMI medium without cells (n = 13). All experiments were performed in accordance with the UK Animals (Scientific Procedures) Act of 1986, and the ARRIVE guidelines.

3.1.2.0 Behavioural assessment of the neurological deficits

All behaviour assessments and analysis were performed blinded. Disease progression was monitored on a daily basis, including assessment of general health (weight) and neurological function. Our standard 10-point scale neurological test was used as described previously in paragraph 2.1.2.0.

3.1.3.0 Evaluation of spinal cord hypoxia

The presence of hypoxia in the spinal cord of rats with passive EAE has been investigated both in-vivo and ex-vivo as following.

3.1.3.1 In-vivo measurement of oxygen partial pressure

Oxygen concentration in the spinal cord of rats with passive EAE (n = 8) and healthy controls (RPMI controls, n = 8) was measured *in-vivo* by inserting an oxygen-sensitive probe (50µm diameter) into the grey matter (as described in Davies *et al.*, 2013). In brief, rats were deeply anesthetized with 5% isoflurane gaseous anesthesia. Next, general anesthesia was maintained with 2.5% isoflurane for the entire duration of the experiment. A laminectomy was performed to expose the spinal cord at the lumbar level (L3), and the oxygen probe was inserted in the posterior ventral horn of the grey matter. When the signal was steady, oxygen tension was recorded for at least 2 minutes before retracting the probe.

3.1.3.2 Tissue probe: pimonidazole

Tissue hypoxia was examined *ex-vivo* by histologically labeling spinal cord cross-sections for pimonidazole adducts. Pimonidazole was injected intravenously in the femoral vein of rats with passive EAE (n = 9) and in RPMI controls (n = 5) under general anesthesia (2.5% isoflurane). Pimonidazole, injected intravenously, readily penetrates all tissues (including the CNS) and it is enzymatically reduced if the oxygen tension is low (approximately < 10mmHg), forming protein adducts that are detectable

immunohistochemically (see also paragraph 1.10.2.0). Rats were then intracardially perfused 4 hours after the injection. The spinal cords were collected and processed for histological analysis.

3.1.4.0 Tissue processing and histology

Rats, under general anaesthesia (2.5% isoflurane), were intracardially perfused with PBS containing heparin followed by 4% PFA in PB solution for tissue fixation. The spinal cords were further post-fixed overnight in 4% PFA in PB solution and then cryoprotected in 30% sucrose in PBS for at least 5 days. Next, the spinal cords were cut in 5 segments of 1 cm each, at the following levels: sacral, lower lumbar, upper lumbar, lower thoracic and upper thoracic, using the lumbar enlargement as reference. The tissue was then embedded in blocks with TissueTek O.C.T and frozen in 2-methylbutan (Sigma) in liquid nitrogen at -150° C. Tissue blocks were stored at -80°C prior to cryosectioning (12 µm transverse sections) and immunohistochemical examination.

3.1.4.1 Neuropathology and immunohistochemistry

Neuropathological staining for myelin with LFB, and DAB immunolabelings of spinal cord cross-sections were performed as described before in paragraph 2.1.5.1. Immunohistochemistry with mouse anti-pimonidazole adducts (Pimo) and rabbit anti-HIF1α were used to disclose tissue hypoxia. Labeling with mouse anti-ED1 was used to mark activated microglia and infiltrated macrophages (Table 3.1).

3.1.4.2 Immunofluorescence

Immunofluorescent labeling was performed as described previously in paragraph 2.1.5.2. A combination of double labeling for Pimo and CNS cell lineage markers was used to examine which types of cell are hypoxic during passive EAE. In particular, primary antibody combinations included rabbit anti-Pimo with mouse anti-neuronal cell nuclei (NeuN, neurons), rabbit anti-Pimo with mouse anti- adenomatous poli coli protein (clone CC1, oligodendrocytes), mouse anti-Pimo with rabbit anti- ionised calcium binding adaptor molecule-1 (Iba1, microglia), and mouse anti-Pimo with rabbit anti- glial fibrillary acidic protein (GFAP, astrocytes) (Table 3.1).

Antibody	Origin	Target	Marker	Dilution	Source
CC1	Mouse (mAb)	Adenomatous poli coli protein,clone CC1	Oligodendrocyte cell body	1/200	Abcam; ab16794
ED-1	Mouse (mAb)	Rat CD68	Activated microglia and macrophages	1/200	AbD Serotec; MCA341G
GFAP	Rabbit (pAb)	Glial fibrillary acidic protein	Astrocytes	1/1000	Dako; Z0334
HIF1α	Rabbit (pAB)	Hypoxia inducible factor-1α	Tissue hypoxia	1/200	Abcam; ab85886
Hydroxyprobe-1-anti-pimonidazole	Mouse (mAb) Rabbit (pAB)	Pimonidazole adducts (Pimo)	Hypoxia	1/500	HPI Inc.
Iba1	Rabbit (pAb)	Ionised calcium binding adaptor-1	Microglia	1/500	Wako; 019-19741
NeuN	Mouse (mAb)	Neuronal nuclei	Neuronal cell body	1/200	Millipore; MAB377

Table 3.1 - Primary antibodies.
Antibodies were used on rat tissue for immunohistochemistry and/or immunofluorescence as described in the material and methods. mAb = monoclonal antibody, pAb = polyclonal antibody.

3.1.5.0 Microscopy and histological analysis

Spinal cord sections stained with DAB and LFB were viewed using an Axiophot light microscope (Zeiss, Germany) and pictures taken with a Nikon D300 camera (Nikon, USA). Quantification was carried out on 10 spinal cord sections per rat at 5 different levels (sacral, lower lumbar, upper lumbar, lower thoracic and upper thoracic; 2 sections per each level). Sections within the same level of the spinal cord were 120µm from each other, whereas 1 cm was the distance between sections in adjacent levels of the spinal cord. ImageJ software (NIH, USA) was used for image analysis. Analysis of DAB labeling for ED1 and Pimo was done by making the images binary, tracing the area around the whole spinal cord sections with the freehand selection tool, before the number of pixels above a set threshold were counted and expressed as the percentage coverage of the total cross-sectional spinal cord area. LFB analysis for demyelination was done by tracing the area around the white matter and measuring the surface covered by LFB above a set threshold. This area was then subtracted to the total area of the selection and expressed as the percentage of demyelination of the white matter. Where no demyelinated lesions were detected a value of zero was given. All the values

were then averaged within each rat and used for statistical analysis. All quantification was carried out in a blinded manner.

Fluorescently labeled tissue was viewed and imaged acquired using an AxioImager-Z.2 confocal microscope (Zeiss, Germany).

3.1.6.0 Oxygen administration

Rats were placed in a chamber (Biospherix, USA) where gaseous concentrations in the air can be selected at will. Oxygen-treated rats were exposed to 75% normobaric oxygen enriched-air, whereas control rats received room air (21% oxygen) as described below.

3.1.6.1 Therapeutic and prophylactic treatment with oxygen

Therapeutic treatment with oxygen was administered from the onset of the disease. In particular, rats with passive EAE (n = 18) were randomly sorted to receive oxygen (75%) for either 24 or 48 hours from the first day of neurological signs (n = 9 per group). Rats were then returned to room air and the neurological deficits assessed up to 4 days after the complete recovery of neurological function.

Prophylactic oxygen treatment (75%, n = 8) was administered before the onset of neurological deficits, and in particular from the day of passive EAE induction, continuously up to 4 days after the complete remission of the disease. Control animals (n = 9) were maintained in room air.

3.1.7.0 Statistical analysis

Graphpad Prism v6.0 (USA) was used for statistical analysis and graph generation. All graphs represent mean ± S.E.M. All statistical analyses were two-tailed and considered significant when $p < 0.05$. Mann Whitney non-parametric U-test was used to compare the severity of neurological deficits between groups. Parametric Student's t-test was used for histological comparisons.

3.2.0.0 Results

3.2.1.0 Disease course of passive EAE

Intraperitoneal injection of encephalitogenic T-cells reactive against MOG in DA rats, induced a neurological disease characterized by ascending motor paresis and paralysis (Figure 3.1). In contrast to rats with active EAE, where neurological deficits appeared around 11 days post-immunisation, passive EAE was characterized by an early development of neurological signs (4 ± 0.6 days post-immunisation), and the peak of disease was reached within 2 days after the onset (3 days in active EAE; Figure 3.1). However, the severity of the neurological deficits in rats with passive EAE was milder compared with rats actively immunized with rMOG (Figure 3.1). Indeed, while rats with active EAE developed both tail and bilateral hind limb paralysis, rats with passive EAE mostly only expressed tail paralysis and hind limb weakness, maintaining the ability to walk with an unsteady gait (score < 6; Figure 3.1). Furthermore, passive EAE caused a monophasic disease course characterized by a complete recovery of the neurological function within few days after the peak of deficits; in contrast active EAE resulted in a relapsing-remitting disease (Figure 3.1).

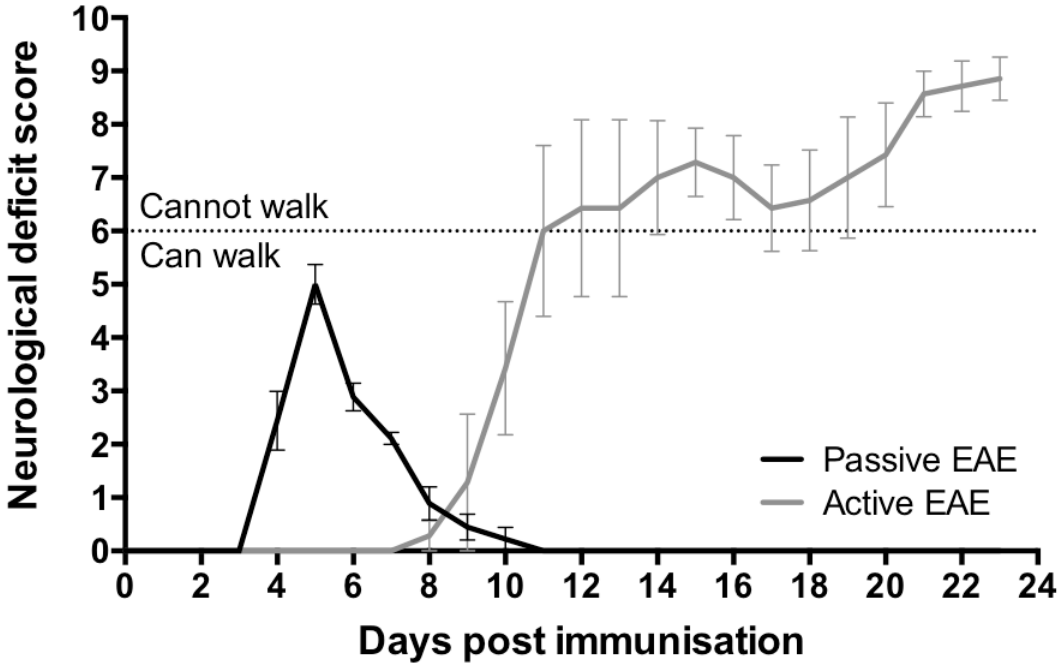

Figure 3.1 - Disease course in rats with passive and active EAE.
Rats with passive EAE (black line) developed neurological deficits 4 (± 0.6) days after the injection of encephalitogenic T-cells. Rats reached the peak of disease within 2 days after the onset, and neurological deficits included tail paralysis and hind limb weakness. The majority of rats with passive EAE maintained the ability to walk using their hind limbs (score < 6, horizontal dashed line). Passive EAE caused a monophasic disease, and normal neurological function was spontaneously and permanently restored within 11 days after the injection of the T-cells. By contrast, active EAE (grey line) caused a relapsing-remitting disease in which rats developed neurological signs 11 (± 2.05) days post-immunisation. In active EAE, neurological deficits included tail and bilateral hind limb paralysis and the peak of disease was reached by the third day after the onset of the first neurological sign. After the first attack of disease, neurological deficits were spontaneously, but partially recovered during the remitting phase. However, a full spectrum of neurological disabilities reappeared a few days after the remission (relapse). Passive EAE, n = 9; active EAE, n = 8.

3.2.2.0 Neuropathological characterization of rats with passive EAE

Histological comparison of spinal cords of rats with active and passive EAE at the peak of neurological deficits, revealed several differences between these two models of MS. Indeed, LFB staining at the peak of disease disclosed a prominent myelin loss in the white matter of rats with active EAE, whereas rats with passive EAE did not show the clear presence of any demyelination ($p = 0.003$; Figure 3.2a, c); consistent with previous reports in active EAE (paragraph 2.2.2.1) and with reports by other groups in passive EAE (Linington *et al*., 1993). Furthermore at the peak of disease, the amount of activated microglia and recruited macrophages labeled for ED-1 was significantly lower in rats with passive EAE compared with active EAE animals ($p = 0.0008$; Figure 3.2b, d). In particular, ED-1 positive cells in passive EAE were detected mainly in the sub-meningeal area and around a few blood vessels, and these cells were not spread in the CNS parenchyma as observed in active EAE (Figure 3.2b, d).

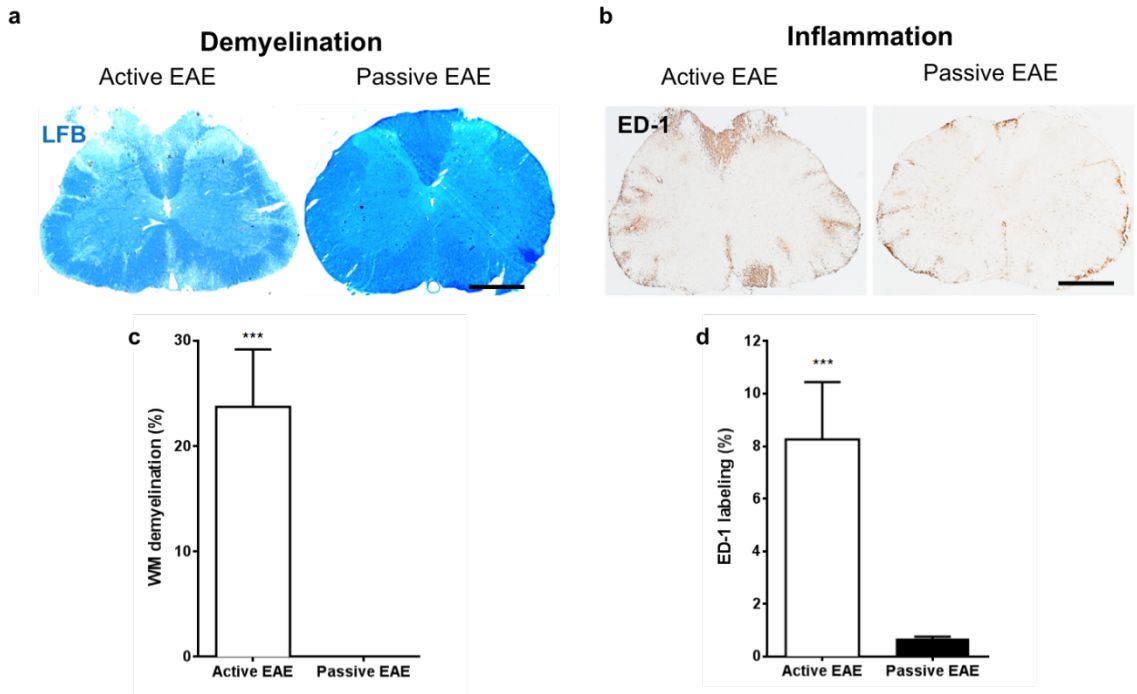

Figure 3.2 - Demyelination, microglial activation and macrophage infiltration in the spinal cord of rats with passive and active EAE.
a, c) Representative images of lumbar spinal cord sections stained with LFB (blue, myelin) of rats with active or passive EAE. Active EAE rats showed demyelination (absence of LFB) in the white matter (WM) at the peak of disease, whereas no demyelination was observed at the peak of neurological deficits in rats with passive EAE. Scale bar = 1mm. Quantification of LFB staining displayed significant demyelination in rats with active EAE ($p = 0.0003$), but no demyelinated lesions in rats with passive EAE. **b, d)** Representative images of lumbar spinal cord sections labeled for ED-1 (brown, activated microglia/macrophages) in rats with active or passive EAE at the peak of neurological deficits. Scale bar = 1mm. Rats with active EAE showed significantly more abundant ED-1 labeling compared with passive EAE rats ($p = 0.0008$). Student's t-test. Active EAE, n = 6; passive EAE, n = 9.

3.2.3.0 Hypoxia in the spinal cord of rats with passive EAE

To investigate whether passive EAE causes spinal cord hypoxia, we measured in-vivo the PaO_2 in rats with passive EAE (n = 8) at the peak of disease, and in RPMI healthy controls (n = 8), by inserting an oxygen-sensitive probe in the ventral horn of the spinal cord grey matter. Interestingly, we observed that whereas in RPMI controls the PaO_2 was at a physiological level (30.26 ± 2.90 mmHg), in rats with passive EAE the PaO_2 was lower (25.03 ± 3.41 mmHg) and comparable with the PaO_2 values observed by Davies et al. (2013) in rats with active EAE which were expressing the same (relatively mild) disease severity (score = 5) (Figure 3.3a, b).

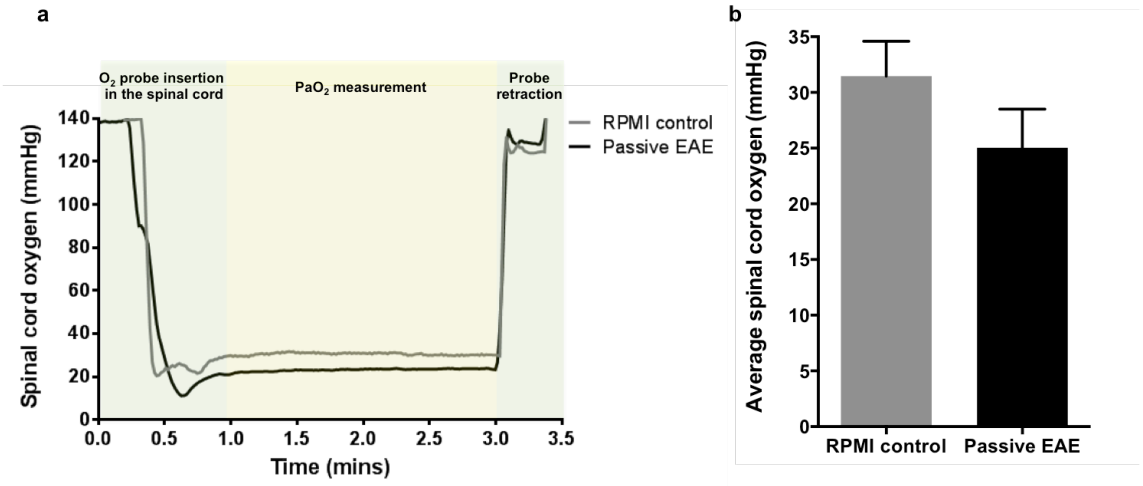

Figure 3.3 - Spinal cord oxygen tension, measured *in-vivo*, is decreased in rats with passive EAE.
a) Measurement *in-vivo* of the oxygen partial pressure (PaO_2) in the spinal cord of two representative animals: one with passive EAE (black line) and one RPMI healthy control (grey line). The rapid drop in oxygen concentration shows when the probe has been inserted in the spinal cord. PaO_2 was recorded for at least 2 minutes, and the values at the steady state were averaged within each rat, and used for comparisons. The increased PaO_2 at the end of the measurement shows when the probe was retracted. The rat with passive EAE had reduced PaO_2 compared with the healthy control. **b)** PaO_2 quantification shows reduced oxygen concentration in the spinal cord of rats with passive EAE compared with RPMI controls. Student's t-test; n = 8 per group.

To confirm this observation and examine whether the decreased oxygen tension can cause tissue hypoxia, we performed an independent trial of passive EAE (n = 9) in which rats were sacrificed at the peak of neurological deficits and the spinal cords labeled for pimonidazole adducts (Pimo, a tissue probe for hypoxia) and HIF1α. RPMI controls (n = 5) were used for comparison. Reassuringly, the labeling for HIF1α, an endogenous, physiological marker of hypoxia, showed a similar pattern to Pimo (Figure 3.4a). At low magnification, both labeling for Pimo and HIF1α were more intense in passive EAE rats than controls, and most obvious in the grey matter (Figure 3.4a). Inspection at higher magnification revealed strong, cell-specific labeling within the white matter, as also observed in immunofluorescence (Figure 3.6). Histological analysis of Pimo revealed that, compared with controls, Pimo labeling was significantly greater in the spinal cord of sick animals compared with healthy (RPMI) controls (p = 0.0001; Figure 3.4b).

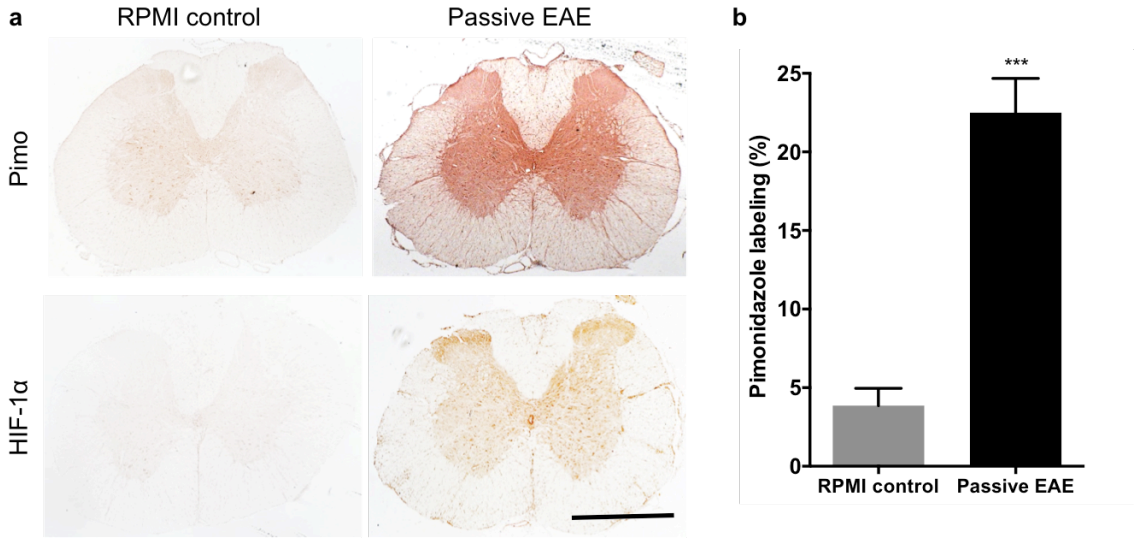

Figure 3.4 - Spinal cord of rats with passive EAE shows increased labeling for marker of tissue hypoxia.
a) Lumbar spinal cord cross-sections labeled for Pimo and HIF1α (markers of tissue hypoxia) in rats with passive EAE and RPMI controls. Pimo and HIF1α labeling show a similar pattern and are more intense in the spinal cord of rats with passive EAE compared to RPMI controls. Scale bar = 1mm. **b)** Histological quantification of Pimo showed a significant increased labeling in rats with passive EAE compared with RPMI controls ($p = 0.0001$). Student's t-test. RPMI control, $n = 5$; passive EAE, $n = 9$.

Moreover, Pimo labeling was significantly stronger in all analysed spinal cord levels (sacral, lumbar and thoracic; Figure 3.5a, b), with the most intense labeling in the lumbar region (Figure 3.5a, b).

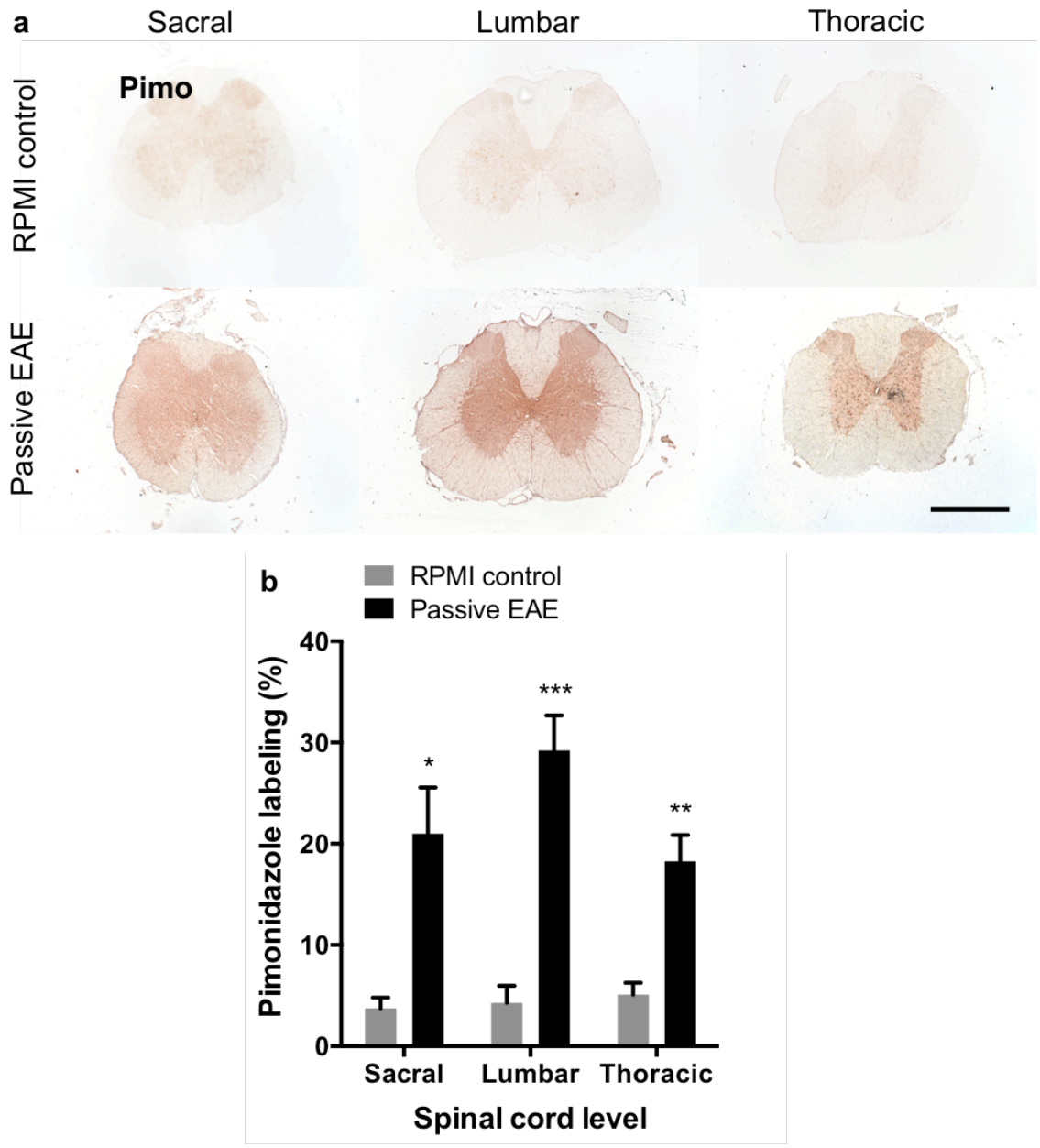

Figure 3.5 - Pimo labeling is increased at the sacral, lumbar and thoracic level of the spinal cord of rats with passive EAE.
a) Representative images of spinal cord sections at the sacral, lumbar and thoracic level labeled for Pimo. Rats with passive EAE showed increased Pimo labeling at all levels of the spinal cord compared with RPMI controls. Scale bar = 1mm. **b)** Histological quantification of Pimo showed a significantly more intense labeling at all levels of the spinal cords (sacral, $p = 0.011$; lumbar, $p = 0.0007$; thoracic, $p = 0.008$) compared with RPMI rats. Student's t-test. RPMI control, $n = 5$; passive EAE, $n = 9$.

Double immunofluorescent labeling for Pimo and cell-specific markers revealed co-localization, and therefore low cellular oxygen concentration, in the majority of NeuN positive neuronal cell bodies, CC1 positive oligodendrocytes and GFAP positive astrocytes, whereas in only few Iba1 positive microglia (Figure 3.6).

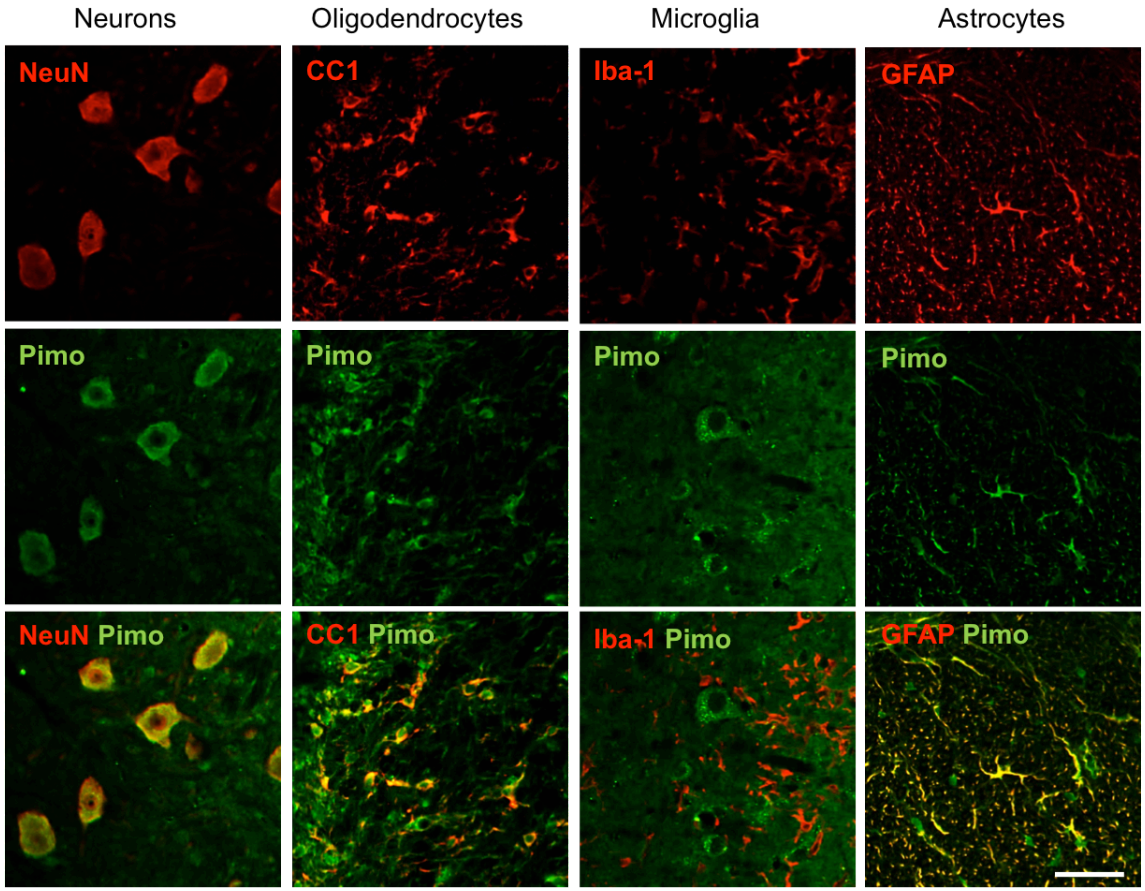

Figure 3.6 - Labeling for Pimo and markers of cell type.
Immunofluorescence for Pimo (green) and markers of CNS cell types (red). Pimo labeled the majority of neurons (NeuN), oligodendrocytes (CC1) and astrocytes (GFAP) although it was detected least commonly in microglia (Iba1). Scale bar = 100µm.

3.2.4.0 Oxygen therapy in passive EAE

To assess whether oxygen can play a beneficial effect on the neurological deficits due to passive EAE, DA rats (n = 35) were injected with encephalitogenic T cells and randomly sorted to receive either oxygen (75%) or room air (n = 9). Oxygen administration was applied either therapeutically for 24 or 48 hours starting at the onset of neurological deficits (n = 9 in each group), or prophylactically (n = 8) starting on the

day of T-cell injection, and administered continuously up to the fourth day after the complete recovery of the neurological function. After the therapeutic treatment with oxygen (24 and 48 hours), rats were returned to room air and the neurological deficits were also monitored up to the fourth day after the complete recovery of the disease.

All animals developed neurological disabilities within 3-4 days from immunization. In contrast with active EAE, oxygen administration at the onset of deficits (therapeutic treatment) for 24 and 48 hours did not ameliorate neurological dysfunction compared with room air controls, and the disease course was similar between treated and untreated rats (Figure 3.7).

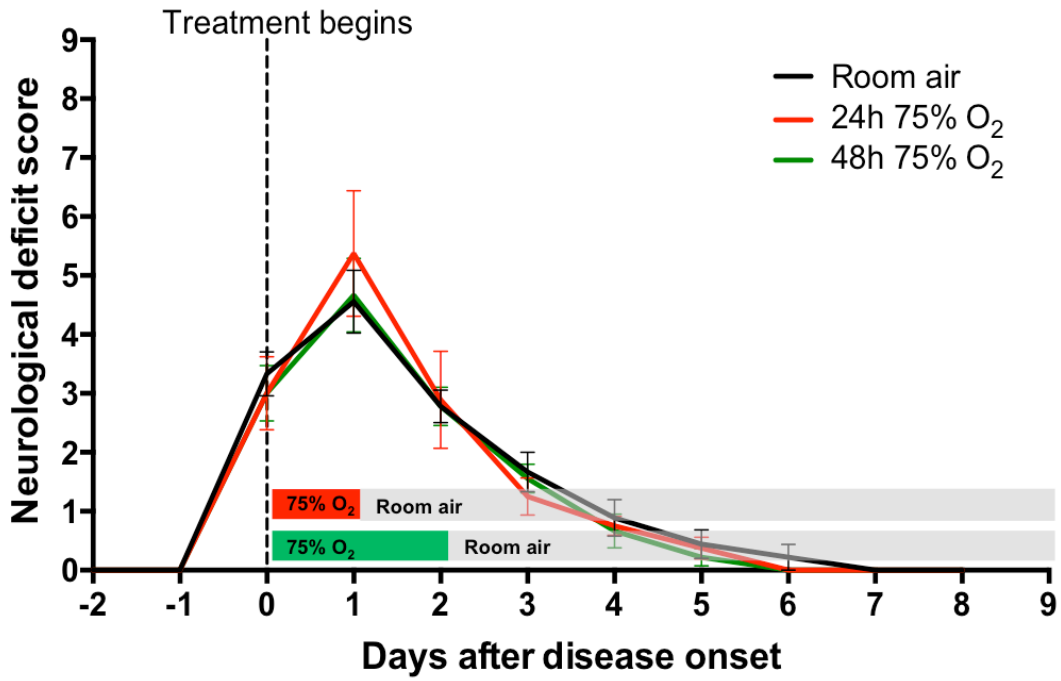

Figure 3.7 - Oxygen (75%) administered therapeutically does not change the disease course in rats with passive EAE.
Rats with passive EAE were randomly sorted to receive oxygen (75%) treatment for 24 or 48 hours from the onset of neurological deficits (day 0, horizontal dashed line). Controls were kept in room air. Oxygen did not change the severity of the neurological deficits and the treated groups (24 and 48 hours) showed a similar disease progression to room air control. Mann-Whitney U-test ($p > 0.05$). Room air, n = 9; 24h 75% O_2, n = 9; 48h 75% O_2, n = 9.

Interestingly, when applied prophylactically, oxygen significantly improved neurological function compared with room air controls (Figure 3.8a), resulting in 58% decrease in the severity of the disease, and a significant reduction of both maximum neurological deficit score ($p = 0.004$) and cumulative score ($p = 0.002$) compared with room air controls (Figure 3.8b, c). Notably, 7 out of 9 rats kept in room air developed tail paralysis and hind limbs weakness ($5 \leq \text{score} \leq 7$), whereas rats treated prophylactically with oxygen displayed tail paresis/paralysis but preserved normal motor function in both their hind limbs (score < 5; Table 3.2). However, differently from what was observed in active EAE, the treatment did not delay the onset of the disease (Figure 3.8 and Table 3.2).

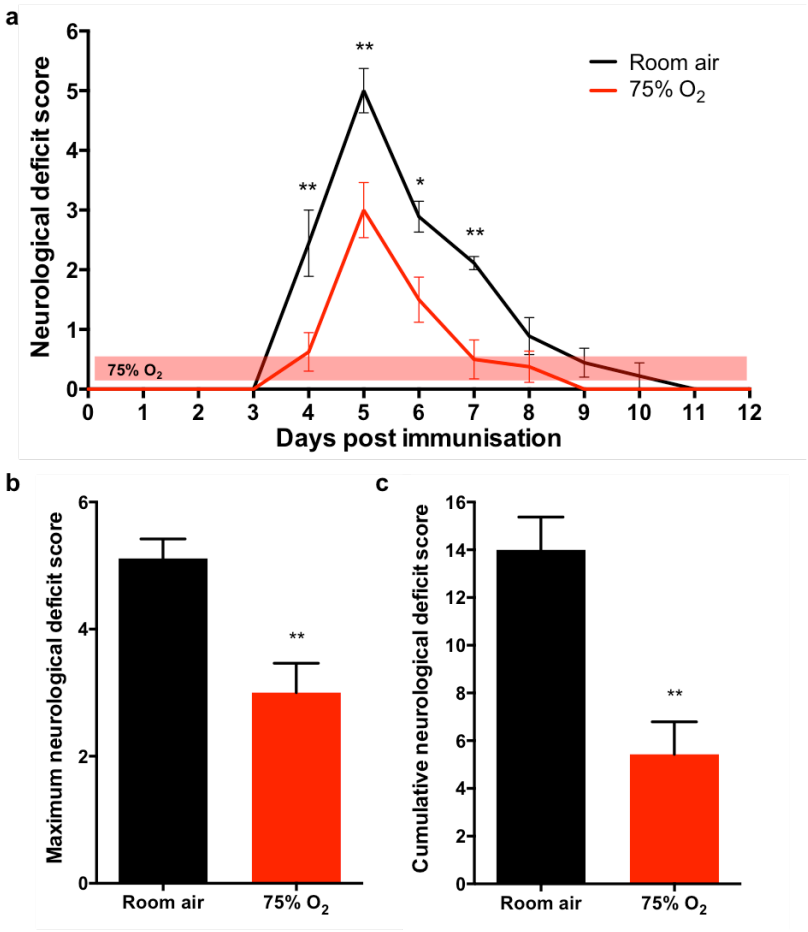

Figure 3.8 - Prophylactic oxygen (75%) treatment ameliorates severity of neurological deficits in rats with passive EAE.
a) Rats with passive EAE were kept in room air or treated with oxygen (75%) from the day of disease induction up to 4 days after the complete remission of the disease. Prophylactic oxygen treatment significantly ameliorated the severity of neurological deficits compared with room air controls. Mann-Whitney U-test (★ = $p < 0.05$; ★★ = $p < 0.01$). **b)** The average maximum score at the neurological test reached by rats treated with oxygen prophylactically was significantly lower compared with room air controls ($p = 0.004$). **c)** Cumulative neurological deficit score at the end of treatment was significantly reduced in rats treated with oxygen prophylactically compared with room air controls ($p = 0.002$). Mann-Whitney U-test. Room air, $n = 9$; 75% O_2, $n = 8$.

	Room air	75% O_2
Number of rats with EAE	9	8
Treatment	No treatment, room air controls	75% oxygen enriched-air applied from the day of T-cells injection up to 12 days
Asymptomatic	0	0
Day of onset	4 ± 0.6	4 ± 0.5
Rats that developed bilateral hind limb weakness (score = 5)	7 (77.7%)	0 (0%)

Table 3.2 - Passive EAE in rats treated with oxygen prophylactically vs. room air controls.

3.3.0.0 Discussion

3.3.1.0 Hypoxia: a feature of the inflamed spinal cord

Neurological deficits in MS and EAE have been mainly attributed to impaired axonal conduction due to extensive inflammation and demyelination. In this regard, the cause of the neurological deficits in passive EAE has previously been puzzling, given that there is no major structural damage and only limited microglial and macrophage activation, but we have found here that the explanation is that the deficit is probably due to spinal hypoxia.

It was previously described that inflammation can cause a number of metabolic changes in the tissue, including nutrient depletion, increased oxygen consumption and ROS/RNS production that can finally result in tissue hypoxia and energy deficit (Kominsky *et al.*, 2010; Colgan *et al.*, 2016). However, the cause of tissue hypoxia in the CNS of patients with MS has been mainly suggested to arise from demyelination and mitochondrial impairment (Trapp and Stys, 2009). In particular, the propagation of the electric impulse through a demyelinated axon, therefore in absence of the normal saltatory conduction allowed by the myelin sheaths, requires more energy in a contest where many axonal mitochondria are not fully functional because they are damaged by the inflammation (Nikic *et al.*, 2011; Sadeghian *et al.*, 2016). Indeed, it has been shown that demyelinated axons have a higher firing rate due to increased spontaneous depolarization of the axolemma (Smith and McDonald, 1980; Felts *et al.*, 1995; Hamada and Kole, 2015), implying augmented energy demand to sustain the increased excitability. At the same time inflammatory mediators such as RNS and ROS can cause mitochondrial damage by a number of mechanisms, making them dysfunctional (Mahad

et al., 2008; Nikic *et al.*, 2011; Witte *et al.*, 2014) (see also Chapter 1; 1.3.2.0). Thus, in demyelinated axons the increased energy demand combined with the inability of mitochondria to sustain it, results in increased mitochondrial stress and ROS/RNS production that leads to an exacerbation of the energy deficit in a vicious cycle that feeds on itself. Trapp et al. (2009) suggested that in demyelinating MS lesions, dysfunctional axonal mitochondria, even in the presence of oxygen, are not able to sustain the cellular energy demand (*virtual hypoxia*), similarly to what happens in a condition with inadequate oxygen supply (*true hypoxia*). Nevertheless, Davies et al. (2013) have demonstrated that in the spinal cord of rats with active EAE there is not a *virtual hypoxia* but an actual shortage of oxygen supply.

Examination of rats with passive EAE revealed that also the inflamed- but non-demyelinated spinal cord of these rats can be hypoxic during the symptomatic phase of the disease. Hypoxia was evaluated using two independent immunohistochemical methods, namely pimonidazole and HIF1α, and optically using an oxygen-sensitive probe to measure the PaO_2. While the measurement of the PaO_2 *in-vivo* suggested a non-significant reduction of the oxygen tension, immunohistochemistry for pimonidazole adducts (Pimo) and HIF1α disclosed a striking labeling for tissue hypoxia in the spinal cord of sick animals compared with healthy controls, underlining a poor correlation between the spinal cord oxygen tension and the labeling for tissue hypoxia. This discrepancy could be explained by the fact that while the oxygen-sensitive probe measures the absolute concentration of oxygen, immunohistochemical detection of tissue hypoxia using pimonidazole does not give an exact indication about the amount of oxygen in the tissue. Indeed, DAB labelling does not follow Beer-Lambert's law, therefore the intensity of the labelling does not linearly correlate with the amount of Pimo in the tissue. Thus, the immunohistochemical valuation of tissue hypoxia provides a merely arbitrary value if considered by itself, but it represents an important indications when different conditions are compared.

Although the measurement of PaO_2 disclosed only a modest reduction of the spinal oxygen concentration, this result was in line with increased Pimo and HIF1α labelling in the spinal cord of sick animals, supporting the conclusion that rats with passive EAE suffer spinal hypoxia. It is reasonable to think that even a mild reduction in the spinal oxygen concentration can affect the overall functionality of a highly energy consuming

organ such as the CNS (LaManna, 2007), leading to the overexpression of hypoxia-related antigens like HIF1α.

Although increased labeling for Pimo and HIF1α have been observed across the entire spinal cord cross-section of rats with passive EAE, the intensity of the signal was higher in the grey matter, and particularly intense in motor neurons. This pattern may be due to the fact that both HIF1α and pimonidazole label mainly the cell bodies, but not axons and myelin of which the white matter is enriched, raising the possibility that the elevated signal in the grey matter may be due to the higher density of cell bodies in this region. Nevertheless, inspection for Pimo at higher magnification, in DAB and immunofluorescence, revealed an increased number of pimo-labeled cells also in the white matter, and in particular in the cell body of oligodendrocytes and astrocytes, while microglial cells were mainly negative. As mentioned before, Pimo and HIF1α labeling were very intense and present in the vast majority of motor neurons. Neurons mainly rely on oxidative phosphorylation to sustain their energy demand (Bélanger *et al.*, 2011), consuming a large amount of oxygen. Therefore, it is possible that even a small decrease in the availability of oxygen in the tissue, as detected using the oxygen-sensitive probe, can result in a marked reduction of cellular oxygen concentration inside neurons, and this could explain the pronounced pimo-labeling in these cells.

Interestingly, a recent study has demonstrated that hypoxia is sufficient to reduce neuronal activity (le Feber *et al.*, 2016). Le Feber and colleagues (2016) used an *in-vitro* model system of the ischaemic penumbra, consisting of networks of cultured cortical neurons. In this model, neurons exposed to different levels of hypoxia for a short period (6 hours), showed a significant reduction in axonal activity at electrophysiological examination, and the dysfunction was completely reversed if a normal oxygen supply was restored within the first 12 hours after exposure to hypoxia (le Feber *et al.*, 2016). However, when the neurons were exposed to hypoxia for longer (30 hours), they found not only a reduction in the axonal firing rate and capacity, but the majority of the functional connections between neurons were disrupted and the damage was largely irreversible upon re-oxygenation (le Feber *et al.*, 2016). Importantly, Le Feber and colleagues (2016) discovered that the severity of the neuronal impairment correlated with the duration of the exposure rather than the depth of hypoxia. Accordingly, it is reasonable to think that even a relatively small, but prolonged

reduction in the spinal oxygenation could reduce the neuronal activity, explaining, at least in part, the neurological deficits occurring in passive EAE. Furthermore, the fact that the hypoxia-mediated impairment of the neuronal activity is more efficiently restored when oxygen is given as early as possible, support our observation that oxygen therapy in both active and passive EAE is more effective when administered at the very early phase of the disease. Also indicates from a therapeutic point of view that intermittent oxygenation should be good – it does not have to be continuous.

The initial cause of tissue hypoxia and metabolic dysfunction in MS as well as in EAE remains unknown. The impairment of mitochondrial respiration caused by microglial/macrophage-derived inflammatory mediators, such as ROS and RNS (Mahad *et al.*, 2008; Nikic *et al.*, 2011; Fischer *et al.*, 2012; Witte *et al.*, 2014) cannot explain the actual reduction in the spinal oxygen concentration. Indeed, the inability of mitochondria to consume oxygen efficiently during the oxidative phosphorylation would imply an increase rather than a reduction of the oxygen available in the tissue.

Two possible explanations are that inflammation *per se* can increase the oxygen consumption and/or impair the oxygen supply to the tissue. Increased oxygen consumption may result from the infiltration of metabolically active inflammatory cells in the CNS, while impairment in the oxygen supply may occur due to alterations in the vasculature, such as: arterial constriction, thrombosis (Koudriavtseva, 2014), adhesion of lymphocytes to the vessels, perivascular cuffs and endothelial damage (Davalos *et al.*, 2012).

Different inflammatory cell lineages have very different oxygen and metabolic demand. Indeed, while myeloid cells (e.g. macrophages) almost entirely rely on glycolysis for their energy (Borregaard and Herlin, 1982; Cramer *et al.*, 2003; Kelly and O'Neill, 2015), lymphocytes predominantly use oxidative respiration (Fox *et al.*, 2005). However, activated inflammatory cells of the myeloid lineage, including microglia and macrophages, can utilize a vast amount of oxygen via the respiratory (or oxidative) burst during phagocytosis (Dahlgren and Karlsson, 1999). The respiratory burst is the process by which neutrophils, macrophages and microglia use oxygen to produce ROS, which then are used to degrade internalized particles during phagocytosis. The respiratory burst can lead up to a 50-fold increase of the oxygen intake in activated

leukocytes (Babior, 1984; Dahlgren and Karlsson, 1999), thereby reducing the amount of oxygen available in the tissue. The respiratory burst is mediated by the oxygen-dependent enzyme NADPH oxidase. This enzyme is comprised of five phagocytic oxidase (phox) subunits: p40phox, p47phox, p67phox, p22phox and p91phox. In resting leukocytes, the enzyme is maintained inactive via the differential distribution of these subunits within the cell. Indeed, p40phox, p47phox and p67phox form a cytosolic complex, whereas p22phox and p91phox are localized in the plasma membrane. During phagocytosis, p47phox is hyperphosphorylated, and this post-translational modification induces the translocation of the cytosolic complex to the plasma membrane, where it binds the other two subunits to form the active oxidase (Babior, 1999). Interestingly the expression of the active form of the NADPH oxidases has been recently demonstrated in active MS lesions (Fischer *et al.*, 2012) and in a number of EAE models (Schuh *et al.*, 2014). However, Schuh and colleagues (2014) revealed a milder expression of the active NADPH oxidase and low levels of markers for oxidative damage such as oxidized DNA and phospholipids in the spinal cord of rats with passive EAE compared with actively immunized animals and active MS lesions (Schuh *et al.*, 2014). In line with this finding, we revealed that the spinal cord of rats with passive EAE is characterized by a narrow expression of the microglial and macrophage phagocytosis marker ED-1. Therefore, the limited phagocytic activity of microglia and macrophages in passive EAE maybe account only for a small part of the reduced spinal oxygen concentration in this model.

By contrast, T-cells intensively use glucose, amino acids and lipids as energy sources (Fox *et al.*, 2005; Kominsky *et al.*, 2010) to fuel oxidative phosphorylation. Indeed, glucose, fatty acids and amino acids are degraded into intermediates such as acetyl coenzyme A, which are then catabolized in the Krebs cycle to form NADH and $FADH_2$, used to generate more ATP via oxidative phosphorylation (Fox *et al.*, 2005). In resting T-cells, oxidative phosphorylation represents the main energetic pathway for the generation of ATP (Fox *et al.*, 2005). As would be expected, activated T-cells increase their energy consumption in order to allow proliferation, migration inside the tissue (cytoskeleton remodeling) and sustain the elevated synthesis and secretion of proteins (e.g. cytokines, chemokines and adhesion molecules) (Fox *et al.*, 2005). One early feature of T-cell activation includes an ATP-dependent alteration of the localization of

cations such as Ca^{2+} from intracellular stores (Fox *et al.*, 2005). Ca^{2+} is released from the ER to the cytosol and it is actively transported into the mitochondria, where it stimulates the general rate of oxidative phosphorylation, in part by allosterically activating several key enzymes such as pyruvate dehydrogenase and ATP synthase (Fox *et al.*, 2005). However, such increase in mitochondrial respiration has been shown to be moderate if compared with the remarkable increase of glycolysis that the T-cells undergo when activated (Fox *et al.*, 2005). Indeed, a great part of the pyruvate produced during glycolysis is converted in lactate rather than entering the Krebs cycle and produce more energy via the oxidative phosphorylation (Fox *et al.*, 2005). It seems paradoxical that an activated T-cell that is facing a number of energy-demanding processes prefers the relatively inefficient glycolysis instead of generating 10-times more ATP via mitochondrial respiration. One explanation is that in activated T-cells, some of the glucose metabolites resulting from glycolysis are used to fuel nucleotide biosynthesis and glutathione production (Fox *et al.*, 2005). Nonetheless, the hyperinduction of glycolysis in activated T-cells correlates with a moderate, although not negligible, increase in mitochondrial respiration and oxygen consumption (Fox *et al.*, 2005). Therefore, if we consider that T-cells consume a lot of oxygen when resting, and their net oxygen consumption further increases when activated (Fox *et al.*, 2005; Kominsky *et al.*, 2010), it is not difficult to image that a massive infiltration of these cells in the CNS, as observed in passive EAE (Schuh *et al.*, 2014), may deprive this organ of an adequate oxygen supply.

In addition, in EAE the adhesion of inflammatory cells at the luminal surface of venules could, at least temporarily, impede the blood flow and oxygenation of the perivenular tissue. Furthermore, the formation of perivascular cuffs could alter the normal diffusion of nutrients and oxygen from the blood stream into the tissue by increasing the distance between the parenchymal cells and the blood vessels. A number of studies showed that the supply of nutrients and oxygen to cells decreases with increasing distance to the blood vessel (Krogh, 1919; Groebe and Vaupel, 1988; Olive *et al.*, 1992; Carmeliet and Jain, 2000). In particular, cells must be within 100-200µm (oxygen diffusion limit) from a vessel to prevent detrimental effects (Carmeliet and Jain, 2000). Moreover, because the distance between the parenchymal cells and the blood vessel is augmented by the interposition of a high number of oxygen-consuming cells (lymphocytes), the amount of

oxygen that from the blood stream diffuses and reaches cells distal from the blood vessel may be even less. Any of these events may contribute to CNS hypoxia, given the high-energy consumption that the CNS has in order to sustain its function.

Interestingly, examination of the spinal oxygen tension in rats with passive EAE at the peak of disease revealed a similar PaO_2 (~25mmHg) to rats with active EAE and the same, relatively mild severity of the neurological deficits (score 5) (Davies *et al.*, 2013). Davies and colleagues (2013) discovered that the reduced oxygen concentration in the spinal cord of rats with active EAE correlates with the severity of the disease. Notably, the oxygen tension was non-significantly reduced in rats with a disease severity of 3-5 points at the neurological score, but it was remarkably decreased in paralyzed rats at the peak of deficits (score 9) (Davies *et al.*, 2013). A number of factors can explain why rats with passive and active EAE, and mild severity of the neurological signs (score 5), have a milder reduction of the spinal oxygen tension compared with rats with active EAE and more severe deficits (score 9). In chapter 2 of this thesis, we have shown that in active EAE, active phagocytic (ED-1 positive) microglia and macrophages appear in the spinal cord and their number increases with the progression of the disease (paragraph 2.2.2.2). This number is lower in rats with milder deficits (score 5) compared with severe ones (score 9; data not shown). Similarly, rats with passive EAE at the peak of disease (score 5) are characterized by a significantly lower number of ED-1 positive cells compared with active EAE rats at the peak of deficits (score 9). It is possible that the higher number of phagocytic cells in rats with more severe deficits (score 9), contributes to a greater extent to the reduction of tissue oxygen via the respiratory burst, explaining the lower PaO_2 measured in these animals (Davies *et al.*, 2013) compared with rats with passive or active EAE, but milder deficits (score 5).

Furthermore, we have previously mentioned that demyelination *per se* may lead to higher energy (and oxygen) consumption due to the increased excitability of demyelinated axons (Smith and McDonald, 1980; Felts *et al.*, 1995; Hamada and Kole, 2015). In addition, demyelination can enhance the recruitment of phagocytic (oxygen-consuming) cells in order to clear the tissue from myelin debris. At the peak of active EAE (score 9) demyelination was prominent and affecting a larger part of the spinal cord parenchyma (see Chapter 2; paragraph 2.2.2.1), whereas it was absent in rats with passive EAE, or rare and confined to few perivenular and sub-meningeal areas in

animals with active EAE and milder deficits (score 3-5; paragraph 2.2.2.1). Therefore, absent (or limited) demyelination in rats with passive EAE (or active EAE and milder deficits) may explain why these animals have a smaller reduction of the spinal oxygen tension compared with actively immunized rats at the peak of disease (Davies *et al.*, 2013). Interestingly, rats with active EAE and treated with oxygen for 24, 48 and 72 hours from the onset of deficits, were protected from demyelination at the peak of disease (third day after onset), and such protection correlated with reduced microglial/macrophage activation and expression of the hypoxic marker HIF1α, even in rats that were returned to room air for 1 or 2 extra days after 48 or 24 hours of oxygen exposure respectively (see Chapter 2; paragraphs 2.2.3.2, 2.2.3.3 and 2.2.3.6). This finding supports the hypothesis that hypoxia may contribute to demyelination and *vice versa*. Indeed, oxygen treatment in rats with active EAE protects from spinal cord demyelination and it is possible that in turn, reduced demyelination contributes to keep lower the oxygen consumption and spinal hypoxia, even when oxygen administration is terminated.

Intriguingly, histological labeling for tissue hypoxia in rats with passive EAE has similar intensity throughout the sacral, lumbar and thoracic levels of the spinal cord. By contrast in active EAE, Davies and colleagues (2013) reported a significantly greater labeling for Pimo in the sacral region compared with the lumbar and thoracic levels of the spinal cord. The reason(s) underlying this different distribution of tissue hypoxia between rats with passive and active EAE are not clear. A possible explanation may lie in a potentially different distribution of the inflammatory cells in the CNS due to the different routes of immunization. In active EAE, rMOG is inoculated subcutaneously at the very base of the tail, followed by the presentation of the antigen in the proximal secondary lymphoid organs (inguinal and abdominal lymph nodes). From these lymph nodes, primed T-cells reactive against MOG migrate in the blood stream and they may possibly first reach the closest CNS regions, namely the sacral and lumbar level of the spinal cord, causing hypoxia. In passive EAE instead, the intraperitoneal injection of already primed T-cells can directly lead to a wide systemic diffusion of these cells in the body that can readily enter and attack different regions of the spinal cord. Nonetheless, in passive EAE, it is still not clear why the inflammation is localized predominantly in the

spinal cord and the presence of encephalitogenic T-cells in the brain is rare (Stromnes and Goverman, 2006b).

3.3.2.0 Contribution of hypoxia to the neurological deficits due to neuroinflammation

To investigate whether hypoxia contributes to the neurological deficits in passive EAE, we administered oxygen-enriched (75%) air either therapeutically for 24 or 48 hours from the onset of neurological deficits; or prophylactically (before the onset of deficits) from the injection of the encephalitogenic T-cells, up to four days after complete remission of the disease.

In contrast to active EAE, in passive EAE oxygen treatment did not reduce neurological deficits when administered therapeutically. However, oxygen significantly decreased the disease severity when applied prophylactically, confirming that an important component in the efficacy of the treatment is the stage when oxygen is administered. The faster development of neurological dysfunction in passive EAE compared with active EAE, may have contributed in reducing the therapeutic window during which the treatment is beneficial. Recently, a study demonstrated that in passive EAE, encephalitogenic T-cells reactive against MBP readily enter the CNS, even before the onset of clinical neurological deficits (Bartholomäus *et al.*, 2009). In this study, encephalitogenic T-cells were retrovirally transduced to express GFP to track their distribution in the body after being injected in the recipient mouse (Bartholomäus *et al.*, 2009). Interestingly, Bartholomaus and colleagues (2009) found that approximately 20% of the injected GFP-positive T-cells migrated in the spinal cord and localized in perivascular areas even 1.5 days after the transfer. It is easily imagined that this pool of infiltrated lymphocytes can initiate subclinical alterations of the CNS including hypoxia and energy dysfunction, and possibly reduce the efficacy of a later therapeutic administration of oxygen. In support to this hypothesis, as mentioned before, le Feber and colleagues (2016) reported that hypoxia impairs the synaptic activity of neurons in proportion to the duration of the exposure, and the ability to reverse the dysfunction by simply restoring a normal oxygenation, decreases as late as oxygen is administered.

In EAE, it is possible that oxygen treatment exerts its beneficial effect first on neurons given that these cells have high metabolic (and oxygen) consumption, and therefore they may be primarily affected by hypoxia; and secondly on other CNS cell types such as oligodendrocytes that, unless damaged, might rely less on oxygen for their energy supply and function (Fünfschilling *et al.*, 2012). However, during demyelination, presumably oligodendrocytes increase their metabolic activity to counteract such damage, possibly consuming oxygen via increased mitochondrial respiration and biosynthesis of membrane lipids (see also paragraphs 2.3.2.0 and 5.3.0.0). Therefore, it is easy to imagine that during demyelination, the detrimental effect of hypoxia may be extended also to oligodendrocytes. This could explain why oxygen treatment, administered therapeutically, is effective in active EAE but not in passive EAE. In passive EAE demyelination does not occur, whereas in rats with active EAE demyelination, oligodendrocyte stress and death are prominent and appear after the onset of neurological deficits (Lin and Popko, 2009) (see chapter 2; paragraph 2.2.3.2 and 2.2.3.5). In addition, therapeutic oxygen in active EAE has been observed to protect oligodendrocytes selectively, promoting their survival and reducing demyelination. In passive EAE instead, such a beneficial effect could not be so pronounced, given that demyelination does not occur. Presumably oligodendrocytes do not need to increase their metabolic activity and oxygen consumption, for example to repair myelin, thereby narrowing the beneficial role of therapeutic oxygen administration in this model.

Alternatively, rats with passive EAE exposed to therapeutic oxygen may have benefited from the treatment but the beneficial effects could not have been detected through our standard 10-point scale neurological test. The 10-point neurological test employed in this study merely assesses changes in the voluntary motor control and muscle tone (paresis/paralysis), whereas several other neurological deficits such as loss of nociception, fatigue and impairment of bladder control can also occur in EAE. Many patients that received HBO in a clinical trial (Fischer *et al.*, 1983) found the treatment particularly helpful in ameliorating fatigue. It is reasonable that an improvement of the CNS metabolism achieved via oxygen administration can result in less fatigue. Although it is relatively easy to assess the intensity of fatigue in patients with MS by subjecting them to physical exercises and/or simply talking with them to find out if they

feel fatigued, the fatigue assessment in animal models is rather difficult to evaluate. Indeed, despite the part that some EAE animals preserve the voluntary motor control of their limbs, maintaining the ability to walk, when sick they generally tend to limit their movements to the minimum necessary and it is difficult to understand if this is due to fatigue, a lack of motivation, or weakness. We believe that new methods capable to assess fatigue in EAE studies are of pivotal importance for a better understanding of the beneficial effects of therapies. Notably, therapies able to ameliorate fatigue can be extremely important in MS, as fatigue severely affects the daily life of patients. Oxygen therapy, by its own nature could be beneficial for the treatment of fatigue due to neuroinflammation and energy deficiency, although in this study, we missed the opportunity to evaluate this aspect.

Furthermore, the fact that passive EAE causes less neurological dysfunctions compared with active EAE, reduces the spectrum and magnitude of disabilities that these rats can improve after treatment. For example, one marked beneficial effect achieved by therapeutic oxygen administration in active EAE was the reduced incidence of hind limb paralysis (paragraph 2.2.3.1), whereas the majority of the oxygen-treated rats still developed hind limb paresis. In passive EAE instead, hind limb paresis represent the most severe neurological dysfunction achieved, therefore the beneficial effect of oxygen in protecting from the development of paralysis cannot be appreciated in this model, underlining the narrower window of neurological deficit that rats with passive EAE can improve after treatment.

The significant benefit achieved with prophylactic administration of oxygen suggests that pathological mechanisms such as hypoxia, energy deficiency and mitochondrial dysfunction may occur even before the onset of neurological deficits and they could represent an interesting therapeutic target to treat or even delay the beginning of new relapses. Furthermore, the efficacy of prophylactic oxygen treatment observed in passive EAE, in which the role of endogenous inflammation is limited and auto-reactive exogenous T-cells are primed in-vitro before being injected in the recipient rats, suggests that oxygen may play its beneficial role through a metabolic-related mechanism rather than an anti-inflammatory effect. However, another mechanism through which prophylactic treatment with oxygen has decreased the severity of neurological deficits may include a reduced trafficking and extravasation of

encephalitogenic T-cells into the CNS, possibly due to a reduction in blood flow caused by the vasoconstriction effect of hyperoxia (Watson *et al.*, 2000; Floyd *et al.*, 2003).

3.3.3.0 Conclusion

We provide evidence that neuroinflammation *per se*, even in absence of demyelination, can cause tissue hypoxia in the spinal cord of rats with passive EAE, and such hypoxia can, at least in part, account for at least some of the neurological deficits in this model. We confirmed that an important factor for the efficacy of oxygen therapy is the stage of disease at which the treatment is administered. The fact that in both passive EAE and active EAE the therapy is particularly effective when applied during the asymptomatic phase consolidates the possibility that metabolic dysfunctions can occur even before the onset of neurological signs.

Our findings in passive EAE suggest that the beneficial effect of oxygen therapy is due to a metabolic action on the hypoxia and energy deficit, rather than an anti-inflammatory role.

We conclude that hypoxia is an important but currently overlooked component in the development of neurological dysfunction due to neuroinflammation, and that oxygen can at least in part protect from the loss of neurological function.

CHAPTER 4

4. ADMINISTRATION OF AN OXYGEN-CARRYING BLOOD SUBSTITUTE FOR THE TREATMENT OF NEUROLOGICAL DEFICITS IN A MODEL OF MULTIPLE SCLEROSIS

4.0.0.0. Background

In accord with the therapeutic effects of oxygen enriched-air discussed previously in this thesis; we have tested an alternative treatment aimed to increase tissue oxygenation in an inflammatory-demyelinating model of MS, active EAE. In particular, we investigated the effects on neurological deficits of treatment with polynitroxylated pegylated hemoglobin (PNPH). PNPH is a novel hemoglobin-based oxygen carrier produced by SynZyme Technology (USA), which consists of bovine hemoglobin coated with nitroxide (NO) and polyethylene glycol (PEG) (Hsia and Ma, 2012; Lewis and Ross, 2014). In addition to the oxygen-carrier function, PNPH has a superoxide dismutase (SOD)-mimetic activity that ameliorates oxidative stress, while the NO moieties enhance vasodilation. Furthermore, both SOD-activity and pegylation, which mask the hemoglobin reducing its interaction with the vascular surface, decrease the free radical cytotoxic effect that cell-free hemoglobin can exert on endothelial cells (Lewis and Ross, 2014). PNPH has also been reported to have a relatively long half-life (20 hours), similar or longer than other hemoglobin-based oxygen carriers (e.g. OxyVita (USA) and MP4 (USA), 6 and 20 hours respectively), giving the possibility of reducing the spare number of injections (Lewis and Ross, 2014).

PNPH is proposed to increase tissue oxygenation via both enriching the oxygen content of the plasma, and NO-mediated vasodilation. Furthermore, the nanoscopic size of PNPH facilitates its delivery in constricted/collapsed capillaries, reaching poorly oxygenated areas of the tissue; and the colloid property of PEG has been reported to increase the intra-vasculature oncotic pressure with significant effects in reducing oedema (Brockman *et al.*, 2013; Lewis and Ross, 2014). Interestingly, recent studies have shown that PNPH is beneficial for the treatment of stroke (Lewis and Ross, 2014),

traumatic brain injury and hemorrhagic hypotension in mice (Shellington *et al.*, 2011; Brockman *et al.*, 2013).

4.0.1.0 Aim

- To investigate whether PNPH administration ameliorates the neurological deficits in rats with active EAE.

4.1.0.0 Material and methods

4.1.1.0 Animal model: active EAE and PNPH administration

Female DA rats (n = 16; 8-9 weeks-old, ~150g, Harlan, UK) were kept in standard cages with food and water *ad libitum* on a twelve-hour light - dark cycle. Active EAE was induced one week after the arrival of the rats to allow acclimatization to the new environment. Active EAE was induced by a subcutaneous injection at the base of the tail of rMOG (100µg) in incomplete Freund's adjuvant (IFA) (Davies *et al.*, 2013). All experiments were performed in accordance with the UK Animals (Scientific Procedures) Act of 1986, and the ARRIVE guidelines.

4.1.2.0 PNPH administration

Rats with active EAE were randomly assigned to receive a daily injection of either PNPH or sterile saline solution (0.9% NaCl; sham controls) on the first three days of neurological deficits (first peak of disease; n = 8 per group). PNPH or saline was injected intravenously in the tail vein (5 mL/Kg). Neurological deficits were monitored up to 7 days after the onset of the disease.

4.1.3.0 Behavioural assessment

All behaviour assessments and analysis were performed blindly. Disease progression was monitored on a daily basis, including assessment of general health (weight) and neurological function. Progression of the neurological deficits was examined using a 10-point behavioural test as described in paragraph 2.1.2.0. To evaluate the acute effect of

the treatment, our detailed 30-point behavioural test (see paragraph 2.1.2.0) was used before and after 1 hour from the injection of PNPH (or saline).

4.1.4.0 Statistical analysis

Graphpad Prism v6.0 (USA) was used for statistical analysis and graph generation. All graphs represent mean ± S.E.M. (standard error of the mean). All statistical analyses were two-tailed and considered significant when $p < 0.05$. Non-parametric Mann-Whitney U-test was used to compare differences in the neurological deficit score between treated and untreated group.

4.2.0.0 Results

4.2.1.0 PNPH treatment for neurological dysfunction in rats with active EAE

To investigate whether PNPH administration can be beneficial for the treatment of neurological deficits due to neuroinflammation, rats with active EAE (n = 16) were randomly sorted to receive intravenous injections (5 mL/Kg/day) of PNPH or saline (sham controls) at the first, second and third day of disease (n = 8 per group). We finely evaluated the acute effect of the treatment by assessing the neurological deficits 1 hour after the administration using our detailed 30-point neurological test. Furthermore, we assessed the effects of the treatment on the progression of the disease by monitoring the severity of neurological deficits up to 7 days after the onset.

PNPH treatment did not significantly change the severity of neurological deficits 1 hour after administration on the first and third day of disease compared with sham controls (Figure 4.1a, c); but it significantly ameliorated the neurological function 1 hour after the administration on the second day of deficits (Figure 4.1b).

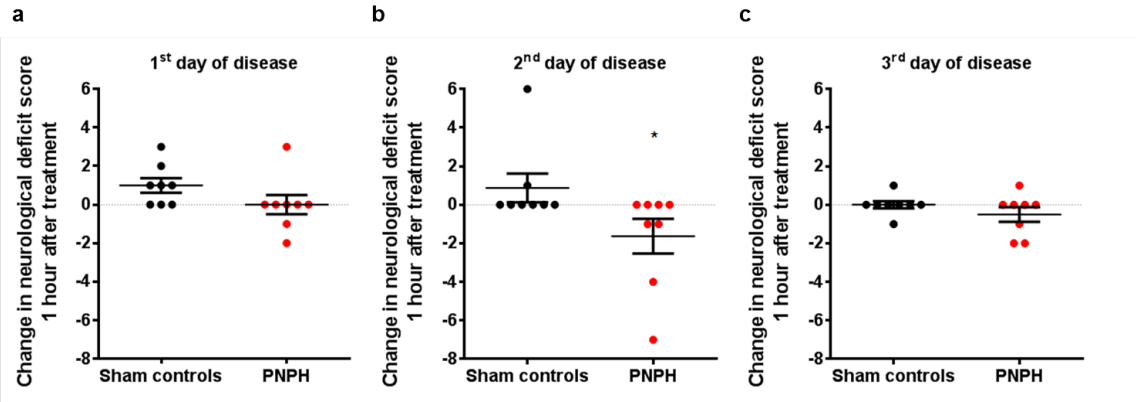

Figure 4.1 - Change in neurological deficit score 1 hour after PNPH administration.
a-c) PNPH was administered intravenously on the first, second and third day of disease. A 30-point behavioural test was used to assess the severity of neurological deficits after 1 hour from the injection, and it was expressed as a difference in the absolute score compared with the score before treatment administration. Zero represents no changes in neurological deficits after 1 hour from the administration, whereas positive and negative scores represent an exacerbation or amelioration of the neurological function respectively. PNPH-treated group did not show acute changes in neurological function for administrations on the first and third day of disease (a, c), whereas PNPH significantly improved the neurological function when administered at the second day of disease compared with sham controls (b; $p = 0.032$). Mann-Whitney U-test. N = 8 per group.

PNPH treatment injected daily on the first three days of disease (first peak of disease) did not ameliorate the progression of the neurological deficits compared with sham controls (Figure 4.2), in contrast with our observation with oxygen treatment (Chapter 2; paragraph 2.2.3.1). Indeed, EAE rats treated with PNPH showed only a mild, non-significant reduction of neurological deficits compared with sham controls (Figure 4.2).

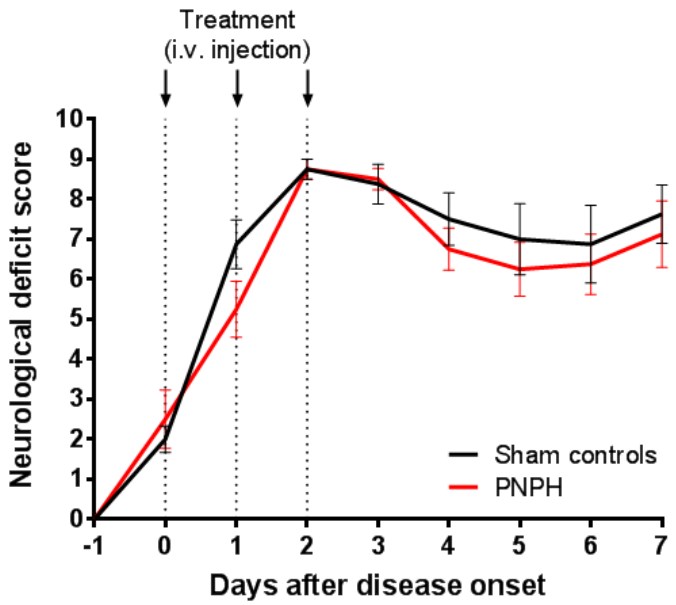

Figure 4.2 - PNPH treatment does not ameliorate the progression of the neurological deficits in rats with active EAE.
Rats with active EAE received an intravenous injection of PNPH or saline (Sham controls) on the first, second and third day of disease. Severity of neurological deficits was assessed for 7 days after the onset of the disease. PNPH treatment did not change the severity of neurological deficits compared with sham controls. Mann-Whitney U-test ($p > 0.05$). N = 8 per group

4.3.0.0 Discussion

4.3.1.0 Use of PNPH to improve tissue oxygenation and overcome the neurological deficits in a model of MS

PNPH is a complex compound that at the hemoglobin-based oxygen-carrying role combines both NO-mediated vasodilation and an antioxidant mechanism played by a SOD-mimetic activity. We speculated that the administration of PNPH would have been beneficial for the treatment of the neurological deficits in active EAE based on previous observations that the inflamed spinal cord is hypoxic (Davies *et al.*, 2013) and that re-oxygenation of the tissue via inspired oxygen-enriched air could ameliorate the neurological dysfunctions. Therefore, we thought that PNPH administration, similarly to what we observed with oxygen treatment, could improve the neurological deficits due to active EAE by reversing hypoxia and in addition reduce the oxidative stress via its SOD-mimetic activity. Although PNPH treatment promptly improved the neurological function in rats with active EAE 1 hour after the injection on the second day of deficits, it

did not significantly ameliorate the overall progression of the disease, in contrast to rats treated with oxygen. The reasons explaining the different efficacy of oxygen and PNPH treatment could include the following.

One mechanism that could limit the therapeutic outcome of PNPH in active EAE may be represented by the NO-mediated effect of the drug in vasodilation. Although increased volume of blood flow due to vasodilation can enhance the amount of oxygen transferred to the tissue, vasodilation may be detrimental during the acute phase of active EAE given the inflammatory/autoimmune nature of this model. Indeed, vasodilation causes a reduction in the velocity of the blood flow, thereby aiding the binding of leukocytes to the endothelial surface and their migration into the tissue (Smith and Lassmann, 2002). Furthermore, it has been described that NO can alter BBB permeability (Mayhan, 2000) and this effect may be further accentuated in animals with active EAE due to the compromised integrity of their BBB (Bennett *et al.*, 2010). Accordingly, it is possible that the NO moieties of PNPH have increased the amount of inflammatory cells and mediators entering into the CNS of rats with active EAE, counteracting the eventual beneficial effect resulting from the increased oxygenation of the tissue.

Another possible explanation for the limited therapeutic effect of PNPH administration in rats with active EAE, could be that the volume injected in our study (5 mL/Kg/day) was below the therapeutic dose. Although our dosage (5 mL/Kg) represents the maximum amount of liquid that we can inject intravenously in rodents according to the Home Office guidelines, other studies have reported beneficial effect on traumatic brain injury and hemorrhagic hypotension in mice by injecting higher volumes of PNPH (8 to 20 mL/kg) (Brockman *et al.*, 2013). Administration of PNPH below the therapeutic dose could explain the rapid improvement of neurological deficits 1 hour after the injection (on the second day of disease) and the absence of a long-lasting amelioration of the disease.

We calculated that a single bolus of 5 mL/Kg of PNPH increases the amount of oxy-hemoglobin in the blood by only 1%. In contrast, we observed that the administration in rats of inspired normobaric oxygen-enriched air (75%) results in an increment of arterial oxy-hemoglobin of approximately 3% (from ~97% to ~100%; data not shown).

Furthermore, it has been demonstrated that the administration of oxygen-enriched air (100%) at normobaric pressure, can increase by about 10%, the amount of hemoglobin-free oxygen dissolved in the arterial plasma (Nemoto and Betterman, 2007). These findings suggest that the administration of oxygen-enriched air can lead to a greater oxygenation of the tissues compared with PNPH, at least for a dose of PNPH of only 5 mL/Kg, thereby explaining the different therapeutic efficacy of these two treatments in active EAE.

4.3.2.0 Conclusion

Despite PNPH treatment during the first three days of deficits (first peak of disease) did not significantly attenuate the disease course compared with sham controls. Both the acute improvement of the neurological function after 1 hour from administration (on the second day of deficits), and the mild (non-significant) amelioration of the disease progression observed in PNPH-treated rats compared with controls, are suggestive of a potential beneficial this drug for the treatment of neurological deficits due to neuroinflammation. However, the treatment with PNPH, at least at a dose of 5 mL/Kg/day, was less effective than oxygen therapy. We think that the low efficacy of PNPH treatment may be due to 1) a modest increment of oxygen concentration in the blood, and/or 2) enhanced inflammatory infiltration in the spinal cord caused by NO-mediated BBB damage. We believe that systemic injection of a higher dose of PNPH can lead to a greater oxygenation of the tissue thereby producing a greater improvement of the disease. In addition, administration of PNPH prophylactically can also be taken in consideration as it could have a more pronounced beneficial outcome on the progression of the disease (as observed for oxygen therapy) and possibly, overcome the NO-mediated detrimental effect on the BBB, given that the BBB is still intact during the asymptomatic phase of the disease. We also note that administration of PNPH may be more acceptable to some patients than regular intake of oxygen, especially if the half-life of PNPH is prolonged. PNPH may also be safer as a “smoother” increase in oxygen over time, rather than regular inspiratory “shots”. Therefore, further studies are needed to assess the optimal therapeutic dose, timing and duration of the treatment, along with the characterization of the pathological effects of PNPH on inflammation, oxidative stress and BBB permeability during active EAE,

before considering or excluding the application of this compound for the treatment of patients with MS.

CHAPTER 5

5. GENERAL DISCUSSION

5.1.0.0 Hypoxia and neuroinflammation

This thesis provides evidence that tissue hypoxia is an important feature of the inflamed CNS in models of MS. Despite increasing evidence reporting the presence of a hypoxia-related energy deficiency in active MS lesions (Aboul-Enein *et al.*, 2003; Graumann *et al.*, 2003; Aboul-Enein and Lassmann, 2005; Paling *et al.*, 2011; Steen *et al.*, 2013; Yang *et al.*, 2015), a role for tissue hypoxia in the pathology of this disease has been largely overlooked.

In normal conditions, hypoxia has to be very severe before it impairs mitochondrial respiration and cause an energy crisis. This is due to the ability of the mitochondrial complex-IV to work at very low oxygen concentration thanks to its high enzymatic affinity (Km) for oxygen (<1μM) (Cooper *et al.*, 2003). However, this advantage seems to be lost in inflammatory condition. A role for NO has been proposed based on the observation that NO has a higher affinity than oxygen for binding to complex-IV. Indeed, even at very low concentration, NO efficiently binds the oxygen-binding site of complex-IV, raising the oxygen Km of this cytochrome (Cleeter *et al.*, 1994; Cooper *et al.*, 2003). Elevated Km means that the enzyme is less prone to bind the substrate and it is not normally saturated when the substrate is present at physiological concentration; so the rate of product formation will depend on the availability of the substrate in the cell. Thus, increased Km of complex-IV means that this complex needs higher concentration of oxygen in the tissue in order to maintain normal the rate of ATP synthesis.

In some MS lesions, NO is largely produced by infiltrated macrophages and reactive microglia (Marik *et al.*, 2007), and the NO-mediated mitochondrial impairment has been suggested to be one of the key mechanisms of axonal damage in MS (Smith and Lassmann, 2002; Kapoor *et al.*, 2003; Trapp and Stys, 2009). Indeed, a study has demonstrated that elevated NO concentration can block axonal conduction of both normal, and especially demyelinated axons (Redford *et al.*, 1997). In addition, in

conditions involving increased release of NO, even a small reduction in oxygen supply to the tissue may have a large effect on the ATP production and the survival of the cells. We believe that NO is involved in the pathology of MS, and its detrimental effect on the mitochondrial respiration can be both a source of tissue hypoxia, as well as further accentuated by decreased oxygen level due to other mechanisms.

Recent evidence showed that inflammation causes a series of metabolic changes within the tissue (Kominsky *et al.*, 2010), which can result in tissue hypoxia. Lymphocytes greedily use glucose, amino acids and lipids as energy sources for oxidative phosphorylation (Kominsky *et al.*, 2010). When reactive, lymphocytes are even more dependent on glucose and oxygen consumption to sustain their proliferation and migration through the tissue, and to support synthesis and secretion of inflammatory mediators (Kominsky *et al.*, 2010). By contrast, inflammatory cells of myeloid lineage (polymorph nuclear leukocytes (PMN), microglia, monocytes and macrophages) are thought to rely predominantly on anaerobic metabolism, and to have a relatively small number of mitochondria. Nevertheless, during phagocytosis PMN and macrophages increase their oxygen consumption through a mechanism known as the respiratory (or oxidative) burst. The respiratory burst is mediated by the enzyme NADPH oxidase, which uses oxygen to generate superoxide anion (O_2^-) (Dahlgren and Karlsson, 1999). This oxygen metabolites gives rise to other ROS that act as pro-inflammatory/ anti-microbial mediators (Dahlgren and Karlsson, 1999). ROS can also damage the surrounding tissue and further disrupt mitochondria, causing mitochondrial DNA mutation and impairment of the respiratory chain (Mahad *et al.*, 2008; Nikic *et al.*, 2011; Guo *et al.*, 2013; Witte *et al.*, 2014), thereby exacerbating the energy deficit. As a result, sites of ongoing inflammatory activity including lymphocytes and/or oxidative-active myeloid leukocytes can become rapidly depleted of both nutrients and oxygen (Kominsky *et al.*, 2010).

Infiltration into the CNS of a large number of energy-consuming lymphocytes (T-cells, B-cells and cytotoxic lymphocytes) and reactive leukocytes of the myeloid lineage (mainly macrophages) has been described in patients with MS (Hemmer *et al.*, 2015). Furthermore, increased levels of the active form of NADPH oxidase have been found within MS active lesions (Fischer *et al.*, 2012) in combination with markers of oxidative damage (oxidized DNA and phospholipids) (Haider *et al.*, 2011; Fischer *et al.*, 2012),

implying that, in MS, cells of the innate immune system are consuming oxygen via the oxidative burst. Studies in rodents demonstrated that a profound, innate immune response in the CNS can be sufficient in causing demyelination. In particular, the infiltration of innate immune cells in the spinal cord triggered by the injection of LPS in the dorsal column, can result in the formation of a demyelinating lesion in rats (Felts *et al.*, 2005). A recent study from our lab has shown that this lesion has hypoxia-related properties including positivity for hypoxic markers such as pimonidazole and HIF1α (Desai *et al.*, 2016). In these rats, the demyelinating lesion is not centered on the site of LPS injection, but occurs slightly distant and in particular at the white-grey matter edge in an area with a relatively lower density of blood vessels (Desai *et al.*, 2016). Interestingly, in this model, oxygen treatment can protect from LPS-mediated demyelination (Desai *et al.*, 2016).

Intriguingly, among the inflammatory-mediated mechanism of tissue hypoxia, the brain of patients with MS can also suffer of reduced blood perfusion (D'haeseleer *et al.*, 2015). It is easy to image that a diminished blood supply to the CNS may cause hypoxia, however the mechanisms underlying this reduction are still unclear. Initially, it was suggested that the decreased cerebral blood flow (CBF) in patients with MS was a consequence of the decreased metabolic demand due to axonal degeneration and CNS atrophy. However, recent evidences have shown that also the NAWM of patients with MS may suffer of decreased blood supply (Paling *et al.*, 2014). Thus, the widespread reduced perfusion of the CNS of patients with MS seems not to be secondary to axonal degeneration and CNS atrophy. A defect in cerebral venous drainage, which could affect the regular perfusion of the brain, has been proposed to correlate with the incidence and severity of MS. Zamboni and colleagues described an association between MS and a condition known as chronic cerebrospinal venous insufficiency (CCSVI) (Zamboni *et al.*, 2009). CCSVI is characterized by high incidence of multiple stenoses in the internal jugular vein and azygos vein, which can impair the cerebral venous outflow of the blood. However, several independent studies failed to confirm any correlation between CCSVI and MS (reviewed in D'haeseleer *et al.*, 2015).
It cannot be excluded that the reduced perfusion in the NAWM of patients with MS could be secondary to a reduced axonal activity and/or astrocyte dysfunction. In normal conditions, the conduction of the electric impulse along the axons releases potassium

ions (K^+) in the extracellular space. K^+ is readily taken by astrocytes through K^+ channels (Kir) and released into the perivascular space in a process that leads to arteriolar vasodilation (Knot and Nelson, 1998; Butt and Kalsi, 2006). Decreased neuronal activity might reduce K^+ axonal release and its subsequent release by astrocytes in the perivascular space, possibly leading to a state of hypo-perfusion (D'haeseleer *et al.*, 2011). Furthermore, this process of K^+ uptake and release is highly energy consuming for the astrocytes due to the activity of the Na^+/K^+ ATPase. Na^+/K^+ ATPase is fundamental in maintaining the negative membrane potential of the astrocytes, necessary for the optimal intracellular K^+ distribution and Kir functioning (Bolton *et al.*, 2006).

In addition, the energy metabolism of astrocytes has been described to be dysfunctional in MS. Indeed, astrocytes in patients with MS have been shown to be deficient in β2-adrenergic receptors (De Keyser *et al.*, 1999), which regulate glycogenolysis, and have reduced phosphocreatine metabolism caused by decreased cytosolic creatine kinase B (Steen *et al.*, 2010). Deficiency in astrocytic ATP synthesis could affect the normal function of the Na^+/K^+ ATPase, resulting in a dysfunctional regulation of vessel tone and decreased blood perfusion.

Davies and colleagues revealed that also the spinal cord of rats with active EAE can be hypoxic, and such hypoxia consists of an actual reduction of the spinal cord oxygen concentration (Davies *et al.*, 2013). Interestingly, they have seen that by giving rats normobaric oxygen-enriched air to breathe, it is possible to reverse the hypoxia and ameliorate the neurological deficits (Davies *et al.*, 2013).

In this thesis, we discovered that neuroinflammation *per se* can cause hypoxia in the spinal cord of rats with passive EAE. In contrast with active EAE, in passive EAE hypoxia occurs in the absence of major structural damage such as demyelination, in the presence of relatively mild microglial activation and macrophage recruitment, and low levels of oxidative stress (Schuh *et al.*, 2014). The mechanisms underlying tissue hypoxia in rats with passive EAE are still unclear. While a role for the oxidative burst and NO-mediated mitochondrial dysfunction may be marginal in causing tissue hypoxia in this model (Schuh *et al.*, 2014), a key part might be played by the infiltration of a large number of oxygen-consuming T-cells (Kominsky *et al.*, 2010) in the spinal cord of these rats (Linington *et al.*, 1993).

Importantly, the absence of demyelination in rats with passive EAE has led to the belief that the neurological deficits are due to inflammation, but via incompletely understood mechanisms. Here, we discovered that tissue hypoxia can help to explain the loss of neurological function in this model.

5.2.0.0 Hypoxia and loss of neurological function: a role for oxygen therapy?

Our findings provide evidence that hypoxia contributes to the neurological deficits due to neuroinflammation, and that by increasing tissue oxygenation it is possible to ameliorate the severity of the disease.

In rats with active EAE, we confirmed that oxygen therapy can reverse tissue hypoxia, and we provide information on the optimal time and duration of the treatment.
We have seen that oxygen therapy can result in a specific, transient improvement of neurological deficits when administered for only 1 hour, whereas it can ameliorate the disease progression when applied for longer.
Although oxygen treatment (for 24 hours) ameliorated the neurological dysfunctions independently from the day of disease at which it was administered, the treatment was more effective when applied from the onset of deficits. Interestingly, when applied from the onset of the disease for 24, 48 or 72 hours, rats displayed a milder progression of the neurological deficits even after treatment cessation compared with room air controls, suggestive of a disease modifying effect of oxygen. In particular, oxygen treatment from the onset of disease resulted in a more pronounced amelioration of the deficits during the remitting phase, especially when applied for 72 hours. In addition, the treatment protected from demyelination at the peak of disease, in proportion to the duration of the exposure, suggesting that the efficacy of oxygen treatment increases not only dependently on the stage of disease at which it is administered (the earlier the better), but also with longer exposure.

Intriguingly, oxygen treatment was remarkably effective when administered prophylactically. The fact that both in active and passive EAE, oxygen treatment significantly ameliorated the disease progression when administered during the

asymptomatic phase, raises the possibility that a metabolic dysfunction may occur even before the onset of neurological signs, and oxygen can change the pathogenesis of the disease. Furthermore, the efficacy of prophylactic oxygen in passive EAE supports our hypothesis that the beneficial effect of oxygen is due to a metabolic-related mechanism rather than an anti-inflammatory role.
However, it remains unclear why therapeutic oxygen treatment in passive EAE, in contrast with active EAE, did not ameliorate the severity of the disease when administered at the onset of the neurological deficits.

In this thesis, we also evaluated the role of a hemoglobin-based oxygen carrier (PNPH) in active EAE, as an alternative approach to deliver oxygen in the inflamed, hypoxic CNS. Although PNPH treatment significantly ameliorated the severity of deficits after 1 hour from the injection on the second day of disease and resulted in a mild attenuation of disease progression compared with controls, its efficacy was lower relative to the treatment with oxygen-enriched air. Therefore, further investigations are needed to ascertain the advantages of administering PNPH as an alternative oxygen-based approach for the treatment of deficits in MS.

5.3.0.0 Oxygen therapy and pathological implications

The most important pathological finding was that oxygen treatment administered in rats with active EAE from the onset of deficits for 24, 48 or 72 hours, reduced oligodendrocyte loss and demyelination at the peak of disease. Furthermore, we have seen that oxygen decreased cellular stress in oligodendrocytes, highlighted by a reduction in eIF2α phosphorylation, which has possibly restored a normal rate of protein synthesis contributing to the greater oligodendrocytes survival achieved after the treatment. Notably, these protective effects of oxygen were proportional to the duration of the treatment and greater in rats treated for 72 hours. When applied from the onset of deficits for 72 hours, oxygen also reduced microglial activation and macrophage recruitment at the peak of disease, but did not change the amount of infiltrated T-cells and pro- and anti- inflammatory markers in the spinal cord. The reduced microglial and macrophage activation, in the absence of other evidence of reduced inflammation, may be a consequence of the reduced demyelination after

oxygen exposure, which may have led to a decreased demand of phagocytic cells for the clearance of myelin debris in the tissue. An alternative explanation for the reduced number of ED-1^{+} cells (macrophages and activated microglia) observed in the spinal cord of rats treated with oxygen, may include a reduced migration of macrophages into the CNS. This could have been caused by the reduced tissue hypoxia achieved with oxygen administration, given that hypoxia can act as a chemo-attractant for the recruitment of these cells within tissues (Murdoch and Lewis, 2005; Chanmee *et al.*, 2014). Furthermore, another important component in the pathogenesis of EAE and MS is represented by B-cells and the consequent antibody-mediated tissue damage (Griot-Wenk *et al.*, 1991; Mann *et al.*, 2012; Pikor *et al.*, 2012) (see also paragraph 2.3.3.3). However in this study we did not evaluate whether the oxygen treatment changes the trafficking and activation of B-cells during active EAE.

Interestingly, the reduced level of eIF2α phosphorylation observed in oligodendrocytes after oxygen treatment, raises the possibility that hypoxia can affect the functionality of these cells. Until now, eIF2α phosphorylation in oligodendrocytes during active EAE has been attributed exclusively to an inflammatory-mediated activation of PERK led by increased levels of IFNγ (Lin and Popko, 2009; Stone and Lin, 2015). Our findings demonstrate that oxygen is able to decrease eIF2α phosphorylation without changing the level of IFNγ or other inflammatory markers, suggesting that in active EAE also the hypoxia can be a source of cellular stress in oligodendrocytes. Nevertheless, it remains unclear how a shortage of oxygen can cause stress in oligodendrocytes, given that these cells have been recently described to rely mainly on the anaerobic glycolysis for their energy need (Fünfschilling *et al.*, 2012).

Although glycolysis may represent the main energy source for oligodendrocytes, some studies reported an important, preserved activity of the mitochondrial respiration in these cells *in-vitro* (Ziabreva *et al.*, 2010), and high susceptibility of oligodendrocytes to ischemic injury *in-vivo* (Dewar *et al.*, 2003).

Furthermore, it is possible that a significant amount of oxygen is used by oligodendrocytes to maintain lipid homeostasis. Indeed, a large amount of α-hydroxy fatty acids such as cerebronic acids are found in the mammalian brain as components of cerebrosides and sulfatides that are cell-membrane lipids of which oligodendrocytes are particularly enriched (Thompson, 1992). These lipids are formed from straight chain

fatty acids via the action of multifunctional oxygenases that require oxygen and NADPH (Thompson, 1992). In addition, lipid peroxidation, which is a mechanism of lipid degradation, can also account for part of the oxygen consumption. Lipid peroxidation can occur either non-enzymatically (via the action of free radicals) or through the action of specific enzymes such as cyclooxygenase and lipoxygenase (Thompson, 1992). As the names suggest, cyclooxygenase and lipoxygenase are enzymes that require oxygen as substrate to catalyze the reactions (Thompson, 1992; Filimonov and Vrzheshch, 2007). It has been estimated that, while under normal conditions lipid peroxidation accounts only for a small portion of lipid degradation, its level can increase 5-fold during severe stress such as malignant growth, deficiency of vitamin E, and X-ray irradiation (Thompson, 1992). In addition, hypoxia has been demonstrated to increase cytosolic phospholipase A2 activity, liberating more unsaturated fatty acids from lipid membranes to act as substrates for cyclooxygenase and lipoxygenases (Barnett *et al.*, 2010).

Oligodendrocytes are characterized by an extensive cell-membrane surface; therefore they may require a consistent amount of oxygen to sustain lipid homeostasis, making them particularly susceptible to hypoxia. In active EAE, myelin disruption could increase the amount of membrane lipids liberated in oligodendrocytes, boosting the cyclooxygenase- and lipoxygenases- mediated degradation. Furthermore, oligodendrocytes may try to repair the membrane damage by increasing the formation of polyunsaturated fatty acids. Therefore, these cellular mechanisms may be enhanced during inflammatory demyelination, augmenting the oxygen demand of oligodendrocytes.

Interestingly, the majority of the cellular lipids are processed in the ER, while other specific fatty acids are metabolized in the mitochondria. In oligodendrocytes, during EAE, the increased lipid homeostasis in addition to the elevated protein synthesis caused by inflammation (Lin and Popko, 2009), may overload the ER working capacity causing ER stress and the consequent phosphorylation of eIF2α.

A safety concern for the use of oxygen in MS is the fact that increased oxygenation can enhance oxidative stress. In active EAE, while nitrative stress may be marginal as indicated by the transient expression of iNOS and mild nitrative damage (e.g. nitrotyrosination of proteins) at the peak of disease (Schuh *et al.*, 2014), oxidative

stress represents an important source of tissue damage. Interestingly, we observed that oxygen exposure up to 72 hours from the onset of the disease does not exacerbate oxidative stress at the peak of deficits, as indicated by markers of oxidative damage like oxidized DNA/RNA and phospholipids. Surprisingly, administration of oxygen for 72 hours from the onset of deficits resulted in a significantly decreased level of oxidized phospholipids.

It is possible that the lower phospholipid oxidation after oxygen exposure may be due to decreased oxidative stress resulting from the reduced hypoxia (Xu *et al.*, 2004; Strapazzon *et al.*, 2016), although the mechanisms through which hypoxia enhances oxidative stress are not entirely understood (see below).

A mechanism involving “reductive stress” has been suggested. Reductive stress is a condition in which cells are in a more reductive state due to increased levels of reducing equivalents such as NADH and $FADH_2$ (Clanton, 2007). These molecules can accumulate in hypoxic condition due to the decreased efficiency of mitochondrial oxidative phosphorylation. In oxidative phosphorylation, oxygen acts as the final electron acceptor, and in low cellular oxygen concentrations the lack of oxygen can slow mitochondrial respiration leading to an accumulation of NADH and $FADH_2$ which are not oxidized upstream in the electron transport chain. NADH and $FADH_2$ contain a pair of electrons with high transfer potential. At elevated concentrations, some NADH and $FADH_2$ molecules can escape the respiratory chain, and directly transfer the electron to oxygen forming superoxide anions (O_2^-, a free radical) (Clanton, 2007).

Reductive stress can be even more severe in the condition of *virtual* (or chemical) hypoxia. *Virtual* hypoxia is caused by an intrinsic impairment of mitochondrial respiration rather than from an actual shortage of oxygen supply. Antagonists of mitochondrial complexes such as NO (which inhibits complex-IV) can cause chemical hypoxia by either slowing down or blocking the electron transport chain. In this condition, the oxidative stress resulting from elevated levels of NADH and $FADH_2$ can be even more severe. Indeed, during chemical hypoxia NADH and $FADH_2$ accumulate in an environment rich in oxygen, so there is more oxygen available to which electrons can be transfered, causing a greater production of ROS (Clanton, 2007).

All together, these findings provide evidence that oxygen therapy applied in a demyelinating model of MS (active EAE) can ameliorate the neurological deficits and

protect from demyelination without exacerbating the oxidative stress, indicating a beneficial role of oxygen with relatively low side effects.

5.4.0.0 Limitations of methods

In this study we examined whether oxygen therapy may be a suitable treatment for neurological dysfunction in MS using two models of MS in rat, namely passive and active EAE. These models are commonly used in pre-clinical research to study the mechanisms involved in the pathology of MS and to test the efficacy and safety of new therapeutic approaches before their application in patients (Stromnes and Goverman, 2006a, 2006b). However, active and passive EAE mimic only a few features of MS and they do not reproduce the entire spectrum of disabilities and pathological mechanisms observed in the human disease (see also Introduction 1.2.0.0). In this regard, the differences between MS and EAE must be taken into consideration before applying to MS patients treatments that have been tested only in EAE. First, EAE is a purely autoimmune-mediated disease, whereas the mechanisms contributing to the pathology of MS are more complex and they remain largely unknown (Noseworthy *et al.*, 2000; Stromnes and Goverman, 2006a), implying that some aspects of MS may not be represented in EAE studies. For example, while an important role for inflammation and autoimmunity has been recognized during the relapsing-remitting phase of MS, other mechanisms such as nitrative and oxidative damage, mitochondrial dysfunction, and energy crisis have been shown to be predominant during the progressive phase of MS (Lassmann *et al.*, 2012; Witte *et al.*, 2014), and these mechanisms are only partially reproduced in EAE. DA rats (Storch *et al.*, 1998) and Biozzi AB/H mice (Baker *et al.*, 1990; Al-Izki *et al.*, 2012), especially during advanced stages of active EAE, mimic some characteristics of progressive MS, but currently no animal models exist that reproduce the entire pathological spectrum of progressive MS (see also Introduction 1.2.0.0). Thus, many treatments that have been proven to be effective in EAE, fail to reproduce a similar beneficial effect in progressive MS.

Furthermore, the rodents used in this study were genetically identical and they were maintained in finely controlled environmental conditions in order to reduce both genetic and environmental variability among animals. This contributes to a decrease in the

number of possible confounding factors that could affect the outcome of the experiments. By contrast, in MS, the high environmental and genetic variability between patients can strongly impact the outcome of a clinical trial. This variability is one of the reasons why many treatments that have proven to be effective in EAE, sometimes do not reproduce the same outcome in MS and they need to be tested in a large number of patients in order to assess accurately whether they are beneficial or not in humans.

As mentioned before in the course of this thesis, another important limitation of EAE models is that the oxidative and nitrative damage in the inflamed CNS is transient and less severe compared with the one occurring in active MS lesions (Schuh *et al.*, 2014). This aspect is of fundamental interest in the characterization of oxygen as a potential treatment for MS, as hyperoxia may contribute to the oxidative damage due to neuroinflammation.

In this study, RT-PCR analysis was performed on lumbar spinal cord cross-sections of rats with active EAE at the first peak of disease in order to evaluate whether treatment with oxygen affects the expression of pro- and anti-inflammatory markers. At the first peak of disease, inflammation is mainly localized in the sub-meningeal area of the spinal cord. Therefore, it is possible that via a gene expression analysis in a whole cross-section we may have diluted small, but possibly significant differences between groups. In this regard, a gene expression analysis on only the inflamed lumbar spinal cord dorsal column could be more precise and possibly highlight even small differences between groups.

5.5.0.0 Oxygen therapy: clinical implications in MS

The use of oxygen therapy in patients with MS has been evaluated in several clinical trials during the 1980s (Fischer *et al.*, 1983; Massey *et al.*, 1985; Murthy *et al.*, 1985; Neiman *et al.*, 1985; Wood *et al.*, 1985; Confavreux *et al.*, 1986; Harpur *et al.*, 1986; Wiles *et al.*, 1986; Barnes *et al.*, 1987; Oriani *et al.*, 1990). In these trials, oxygen was administered at hyperbaric pressure (hyperbaric oxygen treatment, HBOT) in patients with stable, chronic MS. Although many MS patients reported a transient improvement of neurological function after HBOT (Fischer *et al.*, 1983; Murthy *et al.*, 1985; Barnes *et*

al., 1987; Oriani *et al.*, 1990), with some indicating a long-lasting attenuation of the disease severity up to 6 months after treatment cessation (Fischer *et al.*, 1983); several other clinical trials did not detect any beneficial outcome from the use of HBOT in MS (Confavreux *et al.*, 1986; Harpur *et al.*, 1986; Massey *et al.*, 1985; Neiman *et al.*, 1985; Wood *et al.*, 1985). Recently, a meta-analysis of HBOT trials in MS concluded that there is not enough evidence of clinical benefits to support the use of HBOT for the treatment of MS (Bennett and Heard, 2010).

Increasing knowledge about the pathology of MS and use oxygen therapy in animal models is providing a number of observations that could explain the discordant therapeutic effects of HBOT in MS, along with important indications that can lead to a reconsideration of oxygen as a valuable treatment for this disease.

First, the use of HBOT in MS was based on the belief that oxygen could play an anti-inflammatory role (Warren *et al.*, 1978). Instead, our findings in EAE suggest that oxygen treatment does not directly affect inflammation. In particular, we discovered that the beneficial effect of oxygen is mainly due to a metabolic- hypoxic-related mechanism. In this regard, studies revealed that only a subgroup of patients with MS have hypoxia-like lesions and suffer of a CNS energy deficit (Lucchinetti *et al.*, 2000; Steen *et al.*, 2013; Yang *et al.*, 2015); therefore, it is possible that not all patients with MS can benefit from oxygen administration.

The facts that only a subgroup of patients with MS could eventually benefit from oxygen treatment, and that the majority of HBOT clinical trials were performed on relatively small cohorts of cases, sometimes less than 30 patients were examined (Massey *et al.*, 1985; Neiman *et al.*, 1985), it is possible that beneficial effects have been overlooked.

Larger numbers of MS patients, in conjunction with the preventive use of MRI (Paling *et al.*, 2011) or near-infrared spectroscopy (Yang *et al.*, 2015) methods may help in identifying those MS patients that suffer from hypoxia and an energy deficit in the CNS, and that can possibly benefit the most from oxygen administration.

Two other important factors that may also have reduced the efficacy of HBOT in MS could be 1) the stage of disease at which the treatment was applied, and 2) the duration of the exposure. We have seen that oxygen therapy in rats with EAE is more effective when administered at the early phase of disease. However, patients were treated with

HBOT during the chronic stage of MS. This might have reduced the efficacy of the treatment due to the advanced, severe status of the disease, which leaves little opportunity for any improvements following the therapy. Furthermore, our preclinical studies revealed that prolonged exposures to oxygen (≥ 24 hours) are more likely to result in a prominent long-term attenuation of the disease, whereas a short-term administration (1-hour) of oxygen results in a transient amelioration of the neurological function, and the beneficial effects disappear when animals are returned to room air. Interestingly, the great majority of HBOT trials investigated a course of 20 exposures with HBOT administered daily for only 90 minutes over 4 weeks (reviewed in Bennett and Heard, 2010). Similarly to what we observed in 1-hour oxygen-treated rats with active EAE, HBOT for 90 minutes (Fischer *et al.*, 1983; Murthy *et al.*, 1985; Barnes *et al.*, 1987; Oriani *et al.*, 1990) resulted in a mild, transient amelioration of neurological dysfunction in patients with MS; indicating that such short-term administration of oxygen, even if repeated daily, is not enough to establish a long-lasting attenuation of the disease.

In addition, HBOT has been proposed to induce higher superoxide production than oxygen at normobaric pressure, increasing cell toxicity (Nemoto and Betterman, 2007; Singhal, 2007). Instead, normobaric oxygen therapy has been described to be safer and more effective than HBOT in animal models of ischaemic stroke (Singhal, 2007; Weaver and Liu, 2015), resulting in decreased infarct volume without exacerbating the oxidative stress (Singhal, 2007; Weaver and Liu, 2015). Indeed, a number of studies reported reduced levels of oxidative stress in mice with ischaemic stroke after normobaric oxygen treatment compared with untreated controls (reviewed in Weaver and Liu, 2015); whereas HBOT of ischaemic injury was associated with increased oxidative stress, mainly linked to the higher concentration of oxygen dissolved in the plasma (Nemoto and Betterman, 2007; Ding *et al.*, 2014). It is possible that the increased oxidative stress following HBOT administration in patients with MS have counteracted the beneficial effect resulting from the increased oxygenation of the CNS. Nevertheless, MS patients exposed to HBOT did not report deleterious side effects after treatment (Bennett and Heard, 2010).

Therefore, we believe that the failure of HBOT in MS clinical trials can be attributable to: 1) advanced disease stage for therapy administration, 2) short-term exposure to

oxygen, 3) inadequate number of patients included in the trials, and 4) possible exacerbation of the oxidative damage due to pressurized inspired oxygen-enriched air.

In the light of our preclinical studies, we suggest that oxygen therapy at normobaric pressure has a renewed relevance for the treatment of MS. Indeed, we discovered that prolonged exposures (≥ 24 hours) to normobaric oxygen therapy result in a long-lasting amelioration of the neurological deficits when applied from the early stages of the disease, seemingly without side effects. Indeed, consistent with studies in models of ischaemic stroke (Weaver and Liu, 2015), we have seen that, in active EAE, administration of normobaric oxygen does not exacerbate oxidative stress. However, Schuh and colleagues (2014) have demonstrated that animal models of MS, including active and passive EAE, fail in reproducing the same severity of the oxidative and nitrative stress observed in active MS lesions, revealing that EAE is an inadequate model to study the oxidative/nitrative damage occurring in MS. Nevertheless, the presence of only few side effects on both CNS and peripheral organs following normobaric oxygen therapy in patients with ischaemic stroke (Singhal *et al.*, 2005; Singhal, 2007) suggests that oxygen treatment could be similarly safe also in MS. However, we advise caution in the use of oxygen in MS until the safety of oxygen therapy in this disease is fully established.

An interesting opportunity to investigate the efficacy of normobaric oxygen therapy for the treatment of neuroinflammatory diseases in clinic is represented by patients with acute optic neuritis. Optic neuritis shares some pathological similarities with MS and represents a unique scenario for testing oxygen in a relatively simple inflammatory/demyelinating context. Indeed, optic neuritis is characterized by defined inflammatory demyelinating lesions of the optic nerve that cause loss of vision (partial or complete), whereas, in MS, focal lesions can arise everywhere in the CNS leading to a variety of signs and symptoms. Interestingly, recent observations from our lab have shown that sensitization with rMOG of Brown Norway rats often results in the inflammation of the optic nerve and importantly, the inflamed optic nerve is hypoxic (unpublished data). Accordingly, it is possible that patients with optic neuritis suffer tissue hypoxia at the level of the optic nerve, so they may benefit from oxygen administration. We suggest that patients with optic neuritis are treated with oxygen (60-80% for 1 hour) as early as possible, as the earliest treatment is the most likely to

produce the greatest beneficial effect. Based on our preclinical studies, we believe that 1 hour of oxygen exposure may already be sufficient to produce a specific, although probably transient beneficial effect. Furthermore, short-term administrations of oxygen minimize patient's discomfort and are unlikely to induce side effects. Finally, the clinical outcome of the therapy can be simply assessed by measuring the visual evoked potential before and after oxygen administration. This trial may provide preliminary evidence of whether oxygen treatment is beneficial for inflammatory demyelinating diseases in humans, raising the opportunity to target other neuroinflammatory pathologies such as MS.

5.6.0.0 Future perspectives

In this thesis we used prolonged administration of inspired oxygen at high concentrations (≥75% for up to 72 hours) to maximize the effects on disease pathogenesis. Although, it is reasonable to believe that beneficial effects can be achieved even with lower concentrations and/or shorter exposure to the treatment. Indeed, we have seen that 1 hour of oxygen (100%) is already sufficient to promptly ameliorate the deficits, although the beneficial effects were transient. Future research may focus on investigating different doses and durations of oxygen treatment. Longer, daily administration of oxygen (e.g. 4 hours) applied from the early phase of the disease, may be effective in ameliorating neurological function, and protect from a worsening of the deficits. This would help in identifying a good compromise between long-term amelioration of the disease and a reasonable administration of the therapy which could be easily applied in patients' homes, minimizing patient distress and possible side effects.

Furthermore, we showed that oxygen plays a beneficial effect by mainly acting on tissue hypoxia and energy deficit in EAE, with seemingly few effects on the autoimmune response. Future research may focus on the role of oxygen when administered in addition to other therapeutic approaches for MS. Notably, oxygen could be administered in combination with neuroprotective drugs as phenytoin (sodium channel blocker) (Raftopoulos *et al.*, 2016) or immunomodulatory treatments as Fingolimod or BG12. The different mechanisms of action between oxygen and these

drugs could lead to an additive or even synergetic beneficial effect when administered together.

Here we have investigated the role of oxygen in ameliorating disease progression when administered at early stages of EAE (first peak of disease). However, it is possible that oxygen treatment may be effective also at more advanced stages, even though the greatest beneficial effect was achieved when oxygen was administered at the onset of neurological deficits. In advanced stages of MS, neurological deficits are mainly triggered by neuronal degeneration caused by metabolic-related cytodegeneration (Trapp and Stys, 2009; Lassmann, 2013) and inflammation caused by immune cells "trapped" within the CNS rather than new inflammatory cells entering from the blood stream (Lassmann, 2013). Similarly, in rats with active EAE neurodegeneration occurs at later stages of disease (including the second peak). At advanced stages of disease, a more prominent role for mitochondrial dysfunction and tissue hypoxia in neurodegeneration has been suggested in both MS and EAE (Trapp and Stys, 2009; Nikic *et al.*, 2011; Witte *et al.*, 2014). Therefore, it is possible that oxygen therapy, especially if started from the beginning of the neurological deficits, but also when applied during the progressive stage, may result in a long-term amelioration of the disease protecting from neurodegeneration.

In this thesis, we also investigated the use of a hemoglobin-based oxygen carrier (PNPH, SynZyme, USA) as an alternative method to increase oxygen delivery in the inflamed, hypoxic spinal cord of rats with active EAE. Despite our preliminary results suggest that PNPH is less effective than normobaric oxygen-enriched air in ameliorating the severity of the disease, further investigation may help in understand whether an optimization of the time and dosage of the therapy can increase its efficacy. Importantly, while gaseous oxygen therapy is an off-patent treatment (Stoller, 2015) thereby it is not economically attractive for the investment of large amount of money in long and expensive clinical trials; hemoglobin-based oxygen carriers are patentable compounds and they may catalyze the scientific and economic interests of pharmaceutical companies and research agencies in investigating whether oxygen-based therapies are effective for the treatment of patients with MS.

5.7.0.0 Concluding remarks

This thesis provides further evidence that hypoxia may be an important factor in the pathology of neuroinflammatory disease. We discovered that neuroinflammation *per se* is sufficient in causing CNS hypoxia. Interestingly, this hypoxia can contribute to some of the key pathological features of MS including neurological deficits, demyelination and oligodendrocytes loss. Importantly, we discovered that oxygen therapy can protect from demyelination and oligodendrocyte death, and ameliorate the severity of the disease. However, the protective effect of oxygen in EAE was partial and some animals did not benefit from the therapy. These results suggest that hypoxia is only one of the mechanisms contributing to the pathogenesis and progression of the disease.

We provide insights about the optimal time and duration of the treatment, revealing that oxygen therapy is more effective when administered at the very beginning of neurological signs and that the duration of the exposure, at least up to 72 hours, proportionally correlates with the spinal cord protection and long-term attenuation of the disease. Interestingly, oxygen therapy can also delay the onset of deficits if administered prophylactically, suggesting that an energy deficit may occur during the asymptomatic phase of the disease. These findings confirm our hypothesis that hypoxia may be an important player in neuroinflammatory diseases and oxygen therapy can protect from neurological deficits and CNS damage, representing a potential treatment for patients with MS.

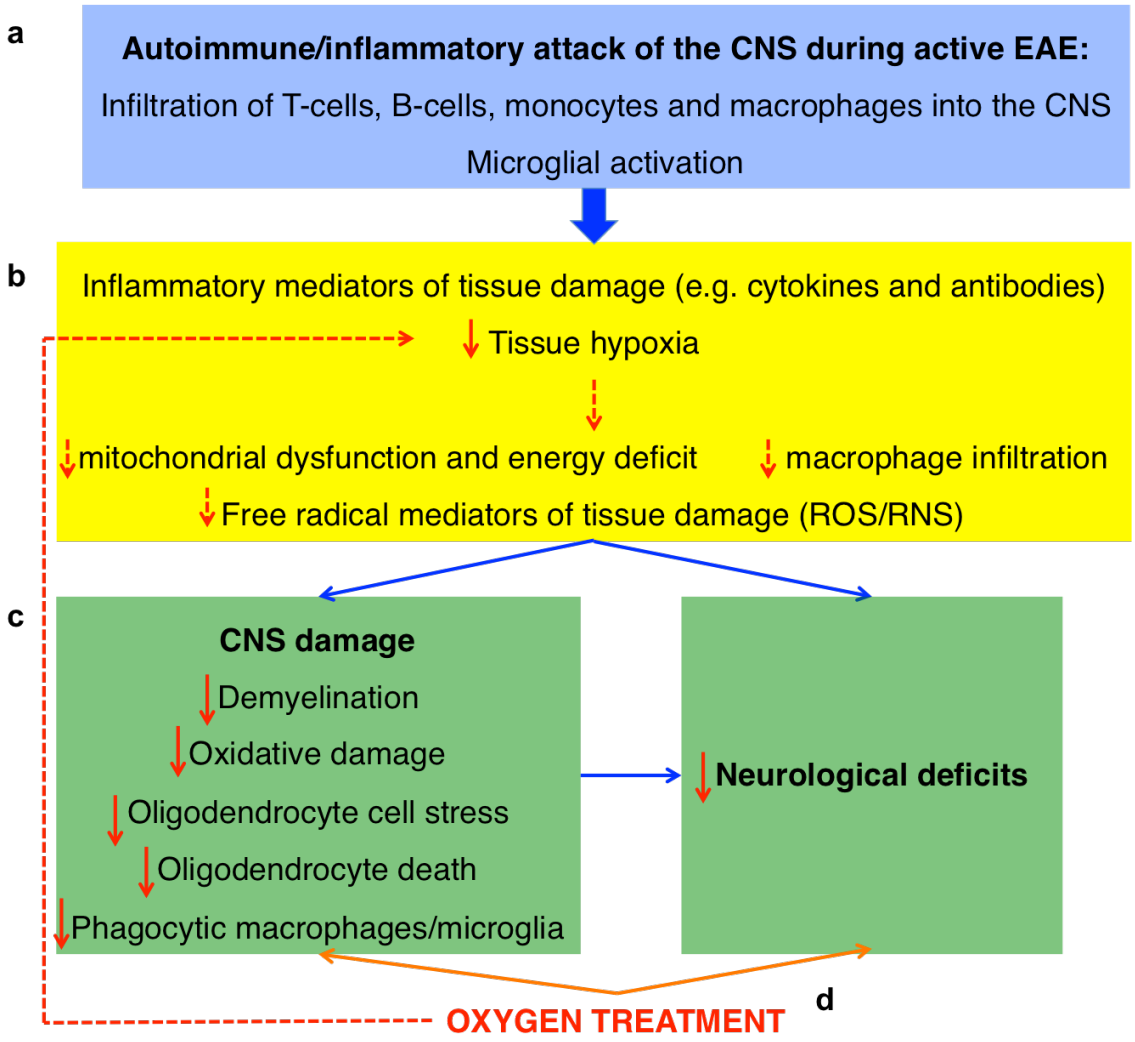

Figure 5.1 – Schematic representation of the likely effects of oxygen treatment in active EAE.

The graph above summarizes the main effects of oxygen therapy (75% for 72 hours from the onset of neurological deficits) in rats with active EAE, and it proposes a possible mechanism of action of the treatment. **a)** Immunisation of DA rats with rMOG (active EAE) leads to an autoimmune/inflammatory response consisting of an infiltration of T-cells, B-cells, and monocytes/macrophages into the CNS, and the activation of resident microglia. **b)** The inflammatory response in the CNS parenchyma is characterized by the release of inflammatory mediators, activation of cytotoxic pathways, tissue hypoxia, production of ROS/RNS, mitochondrial dysfunction and an energy deficit. **c)** The inflammatory insult can cause CNS damage (including demyelination, oxidative damage, phagocytosis, oligodendrocyte stress and death) and neurological deficits. **d)** Administration of oxygen in rats with active EAE ameliorates the severity of the neurological deficits and leads to the reduction of the following pathological features (solid red arrows): tissue hypoxia, demyelination, oxidative damage, oligodendrocyte cell stress and apoptosis, and phagocytic activation of microglia/macrophages. Dashed red arrows highlight a proposed mechanism through which oxygen may have attenuated disease severity. It is possible that by decreasing tissue hypoxia, oxygen leads to a reduced infiltration of macrophages, ROS/RNS production, mitochondrial damage and energy deficit, increasing the endurance of CNS cells at the inflammatory attack.

BIBLIOGRAPHY

Aboul-Enein F, Lassmann H. Mitochondrial damage and histotoxic hypoxia: a pathway of tissue injury in inflammatory brain disease? Acta Neuropathol 2005; 109: 49–55.

Aboul-Enein F, Rauschka H, Kornek B, Stadelmann C, Stefferl A, Bruck W, et al. Preferential loss of myelin-associated glycoprotein reflects hypoxia-like white matter damage in stroke and inflammatory brain diseases. J. Neuropathol. Exp. Neurol. 2003; 62: 25–33.

Airley RE, Loncaster J, Raleigh JA, Harris AL, Davidson SE, Hunter RD, et al. GLUT-1 and CAIX as intrinsic markers of hypoxia in carcinoma of the cervix: relationship to pimonidazole binding. Int J Cancer 2003; 104: 85–91.

Ajami B, Bennett JL, Krieger C, McNagny KM, Rossi FM V. Infiltrating monocytes trigger EAE progression, but do not contribute to the resident microglia pool. Nat. Neurosci. 2011; 14: 1142–9.

Aktas O, Küry P, Kieseier B, Hartung H-P. Fingolimod is a potential novel therapy for multiple sclerosis. Nat. Rev. Neurol. 2010; 6: 373–82.

Al-Izki S, Pryce G, Jackson SJ, Giovannoni G, Baker D. Immunosuppression with FTY720 is insufficient to prevent secondary progressive neurodegeneration in experimental autoimmune encephalomyelitis. Mult. Scler. 2011; 17: 939–48.

Al-Izki S, Pryce G, O'Neill JK, Butter C, Giovannoni G, Amor S, et al. Practical guide to the induction of relapsing progressive experimental autoimmune encephalomyelitis in the Biozzi ABH mouse. Mult. Scler. Relat. Disord. 2012; 1: 29–38.

Albina JE, Henry WL. Suppression of lymphocyte proliferation through the nitric oxide synthesizing pathway. J. Surg. Res. 1991; 50: 403–9.

Alderson NL, Maldonado EN, Kern MJ, Bhat NR, Hama H. FA2H-dependent fatty acid 2-hydroxylation in postnatal mouse brain. J. Lipid Res. 2006; 47: 2772–80.

Alderton WK, Cooper CE, Knowles RG. Nitric oxide synthases: structure, function and inhibition. Biochem. J. 2001; 357: 593–615.

Allen I V, McQuaid S, Mirakhur M, Nevin G. Pathological abnormalities in the normal-appearing white matter in multiple sclerosis. Neurol. Sci. 2001; 22: 141–4.

Allison JD, Meador KJ, Loring DW, Figueroa RE, Wright JC. Functional MRI cerebral activation and deactivation during finger movement. Neurology 2000; 54: 135–42.

Amaral AI, Hadera MG, Tavares JM, Kotter MRN, Sonnewald U. Characterization of glucose-related metabolic pathways in differentiated rat oligodendrocyte lineage cells. Glia 2016; 64: 21–34.

Ames 3rd A. CNS energy metabolism as related to function. Brain Res Brain Res Rev 2000; 34: 42–68.

Ances BM, Greenberg JH, Detre JA. Laser Doppler Imaging of Activation-Flow Coupling in the Rat Somatosensory Cortex. Neuroimage 1999; 10: 716–723.

Ando S, Tanaka Y, Toyoda Y, Kon K. Turnover of myelin lipids in aging brain. Neurochem. Res. 2003; 28: 5–13.

Arteel GE, Thurman RG, Raleigh JA. Reductive metabolism of the hypoxia marker pimonidazole is regulated by oxygen tension independent of the pyridine nucleotide redox state. Eur J Biochem 1998; 253: 743–750.

Attwell D, Laughlin SB. An energy budget for signaling in the grey matter of the brain. J. Cereb. Blood Flow Metab. 2001; 21: 1133–45.

Ayala A, Muñoz MF, Argüelles S, Ayala A, Muñoz MF, Argüelles S, et al. Lipid peroxidation: production, metabolism, and signaling mechanisms of malondialdehyde and 4-hydroxy-2-nonenal. Oxid. Med. Cell. Longev. 2014; 2014: 360438.

Babior BM. The respiratory burst of phagocytes. J. Clin. Invest. 1984; 73: 599–601.

Babior BM. NADPH oxidase: an update. Blood 1999; 93: 1464–76.

Baker D, O'Neill JK, Gschmeissner SE, Wilcox CE, Butter C, Turk JL. Induction of chronic relapsing experimental allergic encephalomyelitis in Biozzi mice. J. Neuroimmunol. 1990; 28: 261–270.

Banati RB, Rothe G, Valet G, Kreutzberg GW. Respiratory burst activity in brain macrophages: a flow cytometric study on cultured rat microglia. Neuropathol. Appl. Neurobiol. 1991; 17: 223–30.

Barnes MP, Bates D, Cartlidge NE, French JM, Shaw DA. Hyperbaric oxygen and multiple sclerosis: final results of a placebo-controlled, double-blind trial. J. Neurol. Neurosurg. Psychiatry 1987; 50: 1402–6.

Barnett JM, McCollum GW, Penn JS. Role of cytosolic phospholipase A(2) in retinal neovascularization. Invest. Ophthalmol. Vis. Sci. 2010; 51: 1136–42.

Barnett MH, Prineas JW. Relapsing and remitting multiple sclerosis: pathology of the newly forming lesion. Ann Neurol 2004; 55: 458–468.

Bartholomäus I, Kawakami N, Odoardi F, Schläger C, Miljkovic D, Ellwart JW, et al. Effector T cell interactions with meningeal vascular structures in nascent autoimmune CNS lesions. Nature 2009; 462: 94–98.

Bauer J, Sminia T, Wouterlood FG, Dijkstra CD. Phagocytic activity of macrophages and microglial cells during the course of acute and chronic relapsing experimental autoimmune encephalomyelitis. J. Neurosci. Res. 1994; 38: 365–375.

Baumann N, Pham-Dinh D. Biology of oligodendrocyte and myelin in the mammalian central nervous system. Physiol. Rev. 2001; 81: 871–927.

Bechtold DA, Smith KJ. Sodium-mediated axonal degeneration in inflammatory

demyelinating disease. J Neurol Sci 2005; 233: 27–35.

Beckman JS, Koppenol WH. Nitric oxide, superoxide, and peroxynitrite: the good, the bad, and ugly. Am. J. Physiol. 1996; 271: C1424-37.

Bélanger M, Allaman I, Magistretti PJ, Ainscow EK, Mirshamsi S, Tang T, et al. Brain energy metabolism: focus on astrocyte-neuron metabolic cooperation. Cell Metab. 2011; 14: 724–38.

Bellavite P. The superoxide-forming enzymatic system of phagocytes. Free Radic. Biol. Med. 1988; 4: 225–61.

Bennett J, Basivireddy J, Kollar A, Biron KE, Reickmann P, Jefferies WA, et al. Blood–brain barrier disruption and enhanced vascular permeability in the multiple sclerosis model EAE. J. Neuroimmunol. 2010; 229: 180–191.

Bennett M, Heard R. Hyperbaric oxygen therapy for multiple sclerosis. CNS Neurosci Ther 2010; 16: 115–124.

Bettelli E, Pagany M, Weiner HL, Linington C, Sobel RA, Kuchroo VK. Myelin Oligodendrocyte Glycoprotein–specific T Cell Receptor Transgenic Mice Develop Spontaneous Autoimmune Optic Neuritis. J. Exp. Med. 2003; 197

Biasutto L, Azzolini M, Szabò I, Zoratti M. The mitochondrial permeability transition pore in AD 2016: An update. Biochim. Biophys. Acta - Mol. Cell Res. 2016; 1863: 2515–2530.

Bielekova B, Sung M-H, Kadom N, Simon R, McFarland H, Martin R. Expansion and functional relevance of high-avidity myelin-specific CD4+ T cells in multiple sclerosis. J. Immunol. 2004; 172: 3893–904.

Bilali F, Kumar P, Feerick J, Berezin S, Farahani R. Hypoxia-induced hypomyelination in the developing brain is mammalian target of rapamycin-4E-binding protein-1 signaling dependent. Neuroreport 2008; 19: 635–639.

Bitsch A, Schuchardt J, Bunkowski S, Kuhlmann T, Brück W. Acute axonal injury in multiple sclerosis. Correlation with demyelination and inflammation. Brain 2000; 123 (Pt 6: 1174–83.

Bitsch A, Wegener C, da Costa C, Bunkowski S, Reimers CD, Prange HW, et al. Lesion development in Marburg's type of acute multiple sclerosis: from inflammation to demyelination. Mult Scler 1999; 5: 138–146.

Blissman G, Menzies S, Beard J, Palmer C, Connor J. The expression of ferritin subunits and iron in oligodendrocytes in neonatal porcine brains. Dev. Neurosci. 1996; 18: 274–81.

Bo L, Dawson TM, Wesselingh S, Mork S, Choi S, Kong PA, et al. Induction of nitric oxide synthase in demyelinating regions of multiple sclerosis brains. Ann. Neurol. 1994; 36: 778–786.

Bolaños JP, Almeida A, Stewart V, Peuchen S, Land JM, Clark JB, et al. Nitric oxide-

mediated mitochondrial damage in the brain: mechanisms and implications for neurodegenerative diseases. J. Neurochem. 1997; 68: 2227–2240.

Bolton S, Greenwood K, Hamilton N, Butt AM. Regulation of the astrocyte resting membrane potential by cyclic AMP and protein kinase A. Glia 2006; 54: 316–328.

Boroujerdi A, Welser-Alves J V, Milner R. Extensive vascular remodeling in the spinal cord of pre-symptomatic experimental autoimmune encephalomyelitis mice; increased vessel expression of fibronectin and the ??5??1 integrin. Exp. Neurol. 2013; 250: 43–51.

Borregaard N, Herlin T. Energy metabolism of human neutrophils during phagocytosis. J. Clin. Invest. 1982; 70: 550–7.

Bosio A, Binczek E, Stoffel W. Functional breakdown of the lipid bilayer of the myelin membrane in central and peripheral nervous system by disrupted galactocerebroside synthesis. Proc. Natl. Acad. Sci. U. S. A. 1996; 93: 13280–5.

Bostock H, Sears TA. The internodal axon membrane: electrical excitability and continuous conduction in segmental demyelination. J. Physiol. 1978; 280: 273–301.

Boullerne AI, Petry KG, Meynard M, Geffard M. Indirect evidence for nitric oxide involvement in multiple sclerosis by characterization of circulating antibodies directed against conjugated S-nitrosocysteine. J. Neuroimmunol. 1995; 60: 117–24.

Bouzier-Sore A-K, Voisin P, Bouchaud V, Bezancon E, Franconi J-M, Pellerin L. Competition between glucose and lactate as oxidative energy substrates in both neurons and astrocytes: a comparative NMR study. Eur. J. Neurosci. 2006; 24: 1687–1694.

Bredt DS. Endogenous nitric oxide synthesis: biological functions and pathophysiology. Free Radic. Res. 1999; 31: 577–96.

Brockman EC, Bayir H, Blasiole B, Shein SL, Fink EL, Dixon C, et al. Polynitroxylated-pegylated hemoglobin attenuates fluid requirements and brain edema in combined traumatic brain injury plus hemorrhagic shock in mice. J. Cereb. Blood Flow Metab. 2013; 33: 1457–1464.

Brown A, McFarlin DE, Raine CS. Chronologic neuropathology of relapsing experimental allergic encephalomyelitis in the mouse. Lab. Invest. 1982; 46: 171–85.

Brown GC, Cooper CE. Nanomolar concentrations of nitric oxide reversibly inhibit synaptosomal respiration by competing with oxygen at cytochrome oxidase. FEBS Lett. 1994; 356: 295–298.

Brück W, Porada P, Poser S, Rieckmann P, Hanefeld F, Kretzschmar HA, et al. Monocyte/macrophage differentiation in early multiple sclerosis lesions. Ann. Neurol. 1995; 38: 788–796.

von Budingen HC, Tanuma N, Villoslada P, Ouallet JC, Hauser SL, Genain CP. Immune responses against the myelin/oligodendrocyte glycoprotein in experimental autoimmune demyelination. J Clin Immunol 2001; 21: 155–170.

Butt AM, Kalsi A. Inwardly rectifying potassium channels (Kir) in central nervous system glia: a special role for Kir4.1 in glial functions. J. Cell. Mol. Med. 2006; 10: 33–44.

van Buul JD, Hordijk PL. Signaling in Leukocyte Transendothelial Migration. Arterioscler. Thromb. Vasc. Biol. 2004; 24

Carmeliet P, Jain RK. Angiogenesis in cancer and other diseases. Nature 2000; 407: 249–257.

Chakrabarty A, Danley MM, LeVine SM. Immunohistochemical localization of phosphorylated protein kinase R and phosphorylated eukaryotic initiation factor-2 alpha in the central nervous system of SJL mice with experimental allergic encephalomyelitis. J Neurosci Res 2004; 76: 822–833.

Chanmee T, Ontong P, Konno K, Itano N. Tumor-associated macrophages as major players in the tumor microenvironment. Cancers (Basel). 2014; 6: 1670–90.

Choi SR, Howell OW, Carassiti D, Magliozzi R, Gveric D, Muraro PA, et al. Meningeal inflammation plays a role in the pathology of primary progressive multiple sclerosis. Brain 2012; 135

Chrast R, Saher G, Nave K-A, Verheijen MHG. Lipid metabolism in myelinating glial cells: lessons from human inherited disorders and mouse models. J. Lipid Res. 2011; 52: 419–34.

Clambey ET, McNamee EN, Westrich JA, Glover LE, Campbell EL, Jedlicka P, et al. Hypoxia-inducible factor-1 alpha-dependent induction of FoxP3 drives regulatory T-cell abundance and function during inflammatory hypoxia of the mucosa. Proc Natl Acad Sci U S A 2012; 109: E2784-93.

Clanton TL. Hypoxia-induced reactive oxygen species formation in skeletal muscle. J. Appl. Physiol. 2007; 102

Clarke D, Sokoloff L. Circulation and energy metabolism. Siegel GJ, Agranoff BW, Albers RW, Fish. SK, Uhler MD. Basic Neurochem. Mol. Cell. Clin. Asp. 6th ed. 1999: 637–669.

Cleeter MWJ, Cooper JM, Darley-Usmar VM, Moncada S, Schapira AHV. Reversible inhibition of cytochrome c oxidase, the terminal enzyme of the mitochondrial respiratory chain, by nitric oxide. FEBS Lett. 1994; 345: 50–54.

Clementi E, Brown GC, Feelisch M, Moncada S. Persistent inhibition of cell respiration by nitric oxide: crucial role of S-nitrosylation of mitochondrial complex I and protective action of glutathione. Proc. Natl. Acad. Sci. U. S. A. 1998; 95: 7631–6.

Coetzee T, Fujita N, Dupree J, Shi R, Blight A, Suzuki K, et al. Myelination in the Absence of Galactocerebroside and Sulfatide: Normal Structure with Abnormal Function and Regional Instability. Cell 1996; 86: 209–219.

Coleman ML, Ratcliffe PJ. Oxygen sensing and hypoxia-induced responses. Essays Biochem 2007; 43: 1–15.

Colgan SP, Campbell EL, Kominsky DJ. Hypoxia and Mucosal Inflammation. Annu. Rev. Pathol. Mech. Dis. 2016; 11: 77–100.

Compston A, Coles A. Multiple sclerosis. Lancet 2008; 372: 1502–1517.

Confavreux C, Mathieu C, Chacornac R, Aimard G, Devic M. Ineffectiveness of hyperbaric oxygen therapy in multiple sclerosis. A randomized placebo-controlled double-blind study. Press. Med 1986; 15: 1319–1322.

Constantinescu CS, Farooqi N, O'Brien K, Gran B. Experimental autoimmune encephalomyelitis (EAE) as a model for multiple sclerosis (MS). Br. J. Pharmacol. 2011; 164: 1079–106.

Cooke MS, Evans MD, Dizdaroglu M, Lunec J. Oxidative DNA damage: mechanisms, mutation, and disease. FASEB J. 2003; 17: 1195–214.

Cooper CE, Davies NA, Psychoulis M, Canevari L, Bates TE, Dobbie MS, et al. Nitric oxide and peroxynitrite cause irreversible increases in the Km for oxygen of mitochondrial cytochrome oxidase: in vitro and in vivo studies. Biochim. Biophys. Acta - Bioenerg. 2003; 1607: 27–34.

Cramer T, Yamanishi Y, Clausen BE, Förster I, Pawlinski R, Mackman N, et al. HIF-1alpha is essential for myeloid cell-mediated inflammation. Cell 2003; 112: 645–57.

Cross AH, Keeling RM, Goorha S, San M, Rodi C, Wyatt PS, et al. Inducible nitric oxide synthase gene expression and enzyme activity correlate with disease activity in murine experimental autoimmune encephalomyelitis. J. Neuroimmunol. 1996; 71: 145–53.

Cunnea P, Mhaille AN, McQuaid S, Farrell M, McMahon J, FitzGerald U. Expression profiles of endoplasmic reticulum stress-related molecules in demyelinating lesions and multiple sclerosis. Mult. Scler. J. 2011; 17: 808–818.

D'haeseleer M, Cambron M, Vanopdenbosch L, De Keyser J, Noseworthy J, Lucchinetti C, et al. Vascular aspects of multiple sclerosis. Lancet Neurol. 2011; 10: 657–666.

D'haeseleer M, Hostenbach S, Peeters I, Sankari S El, Nagels G, De Keyser J, et al. Cerebral hypoperfusion: a new pathophysiologic concept in multiple sclerosis? J. Cereb. Blood Flow Metab. 2015; 35: 1406–1410.

Dahlgren C, Karlsson A. Respiratory burst in human neutrophils. J. Immunol. Methods 1999; 232: 3–14.

Dang E V, Barbi J, Yang HY, Jinasena D, Yu H, Zheng Y, et al. Control of T(H)17/T(reg) balance by hypoxia-inducible factor 1. Cell 2011; 146: 772–784.

Davalos D, Ryu JK, Merlini M, Baeten KM, Le Moan N, Petersen MA, et al. Fibrinogen-induced perivascular microglial clustering is required for the development of axonal damage in neuroinflammation. Nat. Commun. 2012; 3: 1227.

Davies AL, Desai RA, Bloomfield PS, McIntosh PR, Chapple KJ, Linington C, et al. Neurological deficits caused by tissue hypoxia in neuroinflammatory disease. Ann. Neurol. 2013; 74: 815–25.

Desai RA, Davies AL, Tachrount M, Kasti M, Laulund F, Golay X, et al. Cause and prevention of demyelination in a model multiple sclerosis lesion. Ann. Neurol. 2016

Dewar D, Underhill SM, Goldberg MP. Oligodendrocytes and ischemic brain injury. J. Cereb. Blood Flow Metab. 2003; 23: 263–74.

Dhib-Jalbut S. Pathogenesis of myelin/oligodendrocyte damage in multiple sclerosis. Neurology 2007; 68: S13–S21.

Dhib-Jalbut S, Kalvakolanu D V. Microglia and necroptosis: The culprits of neuronal cell death in multiple sclerosis. 2015.

Ding Z, Tong WC, Lu X-X, Peng H-P. Hyperbaric oxygen therapy in acute ischemic stroke: a review. Interv. Neurol. 2014; 2: 201–11.

Donnelly N, Gorman AM, Gupta S, Samali A. The eIF2α kinases: their structures and functions. Cell. Mol. Life Sci. 2013; 70: 3493–511.

Dore-Duffy P, Wencel M, Katyshev V, Cleary K. Chronic mild hypoxia ameliorates chronic inflammatory activity in myelin oligodendrocyte glycoprotein (MOG) peptide induced experimental autoimmune encephalomyelitis (EAE). Adv Exp Med Biol 2011; 701: 165–173.

Dutta R, McDonough J, Yin X, Peterson J, Chang A, Torres T, et al. Mitochondrial dysfunction as a cause of axonal degeneration in multiple sclerosis patients. Ann. Neurol. 2006; 59: 478–489.

Eckersten D, Henningsson R. Nitric oxide (NO)--production and regulation of insulin secretion in islets of freely fed and fasted mice. Regul Pept 2012; 174: 32–37.

Elvidge GP, Glenny L, Appelhoff RJ, Ratcliffe PJ, Ragoussis J, Gleadle JM. Concordant regulation of gene expression by hypoxia and 2-oxoglutarate-dependent dioxygenase inhibition: the role of HIF-1alpha, HIF-2alpha, and other pathways. J Biol Chem 2006; 281: 15215–15226.

Engberink RDO, van der Pol SMA, Walczak P, van der Toorn A, Viergever MA, Dijkstra CD, et al. Magnetic resonance imaging of monocytes labeled with ultrasmall superparamagnetic particles of iron oxide using magnetoelectroporation in an animal model of multiple sclerosis. Mol. Imaging 2010; 9: 268–77.

Engelhardt B, Wolburg H. Mini review: Transendothelial migration of leukocytes: Through the front door or around the side of the house? Eur. J. Immunol. 2004; 34: 2955–2963.

Evangelou N, Konz D, Esiri MM, Smith S, Palace J, Matthews PM. Size-selective neuronal changes in the anterior optic pathways suggest a differential susceptibility to injury in multiple sclerosis. Brain 2001; 124: 1813–1820.

Fayed N, Modrego PJ, Morales H. Evidence of brain damage after high-altitude climbing by means of magnetic resonance imaging. Am J Med 2006; 119: 168 e1-6.

le Feber J, Tzafi Pavlidou S, Erkamp N, van Putten MJAM, Hofmeijer J. Progression of

Neuronal Damage in an In Vitro Model of the Ischemic Penumbra. PLoS One 2016; 11: e0147231.

Felts PA, Kapoor R, Smith KJ. A mechanism for ectopic firing in central demyelinated axons. Brain 1995; 118: 1225–1231.

Felts PA, Woolston AM, Fernando HB, Asquith S, Gregson NA, Mizzi OJ, et al. Inflammation and primary demyelination induced by the intraspinal injection of lipopolysaccharide. Brain 2005; 128: 1649–1666.

Fewou SN, Büssow H, Schaeren-Wiemers N, Vanier MT, Macklin WB, Gieselmann V, et al. Reversal of non-hydroxy : α-hydroxy galactosylceramide ratio and unstable myelin in transgenic mice overexpressing UDP-galactose : ceramide galactosyltransferase. J. Neurochem. 2005; 94: 469–481.

Figley CR, Stroman PW. The role(s) of astrocytes and astrocyte activity in neurometabolism, neurovascular coupling, and the production of functional neuroimaging signals. Eur. J. Neurosci. 2011; 33: 577–588.

Filimonov IS, Vrzheshch P V. Molecular oxygen (a substrate of the cyclooxygenase reaction) in the kinetic mechanism of the bifunctional enzyme prostaglandin-H-synthase. Biochemistry. (Mosc). 2007; 72: 944–53.

Fischer BH, Marks M, Reich T. Hyperbaric-oxygen treatment of multiple sclerosis. A randomized, placebo-controlled, double-blind study. N Engl J Med 1983; 308: 181–186.

Fischer MT, Sharma R, Lim JL, Haider L, Frischer JM, Drexhage J, et al. NADPH oxidase expression in active multiple sclerosis lesions in relation to oxidative tissue damage and mitochondrial injury. Brain 2012; 135: 886–899.

Flammer AJ, Anderson T, Celermajer DS, Creager MA, Deanfield J, Ganz P, et al. The Assessment of Endothelial Function. Circulation 2012; 126

Fleming KK, Bovaird JA, Mosier MC, Emerson MR, LeVine SM, Marquis JG, et al. Statistical analysis of data from studies on experimental autoimmune encephalomyelitis. J. Neuroimmunol. 2005; 170: 71–84.

Fletcher JM, Lalor SJ, Sweeney CM, Tubridy N, Mills KH. T cells in multiple sclerosis and experimental autoimmune encephalomyelitis. Clin Exp Immunol 2010; 162: 1–11.

Floyd TF, Clark JM, Gelfand R, Detre JA, Ratcliffe S, Guvakov D, et al. Independent cerebral vasoconstrictive effects of hyperoxia and accompanying arterial hypocapnia at 1 ATA. J. Appl. Physiol. 2003; 95: 2453–61.

Flügel A, Berkowicz T, Ritter T, Labeur M, Jenne DE, Li Z, et al. Migratory activity and functional changes of green fluorescent effector cells before and during experimental autoimmune encephalomyelitis. Immunity 2001; 14: 547–60.

Foster RE, Whalen CC, Waxman SG. Reorganization of the axon membrane in demyelinated peripheral nerve fibers: morphological evidence. Science 1980; 210: 661–3.

Fox CJ, Hammerman PS, Thompson CB. Fuel feeds function: energy metabolism and the T-cell response. Nat. Rev. Immunol. 2005; 5: 844–852.

Fox PT, Raichle ME. Focal physiological uncoupling of cerebral blood flow and oxidative metabolism during somatosensory stimulation in human subjects. Proc Natl Acad Sci U S A 1986; 83: 1140–1144.

Fox PT, Raichle ME, Mintun MA, Dence C. Nonoxidative glucose consumption during focal physiologic neural activity. Science 1988; 241: 462–464.

Franklin RJM, ffrench-Constant C, Edgar JM, Smith KJ. Neuroprotection and repair in multiple sclerosis. Nat. Rev. Neurol. 2012; 8: 624–634.

Frede S, Berchner-Pfannschmidt U, Fandrey J. Regulation of hypoxia-inducible factors during inflammation. Methods Enzymol. 2007; 435: 405–19.

Freund J, Stern ER, Pisani TM. Isoallergic encephalomyelitis and radiculitis in guinea pigs after one injection of brain and Mycobacteria in water-in-oil emulsion. J Immunol 1947; 57: 179–194.

Friese MA, Schattling B, Fugger L. Mechanisms of neurodegeneration and axonal dysfunction in multiple sclerosis. Nat. Rev. Neurol. 2014; 10: 225–238.

Frischer JM, Bramow S, Dal-bianco A, Lucchinetti CF, Rauschka H, Schmidbauer M, et al. The relation between inflamination and neurodegeneration in multiple sclerosis brains. Brain 2009; 132: 1175–1189.

Fu R, Shen Q, Xu P, Luo JJ, Tang Y. Phagocytosis of microglia in the central nervous system diseases. Mol. Neurobiol. 2014; 49: 1422–34.

Fünfschilling U, Supplie LM, Mahad D, Boretius S, Saab AS, Edgar J, et al. Glycolytic oligodendrocytes maintain myelin and long-term axonal integrity. Nature 2012; 485: 517–21.

Gallagher CN, Carpenter KLH, Grice P, Howe DJ, Mason A, Timofeev I, et al. The human brain utilizes lactate via the tricarboxylic acid cycle: a 13C-labelled microdialysis and high-resolution nuclear magnetic resonance study. Brain 2009; 132

Giovannoni G. Cerebrospinal fluid and serum nitric oxide metabolites in patients with multiple sclerosis. Mult. Scler. 1998; 4: 27–30.

Gold R, Linington C, Lassmann H. Understanding pathogenesis and therapy of multiple sclerosis via animal models: 70 years of merits and culprits in experimental autoimmune encephalomyelitis research. Brain 2006; 129: 1953–1971.

Graumann U, Reynolds R, Steck AJ, Schaeren-Wiemers N. Molecular changes in normal appearing white matter in multiple sclerosis are characteristic of neuroprotective mechanisms against hypoxic insult. Brain Pathol 2003; 13: 554–573.

Graziewicz M, Wink DA, Laval F. Nitric oxide inhibits DNA ligase activity: potential mechanisms for NO-mediated DNA damage. Carcinogenesis 1996; 17: 2501–5.

Griot-Wenk M, Griot C, Pfister H, Vandevelde M. Antibody-dependent cellular cytotoxicity in antimyelin antibody-induced oligodendrocyte damage in vitro. J. Neuroimmunol. 1991; 33: 145–55.

Groebe K, Vaupel P. Evaluation of oxygen diffusion distances in human breast cancer xenografts using tumor-specific in vivo data: role of various mechanisms in the development of tumor hypoxia. Int. J. Radiat. Oncol. Biol. Phys. 1988; 15: 691–7.

De Groot CJ, Bergers E, Kamphorst W, Ravid R, Polman CH, Barkhof F, et al. Post-mortem MRI-guided sampling of multiple sclerosis brain lesions: increased yield of active demyelinating and (p)reactive lesions. Brain 2001; 124: 1635–1645.

Grossman RI, Braffman BH, Brorson JR, Goldberg HI, Silberberg DH, Gonzalez-Scarano F. Multiple sclerosis: serial study of gadolinium-enhanced MR imaging. Radiology 1988; 169: 117–22.

Gunter TE, Gunter KK, Sheu SS, Gavin CE. Mitochondrial calcium transport: physiological and pathological relevance. Am. J. Physiol. 1994; 267: C313-39.

Guo C, Sun L, Chen X, Zhang D. Oxidative stress, mitochondrial damage and neurodegenerative diseases. Neural Regen. Res. 2013; 8: 2003–14.

Haider L, Fischer MT, Frischer JM, Bauer J, Hoftberger R, Botond G, et al. Oxidative damage in multiple sclerosis lesions. Brain 2011; 134: 1914–1924.

Hamada MS, Kole MHP. Myelin loss and axonal ion channel adaptations associated with gray matter neuronal hyperexcitability. J. Neurosci. 2015; 35: 7272–86.

Harpur GD, Suke R, Bass BH, Bass MJ, Bull SB, Reese L, et al. Hyperbaric oxygen therapy in chronic stable multiple sclerosis: double-blind study. Neurology 1986; 36: 988–91.

Hashimoto T, Hussien R, Cho H-S, Kaufer D, Brooks GA. Evidence for the mitochondrial lactate oxidation complex in rat neurons: demonstration of an essential component of brain lactate shuttles. PLoS One 2008; 3: e2915.

Hauser SL, Oksenberg JR. The neurobiology of multiple sclerosis: genes, inflammation, and neurodegeneration. Neuron 2006; 52: 61–76.

Hausladen A, Fridovich I. Superoxide and peroxynitrite inactivate aconitases, but nitric oxide does not. J. Biol. Chem. 1994; 269: 29405–8.

Hemmer B, Kerschensteiner M, Korn T. Role of the innate and adaptive immune responses in the course of multiple sclerosis. Lancet Neurol. 2015; 14: 406–419.

Henderson APD, Barnett MH, Parratt JDE, Prineas JW. Multiple sclerosis: Distribution of inflammatory cells in newly forming lesions. Ann. Neurol. 2009; 66: 739–753.

Hickey WF. Basic principles of immunological surveillance of the normal central nervous system. Glia 2001; 36: 118–24.

Hochmeister S, Grundtner R, Bauer J, Engelhardt B, Lyck R, Gordon G, et al. Dysferlin

Is a New Marker for Leaky Brain Blood Vessels in Multiple Sclerosis. J. Neuropathol. Exp. Neurol. 2006; 65

Hohlfeld R, Wekerle H. Immunological update on multiple sclerosis. Curr Opin Neurol 2001; 14: 299–304.

Holley JE, Newcombe J, Whatmore JL, Gutowski NJ. Increased blood vessel density and endothelial cell proliferation in multiple sclerosis cerebral white matter. Neurosci Lett 2010; 470: 65–70.

van Horssen J, Singh S, van der Pol S, Kipp M, Lim JL, Peferoen L, et al. Clusters of activated microglia in normal-appearing white matter show signs of innate immune activation. J. Neuroinflammation 2012; 9: 156.

Hsia CJC, Ma L. A hemoglobin-based multifunctional therapeutic: polynitroxylated pegylated hemoglobin. Artif. Organs 2012; 36: 215–20.

Imtiyaz HZ, Simon MC. Hypoxia-inducible factors as essential regulators of inflammation. Curr. Top. Microbiol. Immunol. 2010; 345: 105–20.

Itoh Y, Esaki T, Shimoji K, Cook M, Law MJ, Kaufman E, et al. Dichloroacetate effects on glucose and lactate oxidation by neurons and astroglia in vitro and on glucose utilization by brain in vivo. Proc. Natl. Acad. Sci. U. S. A. 2003; 100: 4879–84.

Ivan M, Kondo K, Yang H, Kim W, Valiando J, Ohh M, et al. HIFalpha targeted for VHL-mediated destruction by proline hydroxylation: implications for O2 sensing. Science (80-.). 2001; 292: 464–468.

Jaakkola P, Mole DR, Tian YM, Wilson MI, Gielbert J, Gaskell SJ, et al. Targeting of HIF-alpha to the von Hippel-Lindau ubiquitylation complex by O2-regulated prolyl hydroxylation. Science (80-.). 2001; 292: 468–472.

Jacobowitz DM, Cole JT, McDaniel DP, Pollard HB, Watson WD. Microglia activation along the corticospinal tract following traumatic brain injury in the rat: A neuroanatomical study. Brain Res. 2012; 1465: 80–89.

Janssen HL, Haustermans KM, Sprong D, Blommestijn G, Hofland I, Hoebers FJ, et al. HIF-1A, pimonidazole, and iododeoxyuridine to estimate hypoxia and perfusion in human head-and-neck tumors. Int J Radiat Oncol Biol Phys 2002; 54: 1537–1549.

Johns TG, Kerlero de Rosbo N, Menon KK, Abo S, Gonzales MF, Bernard CC. Myelin oligodendrocyte glycoprotein induces a demyelinating encephalomyelitis resembling multiple sclerosis. J Immunol 1995; 154: 5536–5541.

Johnston AJ, Czosnyka M. Measuring cerebral autoregulation in stroke patients. Stroke 2003; 34: e39-40-40.

Jones R. Glia: Oligodendrocyte transporters feed axons. Nat. Rev. Neurosci. 2012; 13: 601–601.

Julien-Dolbec C, Tropres I, Montigon O, Reutenauer H, Ziegler A, Decorps M, et al. Regional response of cerebral blood volume to graded hypoxic hypoxia in rat brain. Br J

Anaesth 2002; 89: 287–293.

Jurewicz A, Matysiak M, Andrzejak S, Selmaj K. TRAIL-induced death of human adult oligodendrocytes is mediated by JNK pathway. Glia 2006; 53: 158–166.

Jurewicz A, Matysiak M, Tybor K, Kilianek L, Raine CS, Selmaj K. Tumour necrosis factor-induced death of adult human oligodendrocytes is mediated by apoptosis inducing factor. Brain 2005; 128: 2675–2688.

Juurlink BHJ. The evidence for hypoperfusion as a factor in multiple sclerosis lesion development. Mult. Scler. Int. 2013; 2013: 598093.

Kapoor R, Davies M, Blaker PA, Hall SM, Smith KJ. Blockers of sodium and calcium entry protect axons from nitric oxide-mediated degeneration. Ann. Neurol. 2003; 53: 174–180.

Keeney JT, Swomley AM, Forster S, Harris JL, Sultana R, Butterfield DA. Apolipoprotein A-I: insights from redox proteomics for its role in neurodegeneration. Proteomics Clin Appl 2013; 7: 109–122.

Kelly B, O'Neill LA. Metabolic reprogramming in macrophages and dendritic cells in innate immunity. Cell Res. 2015; 25: 771–784.

Kettenmann H, Sonnhof U, Schachner M. Exclusive potassium dependence of the membrane potential in cultured mouse oligodendrocytes. J. Neurosci. 1983; 3: 500–5.

Kety SS, Schmidt CF. The Effects of Altered Arterial Tensions of Carbon Dioxide and Oxygen on Cerebral Blood Flow and Cerebral Oxygen Consumption of Normal Young Men. J Clin Invest 1948; 27: 484–492.

De Keyser J, Wilczak N, Leta R, Streetland C. Astrocytes in multiple sclerosis lack beta-2 adrenergic receptors. Neurology 1999; 53: 1628–33.

Klimova T, Chandel NS. Mitochondrial complex III regulates hypoxic activation of HIF. Cell Death Differ 2008; 15: 660–666.

Knot HJ, Nelson MT. Regulation of arterial diameter and wall [Ca2+] in cerebral arteries of rat by membrane potential and intravascular pressure. J. Physiol. 1998: 199–209.

Kobari M, Fukuuchi Y, Tomita M, Tanahashi N, Yamawaki T, Takeda H, et al. Transient cerebral vasodilatory effect of neuropeptide y mediated by nitric oxide. Brain Res. Bull. 1993; 31: 443–448.

Kominsky DJ, Campbell EL, Colgan SP. Metabolic shifts in immunity and inflammation. J. Immunol. 2010; 184: 4062–8.

Koprowski H, Zheng YM, Heber-Katz E, Fraser N, Rorke L, Fu ZF, et al. In vivo expression of inducible nitric oxide synthase in experimentally induced neurologic diseases. Proc. Natl. Acad. Sci. U. S. A. 1993; 90: 3024–7.

Koudriavtseva T. Thrombotic processes in multiple sclerosis as manifestation of innate immune activation. Front. Neurol. 2014; 5: 119.

Koumenis C, Naczki C, Koritzinsky M, Rastani S, Diehl A, Sonenberg N, et al. Regulation of protein synthesis by hypoxia via activation of the endoplasmic reticulum kinase PERK and phosphorylation of the translation initiation factor eIF2alpha. Mol. Cell. Biol. 2002; 22: 7405–16.

Krogh A. The supply of oxygen to the tissues and the regulation of the capillary circulation. J. Physiol. 1919; 52: 457–474.

Kuchroo VK, Anderson AC, Waldner H, Munder M, Bettelli E, Nicholson LB. T cell response in experimental autoimmune encephalomyelitis (EAE): role of self and cross-reactive antigens in shaping, tuning, and regulating the autopathogenic T cell repertoire. Annu. Rev. Immunol. 2002; 20: 101–23.

Kumagami T, Kato S, Ishikura R, Nagata M, Tamai A, Ohama E. Expression of stress-response protein 60 in iritis associated with experimental autoimmune encephalomyelitis. Jpn J Ophthalmol 1999; 43: 458–465.

Kutzelnigg, A.; Lucchinetti, C.F.; Stadelmann, C.; Brück, W.; Rauschka, H.; Bergmann, M.; Schmidbauer, M.; Parisi, J.E.; Lassmann H. Cortical demyelination and diffuse white matter injury in multiple sclerosis. Brain 2005; 128: 2705–2712.

van Laarhoven HW, Kaanders JH, Lok J, Peeters WJ, Rijken PF, Wiering B, et al. Hypoxia in relation to vasculature and proliferation in liver metastases in patients with colorectal cancer. Int J Radiat Oncol Biol Phys 2006; 64: 473–482.

LaManna JC. Hypoxia in the central nervous system. Essays Biochem 2007; 43: 139–151.

LaManna JC, Chavez JC, Pichiule P. Structural and functional adaptation to hypoxia in the rat brain. J Exp Biol 2004; 207: 3163–3169.

Larochelle C, Alvarez JI, Prat A. How do immune cells overcome the blood-brain barrier in multiple sclerosis? FEBS Lett. 2011; 585: 3770–3780.

Lassmann H. Hypoxia-like tissue injury as a component of multiple sclerosis lesions. J Neurol Sci 2003; 206: 187–191.

Lassmann H. Pathology and disease mechanisms in different stages of multiple sclerosis. J. Neurol. Sci. 2013; 333: 1–4.

Lassmann H, Van Horssen J. The molecular basis of neurodegeneration in multiple sclerosis. FEBS Lett. 2011; 585: 3715–3723.

Lassmann H, van Horssen J, Mahad D. Progressive multiple sclerosis: pathology and pathogenesis. Nat. Rev. Neurol. 2012; 8: 647–656.

Lawrence T, Natoli G. Transcriptional regulation of macrophage polarization: enabling diversity with identity. Nat Rev Immunol 2011; 11: 750–761.

Lee Y, Morrison BM, Li Y, Lengacher S, Farah MH, Hoffman PN, et al. Oligodendroglia metabolically support axons and contribute to neurodegeneration. Nature 2012; 487: 443–448.

Leonard MO, Cottell DC, Godson C, Brady HR, Taylor CT. The role of HIF-1 alpha in transcriptional regulation of the proximal tubular epithelial cell response to hypoxia. J Biol Chem 2003; 278: 40296–40304.

Lewis CJ, Ross JD. Hemoglobin-based oxygen carriers: an update on their continued potential for military application. J. Trauma Acute Care Surg. 2014; 77: S216-21.

Lin W, Bailey SL, Ho H, Harding HP, Ron D, Miller SD, et al. The integrated stress response prevents demyelination by protecting oligodendrocytes against immune-mediated damage. J. Clin. Invest. 2007; 117: 448–56.

Lin W, Kemper A, Dupree JL, Harding HP, Ron D, Popko B. Interferon-gamma inhibits central nervous system remyelination through a process modulated by endoplasmic reticulum stress. Brain 2006; 129: 1306–18.

Lin W, Lin Y, Li J, Fenstermaker AG, Way SW, Clayton B, et al. Oligodendrocyte-specific activation of PERK signaling protects mice against experimental autoimmune encephalomyelitis. J. Neurosci. 2013; 33: 5980–91.

Lin W, Popko B. Endoplasmic reticulum stress in disorders of myelinating cells. Nat Neurosci 2009; 12: 379–385.

Lin Y, Jamison S, Lin W. Interferon-γ activates nuclear factor-κ B in oligodendrocytes through a process mediated by the unfolded protein response. PLoS One 2012; 7: e36408.

Linington C, Berger T, Perry L, Weerth S, Hinze-Selch D, Zhang Y, et al. T cells specific for the myelin oligodendrocyte glycoprotein mediate an unusual autoimmune inflammatory response in the central nervous system. Eur. J. Immunol. 1993; 23: 1364–72.

Link H, Huang Y-M. Oligoclonal bands in multiple sclerosis cerebrospinal fluid: An update on methodology and clinical usefulness. J. Neuroimmunol. 2006; 180: 17–28.

Liu JS, Zhao ML, Brosnan CF, Lee SC. Expression of inducible nitric oxide synthase and nitrotyrosine in multiple sclerosis lesions. Am. J. Pathol. 2001; 158: 2057–66.

Liu L, Cash TP, Jones RG, Keith B, Thompson CB, Simon MC. Hypoxia-induced energy stress regulates mRNA translation and cell growth. Mol. Cell 2006; 21: 521–31.

Liu L, Wise DR, Diehl JA, Simon MC. Hypoxic reactive oxygen species regulate the integrated stress response and cell survival. J. Biol. Chem. 2008; 283: 31153–62.

Liu S, Liu W, Ding W, Miyake M, Rosenberg GA, Liu KJ. Electron paramagnetic resonance-guided normobaric hyperoxia treatment protects the brain by maintaining penumbral oxygenation in a rat model of transient focal cerebral ischemia. J. Cereb. Blood Flow Metab. 2006; 26: 1274–84.

Liu Y, Shaw SK, Ma S, Yang L, Luscinskas FW, Parkos CA. Regulation of Leukocyte Transmigration: Cell Surface Interactions and Signaling Events. J. Immunol. 2003; 172

Lizasoain I, Moro MA, Knowles RG, Darley-Usmar V, Moncada S. Nitric oxide and

peroxynitrite exert distinct effects on mitochondrial respiration which are differentially blocked by glutathione or glucose. Biochem. J. 1996: 877–80.

Lu H, Patel S, Luo F, Li S-J, Hillard CJ, Ward BD, et al. Spatial correlations of laminar BOLD and CBV responses to rat whisker stimulation with neuronal activity localized by Fos expression. Magn. Reson. Med. 2004; 52: 1060–1068.

Lucchinetti C, Bruck W, Parisi J, Scheithauer B, Rodriguez M, Lassmann H. Heterogeneity of multiple sclerosis lesions: implications for the pathogenesis of demyelination. Ann Neurol 2000; 47: 707–717.

Ludowyk PA, Willenborg DO, Parish CR. Selective localisation of neuro-specific T lymphocytes in the central nervous system. J. Neuroimmunol. 1992; 37: 237–250.

Magistretti PJ, Pellerin L. Cellular mechanisms of brain energy metabolism and their relevance to functional brain imaging. Philos. Trans. R. Soc. Lond. B. Biol. Sci. 1999; 354: 1155–63.

Magliozzi R, Howell O, Vora A, Serafini B, Nicholas R, Puopolo M, et al. Meningeal B-cell follicles in secondary progressive multiple sclerosis associate with early onset of disease and severe cortical pathology. Brain 2007; 130: 1089–1104.

Magliozzi R, Howell OW, Reeves C, Roncaroli F, Nicholas R, Serafini B, et al. A Gradient of neuronal loss and meningeal inflammation in multiple sclerosis. Ann. Neurol. 2010; 68: 477–493.

Mahad D, Ziabreva I, Lassmann H, Turnbull D. Mitochondrial defects in acute multiple sclerosis lesions. Brain 2008; 131: 1722–1735.

Mahad DH, Trapp BD, Lassmann H. Pathological mechanisms in progressive multiple sclerosis. Lancet. Neurol. 2015; 14: 183–93.

Manalo DJ, Rowan A, Lavoie T, Natarajan L, Kelly BD, Ye SQ, et al. Transcriptional regulation of vascular endothelial cell responses to hypoxia by HIF-1. Blood 2005; 105: 659–669.

Mann MK, Ray A, Basu S, Karp CL, Dittel BN. Pathogenic and regulatory roles for B cells in experimental autoimmune encephalomyelitis. Autoimmunity 2012; 45: 388–99.

Mannie M, Swanborg RH, Stepaniak JA. Experimental autoimmune encephalomyelitis in the rat. Curr. Protoc. Immunol. 2009; Chapter 15: Unit 15 2.

Marik C, Felts PA, Bauer J, Lassmann H, Smith KJ. Lesion genesis in a subset of patients with multiple sclerosis: a role for innate immunity? Brain 2007; 130: 2800–2815.

Martinelli R, Gegg M, Longbottom R, Adamson P, Turowski P, Greenwood J. ICAM-1-mediated endothelial nitric oxide synthase activation via calcium and AMP-activated protein kinase is required for transendothelial lymphocyte migration. Mol. Biol. Cell 2009; 20: 995–1005.

Massey E, Shelton D, Pact V, Greenburg J, Erwin W, Satzman H, et al. Hyperbaric

oxygen in multiple sclerosis: a double-blind crossover study of 18 patients. Neurology 1985; 35: 104.

Masson N, Ratcliffe PJ. HIF prolyl and asparaginyl hydroxylases in the biological response to intracellular O2 levels. J. Cell Sci. 2003; 116

Maxwell PH, Wiesener MS, Chang GW, Clifford SC, Vaux EC, Cockman ME, et al. The tumour suppressor protein VHL targets hypoxia-inducible factors for oxygen-dependent proteolysis. Nature 1999; 399: 271–275.

Mayhan WG. Nitric oxide donor-induced increase in permeability of the blood–brain barrier. Brain Res. 2000; 866: 101–108.

McDonald WI. The Role of Evoked Potentials in the Diagnosis of Multiple Sclerosis. In: Progress in Multiple Sclerosis Research. Berlin, Heidelberg: Springer Berlin Heidelberg; 1980. p. 564–568.

McDonald WI, Sears TA. The effects of experimental demyelination on conduction in the central nervous system. Brain 1970; 93: 583–98.

McFarland HF, Martin R. Multiple sclerosis: a complicated picture of autoimmunity. Nat. Immunol. 2007; 8: 913–919.

McMahon JM, McQuaid S, Reynolds R, FitzGerald UF. Increased expression of ER stress- and hypoxia-associated molecules in grey matter lesions in multiple sclerosis. Mult Scler 2012; 18: 1437–1447.

Miller DH, Rudge P, Johnson G, Kendall BE, Macmanus DG, Moseley IF, et al. Serial gadolinium enhanced magnetic resonance imaging in multiple sclerosis. Brain 1988; 111 (Pt 4: 927–939.

Miron VE, Boyd A, Zhao JW, Yuen TJ, Ruckh JM, Shadrach JL, et al. M2 microglia and macrophages drive oligodendrocyte differentiation during CNS remyelination. Nat Neurosci 2013; 16: 1211–1218.

Mitrovic B, Ignarro LJ, Montestruque S, Smoll A, Merrill JE. Nitric oxide as a potential pathological mechanism in demyelination: its differential effects on primary glial cells in vitro. Neuroscience 1994; 61: 575–85.

Mitrovic B, Ignarro LJ, Vinters HV, Akers M-A, Schmid I, Uittenbogaart C, et al. Nitric oxide induces necrotic but not apoptotic cell death in oligodendrocytes. Neuroscience 1995; 65: 531–539.

Moncada S, Bolanos JP. Nitric oxide, cell bioenergetics and neurodegeneration. J Neurochem 2006; 97: 1676–1689.

Monson NL, Ortega SB, Ireland SJ, Meeuwissen AJ, Chen D, Plautz EJ, et al. Repetitive hypoxic preconditioning induces an immunosuppressed B cell phenotype during endogenous protection from stroke. J Neuroinflammation 2014; 11: 22.

Moreau T, Coles A, Wing M, Isaacs J, Hale G, Waldmann H, et al. Transient increase in symptoms associated with cytokine release in patients with multiple sclerosis. Brain

1996; 119 (Pt 1: 225–237.

Morell P, Toews AD. In Vivo Metabolism of Oligodendroglial Lipids. In: Oligodendroglia. Boston, MA: Springer US; 1984. p. 47–86.

Muller DM, Pender MP, Greer JM. A neuropathological analysis of experimental autoimmune encephalomyelitis with predominant brain stem and cerebellar involvement and differences between active and passive induction. Acta Neuropathol. 2000; 100: 174–82.

Murdoch C, Lewis CE. Macrophage migration and gene expression in response to tumor hypoxia. Int. J. Cancer 2005; 117: 701–708.

Murphy ÁC, Lalor SJ, Lynch MA, Mills KHG. Infiltration of Th1 and Th17 cells and activation of microglia in the CNS during the course of experimental autoimmune encephalomyelitis. Brain. Behav. Immun. 2010; 24: 641–651.

Murphy MP. Nitric oxide and cell death. Biochim. Biophys. Acta - Bioenerg. 1999; 1411: 401–414.

Murphy MP. How mitochondria produce reactive oxygen species. Biochem. J. 2009; 417: 1–13.

Murthy K, Maurice P, Wilmeth J. Double-blind randomised study of hyperbaric oxygen (HBO) versus placebo in multiple sclerosis (MS). Neurology 1985; 35: 104.

Naegele M, Tillack K, Reinhardt S, Schippling S, Martin R, Sospedra M. Neutrophils in multiple sclerosis are characterized by a primed phenotype. J. Neuroimmunol. 2012; 242: 60–71.

Neiman J, Nilsson BY, Barr PO, Perrins DJ. Hyperbaric oxygen in chronic progressive multiple sclerosis: visual evoked potentials and clinical effects. J. Neurol. Neurosurg. Psychiatry 1985; 48: 497–500.

Nemoto EM, Betterman K. Basic physiology of hyperbaric oxygen in brain. Neurol. Res. 2007; 29: 116–126.

Newton K, Manning G. Necroptosis and Inflammation. Annu. Rev. Biochem. 2016; 85: 743–763.

Ngo ST, Steyn FJ, McCombe PA. Gender differences in autoimmune disease. Front. Neuroendocrinol. 2014; 35: 347–369.

Ní Fhlathartaigh M, McMahon J, Reynolds R, Connolly D, Higgins E, Counihan T, et al. Calreticulin and other components of endoplasmic reticulum stress in rat and human inflammatory demyelination. Acta Neuropathol. Commun. 2013; 1: 37.

Nicot A, Ratnakar P V, Ron Y, Chen C-C, Elkabes S. Regulation of gene expression in experimental autoimmune encephalomyelitis indicates early neuronal dysfunction. Brain 2003; 126: 398–412.

Nikic I, Merkler D, Sorbara C, Brinkoetter M, Kreutzfeldt M, Bareyre FM, et al. A

reversible form of axon damage in experimental autoimmune encephalomyelitis and multiple sclerosis. Nat Med 2011; 17: 495–499.

van Noort JM, Bsibsi M, Gerritsen WH, van der Valk P, Bajramovic JJ, Steinman L, et al. Alphab-crystallin is a target for adaptive immune responses and a trigger of innate responses in preactive multiple sclerosis lesions. J. Neuropathol. Exp. Neurol. 2010; 69: 694–703.

Noseworthy JH, Lucchinetti C, Rodriguez M, Weinshenker BG. Multiple Sclerosis. N. Engl. J. Med. 2000; 343: 938–952.

O'Brien K, Gran B, Rostami A. T-cell based immunotherapy in experimental autoimmune encephalomyelitis and multiple sclerosis. Immunotherapy 2010; 2: 99–115.

Ofengeim D, Ito Y, Trapp B, Correspondence JY, Najafov A, Zhang Y, et al. Activation of Necroptosis in Multiple Sclerosis. CellReports 2015; 10: 1836–1849.

Ohno N, Chiang H, Mahad DJ, Kidd GJ, Liu L, Ransohoff RM, et al. Mitochondrial immobilization mediated by syntaphilin facilitates survival of demyelinated axons. Proc. Natl. Acad. Sci. U. S. A. 2014; 111: 9953–8.

Oleszak EL, Zaczynska E, Bhattacharjee M, Butunoi C, Legido A, Katsetos CD. Inducible nitric oxide synthase and nitrotyrosine are found in monocytes/macrophages and/or astrocytes in acute, but not in chronic, multiple sclerosis. Clin. Diagn. Lab. Immunol. 1998; 5: 438–45.

Olive PL, Vikse C, Trotter MJ. Measurement of oxygen diffusion distance in tumor cubes using a fluorescent hypoxia probe. Int. J. Radiat. Oncol. 1992; 22: 397–402.

Oriani G, Barbieri S, Cislaghi G, Albonico G, Scarlato G, Mariani C, et al. Long - term Hyperbaric Oxygen in Multiple Sclerosis: A Placebo - controlled, Double - blind Trial With Evoked Potentials Studies. 1990

Orihuela R, McPherson CA, Harry GJ. Microglial M1/M2 polarization and metabolic states. Br. J. Pharmacol. 2016; 173: 649–665.

Orrenius S, Zhivotovsky B, Nicotera P. Calcium: Regulation of cell death: the calcium–apoptosis link. Nat. Rev. Mol. Cell Biol. 2003; 4: 552–565.

Pacher P, Beckman JS, Liaudet L. Nitric oxide and peroxynitrite in health and disease. Physiol. Rev. 2007; 87: 315–424.

Packer MA, Murphy MP. Peroxynitrite causes calcium efflux from mitochondria which is prevented by Cyclosporin A. FEBS Lett. 1994; 345: 237–40.

Packer MA, Murphy MP. Peroxynitrite formed by simultaneous nitric oxide and superoxide generation causes cyclosporin-A-sensitive mitochondrial calcium efflux and depolarisation. Eur. J. Biochem. 1995; 234: 231–9.

Paling D, Golay X, Wheeler-Kingshott C, Kapoor R, Miller D. Energy failure in multiple sclerosis and its investigation using MR techniques. J. Neurol. 2011; 258: 2113–2127.

Paling D, Thade Petersen E, Tozer DJ, Altmann DR, Wheeler-Kingshott CA, Kapoor R, et al. Cerebral arterial bolus arrival time is prolonged in multiple sclerosis and associated with disability. J. Cereb. Blood Flow Metab. 2014; 34: 34–42.

Di Paola M, Bozzali M, Fadda L, Musicco M, Sabatini U, Caltagirone C. Reduced oxygen due to high-altitude exposure relates to atrophy in motor-function brain areas. Eur J Neurol 2008; 15: 1050–1057.

Parsa R, Andresen P, Gillett A, Mia S, Zhang XM, Mayans S, et al. Adoptive transfer of immunomodulatory M2 macrophages prevents type 1 diabetes in NOD mice. Diabetes 2012; 61: 2881–2892.

Pasparakis M, Vandenabeele P. Necroptosis and its role in inflammation. Nature 2015; 517: 311–320.

Peña JR, Fitzpatrick D, Saidman SL. Complement-Dependent Cytotoxicity Crossmatch. 2013. p. 257–283.

Petito CK, Olarte J-P, Roberts B, Nowak TS, Pulsinell WA. Selective Glial Vulnerability following Transient Global Ischemia in Rat Brain. J. Neuropathol. Exp. Neurol. 1998; 57

Pikor N, Gommerman JL, Archelos JJ, Storch MK, Hartung HP, Bar-Or A, et al. B cells in MS: Why, where and how? Mult. Scler. Relat. Disord. 2012; 1: 123–30.

Poitz DM, Augstein A, Gradehand C, Ende G, Schmeisser A, Strasser RH. Regulation of the Hif-system by micro-RNA 17 and 20a - role during monocyte-to-macrophage differentiation. Mol Immunol 2013; 56: 442–451.

Polman CH, Reingold SC, Banwell B, Clanet M, Cohen JA, Filippi M, et al. Diagnostic criteria for multiple sclerosis: 2010 revisions to the McDonald criteria. Ann. Neurol. 2011; 69: 292–302.

Popescu BFG, Pirko I, Lucchinetti CF. Pathology of multiple sclerosis: Where do we stand? Contin. Lifelong Learn. Neurol. 2013; 19: 901–921.

Prineas JW, Kwon EE, Cho E-S, Sharer LR, Barnett MH, Oleszak EL, et al. Immunopathology of secondary-progressive multiple sclerosis. Ann. Neurol. 2001; 50: 646–657.

Radi R, Rodriguez M, Castro L, Telleri R. Inhibition of Mitochondrial Electron Transport by Peroxynitrite. Arch. Biochem. Biophys. 1994; 308: 89–95.

Raftopoulos R, Hickman SJ, Toosy A, Sharrack B, Mallik S, Paling D, et al. Phenytoin for neuroprotection in patients with acute optic neuritis: a randomised, placebo-controlled, phase 2 trial. Lancet. Neurol. 2016; 15: 259–69.

Raleigh JA, Calkins-Adams DP, Rinker LH, Ballenger CA, Weissler MC, Fowler Jr. WC, et al. Hypoxia and vascular endothelial growth factor expression in human squamous cell carcinomas using pimonidazole as a hypoxia marker. Cancer Res 1998; 58: 3765–3768.

Ramagopalan S V, Dobson R, Meier UC, Giovannoni G, Noseworthy J, Lucchinetti C,

et al. Multiple sclerosis: risk factors, prodromes, and potential causal pathways. Lancet Neurol. 2010; 9: 727–739.

Redford EJ, Kapoor R, Smith KJ. Nitric oxide donors reversibly block axonal conduction: demyelinated axons are especially susceptible. Brain 1997; 120 (Pt 1: 2149–2157.

Rejdak K, Eikelenboom MJ, Petzold A, Thompson EJ, Stelmasiak Z, Lazeron RHC, et al. CSF nitric oxide metabolites are associated with activity and progression of multiple sclerosis. Neurology 2004; 63: 1439–45.

Renganathan M, Cummins TR, Waxman SG. Nitric Oxide Blocks Fast, Slow, and Persistent Na+ Channels in C-Type DRG Neurons by S-Nitrosylation. J. Neurophysiol. 2002; 87

Riboldi E, Porta C, Morlacchi S, Viola A, Mantovani A, Sica A. Hypoxia-mediated regulation of macrophage functions in pathophysiology. Int Immunol 2013; 25: 67–75.

Richter C, Gogvadze V, Schlapbach R, Schweizer M, Schlegel J. Nitric oxide kills hepatocytes by mobilizing mitochondrial calcium. Biochem. Biophys. Res. Commun. 1994; 205: 1143–50.

Rinholm JE, Hamilton NB, Kessaris N, Richardson WD, Bergersen LH, Attwell D. Regulation of oligodendrocyte development and myelination by glucose and lactate. J. Neurosci. 2011; 31: 538–48.

Rinholm JE, Vervaeke K, Tadross MR, Tkachuk AN, Kopek BG, Brown TA, et al. Movement and structure of mitochondria in oligodendrocytes and their myelin sheaths. Glia 2016; 64: 810–825.

Ritchie JM, Rogart RB. Density of sodium channels in mammalian myelinated nerve fibers and nature of the axonal membrane under the myelin sheath. Proc. Natl. Acad. Sci. U. S. A. 1977; 74: 211–215.

Rodriguez M, Scheithauer B. Ultrastructure of multiple sclerosis. Ultrastruct. Pathol. 1994; 18: 3–13.

Rothman DL, Behar KL, Hyder F, Shulman RG. In vivo NMR studies of the glutamate neurotransmitter flux and neuroenergetics: implications for brain function. Annu Rev Physiol 2003; 65: 401–427.

Roussel BD, Kruppa AJ, Miranda E, Crowther DC, Lomas DA, Marciniak SJ, et al. Endoplasmic reticulum dysfunction in neurological disease. Lancet Neurol. 2013; 12: 105–118.

Rubbo H, Denicola A, Radi R. Peroxynitrite Inactivates Thiol-Containing Enzymes of Trypanosoma cruzi Energetic Metabolism and Inhibits Cell Respiration. Arch. Biochem. Biophys. 1994; 308: 96–102.

Rumble JM, Huber AK, Krishnamoorthy G, Srinivasan A, Giles DA, Zhang X, et al. Neutrophil-related factors as biomarkers in EAE and MS. J. Exp. Med. 2015; 212: 23–35.

Sadeghian M, Mastrolia V, Rezaei Haddad A, Mosley A, Mullali G, Schiza D, et al. Mitochondrial dysfunction is an important cause of neurological deficits in an inflammatory model of multiple sclerosis. Sci. Rep. 2016; 6: 33249.

Saibil H. Chaperone machines for protein folding, unfolding and disaggregation. Nat. Rev. Mol. Cell Biol. 2013; 14: 630–42.

Scarlett JL, Packer MA, Porteous CM, Murphy MP. Alterations to glutathione and nicotinamide nucleotides during the mitochondrial permeability transition induced by peroxynitrite. Biochem. Pharmacol. 1996; 52: 1047–55.

Schofield CJ, Ratcliffe PJ. Oxygen sensing by HIF hydroxylases. Nat. Rev. Mol. Cell Biol. 2004; 5: 343–354.

Schofield CJ, Zhang Z. Structural and mechanistic studies on 2-oxoglutarate-dependent oxygenases and related enzymes. Curr Opin Struct Biol 1999; 9: 722–731.

Schuh C, Wimmer I, Hametner S, Haider L, Van Dam AM, Liblau RS, et al. Oxidative tissue injury in multiple sclerosis is only partly reflected in experimental disease models. Acta Neuropathol 2014; 128: 247–266.

Schurr A. Lactate: the ultimate cerebral oxidative energy substrate? J. Cereb. Blood Flow Metab. 2006; 26: 142–152.

Schurr A, Miller JJ, Payne RS, Rigor BM. An Increase in Lactate Output by Brain Tissue Serves to Meet the Energy Needs of Glutamate-Activated Neurons. J. Neurosci. 1999; 19

Sciamanna MA, Lee CP. Ischemia/reperfusion-induced injury of forebrain mitochondria and protection by ascorbate. Arch Biochem Biophys 1993; 305: 215–224.

Seabrook TJ, Littlewood-Evans A, Brinkmann V, Pollinger B, Schnell C, Hiestand PC. Angiogenesis is present in experimental autoimmune encephalomyelitis and pro-angiogenic factors are increased in multiple sclerosis lesions. J Neuroinflammation 2010; 7: 95.

Selmaj KW, Raine CS. Tumor necrosis factor mediates myelin and oligodendrocyte damage in vitro. Ann. Neurol. 1988; 23: 339–346.

Semenza G. Signal transduction to hypoxia-inducible factor 1. Biochem Pharmacol 2002; 64: 993–998.

Sharief MK, Hentges R. Association between tumor necrosis factor-alpha and disease progression in patients with multiple sclerosis. N. Engl. J. Med. 1991; 325: 467–472.

Shellington DK, Du L, Wu X, Exo J, Vagni V, Ma L, et al. Polynitroxylated pegylated hemoglobin: a novel neuroprotective hemoglobin for acute volume-limited fluid resuscitation after combined traumatic brain injury and hemorrhagic hypotension in mice. Crit Care Med 2011; 39: 494–505.

Shi LZ, Wang R, Huang G, Vogel P, Neale G, Green DR, et al. HIF1alpha-dependent glycolytic pathway orchestrates a metabolic checkpoint for the differentiation of TH17

and Treg cells. J Exp Med 2011; 208: 1367–1376.

Shin HK, Dunn AK, Jones PB, Boas DA, Lo EH, Moskowitz MA, et al. Normobaric hyperoxia improves cerebral blood flow and oxygenation, and inhibits peri-infarct depolarizations in experimental focal ischaemia. Brain 2007; 130: 1631–42.

Shockley RP, LaManna JC. Determination of rat cerebral cortical blood volume changes by capillary mean transit time analysis during hypoxia, hypercapnia and hyperventilation. Brain Res 1988; 454: 170–178.

Sibson NR, Dhankhar A, Mason GF, Rothman DL, Behar KL, Shulman RG. Stoichiometric coupling of brain glucose metabolism and glutamatergic neuronal activity. Proc Natl Acad Sci U S A 1998; 95: 316–321.

Sica A, Mantovani A. Macrophage plasticity and polarization: in vivo veritas. J Clin Invest 2012; 122: 787–795.

Sicher SC, Vazquez MA, Lu CY. Inhibition of macrophage Ia expression by nitric oxide. J. Immunol. 1994; 153: 1293–300.

Simmons RD, Bernard CC, Singer G, Carnegie PR. Experimental autoimmune encephalomyelitis. An anatomically-based explanation of clinical progression in rodents. J Neuroimmunol 1982; 3: 307–318.

Simons M, Alitalo K, Annex BH, Augustin HG, Beam C, Berk BC, et al. State-of-the-Art Methods for Evaluation of Angiogenesis and Tissue Vascularization. Circ. Res. 2015; 116

Singhal AB. A review of oxygen therapy in ischemic stroke. Neurol Res 2007; 29: 173–183.

Singhal AB, Benner T, Roccatagliata L, Koroshetz WJ, Schaefer PW, Lo EH, et al. A pilot study of normobaric oxygen therapy in acute ischemic stroke. Stroke. 2005; 36: 797–802.

Smith D, Pernet A, Hallett WA, Bingham E, Marsden PK, Amiel SA. Lactate: a preferred fuel for human brain metabolism in vivo. J Cereb Blood Flow Metab 2003; 23: 658–664.

Smith KJ. Conduction properties of central demyelinated and remyelinated axons, and their relation to symptom production in demyelinating disorders. Eye 1994; 8: 224–237.

Smith KJ. Sodium channels and multiple sclerosis: Roles in symptom production, damage and therapy. Brain Pathol. 2007; 17: 230–242.

Smith KJ. Newly lesioned tissue in multiple sclerosis--a role for oxidative damage? Brain 2011; 134: 1877–81.

Smith KJ, Blakemore WF, McDonald WI. Central remyelination restores secure conduction. Nature 1979; 280: 395–6.

Smith KJ, McDonald WI. Spontaneous and mechanically evoked activity due to central demyelinating lesion. Nature 1980; 286: 154–5.

Smith KJK, Lassmann H. The role of nitric oxide in multiple sclerosis. Lancet Neurol. 2002; 1: 232–241.

Solaini G, Baracca A, Lenaz G, Sgarbi G. Hypoxia and mitochondrial oxidative metabolism. Biochim. Biophys. Acta - Bioenerg. 2010; 1797: 1171–1177.

Stadelmann C, Ludwin S, Tabira T, Guseo A, Lucchinetti CF, Leel-Ossy L, et al. Tissue preconditioning may explain concentric lesions in Balo's type of multiple sclerosis. Brain 2005; 128: 979–987.

Steen C, D'haeseleer M, Hoogduin JM, Fierens Y, Cambron M, Mostert JP, et al. Cerebral white matter blood flow and energy metabolism in multiple sclerosis. Mult. Scler. J. 2013; 19: 1282–1289.

Steen C, Wilczak N, Hoogduin JM, Koch M, De Keyser J. Reduced creatine kinase B activity in multiple sclerosis normal appearing white matter. PLoS One 2010; 5: e10811.

Stoller KP. All the right moves: the need for the timely use of hyperbaric oxygen therapy for treating TBI/CTE/PTSD. Med. Gas Res. 2015; 5: 7.

Stone S, Lin W. The unfolded protein response in multiple sclerosis. Front Neurosci 2015; 9: 264.

Storch MK, Stefferl A, Brehm U, Weissert R, Wallstrom E, Kerschensteiner M, et al. Autoimmunity to myelin oligodendrocyte glycoprotein in rats mimics the spectrum of multiple sclerosis pathology. Brain Pathol 1998; 8: 681–694.

Strapazzon G, Malacrida S, Vezzoli A, Dal Cappello T, Falla M, Lochner P, et al. Oxidative stress response to acute hypobaric hypoxia and its association with indirect measurement of increased intracranial pressure: a field study. Sci. Rep. 2016; 6: 32426.

Stromnes IM, Goverman JM. Active induction of experimental allergic encephalomyelitis. Nat Protoc 2006a; 1: 1810–1819.

Stromnes IM, Goverman JM. Passive induction of experimental allergic encephalomyelitis. Nat Protoc 2006b; 1: 1952–1960.

Stys P, Waxman S, Ransom B. Ionic mechanisms of anoxic injury in mammalian CNS white matter: role of Na+ channels and Na(+)-Ca2+ exchanger. J. Neurosci. 1992; 12

Stys PK. Anoxic and ischemic injury of myelinated axons in CNS white matter: from mechanistic concepts to therapeutics. J. Cereb. Blood Flow Metab. 1998; 18: 2–25.

Stys PK. Multiple sclerosis: autoimmune disease or autoimmune reaction? Can. J. Neurol. Sci. J. Can. des Sci. Neurol. 2010; 37 Suppl 2: S16-23.

Su Z, Yang Z, Xie L, DeWitt JP, Chen Y. Cancer therapy in the necroptosis era. Cell Death Differ. 2016; 23: 748–756.

Tabas I, Ron D. Integrating the mechanisms of apoptosis induced by endoplasmic reticulum stress. Nat. Cell Biol. 2011; 13: 184–90.

Thompson GA. The regulation of membrane lipid metabolism. CRC Press; 1992.

Todorich B, Pasquini JM, Garcia CI, Paez PM, Connor JR. Oligodendrocytes and myelination: The role of iron. Glia 2009; 57: 467–478.

Trapp BD, Peterson J, Ransohoff RM, Rudick R, Mork S, Bo L. Axonal transection in the lesions of multiple sclerosis. N Engl J Med 1998; 338: 278–285.

Trapp BD, Stys PK. Virtual hypoxia and chronic necrosis of demyelinated axons in multiple sclerosis. Lancet Neurol. 2009; 8: 280–291.

Tugal D, Liao X, Jain MK. Transcriptional control of macrophage polarization. Arter. Thromb Vasc Biol 2013; 33: 1135–1144.

Varga AW, Johnson G, Babb JS, Herbert J, Grossman RI, Inglese M. White matter hemodynamic abnormalities precede sub-cortical gray matter changes in multiple sclerosis. J Neurol Sci 2009; 282: 28–33.

van der Veen RC, Roberts LJ. Contrasting roles for nitric oxide and peroxynitrite in the peroxidation of myelin lipids. J. Neuroimmunol. 1999; 95: 1–7.

Verreck FA, de Boer T, Langenberg DM, van der Zanden L, Ottenhoff TH. Phenotypic and functional profiling of human proinflammatory type-1 and anti-inflammatory type-2 macrophages in response to microbial antigens and IFN-gamma- and CD40L-mediated costimulation. J Leukoc Biol 2006; 79: 285–293.

Vidaurre OG, Haines JD, Katz Sand I, Adula KP, Huynh JL, McGraw CA, et al. Cerebrospinal fluid ceramides from patients with multiple sclerosis impair neuronal bioenergetics. Brain 2014; 137: 2271–86.

Wacker BK, Perfater JL, Gidday JM. Hypoxic preconditioning induces stroke tolerance in mice via a cascading HIF, sphingosine kinase, and CCL2 signaling pathway. J Neurochem 2012; 123: 954–962.

Walz W, Mukerji S. Lactate production and release in cultured astrocytes. Neurosci. Lett. 1988; 86: 296–300.

Wang GL, Jiang BH, Rue EA, Semenza GL. Hypoxia-inducible factor 1 is a basic-helix-loop-helix-PAS heterodimer regulated by cellular O2 tension. Proc Natl Acad Sci U S A 1995; 92: 5510–5514.

Wang N, Liang H, Zen K. Molecular Mechanisms That Influence the Macrophage M1-M2 Polarization Balance. Front. Immunol. 2014; 5: 614.

Warren J, Sacksteder MR, Thuning CA. Oxygen immunosuppression: modification of experimental allergic encephalomyelitis in rodents. J. Immunol. 1978; 121: 315–20.

Watson NA, Beards SC, Altaf N, Kassner A, Jackson A. The effect of hyperoxia on cerebral blood flow: a study in healthy volunteers using magnetic resonance phase-contrast angiography. Eur. J. Anaesthesiol. 2000; 17: 152–9.

Waxman SG. Axonal conduction and injury in multiple sclerosis: the role of sodium

channels. Nat. Rev. Neurosci. 2006; 7: 932–941.

Waxman SG, WI M, Mayer RF D-BD, JL H, McDonald WI ST, RF M, et al. Conduction in Myelinated, Unmyelinated, and Demyelinated Fibers. Arch. Neurol. 1977; 34: 585–589.

Way SW, Popko B, Hauser S, Dawson D, Lehrich J, al. et, et al. Harnessing the integrated stress response for the treatment of multiple sclerosis. Lancet Neurol. 2016; 15: 434–443.

Weaver J, Liu KJ. Does normobaric hyperoxia increase oxidative stress in acute ischemic stroke? A critical review of the literature. Med Gas Res 2015; 5: 11.

Wekerle H, Linington C, Lassmann H, Meyermann R, Thomas L, Burnet FM, et al. Cellular immune reactivity within the CNS. Trends Neurosci. 1986; 9: 271–277.

Wensky AK, Furtado GC, Marcondes MCG, Chen S, Manfra D, Lira SA, et al. IFN-gamma determines distinct clinical outcomes in autoimmune encephalomyelitis. J. Immunol. 2005; 174: 1416–23.

Wildner G, Kaufmann U. What causes relapses of autoimmune diseases? The etiological role of autoreactive T cells. Autoimmun. Rev. 2013; 12: 1070–1075.

Wiles CM, Clarke CRA, Irwin HP, Edgar EF, Swan A V. Hyperbaric Oxygen In Multiple Sclerosis: A Double Blind Trial. Br. Med. J. 1986; 292: 367–371.

Wilson EH, Weninger W, Hunter CA, Goldmann E, Hawkins B, Davis T, et al. Trafficking of immune cells in the central nervous system. J. Clin. Invest. 2010; 120: 1368–79.

Winkelmann A, Loebermann M, Reisinger EC, Hartung H-P, Zettl UK. Disease-modifying therapies and infectious risks in multiple sclerosis. Nat. Rev. Neurol. 2016; advance on

Witte ME, Mahad DJ, Lassmann H, van Horssen J. Mitochondrial dysfunction contributes to neurodegeneration in multiple sclerosis. Trends Mol. Med. 2014; 20: 179–187.

Wood J, Stell R, Unsworth I, Lance JW, Skuse N. A double-blind trial of hyperbaric oxygen in the treatment of multiple sclerosis. Med. J. Aust. 1985; 143: 238–40.

Wouters BG, Koritzinsky M. Hypoxia signalling through mTOR and the unfolded protein response in cancer. Nat. Rev. Cancer 2008; 8: 851–864.

Wykoff CC, Beasley NJ, Watson PH, Turner KJ, Pastorek J, Sibtain A, et al. Hypoxia-inducible expression of tumor-associated carbonic anhydrases. Cancer Res 2000; 60: 7075–7083.

Xia X, Lemieux ME, Li W, Carroll JS, Brown M, Liu XS, et al. Integrative analysis of HIF binding and transactivation reveals its role in maintaining histone methylation homeostasis. Proc Natl Acad Sci U S A 2009; 106: 4260–4265.

Xu K, Lamanna JC. Chronic hypoxia and the cerebral circulation. J Appl Physiol 2006; 100: 725–730.

Xu W, Chi L, Row B., Xu R, Ke Y, Xu B, et al. Increased oxidative stress is associated with chronic intermittent hypoxia-mediated brain cortical neuronal cell apoptosis in a mouse model of sleep apnea. Neuroscience 2004; 126: 313–323.

Yang EJ, Lee J, Lee SY, Kim EK, Moon YM, Jung YO, et al. EGCG attenuates autoimmune arthritis by inhibition of STAT3 and HIF-1alpha with Th17/Treg control. PLoS One 2014; 9: e86062.

Yang R, Dunn JF, Dotti CG, Strooper B De, Alexandre F, Heraud N, et al. Reduced cortical microvascular oxygenation in multiple sclerosis: a blinded, case-controlled study using a novel quantitative near-infrared spectroscopy method. Sci. Rep. 2015; 5: 16477.

Zamboni P, Galeotti R, Menegatti E, Malagoni AM, Tacconi G, Dall'Ara S, et al. Chronic cerebrospinal venous insufficiency in patients with multiple sclerosis. J. Neurol. Neurosurg. Psychiatry 2009; 80: 392–9.

Zhang J, Dawson VL, Dawson TM, Snyder SH. Nitric oxide activation of poly(ADP-ribose) synthetase in neurotoxicity. Science 1994; 263: 687–9.

Zhang J, Jin B, Li L, Block ER, Patel JM. Nitric oxide-induced persistent inhibition and nitrosylation of active site cysteine residues of mitochondrial cytochrome-c oxidase in lung endothelial cells. Am. J. Physiol. - Cell Physiol. 2005; 288

Ziabreva I, Campbell G, Rist J, Zambonin J, Rorbach J, Wydro MM, et al. Injury and differentiation following inhibition of mitochondrial respiratory chain complex IV in rat oligodendrocytes. Glia 2010; 58: 1827–37.

ACKNOWLEDGEMENTS

I would like to express my gratitude to Prof Kenneth Smith, for the scientific support, guidance, patience and advices that he dedicated to me throughout my Ph.D. Also, I want to thank Ken for giving me the opportunity to work in his laboratory, without him, this project and the wonderful experience in London would not have been possible.

I would like to thank Prof Christopher Linington and Daniel McElroy for the help and teaching about the passive EAE model. I would also further thank Daniel for his help with the RT-PCR experiment.

A Big thank goes to my dear colleagues: Ana, Greg, Catherine, Claudio, Cristina, Helen, Joe, Kat, Lars, Lukasz, Marija, Michael, Pablito, Radha, Sharmeen and Tom. They all contributed in making special my PhD experience.
Many thanks go to Roshni and Andrew for their mentoring when I first started in the lab. I would like to thank also Alina and Kate for their help with the experiments, it has been a pleasure to have the chance to work with them. I would like to thank Charlotte for helping me with administrative issues and for the funny chats (in brummie) that we had in the office. A thank goes to The German for sorting out my foolish IT problems and for the bruises that he caused me playing squash. I would also like to thank the B-club: Alina (again), Dimitra, Kim and Philip (or Alex at wish): to the Greek for her funny grumpiness and for having cleaned up my lab mess when I was not able to do so by myself, to Kim for her evergreen super-excitement and craziness, and to Alex for her (with Claudio) help and patience in tissue culture, and for the English lessons that have left me flabbergasted. The moments we spent together have made my experience in London amaaaaziiing and, apart the jokes, I consider you friends rather than colleagues.

Thanks to my flatmates, they also contributed in making interesting my life in London.

I would like to thank for their support and friendship also the Little Italy community: Alberto, Andrea, Baby, Eleonora, Giulia, Gubbbi, Rosellina and Stefano. Thanks to them, it has been like having the “taste” of home always with me.

I would like to thank all my friends in Oxford for the nice weekends spent together in the countryside.

A special thank goes to Federica for her support and love, and for continuously encouraging me even in the more difficult situations. This PhD would not have been so pleasant without her.

I would like to dedicate this thesis to my family: my father Giuseppe, my mother Ottavia, and my siblings Decio and Mafalda. The smiles, the trust and the affection shown to me continually are one of the most beautiful things in my life.

Vorrei dedicare questa tesi alla mia famiglia: a mio padre Giuseppe, mia madre Ottavia, e ai miei fratelli Decio e Mafalda. I sorrisi, la fiducia e l'affetto che mi dimostrano continuamente sono una delle cose piú belle della mia vita.